



National Library
of Canada

Bibliothèque nationale
du Canada

Canadian Theses Service

Services des thèses canadiennes

Ottawa, Canada
K1A 0N4

CANADIAN THESES

NOTICE

The quality of this microfiche is heavily dependent upon the quality of the original thesis submitted for microfilming. Every effort has been made to ensure the highest quality of reproduction possible.

If pages are missing, contact the university which granted the degree.

Some pages may have indistinct print especially if the original pages were typed with a poor typewriter ribbon or if the university sent us an inferior photocopy.

Previously copyrighted materials (journal articles, published tests, etc.) are not filmed.

Reproduction in full or in part of this film is governed by the Canadian Copyright Act, R.S.C. 1970, c. C-30.

**THIS DISSERTATION
HAS BEEN MICROFILMED
EXACTLY AS RECEIVED**

THÈSES CANADIENNES

AVIS

La qualité de cette microfiche dépend grandement de la qualité de la thèse soumise au microfilmage. Nous avons tout fait pour assurer une qualité supérieure de reproduction.

S'il manque des pages, veuillez communiquer avec l'université qui a conféré le grade.

La qualité d'impression de certaines pages peut laisser à désirer, surtout si les pages originales ont été dactylographiées à l'aide d'un ruban usé ou si l'université nous a fait parvenir une photocopie de qualité inférieure.

Les documents qui font déjà l'objet d'un droit d'auteur (articles de revue, examens publiés, etc.) ne sont pas microfilmés.

La reproduction, même partielle, de ce microfilm est soumise à la Loi canadienne sur le droit d'auteur, SRC 1970, c. C-30.

**LA THÈSE A ÉTÉ
MICROFILMÉE TELLE QUE
NOUS L'AVONS REÇUE**

THE UNIVERSITY OF ALBERTA

The Renal Excretion of Radioiodinated Peanut Lectin

by

Graeme Rex Boniface

A THESIS

SUBMITTED TO THE FACULTY OF GRADUATE STUDIES AND RESEARCH

IN PARTIAL FULFILMENT OF THE REQUIREMENTS FOR THE DEGREE

OF Doctor of Philosophy

IN

Pharmaceutical Sciences-(Bionucleonics)

Faculty of Pharmacy and Pharmaceutical Sciences

EDMONTON, ALBERTA

Spring 1986

Permission has been granted to the National Library of Canada to microfilm this thesis and to lend or sell copies of the film.

The author (copyright owner) has reserved other publication rights, and neither the thesis nor extensive extracts from it may be printed or otherwise reproduced without his/her written permission.

L'autorisation a été accordée à la Bibliothèque nationale du Canada de microfilmer cette thèse et de prêter ou de vendre des exemplaires du film.

L'auteur (titulaire du droit d'auteur) se réserve les autres droits de publication; ni la thèse ni de longs extraits de celle-ci ne doivent être imprimés ou autrement reproduits sans son autorisation écrite.

ISBN 0-315-30191-0

THE UNIVERSITY OF ALBERTA

RELEASE FORM

NAME OF AUTHOR Graeme Rex Boniface

TITLE OF THESIS The Renal Excretion of Radiiodinated Peanut Lectin

DEGREE FOR WHICH THESIS WAS PRESENTED Doctor of Philosophy

YEAR THIS DEGREE GRANTED Spring 1986

Permission is hereby granted to THE UNIVERSITY OF ALBERTA LIBRARY to reproduce single copies of this thesis and to lend or sell such copies for private, scholarly or scientific research purposes only.

The author reserves other publication rights, and neither the thesis nor extensive extracts from it may be printed or otherwise reproduced without the author's written permission.

(SIGNED) 

PERMANENT ADDRESS:

..... 9 Landscape Road,

..... Mt. Eden, Auckland,

..... NEW ZEALAND

DATED 6 February 1986

THE UNIVERSITY OF ALBERTA
FACULTY OF GRADUATE STUDIES AND RESEARCH

The undersigned certify that they have read, and recommend to the Faculty of Graduate Studies and Research, for acceptance, a thesis entitled **The Renal Excretion of Radioiodinated Peanut Lectin** submitted by **Graeme Rex Boniface** in partial fulfilment of the requirements for the degree of **Doctor of Philosophy in Pharmaceutical Sciences (Bionucleonics)**.

Tracy
.....
Supervisor

She Shun
.....

[Signature]
.....

[Signature]
.....

Date.....6..February..1986.....

TO SHONA, MY MOTHER AND THE MEMORY OF MY FATHER.

Abstract

Peanut lectin (PNA) is a plant protein of 110,000 daltons which binds specifically to the disaccharide β -D-Gal-(1 \rightarrow 3)- α -GalNAc, the immunodeterminant structure of the Thomsen-Friedenreich (T-F) antigen. This antigen is found in unmasked form in a variety of carcinomas, as well as in cryptic form in many normal tissues. Iodinated (125 I or 131 I)-PNA has been used as a radiopharmaceutical for the *in vivo* scintigraphy of both animal and human tumours, however during biodistribution studies, rapid and selective renal excretion of iodinated PNA was noted. I here report on the investigation of the mechanism of renal excretion of radioiodinated PNA, and its use in the quantification of renal function.

Peanut lectin was successfully iodinated with 131 I and 125 I using the iodogen method, resulting in a stable radiolabelled protein which retained its sugar-binding characteristics. 125 I-PNA or 131 I-PNA was administered intravenously (i.v.) into various strains of mice (AJ, CBA/CAJ, c57b, CAF1/J), NZW rabbits, mongrel dogs and humans, and the rate of renal uptake and excretion was quantitated using nuclear medicine techniques. Rapid renal accumulation of PNA was noted in mice, rabbits, dogs and humans, with resultant radioactivity noted in the urine following renal excretion. In normal rabbits, the renal activity peaked at 37.2 ± 6.9 min P.I., with $19.6 \pm 4.3\%$ of the injected dose-at-peak in the kidneys. The bladder contained $12.6 \pm 3.9\%$ of the injected dose at 1 h P.I., and the kidney/liver ratio was determined as 18.9 ± 1.8 . The renal uptake and excretion of 131 I-PNA was inhibited by the prior administration of anti-PNA IgG antibodies and the glycoprotein epiglycanin, or if 131 I-PNA was complexed to the glycosylated HSA analogue asialo-GM₁-HSA. The renal uptake and excretion of 131 I-PNA was not affected by furosemide or probenecid.

In normal dogs, the renal uptake and excretion of 131 I-PNA was kinetically similar to rabbits (time-to-peak 44.6 ± 4.8 min, % inj. dose-at-peak $21.8 \pm 3.3\%$) with $12.8 \pm 5.3\%$ of the injected dose contained in the bladder at 1 h P.I. The renal uptake of 131 I-PNA was inhibited by the concomitant infusion of D-galactose. The plasma pharmacokinetics of 131 I-PNA in dogs were best described by a two compartment exponential model ($A_0 = 68.23\%$, $t_{1/2\alpha} = 0.31$ h, B_0

= 39.75%, $t_{1/2} \beta = 1.19$ h), and a volume of distribution of 1.27 L and clearance of 17.52 mL.min⁻¹ calculated.

Immunoperoxidase renal histopathology revealed that PNA was primarily cleared from the blood of mice, rabbits and dogs by binding to the basement membrane of the proximal tubules, with a small proportion of binding also noted on the basement membrane of intercalated cells of the collecting duct. Following basement membrane binding, PNA was demonstrated within the tubular cells, and at later time points, within the lumen of the nephron. Urine analysis revealed that the radioactivity in the urine at early time points was primarily associated with intact PNA, along with smaller molecular weight protein fragments, and a small proportion of free I⁻. At later time, the relative proportion of free iodide increased in both plasma and urine. The renal excretion of radioiodinated PNA appears to involve a specific process of transport from the peritubular capillaries to the lumen by the tubular cells.

The tubular toxic chemotherapeutic agent cis-platinum had a pronounced effect on the renal uptake and plasma clearance rate of ¹³¹I-PNA in dogs. At comparable therapeutic doses for human treatment, a decline in ¹³¹I-PNA clearance of 71.3 ± 6.6% was observed, while ERPF and GFR was only noted to drop by 20.9 ± 11.8% and 46.6 ± 8.9% respectively. Dynamic renal scintigraphic analysis confirmed a similar decline in % inj. dose-at-peak (65.8 ± 12.7%) and % inj. dose in bladder at 60 min P.I. (67.6 ± 18.1%) when compared with pretreatment estimates.

Studies in humans revealed a similar mechanism of ¹³¹I-PNA renal excretion, although of slower rate than that for other animals (time-to-peak = 90 ± 12 min, % inj. dose-at-peak = 20.2 ± 4.6%). Patients injected with up to three doses of ¹³¹I-PNA at six week intervals, did not show elevated titres of anti-PNA IgG, IgM, or IgE antibodies in serum, as determined by ELISA assay, nor have any patients shown acute or chronic side effects from multiple administrations of ¹³¹I-PNA.

Sequential ¹³¹I-PNA renal uptake studies in patients undergoing cis-platinum chemotherapy have not, to date, revealed significant changes in renal uptake, which could be

attributed to renal tubular dysfunction or toxicity. Variations in the renal uptake rate of

^{131}I -PNA have been demonstrated in patients with normal creatinine clearance and appear to be

due to normal variations in the renal tubular receptor binding rate of ^{131}I -PNA.

Acknowledgements

I wish to extend my appreciation to my supervisor, Dr Tony Noujaim, whose constant encouragement, guidance, and enthusiasm was present throughout this research project. His help and friendship will always be remembered. To Dr Alex Shysh, I wish to extend my thanks for his co-operation and help.

Sincere thanks for invaluable assistance with parts of this project go to Dr Dave Willans of the Edmonton General Hospital, Drs Tam and Suresh of the Faculty of Pharmacy and Pharmaceutical Sciences, Dr Dossetor of the Faculty of Medicine, and to Drs Brian Lentle, and Rick Hooper and all of the technical staff of the Dept of Nuclear Medicine, Cross Cancer Institute, for their help in the clinical studies.

To all my colleagues and friends in Bionucleonics, including Lindsay MacQueen, Connie Turner, Steve MacQuarrie, Chris Ediss, Drs Doug Abrams, Tom Sykes, John Mercer and Richard Flanagan, a special thanks for your constant help, support, and friendship. To the many others, whose professional skills and friendship made the day-to-day rigours much more enjoyable, I will always be grateful.

I wish to acknowledge the financial assistance of the Alberta Heritage Foundation for Medical Research, for their award of a Studentship, and the Alberta Cancer Board for their contribution towards some of the research expenditure.

Table of Contents

Chapter	Page
1. INTRODUCTION	1
2. SURVEY OF THE LITERATURE	2
2.1 RENAL FUNCTION TESTS	2
2.1.1 Radiopharmaceuticals for Renal Evaluation	2
2.1.1.1 Static Renal Imaging Agents	3
2.1.1.2 ^{99m}Tc -Labelled Radiopharmaceuticals	3
2.1.1.3 Radiopharmaceuticals for Glomerular Filtration Rate (GFR) estimation	7
2.1.1.4 Radioiodinated Urological Contrast Agents	8
2.1.1.5 Radiometal Chelates	9
^{99m}Tc -DTPA	10
2.1.1.6 Radiopharmaceuticals for Effective Renal Plasma Flow (ERPF) estimation	11
2.1.1.7 Orthoiodohippurate (OIH)	11
2.1.1.8 Ruthenium-Labelled Renal Radiopharmaceuticals	13
2.1.1.9 Radiopharmaceuticals for the Assessment of Renal Perfusion	14
2.1.1.10 Quantitative Considerations in Radionuclide Renal Function Studies	14
2.1.1.11 Determination of Global and Differential ERPF	15
2.1.1.12 Quantification of Global and Differential GFR	17
2.1.2 Clinical Indications for Radionuclide Renal Investigation	17
2.1.2.1 Space-Occupying Lesions of the Kidney	17
2.1.2.2 Renovascular Hypertension	19
2.1.2.3 Acute and Chronic Renal Failure	20
2.1.2.4 Renal Allograft Studies	21
2.1.3 Biochemical Methods of Renal Function Estimation	22
2.1.3.1 Serum Creatinine and Creatinine Clearance	22

2.1.3.2	β_2 -Microglobulin.	23
2.1.3.3	Blood Urea Nitrogen (BUN).	24
2.1.3.4	γ -Glutamyltransferase (γ -GT).	25
2.1.3.5	Miscellaneous Biochemical Markers of Renal Function.	25
2.1.3.6	Tamm-Horsfall Glycoprotein	27
2.2	CIS-PLATINUM NEPHROTOXICITY	28
2.2.0.1	Pathology	28
2.2.0.2	Diagnosis of Cis-Platinum Nephrotoxicity.	29
2.3	THE THOMSEN-FRIEDENREICH ANTIGEN.	30
2.3.1	Anti T-F antibodies.	30
2.3.2	M-, N-, T-F- and Tn- Glycoproteins.	31
2.3.3	Composition and structure of the T-F and related antigens.	31
2.3.4	T-F and Tn antigens in Tumour Aggressiveness and Adhesion.	35
2.4	LECTINS.	36
2.4.1	Definition and Classification.	36
2.4.1.1	Macromolecular Properties.	37
2.4.1.2	Functional Roles of Lectins	37
2.4.2	Lectin Carbohydrate Specificity	38
2.4.3	Uses of Lectins.	40
2.5	PEANUT LECTIN (PNA).	41
2.5.1	Macromolecular Properties of PNA.	42
2.5.2	Isolation and purification of PNA.	44
2.5.2.1	Isolectins: Multiple Molecular Forms of PNA.	44
2.5.3	Carbohydrate-Binding Specificity of PNA	45
2.5.4	Biological Binding of PNA.	48
2.5.4.1	Erythrocytes	49
2.5.4.2	Lymphocytes	50

2.5.4.3	Platelets	51
2.5.5	PNA binding to tumour cells	52
2.5.5.1	Embryonal Carcinoma	52
2.5.5.2	Mammary Carcinomas	52
2.5.5.3	Carcinomas of the G.I.T.	55
2.5.5.4	Carcinomas of the bladder	56
2.5.5.5	PNA binding in the skin	57
2.5.6	PNA binding in the Kidney	57
2.5.7	In-vivo Studies with PNA	60
3.	EXPERIMENTAL.	63
3.1	MATERIALS AND METHODS.	63
3.1.1	Protein solutions.	63
3.1.1.1	Peanut lectin.	63
3.1.1.2	Bovine Serum Albumin and Human Serum Albumin.	63
3.1.1.3	Asialo-GM ₁ -HSA.	63
3.1.2	Radioiodination.	63
3.1.3	Chromatographic Separation of Iodinated Protein.	64
3.1.4	Quality Control.	65
3.1.4.1	Estimation of Protein Concentration.	65
3.1.4.2	Trichloroacetic Acid Precipitation.	65
3.1.4.3	Instant Thin Layer Chromatography (ITLC).	66
3.1.4.4	Carbohydrate Binding Specificity of Iodinated PNA.	66
3.1.5	¹³¹ I-PNA for Human Administration.	66
3.1.5.1	Sterile Production of ¹³¹ I-PNA.	67
3.1.5.2	Sterility Testing.	68
3.1.5.3	Pyrogen Testing.	68
3.2	ANIMAL STUDIES.	68

3.2.1 ^{125}I -PNA Biodistribution Studies in Mice.	68
3.2.1.1 Dose-Response in CBA/CAJ Mice.	69
3.2.1.2 ^{125}I -PNA Biodistribution in AJ, c57b, CBA/CAJ and CAF1/J Strain Mice.	69
3.2.1.3 Effect of Multiple Doses of PNA on the Biodistribution of ^{125}I -PNA in CBA/CAJ Mice.	69
3.2.2 Dynamic ^{125}I -PNA Renal Scintigraphy in NZW Rabbits.	70
3.2.2.1 Normals.	70
3.2.2.2 Comparative Studies.	71
3.2.3 Studies with asialo- GM_1 -HSA.	72
3.2.3.1 ^{125}I -PNA: ^{125}I -a- GM_1 -HSA Biodistribution Studies in TA_1 -Ha Tumour-Bearing CBA/CAJ and CAF1/J Mice.	73
3.2.4 Dynamic and Static ^{125}I -PNA Scintigraphy in Dogs.	74
3.2.5 ^{125}I -PNA Plasma Pharmacokinetics and Clearance Studies in Dogs.	75
3.2.5.1 Pharmacokinetic Model Calculations.	75
3.2.5.2 Red cell Binding.	76
3.2.5.3 Urine Collection and Analysis.	76
3.2.5.4 ^{125}I -PNA Renal Scintigraphy during Galactose Perfusion in Dogs.	77
3.2.6 Renal PNA Deposition by Histopathology Techniques.	77
3.2.7 ^{125}I -PNA Renal Parameters in Cis-platinum Induced Renal Toxicity in Dogs.	78
3.2.7.1 Cis-platinum Treatment Regimen.	79
3.2.7.2 Serum Biochemistry.	79
3.2.7.3 Serum circulating T-F antigen titres.	80
3.2.7.4 ERPF and GFR Estimations.	80
3.2.7.5 ^{125}I -PNA Plasma Clearance and Renal Studies in Cis-platinum Treated Dogs.	81
3.2.7.6 Renal Histopathology after Cis-platinum Treatment in Dogs.	81
3.3 HUMAN STUDIES.	81

3.3.1	¹³¹ I-PNA Scintigraphy in Patients with Metastatic Disease	81
3.3.2	¹³¹ I-PNA Renal Studies in Patients undergoing Cis-platinum Chemotherapy	83
3.3.2.1	Patient Eligibility	83
3.3.2.2	¹³¹ I-PNA Renal Scanning and Pharmacokinetic Protocol	83
3.3.2.3	Serum Biochemistry and Creatinine Clearance	84
3.3.2.4	Anti-PNA Antibody Determinations	85
4.	RESULTS AND DISCUSSION	86
4.1	RADIOIODINATION AND QUALITY CONTROL OF PEANUT LECTIN	86
4.1.0.1	Protein concentration determinations	87
4.1.0.2	Sterile preparation of ¹³¹ I-PNA	88
4.2	PNA BIODISTRIBUTION STUDIES IN ANIMALS AND HUMANS	90
4.2.1	¹²⁵ I-PNA Biodistribution studies in mice	90
4.2.1.1	Dose-response in mice	90
4.2.1.2	Renal uptake of ¹²⁵ I-PNA in different strains of mice	90
4.2.2	Dynamic ¹³¹ I-PNA renal scintigraphy in NZW Rabbits	95
4.2.3	¹³¹ I-PNA Dynamic and Static Renal Scintigraphy in Dogs	98
4.2.4	¹³¹ I-PNA Scintigraphy in Patients with Metastatic Disease	101
4.2.4.1	Toxicity of PNA	102
4.2.4.2	Tumour Scintigraphy with ¹³¹ I-PNA in Humans	102
4.2.4.3	Renal Uptake and Excretion of ¹³¹ I-PNA in Humans	103
4.3	THE MECHANISM OF RENAL UPTAKE AND EXCRETION OF ¹³¹ I-PNA	106
4.3.1	¹³¹ I-PNA Plasma Pharmacokinetics and Clearance Studies in Dogs	106
4.3.1.1	Plasma Pharmacokinetics and Clearance Determinations	106
4.3.1.2	Urine analysis	107
4.3.2	Histological determination of PNA binding in the kidneys of CBA/CAJ mice, NZW rabbits, and dogs	112
4.3.3	Proposed proximal tubular transport mechanism for PNA	116

4.4	FACTORS AFFECTING THE RENAL UPTAKE AND EXCRETION OF ¹³¹ I-PNA.	120
4.4.1	Agents present in the Circulation.	120
4.4.1.1	¹³¹ I-PNA :asialo GM ₁ disaccharide renal scintigraphy in NZW rabbits.	120
4.4.1.2	¹³¹ I-PNA renal scintigraphy in Probenecid and Furosemide treated NZW rabbits.	121
4.4.1.3	¹³¹ I-PNA Renal Scintigraphy in NZW Rabbits injected with anti-PNA IgG Antibodies.	121
4.4.1.4	¹³¹ I-PNA Renal Scintigraphy in NZW Rabbits injected with Epiglycanin.	122
4.4.2	Studies with asialo-GM ₁ -HSA and PNA in NZW rabbits and TA ₃ -Ha tumour-bearing CBA/CAJ and CAF1/J mice.	126
4.4.2.1	Renal scintigraphy with a-GM ₁ -HSA/ ¹³¹ I-PNA in NZW rabbits. .	127
4.4.2.2	¹³¹ I-PNA and ¹²⁵ I-asialo-GM ₁ -HSA dual isotope biodistribution studies in CAF1/J mice bearing s.c. TA ₃ -Ha tumours.	130
4.4.3	The Effect of Multiple Doses of PNA on the Biodistribution of ¹²⁵ I-PNA in CBA/CAJ mice.	136
4.5	THE EFFECT OF RENAL CELL FUNCTION ON THE RATE OF PNA RENAL BINDING AND EXCRETION.	137
4.5.1	¹³¹ I-PNA Renal Kinetics of Cis-Platinum induced Nephrotoxicity in Dogs. .	137
4.5.2	¹³¹ I-PNA Renal kinetics in Patients undergoing Cis-Platinum chemotherapy.	146
5.	CONCLUSIONS:	152
6.	REFERENCES	155
7.	APPENDICES	185

List of Tables

Table	Page
2.1 ^{99m} Tc-Labelled Renal Agents	5
2.2 Renal Diseases in which Radiofluclide Methods are of diagnostic value.	18
2.3 Common Lectin Carbohydrate-binding Specificities.	39
2.4 Inhibitory effect of Carbohydrates on PNA hemagglutination or glycoprotein precipitation	47
2.5 PNA binding patterns in kidney sections of various animal species	58
4.1 Radioiodination efficiencies and quality control results of ¹²⁵ I and ¹³¹ I-PNA batches.	86
4.2 Dose-response of ¹²⁵ I-PNA in CBA/CAJ mice (Blood and Kidney levels).	91
4.3 Renal uptake of ¹²⁵ I-PNA in AJ, c57b, CBA/CAJ, and CAF1/J strain mice	94
4.4 ¹³¹ I-PNA renal and bladder kinetics in NZW rabbits	96
4.5 Dynamic ¹³¹ I-PNA renal parameters in control and D-galactose infused dogs.	98
4.6 ¹³¹ I-PNA Dynamic Renal Parameters in Humans.	104
4.7 Normalized biexponential curve fitting estimates of ¹³¹ I-PNA plasma radioactivity, in dogs.	108
4.8 Urine analysis following i.v. ¹³¹ I-PNA administration in dogs.	109
4.9 The effect of asialo-GM ₁ -HSA on gamma-camera derived ¹³¹ I-PNA kidney and liver parameters.	128
4.10 ¹³¹ I-PNA biodistribution in CAF1/J mice with s.c. TA ₃ -Ha tumours; effect of a-GM ₁ -HSA on tissue uptake at 30 min P.I.	133
4.11 ¹³¹ I-PNA biodistribution in CAF1/J mice with s.c. TA ₃ -Ha tumours; effect of a-GM ₁ -HSA on tissue uptake at 24 h. P.I.	134
4.12 Effect of Multiple doses of PNA on the biodistribution of ¹²⁵ I-PNA in CBA/CAJ mice.	138
4.13 Serum biochemistry of dogs pre and post cis-platinum chemotherapy.	141
4.14 Renal function estimates in dogs pre and post cis-platinum chemotherapy.	142

Table	Page
4.15 ¹³¹ I-PNA gamma-camera renal dynamic parameters in dogs pre and post cis-platinum chemotherapy.	143
4.16 Serum creatinine, Creatinine clearance, and Specific anti-PNA antibody titres in Patients undergoing Cis-Platinum chemotherapy.	148
4.17 ¹³¹ I-PNA Plasma and Renal Parameters in Patients undergoing Cis-Platinum chemotherapy.	149

List of Figures

Figure	Page
2.1 The chemical structure of the MN, T-F, and Tn antigens.	33
2.2 The chemical structure of the GM, and asialo-GM ₁ antigens.	34
3.1 Protocol of renal investigation for Cis-platinum treated dogs.	79
4.1 Calculated vs. Actual PNA concentration by u.v. spectroscopy at 280 nm.	88
4.2 OD ₂₈₀ vs. concentration of bovine gamma globulin and PNA (20 µg-1.6 mg/mL) with the standard Bio-rad® protein assay.	89
4.3 OD ₂₈₀ vs. concentration of bovine gamma globulin and PNA (1-16 µg/mL) with the Bio-rad® microassay.	89
4.4 Kidney/blood ratio vs. injected dose of ¹²⁵ I-PNA in CBA/CAJ mice.	92
4.5 Static ¹²⁵ I-PNA renal scintigram 60 min P.I. in NZW Rabbit	97
4.6 Dynamic Activity/time curve of ¹²⁵ I-PNA in kidneys of NZW rabbit.	97
4.7 The % injected dose of ¹²⁵ I-PNA remaining in kidney ROIs vs time in dogs.	99
4.8 ¹²⁵ I-PNA renal and bladder Activity/time curves in control dogs and dogs infused with D-galactose.	100
4.9 Typical Static ¹²⁵ I-PNA renal scintigrams 0-60 min P.I. in humans.	105
4.10 Normalized Plasma Activity/time curves of total and protein-bound radioactivity following i.v. administration of ¹²⁵ I-PNA in dogs.	110
4.11 Biogel P100 gel column elution profile of urine contents 1 h following i.v. administration of ¹²⁵ I-PNA in dogs.	111
4.12 Fluorescent microscopical cortical section of CBA/CAJ mouse kidney 3 h following i.v. administered FITC-PNA.	113
4.13 Immunoperoxidase stained section of whole CBA/CAJ mouse kidney (1 h P.I. PNA).	113
4.14 Immunoperoxidase stained cortical kidney section of CBA/CAJ mouse injected with PNA (1 h P.I.).	114
4.15 Immunoperoxidase stained medullary kidney section of CBA/CAJ mouse injected with PNA (1 h P.I.).	114
4.16 Proposed mechanism of PNA transport by proximal tubular cells of mouse, rabbit and dog.	118

Figure	Page
4.17 Static ^{131}I -PNA renal scintigram 60 min P.I. following administration of anti-PNA antibody in a NZW rabbit.	123
4.18 Dynamic liver Activity/time curve of ^{131}I -PNA following administration of anti-PNA antibody in a NZW rabbit.	123
4.19 Static ^{131}I -PNA renal scintigram 60 min P.I. following administration of epiglycanin in a NZW rabbit.	125
4.20 Dynamic liver Activity/time curve of ^{131}I -PNA following administration of epiglycanin in a NZW rabbit.	125
4.21 Static scintigram of ^{131}I -a-GM ₁ -HSA in a NZW rabbit (60 min P.I.).	129
4.22 Dynamic Liver Activity/time curve following the administration of ^{131}I -a-GM ₁ -HSA in a NZW rabbit (0-60 min P.I.).	129
4.23 Static scintigrams of various molar ratios of ^{131}I -PNA:a-GM ₁ -HSA at 1 h post injection.	131
4.24 The blood, renal, liver and tumour % injected dose/g vs. time curves of ^{131}I -PNA, and ^{131}I -PNA:a-GM ₁ -HSA(4:1 and 1:2 molar ratios) in TA ₇ -Ha tumour-bearing CAF1/J mice.	135
4.25 Liver/kidney ratios in CBA/CAJ mice previously exposed to multiple doses of PNA.	139
4.26 Static Renal ^{131}I -PNA scintigrams 1 h P.I. in dogs following cis-platinum chemotherapy.	145
4.27 ^{131}I -PNA Mean Normalized Renal Slope Estimates in Patients before and after Cis-platinum chemotherapy.	150

List of Abbreviations

a-GM ₁	asialo-GM ₁
a-GM ₁ -sorb	asialo-GM ₁ synsorb
a-GM ₁ -HSA	asialo-GM ₁ -HSA
ANOVA	analysis of variance
β_2 -MG	β_2 -microglobulin
BSA	bovine serum albumin
BUN	blood urea nitrogen
cis-pt	cis-platinum
Cl/Tb	clearance (total body)
CNS	central nervous system
CrCl	creatinine clearance
ELISA	enzyme-linked immunosorbant assay
ERPF	effective renal plasma flow
FITC	fluorescein isothiocyanate
GBM	glomerular basement membrane
GIT	gastrointestinal tract
GFR	glomerular filtration rate
HRPO	horseradish peroxidase
HSA	human serum albumin
i.p.	intraperitoneal
i.m.	intramuscular
i.v.	intravenous
LAL	limulus amoebocyte lysate
Mab	monoclonal antibody
MCU	micturating cystourethrogram
OD	optical density
PBS	phosphate buffered saline
P.I.	post injection
PNA	peanut lectin
RES	reticuloendothelial system
Rho	rhodamine
RIA	radioimmunoassay
ROI	region of interest
s.c.	subcutaneous
SMRI	Surgical Medical Research Institute (University of Alberta)
TCA	trichloroacetic acid
T-F antigen	Thomsen Freidenreich antigen
T-H glycoprotein	Tamm Horsfall glycoprotein
T-sorb	T-synsorb
USP	United States Pharmacopeia

1. INTRODUCTION

There exists a need in nuclear medicine for a radiopharmaceutical which would be suitable for the quantification of renal tubular function. Current compounds available often suffer from a lack of tubular specificity, non-specific mechanisms of tubular transport, or the presence of competing elimination pathways.

During the *in vivo* investigation of radioiodinated peanut lectin for the scintigraphic detection of tumours expressing the T-F antigen, both in animals and in humans, the rapid renal uptake and subsequent urinary excretion of this large molecular weight (110,000 dalton) protein was noted. Its excretion could not be explained in terms of known renal elimination mechanisms, such as glomerular filtration, nor did its behaviour correspond to that of free inorganic iodide. Several hypotheses were subsequently considered to explain this interesting phenomenon, one of which postulated that the excretion of PNA was due to a tubular transport mechanism, which appeared related to the specificity PNA exhibits for membrane glycoproteins expressing the T-F antigen.

The experiments presented in this thesis were undertaken, initially to establish a radioiodination procedure, quality control techniques and methods which would allow the safe administration of ^{131}I -PNA to humans. Following the establishment of such methods, experiments were performed to elucidate the mechanism of renal excretion of radioiodinated (both ^{125}I and ^{131}I) PNA in animal models, to investigate the effect of various pharmacological agents on the excretion of PNA, and to establish kinetic models for the quantification of renal excretion rate. Further experiments were performed to assess if the rate of elimination could be related to the functional status of renal tubules, hence allowing quantification of tubular cell function using nuclear medicine dynamic imaging techniques. Thus, the primary aim of this work was ultimately to determine if ^{131}I -PNA renal scintigraphy would be a valuable addition to existing methods of renal function quantification, by comparing the behaviour of ^{131}I -PNA with the more established methods of assessing renal function.

2. SURVEY OF THE LITERATURE

2.1 RENAL FUNCTION TESTS

2.1.1 Radiopharmaceuticals for Renal Evaluation

The development of radionuclide methods for the evaluation of renal function and morphology has been achieved by parallel developments in three main areas i) Radioisotope production ii) Instrumentation for the detection and quantification of *in vivo* distribution, and iii) Design and synthesis of appropriate radiopharmaceuticals which are localized and/or excreted by the kidney. Advances in all three areas have resulted in renal nuclear medicine becoming one of the most useful tools available for the nephrologist in the diagnosis of renal function disorders.

Oeser and Billion¹ were the first to describe the use of an *in vivo* administered radiopharmaceutical for determining renal function. They measured the urinary elimination of ¹³¹I-Uroselectan B and Iopax using scintillation probes, however they failed to recognize the usefulness of monitoring the radioactivity in the region of the kidney. This was attempted initially by Kimbel² who generated an activity/time curve over the kidney regions after the administration of ¹³¹I-Perabrodil and ¹³¹I-Urographin. Taplin *et al.*³ were responsible for the development of renography as we now know it. They obtained activity/time curves over the kidneys following ¹³¹I-Urokon administration using two collimated scintillation detectors and two ratemeters connected to dual chart recorders. Although these initial attempts were unsuccessful, the substitution of ¹³¹I-Diotrast as the radiopharmaceutical resulted in activity/time curves which closely resemble the modern renogram⁴. The above radiopharmaceuticals however, suffered from slow renal accumulation and high extrarenal background. This was overcome by the introduction of ¹³¹I-orthoiodohippurate (¹³¹I-OIH) in 1960⁵. Swick⁶ had previously shown that OIH was rapidly accumulated and excreted by the kidneys and its kinetics were known to be similar to those of para-aminohippuric acid (PAH)⁷.

The development of radiolabelling methods for the incorporation of ^{131}I , ^{125}I , and more recently ^{123}I into OIH has resulted in the widespread use of radioiodinated OIH as the agent of choice for renography¹³⁻¹⁴.

2.1.1.1 Static Renal Imaging Agents

Renal static imaging was first attempted by Winter and Taplin⁴ using ^{131}I -Diodrast, however this was unsuccessful. Haynie *et al.*¹⁵ were able to demonstrate renal infarctions in dogs but the high radiation burden limited clinical application with this radiopharmaceutical. In 1956 chlormerodrin, a mercurial diuretic, was labelled with ^{203}Hg and subsequently was used clinically for renal imaging¹⁶. The long half-life of ^{203}Hg (46.8 d)¹ and high gamma-energy (279 keV) resulted in a high radiation dose. The substitution of ^{197}Hg -Chlormerodrin by Sodee¹⁷ reduced the radiation dose to the patient due to the shorter half-life of ^{197}Hg (65 h), however the lower gamma-energy of this isotope (77 keV, 91% abundance) resulted in poorer spatial resolution due to tissue attenuation.

The mercurial diuretics are highly bound to plasma proteins, mainly albumin, and are unable to be filtered by the glomerulus¹⁸. They are extracted by the renal tubules and are bound to sulphhydryl groups of functioning cortical tubules, directly from renal vascular capillaries¹⁸. Approximately 45% of the radioactivity is localized in the cortical tubules 2 h post injection in patients with normal renal function¹⁹. The biological half-life of the renally trapped activity is prolonged, allowing static imaging several days after administration. The quantification of relative renal accumulation has been reported by Reba *et al.*²⁰ and others²¹⁻²³ as a measure of differential function.

2.1.1.2 $^{99\text{m}}\text{Tc}$ -Labelled Radiopharmaceuticals

Perhaps the greatest advance in the use of radiopharmaceuticals for renal imaging has been made because of the development of techniques for the incorporation of technetium-99m ($^{99\text{m}}\text{Tc}$) into radioligands which are subsequently handled by the kidneys.

.....
¹All radioisotope data extracted from Table of Isotopes, 7th Ed, Lederer, C.M., *et al.* John Wiley & Son Inc., New York, 1977.

This radionuclide possesses almost ideal physical properties for imaging with the Anger camera (gamma-energy 140 keV, abundance 90%) and its short half-life (6 h) allows the administration of relatively large amounts of activity (30-600 MBq) without the burden of high radiation doses to the patient. In its generated form, ^{99m}Tc pertechnetate ($^{99m}\text{TcO}_4^-$) is used extensively for perfusion studies utilizing dynamic first-pass acquisition. The urinary excretion of $^{99m}\text{TcO}_4^-$ is relatively low and although it is freely filtered by the glomerulus, about 85% of the filtered activity is reabsorbed by the renal tubules, precluding its use for renal function studies²⁴. $^{99m}\text{TcO}_4^-$ is routinely used for the detection of vesicoureteric reflux by the isotopic micturating-cystourethrogram (MCU) technique^{25,26}. The radionuclide is instilled directly into the bladder by either bladder puncture or catheterization and evidence of reflux is determined by passage of $^{99m}\text{TcO}_4^-$ up the ureter during micturation.

The reduction of $^{99m}\text{Tc(VII)}$ to the lower valency states by various reducing agents allows the complexation of this more reactive chemical form to a variety of ligands. Many complexes of ^{99m}Tc have been reported and a chronological list is summarized in Table 2.1.

Of the radiopharmaceuticals listed in Table 2.1 the most useful agents for the evaluation of renal morphology appear to be ^{99m}Tc -gluconate^{30,31}, ^{99m}Tc -glucoheptonate (^{99m}Tc -GH)³², ^{99m}Tc -penicillamine^{33,34}, and ^{99m}Tc -DMSA^{35,37}. ^{99m}Tc -GH and ^{99m}Tc -DMSA have been used extensively for the evaluation of renal morphology as well as unilateral renal function estimation.

^{99m}Tc -GH complex is prepared by reacting the acid or Na salt of GH with chemically reduced pertechnetate (Stannous chloride (SnCl_2), or formamidinium sulphonate (FSA)). After administration, ^{99m}Tc -GH is filtered by the glomerulus, however 20-30% of the filtrate is reabsorbed by the tubules (both proximal and distal). The remaining activity is eliminated into the bladder³². Good cortical scintigrams are obtained 2-3 h post-injection (P.I.) after transit of activity from the renal pelvis, in patients with

Table 2.1 ^{99m}Tc -Labelled Renal Agents

Agent	Mechanism of Localization	Author	Year
^{99m}Tc -Fe-Ascorbate	Tubular reabsorption	Harper <i>et al.</i> ²⁷	1966
^{99m}Tc -Citrate	Glomerular filtration	Kountz <i>et al.</i> ²⁸	1967
^{99m}Tc -EDTA	Glomerular filtration	Fleay ²⁹	1968
^{99m}Tc -Sn-Gluconate	Tubular reabsorption	Charamaza <i>et al.</i> ³⁰	1969
^{99m}Tc -Sn-Mannionate	Tubular reabsorption	Charamaza <i>et al.</i> ³⁰	1969
^{99m}Tc -DTPA	Glomerular filtration	Eckelman <i>et al.</i> ³¹	1970
^{99m}Tc -Fe-ascorbate-DTPA	Glomerular filtration	Brookeman <i>et al.</i> ³²	1970
^{99m}Tc -Mannitol	Glomerular filtration	Subramanian <i>et al.</i> ³³	1971
^{99m}Tc -Sn-Inulin	Glomerular filtration	Subramanian <i>et al.</i> ³³	1971
^{99m}Tc -Sn-Meglumine diatrizoate	Glomerular filtration	Subramanian <i>et al.</i> ³³	1971
^{99m}Tc -Sn- β -Glycerol phosphate	Glomerular filtration	Subramanian <i>et al.</i> ³³	1971
^{99m}Tc -Sn-Sorbitol	Glomerular filtration	Subramanian <i>et al.</i> ³³	1971
^{99m}Tc -Sn-n-methyl glucamine	Glomerular filtration	Subramanian <i>et al.</i> ³³	1971
^{99m}Tc -Sn-Gelatin	Tubular fixation	Lebowitz <i>et al.</i> ³⁴	1971
^{99m}Tc -Sn-Caseidin	Tubular fixation	Winchell <i>et al.</i> ³⁵	1971
^{99m}Tc -Penicillamine Acetazolamide	Tubular fixation	Halpern <i>et al.</i> ³⁶	1972
^{99m}Tc -Sn-tetracycline	Tubular fixation	Fliegel <i>et al.</i> ³⁷	1974
^{99m}Tc -Sn-DMSA	Tubular fixation	Lin <i>et al.</i> ³⁸	1974
^{99m}Tc -Sn-Calceidin blue	Tubular fixation	Arnold <i>et al.</i> ³⁹	1975
^{99m}Tc -Sn-Lactobionate	Tubular fixation	Arnold <i>et al.</i> ³⁹	1975
^{99m}Tc -Sn-Glucoheptonate	Tubular reabsorption	Arnold <i>et al.</i> ³⁹	1975
^{99m}Tc -Thiomalic Acid	Tubular fixation	Hagan <i>et al.</i> ⁴⁰	1975
^{99m}Tc -Sn-Acetyl cysteine	Tubular fixation	Subramanian <i>et al.</i> ⁴¹	1976
^{99m}Tc -Sn-Malate	Tubular fixation	Machida <i>et al.</i> ⁴²	1977
^{99m}Tc -Penicillamine	Tubular fixation	Robinson <i>et al.</i> ⁴³	1977
^{99m}Tc -Ethylthiomethyl phosphonate	Tubular fixation	Fritzberg <i>et al.</i> ⁴⁴	1977
^{99m}Tc -Glutathione	Tubular fixation	Fritzberg <i>et al.</i> ⁴⁵	1978
^{99m}Tc -2,3 Dimercapto -propanesulphonate	Tubular fixation	Vanlic-Razumenic <i>et al.</i> ⁴⁶	1979
^{99m}Tc -DADS	Tubular excretion	Fritzberg <i>et al.</i> ⁴⁷	1981
^{99m}Tc -CO ₂ -DADS	Tubular excretion	Fritzberg <i>et al.</i> ⁴⁸	1982
^{99m}Tc -PAHIDA	Tubular excretion	Chervu <i>et al.</i> ⁴⁹	1984

normal renal function". The liver accumulation of ^{99m}Tc -GH is low and about 10% of the administered activity remains in the renal cortex at 24 h". The behaviour of ^{99m}Tc -gluconate⁵¹ and ^{99m}Tc -Fe-Ascorbate⁵² is similar to that of ^{99m}Tc -GH.

^{99m}Tc -DMSA (dimercaptosuccinic acid) is currently the radiopharmaceutical of choice for the study of renal morphology, the estimation of functional cortical mass and differential renal function. This dimercaptodicarboxylic acid was first used in China for the treatment of heavy-metal poisoning⁵³ and later developed as a renal imaging agent by Lin *et al.*⁵⁴ as an alternative to the radiomercurial diuretics. High cortical uptake of ^{99m}Tc -DMSA is demonstrated in both animals⁵⁵ and humans (55% at 1hr. P.I.)⁵⁶. A small fraction (5-7%) is filtered into the urinary bladder and about 5% localizes in the liver and spleen⁵⁷. The mechanism of tubular fixation is thought to be analogous to that of the mercurials⁵⁸. ^{99m}Tc -DMSA is highly bound to plasma proteins after administration (>90%), which precludes its filtration by the glomerulus, and is thought to be absorbed directly from the peritubular capillaries by both proximal and distal tubules^{59,61}. Conflicting data exists for this mechanism, as results generated in patients with tubular disorders suggests that ^{99m}Tc -DMSA may be reabsorbed from the lumen of the nephron after glomerular filtration⁶².

Autoradiographical studies by several investigators have demonstrated the intracellular localization of radioactivity in the proximal and distal tubules of the cortex while activity in the medulla, glomerulus and collecting tubules was virtually absent^{60,61,63}. Hosokawa *et al.*⁶⁰ calculated the cortex/medullary ratio as 22:1 and the tubular/glomerular ratio as 27:1. Subcellular studies have shown that ^{99m}Tc -DMSA is mainly bound to cytosol proteins and to mitochondria, with less binding seen in nuclei and microsomes⁶¹. A hypothesis to explain the tubular accumulation has been proposed which involves ^{99m}Tc -DMSA binding to the metal binding protein metallothionein (MW 10,000 daltons)⁶⁴.

Several research groups have investigated the chemical composition of the ^{99m}Tc -DMSA complex, and alluded to variability in biodistribution resulting from

formulation conditions and stability⁶⁵⁻⁶⁸. Ikeda *et al.*^{65,68} have shown that four different ^{99m}Tc-DMSA complexes may be produced by using different reaction conditions. They also demonstrated that each complex had a unique biodistribution pattern⁶⁸. The complex most suitable for cortical imaging is formed at pH 2.5 via a short-lived intermediate, and must be left for 10 min after reconstitution prior to injection⁶⁸. Care must also be taken to exclude oxygen from the reaction vial due to the possible oxidation and degradation of this complex which may result in increased liver accumulation⁶⁹.

2.1.1.3 Radiopharmaceuticals for Glomerular Filtration Rate (GFR) estimation.

For the proper interpretation and evaluation of renal function studies it is important to understand the concepts of renal clearance. The function of the kidney and its physiological unit, the nephron, can be divided into two main processes i) Glomerular filtration, and ii) Tubular transport. The rate of nephron filtration is dependent on i) rate of nephron plasma flow ii) systemic oncotic pressure iii) the gradient of hydrostatic pressure between the glomerular capillary and Bowman's capsule, and iv) the glomerular hydraulic permeability coefficient⁷⁰⁻⁷². GFR can be quantified with a variety of chemical and radionuclide methods providing the radiopharmaceutical fits the criteria originally proposed by Smith⁷³, i.e. i) it must be metabolically inert and non toxic, ii) must have no intrinsic effect on renal function, iii) must be freely filtered by the glomerulus, iv) must neither be reabsorbed nor secreted by renal tubules, v) its clearance rate must not be affected by other substances, vi) its clearance rate must not be affected by changes in plasma concentration or urine flow, and vii) it must be able to be accurately measured in plasma and urine.

The "gold standard" method for the measurement of GFR has been that of inulin clearance^{74,75}. Inulin is a polysaccharide of molecular weight 5000 daltons which is freely filtered by the glomerulus. Both "cold" inulin and radioactive derivatives have been reported for the estimation of GFR, using the standard constant infusion technique⁷⁶.

¹⁴C-carboxyl-inulin⁷⁷, ¹⁴C-methoxy-inulin⁷⁸ and ³H-methoxy-inulin⁷⁶ have all been

reported for the measurement of GFR. ^{14}C -carboxyl-inulin has been shown to have a significantly different rate of clearance than inulin, whereas the two methoxy derivatives correlate well with "cold" inulin clearance values⁷⁴. Their widespread clinical utilization has been limited due to the necessity of using liquid scintillation counting techniques, however for animal and laboratory use, these agents are extremely useful.

Radioiodinated (^{131}I and ^{125}I) inulin has been reported via the incorporation of an allyl ether group into the molecule⁷⁹. A good correlation was observed with the clearance rate of these derivatives when compared to that of native inulin⁸⁰. Other iodinated derivatives (Chloro-iodo-propyl and propargyl inulin) have also been reported but their clearance is slightly lower than that of "cold" inulin^{81,82}. They, however, show poor *in vitro* and *in vivo* stability with the liberation of free iodide with time⁸³ and may result in underestimation of GFR due to the longer biological half-life of inorganic iodide. ^{51}Cr -inulin has been reported as a more stable compound than the iodinated derivatives, however it is less suitable for imaging purposes because of low density photon flux⁸⁴.

The radioactive cobalt (^{57}Co , ^{60}Co) derivatives of Vitamin B₁₂ (cyanocobalamin and hydroxocobalamin) are worth historical mention for the estimation of GFR due to their similarities in clearance rate to native Vitamin B₁₂⁸⁵. The clearance rates are lower than that of inulin because of variabilities in plasma protein binding and radiolabel exchange with inactivated vitamin⁸⁶. Expense, and the non ideal characteristics of the cobalt radionuclides have, however, limited their clinical application.

2.1.1.4 Radioiodinated Urological Contrast Agents.

The radiological contrast agents diatrizoate (Na salt: Hypaque, Methyl glucamine salt: Renografin) and iothalamate (Conray, Glofil) have been reported as agents for the estimation of GFR when substituted with radioiodide (^{131}I and ^{125}I)⁸⁷⁻⁹¹. ^{131}I -diatrizoate was first introduced in 1956 by Kimbel and Borner⁹² and used for the study of renal function by Winter and Taplin⁹³. Several investigators⁹⁰⁻⁹³ reported on the biological distribution of this agent and compared its clearance rate to that of inulin. Plasma binding

was reported low, and tubular reabsorption or secretion negligible^{93,94}. Autoradiolysis has been demonstrated on storage but is dependent on the specific activity of the preparation⁹⁵. With adequate quality control ¹³¹I-diatrizoate is accurate for the measurement of GFR.

Iothalamate has very similar chemical structure and renal clearance to that of Diatrizoate. Radioiodinated iothalamate (¹³¹I and ¹²⁵I) has been used as a radiopharmaceutical for accurately measuring GFR in both animals and humans, showing low plasma protein binding and negligible tubular reabsorption and secretion^{91,96}. ¹²⁵I-iothalamate is available commercially as a highly pure agent and with acceptable levels of free iodide even after storage up to 2 months.

2.1.1.5 Radiometal Chelates.

The chelates ethylene diaminetetraacetic acid (EDTA) and diethylene triamine pentaacetic acid (DTPA) form highly stable complexes with a variety of metal ions. They have also been shown to be cleared from the plasma via glomerular filtration, making them ideal agents for quantifying GFR, and are now routinely used for clinical studies.

Foreman *et al.*^{97,98} studied the metabolism of ¹⁴C-EDTA in rats and man and showed renal elimination of unchanged compound. Tubular excretion was negligible and 96-98% of the injected dose was recovered in urine within 6 h. Heller and Vostal⁹⁹ found the clearance to be slightly higher than inulin. The metabolism of ¹⁴C-DTPA was reported to be similar to that of EDTA¹⁰⁰ and a large number of stable radiometal chelates have been reported. These include ⁵¹Cr, ⁵⁹Co, ⁶⁷Ga, ^{99m}Tc, ¹¹¹In, ^{113m}In, ¹⁴⁰La, ¹⁶⁹Yb and ¹⁹⁷Hg although the physical properties of many of these radionuclides are far from ideal for patient studies¹⁰¹⁻¹⁰⁶. All these complexes have been shown to be cleared by glomerular filtration and exhibit low plasma protein binding, with an absence of tubular excretion. ¹⁶⁹Yb-DTPA, ^{113m}In and ¹⁴⁰La-DTPA have been studied in some detail and the effect of increased plasma concentration and varied urine flows has been reported to have no effect on renal clearance^{103,106}. Sziklas *et al.*¹⁰³ compared clearance rates of

^{169}Yb -DTPA,¹¹³ In and ^{14}C -inulin in patients, demonstrating good correlation with each radiopharmaceutical.

Two chelates which have been extensively studied for the determination of GFR are ^{51}Cr -EDTA and $^{99\text{m}}\text{Tc}$ -DTPA. Stacy and Thorburn¹⁰⁷, and Winter and Meyers¹⁰⁸ first reported the use of ^{51}Cr -EDTA for renal studies. It exhibits a high degree of radiochemical stability, which is not always the case with radioiodinated agents, and is available outside North America in a highly purified form for GFR measurement. Plasma protein binding is reported to be less than 2%, tubular clearance insignificant, and extrarenal clearance is negligible¹⁰⁹. Several studies have been reported comparing ^{51}Cr -EDTA clearance, both by single injection and constant infusion, with that of inulin¹¹⁰⁻¹¹². Lower clearance values of between 5 and 20% were noted for ^{51}Cr -EDTA in comparison to inulin in animals and man, although this did not preclude the accurate estimation of GFR in clinical testing. It is particularly useful in dual isotope studies of GFR and effective renal plasma flow (ERPF) with ^{125}I -OIH using the plasma sampling protocol to be discussed later. The high gamma-energy of ^{51}Cr (320keV) allows good separation of the isotope peak from that of ^{125}I using gamma-spectrometry. The low photon abundance (9%), however, limits its usefulness for gamma-camera imaging studies.

$^{99\text{m}}\text{Tc}$ -DTPA

The ideal radioisotopic properties of $^{99\text{m}}\text{Tc}$ for *in vivo* imaging and the ability of this radionuclide to form a stable complex with DTPA have resulted in this agent's wide use for renographic studies of the kidney and for the determination of GFR¹¹³⁻¹²². $^{99\text{m}}\text{Tc}$ -DTPA exhibits a small degree of plasma protein binding (2-5%) and this is dependent on the salt used in formulation¹²⁰⁻¹²². Extrarenal excretion is insignificant and only 4-5% of the radioactivity remains in the body 24 h post injection (P.I.) in patients with normal renal function¹²¹. A slightly lower clearance than that for iothalamate has been reported in patients and this may introduce a significant error in the calculation of GFR below $20 \text{ mL} \cdot \text{min}^{-1}$ ¹²¹. Although the use of

^{99m}Tc -DTPA may result in the underestimation of GFR by single injection or by constant infusion techniques, it still comes closest to the ideal clinical radiopharmaceutical for routine application.

2.1.1.6 Radiopharmaceuticals for Effective Renal Plasma Flow (ERPF) estimation.

The clearance of a compound which is totally extracted by the kidney on first pass allows the calculation of renal plasma flow. For all practical purposes this is an idealized parameter unobtainable with current radiopharmaceuticals, however the term 'effective' is introduced into the term (ERPF) which allows the quantification of renal blood flow with agents that have a high but non unit extraction ratio. Iodo-pyrocet (Diodrast) was the first agent to be used for the measurement of ERPF, however its significant extrarenal clearance introduced errors in the calculation. Para-aminohippuric acid (PAH) is currently the agent of choice for the chemical estimation of ERPF and is the standard procedure for quantifying ERPF⁷. Its extraction ratio is close to 0.90 on first-pass, 20% being eliminated by glomerular filtration and 80% by tubular excretion. Orthoiodohippuric acid (OIH) has been reported as a substitute for PAH in determining ERPF⁷³. The ability to iodinate OIH with ^{131}I resulted in this radiopharmaceutical being used extensively for ERPF and renographic assessment of kidney function⁷⁴.

2.1.1.7 Orthoiodohippurate (OIH).

Tubis *et al.*⁵ first reported the exchange labelling of ^{131}I with OIH and this simple method has been modified by several investigators for labelling with other iodide (^{125}I , ^{123}I) radionuclides⁸⁻¹². Radiochemical stability of OIH has been the subject of many studies and is reported to be adversely affected by temperature, light and the specific-activity of the radioiodinated product^{123,124}. Inorganic iodide is the main radiocontaminant and the levels of free radioiodide increase on storage. In order to maintain accurate ERPF estimates, free radioiodide levels should remain below 2% and consequently quality control of this radiopharmaceutical is crucial.

Renal clearance of ^{131}I -OIH has been compared to PAH clearance in man by both Burbank *et al.*¹²⁵ and Schwartz and Madeloff¹²⁶. They found that ^{131}I -OIH clearance was 10-15% lower than PAH. This has been further verified by Mailloux *et al.*¹²⁷ who studied in detail the clearance mechanism in animals and man. The lower clearance values for OIH have been explained by differences in protein-binding, tubular transport and in free iodide contamination. It has been shown that 70% of OIH, at the normal administered doses, is weakly bound to plasma protein, whereas PAH binds to a lesser degree. OIH, being a slightly weaker acid also tends to be in a non-ionized form in the distal tubular lumen, resulting in a small amount of back diffusion. Detailed studies by Blaufox *et al.*¹²⁸⁻¹³⁰ have elucidated the mechanism of excretion and the pharmacokinetic models for clearance estimation. The injected material is almost completely excreted by the kidney, 15-20% by glomerular filtration and 80-85% by tubular secretion, with minimal hepatic clearance. The mixed mode of excretion does not allow ^{131}I -OIH clearance to be an indicator of any particular cellular process within the kidney, and is perhaps the major limitation of its use.

Because of the less than ideal radionuclidic properties of ^{131}I , scintigrams of ^{131}I -OIH are of low quality and the radiation dose to the kidneys is higher than with $^{99\text{m}}\text{Tc}$ -DTPA renography. The introduction of ^{123}I for labelling to OIH has major advantages for patient studies and several recent reports have noted the suitability of ^{123}I -OIH for renal perfusion, clearance and imaging studies¹³¹⁻¹³³. ^{123}I -OIH renal extraction and clearance has been demonstrated to be similar to ^{131}I -OIH and PAH¹³³ and is currently available commercially in North America, although it is considerably more expensive than ^{131}I -OIH¹³⁴.

Recently, there has been an effort to develop $^{99\text{m}}\text{Tc}$ labelled radiopharmaceuticals which are handled by the kidney in a similar manner to OIH. The advantage of these compounds would be higher photon flux and lower patient radiation dose, resulting in better quality scintigrams. Fritzberg *et al.*⁴⁷ have reported the synthesis and early biological data on $^{99\text{m}}\text{Tc}$ -N,N'-bis (mercaptoacetamido) ethylenediamine ($^{99\text{m}}\text{Tc}$ -DADS) as a

potential replacement for ^{131}I -OIH. Clearance of this compound is significantly greater than $^{99\text{m}}\text{Tc}$ -DTPA, but lower than ^{131}I -OIH in rats. Significant biliary excretion of this compound in rats and humans represents a major limitation to its use for measuring ERPF and for renography¹³⁵. A further analogue of this compound $^{99\text{m}}\text{Tc}$ -N,N'-bis (mercaptoacetyl)-2,3-diamino propanoate ($^{99\text{m}}\text{Tc}$ -CO₂-DADS) has been synthesized by the same workers and been shown to undergo less biliary excretion than $^{99\text{m}}\text{Tc}$ -DADS¹³⁶. Complicated purification using HPLC is necessary for separation of the most appropriate component of the reaction and this may preclude its universal acceptance as a substitute for ^{131}I -OIH. Schneider *et al.*^{136,137} have synthesized over 20 analogues of $^{99\text{m}}\text{Tc}$ -DADS, however none of the complexes studied have approached the clearance rate of OIH in animals or in human studies.

Chervu *et al.*⁴⁹ have recently reported the synthesis and animal biodistribution of a $^{99\text{m}}\text{Tc}$ labelled PAH analogue ($^{99\text{m}}\text{Tc}$ -PAHIDA) as a potential replacement for ^{131}I -OIH. The derivative contains an imido diacetic acid group (IDA), which is capable of chelating the technetium, and the R-CO-NH-CH₂-COOH group, which is analogous to hippurate. In animals, the clearance rate has been shown to be lower than ^{131}I -OIH, with no extrarenal excretion pathway. The reduced clearance is thought to be due to high plasma protein binding *in vivo*. This class of compounds may be a useful alternative to ^{131}I -OIH providing that derivatives are found which elicit lower protein binding.

2.1.1.8 Ruthenium-Labelled Renal Radiopharmaceuticals

Ruthenium isotopes have recently been suggested for use in nuclear medicine imaging. In particular ^{97}Ru has the physical properties suitable for imaging purposes with a half-life of 2.9 d, no β emission and a gamma energy of 215 keV (85% abundance) which is suitable for gamma-camera detection. The patient radiation dose is higher than that of $^{99\text{m}}\text{Tc}$ but comparable to ^{123}I and lower than ^{131}I ¹³⁸. Several radiopharmaceuticals have been produced with ^{97}Ru which may be suitable for evaluation of the kidney. ^{97}Ru forms a stable complex with DMSA in the presence of Stannous (Sn II) ions, and has been

reported as a useful static imaging agent, particularly when prolonged follow-up imaging is required¹³⁸. ⁹⁷Ru-2,3 dimercaptpropansulphonic acid complex has also been synthesized for static renal imaging¹³⁹.

Wenzel *et al.*¹⁴⁰ have very recently reported the synthesis and biodistribution of two ruthenium labelled glycine derivatives (Ruthenocenoyl-glycine (ruppuran) and Ruthenocenoyl-1,1'-diglycine) which appear very promising for renography and ERPF estimation. In rabbits, both ruppuran and the diglycine derivative showed higher clearance rates than ¹²⁵I-OIH. Both were totally excreted within 48 h P.I. via the kidney, with no extrarenal pathway discernible. When translated into human terms the clearance rate was in the order of 500-600 mL.min⁻¹, although human studies have not yet been presented with these compounds.

2.1.1.9 Radiopharmaceuticals for the Assessment of Renal Perfusion.

Renal perfusion can be studied with a variety of compounds. The main criteria for their use are high photon flux and low radiation dose to the patient, allowing high doses to be administered to provide good counting statistics with short dynamic framing rates.

Dynamic data during the first few seconds of renal transit is normally acquired and can indicate the patency of the renal artery and kidney vasculature as well as quantitative data useful for follow-up. The agents of choice are ^{99m}TcO₄ and ^{99m}Tc-DTPA although several other compounds have also been reported including ^{113m}In-DTPA, ¹⁶⁹Yb-DTPA and ¹²⁵I-OIH.

2.1.1.10 Quantitative Considerations in Radionuclide Renal Function Studies

As previously mentioned, there are a number of radiopharmaceuticals available for the determination of renal function, both ERPF and GFR, using nuclear medicine techniques. The accurate determination of these parameters is dependent on the application of appropriate pharmacokinetic models and plasma sampling or dynamic data manipulation. A review by Dubrovsky and Russel¹⁴¹ has summarized many of the

techniques currently available for the determination of both global (both kidneys) and individual kidney (differential) ERPF and GFR. In the same volume Taylor¹⁴² has reviewed the quantification of differential renal function by the use of static renal imaging agents including ^{99m}Tc-DMSA. The validity of some of these techniques is still open to some debate, but clinical utilization has aided in the diagnosis of a variety of renal function disorders.

2.1.1.11 Determination of Global and Differential ERPF.

The plasma disappearance of intravenously (i.v.) administered OIH follows a two compartment exponential model as originally described by Blaurox *et al.*^{128,143} and can be analysed by the methods suggested by Sapirstein *et al.*¹⁴⁴. The ERPF can be calculated directly from this curve by area under-the-curve and volume of distribution (Vd) measurements or other standard pharmacokinetic calculations. For an accurate measure of the plasma curves, numerous plasma samples are required, which is impractical for clinical utility. Blaurox¹²⁹ simplified the method to include only two blood samples between 15 and 30 min P.I. The clearance is calculated using the slope of the line between these two points and the Vd determined by dividing the injected dose by the counts in plasma at $t=0$ from the extrapolated line between these points. Tauxe *et al.*^{145,146} further simplified the technique by studying in detail the correlation of the concentration reciprocal at various times with the clearance determined from the total curve. They demonstrated that there was good correlation between the ERPF and the plasma concentration at 45 min P.I. and advocated that ERPF could be calculated within $\pm 30 \text{ mL} \cdot \text{min}^{-1}$ using only one plasma sample. This method has been verified by other investigators^{147,148} and is sufficiently accurate over a wide range of values to be useful clinically. Care, however, must be taken to obtain reproducible results. Using Mathews compartmental algorithm¹⁴⁹, it is also possible to predict the % of injected dose in any compartment at a given time.

Good correlation was shown by Tauxe *et al.*¹⁵⁰ with predicted versus actual urinary excretion and a regression expression derived for comparing predicted and observed data.

Further work has been described to eliminate the necessity of multiple blood sampling to obtain the activity/time curve, by using external counting probes or the gamma-camera activity/time curves over the head or precordium as a measure of the plasma disappearance rate^{131,132}. These curves have been shown to be an accurate indicator of the plasma clearance curve. Further accuracy can be obtained by correcting the curves to collected blood samples (one at 3-5 min, and another at 60 min P.I.).

In patients who have a renal transplant or only one kidney, global ERPF is a measure of the single kidney function, however for the majority of patients further division of the total function is required for differential kidney estimation. Taplin¹³³ first introduced a method for determining individual function using ¹³¹I-OIH and probe renography. He concluded that the ratio of the slope of the second segment of the renogram for each kidney (that corresponding to renal parenchymal uptake) was an estimation of split renal function. This technique, however, required background correction using ¹³¹I-HSA, due to the considerable extrarenal accumulation of OIH¹³⁴. With the introduction of gamma-cameras, and more recently the on-line computers, background correction can now be made using appropriate regions-of-interest (ROIs). The normal intrarenal transit time of OIH, as determined by deconvolution analysis, is between 2.2-2.3 min in well hydrated patients¹³⁵, making it wise to select points within this time for comparison. The most widely used technique for calculating relative renal function with ¹³¹I-OIH, is to compare the summed counts in each kidney between 1 and 2 min P.I.^{136,137}.

A more simple approach to determine relative renal ERPF relies on the comparison of individual renal uptake of ^{99m}Tc-DMSA at 2-6 h P.I. Numerous investigators have shown good correlation between this technique and that determined by ureteric catheterization and other scintigraphic techniques¹³⁸⁻¹⁶¹. Patient positioning, variability in renal size and depth, as well as the selection of ROIs will affect the computation and must be adequately corrected for, to obtain accurate determinations of split renal function.

2.1.1.12 Quantification of Global and Differential GFR

Global GFR can be calculated from the plasma disappearance curve and/or urine samples of any of the previously mentioned radiopharmaceuticals that undergo glomerular filtration. A bi-exponential curve or a single exponential fitted to the slow component of the plasma curve may be used for accurate determination of GFR analogous to that of the ERPF calculation previously described. Again single blood sample, whole body clearance and gamma-camera techniques using precordial ROIs have all been used yielding reliable and reproducible results¹⁴¹.

Differential GFR can be calculated from the ^{99m}Tc -DTPA renogram in a manner analogous to that described for ^{131}I -OIH. Numerous reports have confirmed the validity of this technique in comparison to ureteric catheterization and split creatinine clearance measurements^{142,143}.

2.1.2 Clinical Indications for Radionuclide Renal Investigation

Nuclear medicine imaging and quantitative renal determinations are useful in a variety of clinical conditions which are summarized in Table 2.2. Further specific discussion of these clinical indications follows.

2.1.2.1 Space-Occupying Lesions of the Kidney

Renal scintigraphy using static imaging radiopharmaceuticals such as ^{99m}Tc -DMSA and ^{99m}Tc -GH will often demonstrate "cold" parenchymal areas in the renal cortex consistent with a space-occupying lesion (SOL)¹⁴⁴. This type of scintigraphic pattern is non-specific, and may be due to the presence of renal tumours (renal cell carcinomas, transitional cell tumours, squamous cell carcinomas, Wilm's tumour, diffuse tubular cell tumour), renal cysts, renal pseudotumours, renal abscesses, A-V malformations, trauma, or cortical scarring¹⁴⁵. The diagnosis or exclusion of renal malignancy by scintigraphy alone is not possible, although the scintigraphic pattern may reveal the nature of the SOL in some cases. The initial detection of SOLs is usually made by

Table 2.2 Renal Diseases in which Radionuclide Methods are of diagnostic value.

Condition	Radionuclide Study	Typical Observations
Space Occupying Lesion	Static Imaging: ^{99m}Tc -DMSA, ^{99m}Tc -GH	Cortical "cold spot".
Renovascular hypertension	Perfusion: $^{99m}\text{TcO}_4$, DTPA, and Renography: OIH	Reduced perfusion, cortical/medullary ERPF.
Cortical necrosis	$^{99m}\text{TcO}_4$, DTPA, DMSA, OIH	Reduced RBF & cortical visualization.
Renal artery stenosis	$^{99m}\text{TcO}_4$, DTPA, OIH, DMSA, GH	Reduced RBF, often ⁶ asymmetrical. Asymmetrical size.
Renal artery embolism	$^{99m}\text{TcO}_4$, DTPA, OIH, DMSA, GH	Absence of uptake, segmental, unilateral or bilateral.
Acute tubular necrosis (ATN)	^{131}I -OIH	Normal uptake, delayed excretion.
Acute pyelonephritis	^{67}Ga -citrate, ^{111}In -WBC ^{99m}Tc -DMSA, GH	Renal uptake; Cortical defects.
Acute interstitial nephritis	^{67}Ga -citrate	Renal uptake.
Obstructive nephropathy	^{99m}Tc -DTPA, ^{131}I -OIH	delayed uptake, prolonged excretion, pelvic retention.
Chronic pyelonephritis	^{99m}Tc -DMSA, GH	Cortical defects.
Reflux nephropathy	^{99m}Tc -DMSA, GH MCU: $^{99m}\text{TcO}_4$, DTPA	Cortical defects. • Ureteropelvic reflux.
<u>Renal Transplantation</u>		
Acute tubular necrosis	OIH, ^{99m}Tc -DTPA	Good perfusion, impaired or absent renal transit.
Graft rejection	OIH, ^{99m}Tc -DTPA ^{111}In -platelets ^{99m}Tc -Sulphur colloid	Reduced perfusion and renal transit. Graft deposition. Graft deposition.

RBF = Renal blood flow

 ^{111}In -WBC = Indium 111 labelled white blood cells

MCU = Micturating Cystoureterogram.

Table derived from references 141, 142, 154, 164, 165, 171, 172, 174 and 175.

excretion urography, and the introduction of CT scanning and renal ultrasonography have generally replaced the renal scintiscan as more sensitive techniques for the differentiation of benign vs malignant SOLs. Renal scintigraphy may be of value in distinguishing renal from non-renal SOLs such as from tumours of the adrenal gland, although it remains a confirmatory procedure in the majority of situations. The scintigraphic patterns observed in renal SOLs have been well reviewed¹⁴⁵ and will not be discussed further.

2.1.2.2 Renovascular Hypertension

In patients with hypertension, the kidneys may be damaged as a result of the elevated blood pressure, or may contribute to the hypertension directly. Renovascular hypertension is a specific entity produced by obstruction of the main renal artery or of any of its branches¹⁴⁶. This condition can often be corrected by surgical intervention, balloon angioplasty or nephrectomy, and as such, the diagnosis of renovascular hypertension is important for the appropriate treatment of patients presenting with elevated blood pressure. Arteromatous changes and fibromuscular hyperplasia account for about 78% of all cases of renal hypertension although trauma, tumours, compression by external bands, aneurysms, chronic pyelonephritis, radiation nephritis, hypoplasia, pelviureteric junction (PUJ) obstruction, A-V malformations, and renin-secreting tumours may be underlying causes¹⁴⁷.

Renal perfusion studies using $^{99m}\text{TcO}_4$ and $^{99m}\text{Tc-DTPA}$ may be of value in determining reduced renal blood flow, although the demonstration of diminished RBF is non-specific. It is also of value in the follow-up of patients who have undergone intervention, and can aid in the confirmation of restored blood flow. ^{131}I and $^{123}\text{I-OIH}$ renography have been reported of value in the study of renal hypertension¹⁴⁸.

Britton¹⁴⁸ has recently postulated that essential hypertension may be a consequence of altered cortical nephron flow. Using $^{123}\text{I-OIH}$ and quantitative techniques which can independently determine cortical vs medullary delivery of radionuclide, a difference in cortical blood flow was demonstrated in patients with essential hypertension. This elegant

technique has been used to demonstrate the changes in intrarenal blood flow with captopril treatment in animals and patients with renal hypertension and may be of considerable value in the sequential study of patients during pharmacological treatment.

Clorius *et al.*¹⁶⁹ have reported the usefulness of renography for the identification of bilateral orthostatic renal dysfunction (BORD) as a cause of hypertension. Exercise renography has also been reported by the same author¹⁷⁰ as a sensitive procedure to identify renal involvement in hypertension. These methods may provide an accurate means of quantifying the transient posture and exercise mediated changes in cortical blood flow in hypertensive patients, aid in determining the aetiology of such conditions *in vivo*, and allow a means of quantitatively monitoring the effect of treatment.

2.1.2.3 Acute and Chronic Renal Failure

Acute renal failure occurs when there is a significant and sudden decrease in GFR and may result from a variety of causes further subclassified as i) pre-renal, ii) renal, and iii) post-renal failure¹⁶⁹. A variety of radionuclide procedures exist which can aid in the diagnosis of renal failure, the most useful being the ^{99m}Tc-DTPA or ¹³¹I-OIH renogram. Abnormalities in the normal transit of these radiopharmaceuticals through the kidney can distinguish between blood flow, glomerular or tubular transit and ureteric passage. These three entities are distinguishable and quantifiable from the renogram. Although the renogram findings may be non specific, they often complement other diagnostic modalities and clinical findings to increase the accuracy of diagnosis. Of particular usefulness is the ability to use renography to quantitate progression or recovery of a disease by sequential studies.

Chronic renal failure can also be studied in a similar manner using renography. Again the results may be non-specific but are of value in following the disease process.

2.1.2.4 Renal Allograft Studies.

Renal transplant recipients can undergo a multitude of complications post-transplantation. These include i) parenchymal graft failure due to acute tubular necrosis, cell mediated or humoral rejection, tubular acidosis or glomerular nephritis, and ii) surgical complications such as incomplete anastomosis in blood vessels and ureter, tears in the kidney, and lymphocoeles¹⁷¹⁻¹⁷². Radionuclide investigations are invaluable in the non-invasive investigation of graft blood flow and parenchymal function in allograft recipients. Perfusion imaging with $^{99m}\text{TcO}_4$ or $^{99m}\text{Tc-DTPA}$ is a reliable and safe method to determine the patency of blood supply to the graft while renographic studies using $^{99m}\text{Tc-DTPA}$ or $^{131}\text{I-OIH}$ can give valuable information on glomerular and tubular function as well as ureteric patency¹⁷¹⁻¹⁷².

Methods of quantifying graft blood flow usually employ a relationship of graft to iliac blood flow such as that described by Hilson *et al.*¹⁷³. $^{99m}\text{Tc-DTPA}$ bolus injection and subsequent renography is the procedure of choice as it also provides information on glomerular function and urine flow. Serial studies allow the monitoring of patients over both the short and long term, and permits the diagnosis of both acute and chronic rejection. $^{131}\text{I-OIH}$ renography is reported as being more sensitive for distinguishing ATN from acute rejection in the early post-transplant period¹⁷¹. ATN is generally characterized by poor tubular function in spite of good graft perfusion, where rejection is generally associated with diminished blood flow and cellular function. The use of $^{99m}\text{Tc-Sulphur colloid}$ ¹⁷⁴ and radiolabelled blood components such as $^{111}\text{In-platelets}$ ¹⁷⁵ and leukocytes¹⁷⁶ can demonstrate the increased sequestration of blood cells in the rejecting allograft. Diagnostic difficulties remain in distinguishing immunological rejection from drug toxicity, as elicited by cyclosporin therapy using current radiopharmaceutical methods.

2.1.3 Biochemical Methods of Renal Function Estimation

2.1.3.1 Serum Creatinine and Creatinine Clearance

Creatinine is an amino-acid by-product of protein metabolism, derived from creatine. Creatine synthesis occurs in the liver, pancreas and kidney but the main concentration of creatine is the striated muscle where it is stored unchanged or as phosphocreatine. It is metabolized in muscle fibres and released into the circulation as creatinine. Creatinine has been shown to be excreted by the kidney and its serum concentration and clearance advocated as an endogenous measure of renal function¹⁷⁷⁻¹⁷⁹. Several methods are available for the measurement of creatinine in plasma, serum, and urine¹⁷⁷. The modified Jaffe reaction measures not only creatinine but other chromogens such as acetone, pyruvate, ascorbate, proteins, barbiturates and other unknown substances¹⁷⁸. This method tends to overestimate creatinine concentrations in serum (up to 20%) and to a lesser extent in the urine, due to the non filtration of many of the chromogens. Another assay based on the Folin-Wu reaction measures only true creatinine chromogens¹⁷⁹. A significant improvement in the assay of creatinine has been achieved by the use of autoanalyser methods based on the Jaffe reaction¹⁸⁰. Measurements of creatinine and creatinine clearance (CrCl) by the autoanalyzer have been compared to inulin clearance and show acceptable correlation ($\pm 8\%$) with normal renal function¹⁸¹. As renal function diminishes however, there is an increased discrepancy between CrCl and inulin clearance. Below a GFR of $20 \text{ mL} \cdot \text{min}^{-1}$ it is generally recognized as being inaccurate for the measurement of GFR¹⁸².

The reason for the increased discrepancy found with GFR measurement by CrCl is due to significant tubular secretion of creatinine by renal tubules, a process which is known to increase with increasing serum concentration¹⁸³. In the patient with normal or only minor renal dysfunction CrCl is sufficiently accurate for routine GFR estimation. The protocol requires both a blood sample and urine collection (usually 24 h) and is generally considered as the first investigation choice to exclude renal dysfunction. Because of the

many variables in both serum creatinine and CrCl (including sex, age, muscle bulk, stress, and exercise) further investigation using radioisotope methods is advocated in cases where CrCl is diminished¹⁷⁷.

2.1.3.2 β_2 -Microglobulin.

β_2 -Microglobulin (β_2 -MG) is a low molecular weight protein (11,800 daltons) first isolated from urine in 1964 and characterized in 1968¹⁷⁴. It is completely filtered by the glomerulus, but unlike creatinine is reabsorbed and catabolized by the proximal tubules¹⁷⁵. The reabsorption is via a process of endocytosis and the endocytotic vesicles fuse with the lysosomes, where the protein is enzymatically cleaved to its amino acid constituents. The normal kidney is able to reabsorb about 99.9% of the filtered β_2 -MG, resulting in minimal amounts in the urine. In animals and patients with impaired tubular function, β_2 -MG tubular reabsorption is incomplete and increased levels are detected in urine¹⁷⁵.

β_2 -MG is produced by all nucleated cells and located on the cell surface¹⁷⁵. Cunningham *et al.*¹⁷⁶ resolved the amino acid sequence of β_2 -MG and further work has shown relationship between the C₁ heavy chain of IgG₁ and β_2 -MG¹⁷⁷. It appears that β_2 -MG is related to the glycoproteins of the major histocompatibility complex in man, genetically located in the HLA region of the sixth chromosome. The HLA molecule is composed of a β light chain, which is β_2 -MG and an α heavy chain giving the HLA complex its specificity¹⁷⁷. Serological specificity is lost when not attached to β_2 -MG. Tumour antigens have many similarities with HLA antigens and have been shown to bind to β_2 -MG¹⁷⁸. Lymphocytes are able to produce relatively large quantities of β_2 -MG and 'shedding' occurs due to *in vivo* metabolism and degradation, resulting in serum concentrations of 1.0-2.7 mg.L⁻¹ in normal patients¹⁷⁹. Serum concentration varies with age and with renal dysfunction¹⁷⁵.

Serum β_2 -MG and β_2 -MG clearance are useful techniques for the clinical determination of renal function. Serum levels are indicative of glomerular function and

correlate to those of inulin clearance, whilst those of clearance (using the pharmacokinetic relationship between serum and urine concentrations to determine clearance rate) can be related to proximal tubular function^{188,190}. A commercial radioimmunoassay (RIA)² is available for the determination of human β_2 -MG in serum and urine, however there are several technical difficulties with the estimations. β_2 -MG degrades rapidly and irreversibly in urine at a pH lower than 6.0. Because urine remains in the bladder beyond that which ensures stability, patients must receive alkaline agents such as Na bicarbonate to diminish the pH degradation. Patients with malignancies (leukemias, lymphomas, multiple myeloma, and Hodgkin's disease) may show elevated serum concentrations, and non malignant conditions (rheumatoid arthritis, SLE, sarcoidosis, Sjögrens disease, Crohn's disease, and angioimmunoblastic lymphadenopathy) or liver dysfunction (hepatitis, cirrhosis) may negate the diagnostic usefulness of serum values. Clearance appears a more suitable technique to increase the specificity in patients with underlying disease other than that of renal origin¹⁸⁵.

The renal clearance of β_2 -MG is reported as between 50-200 $\mu\text{g}/24\text{ h}$ and tends to increase with age in normal patients¹⁹⁰. Clearance is elevated in a variety of renal tubular disorders including aminoglycoside, heavy metal, and cis-platinum nephrotoxicity, Balkan nephropathy, Fanconi's syndrome, and in non-parenchymal renal diseases such as obstructive nephropathies or upper urinary tract infections¹⁸⁵. β_2 -MG has also been reported in the monitoring of renal transplant recipients¹⁹¹. Elevated serum levels are suggestive of acute rejection although definitive diagnosis cannot be made using β_2 -MG clearance alone.

2.1.3.3 Blood Urea Nitrogen (BUN).

The concentration of urea in blood to that in the urine can be related in a similar way to creatinine, providing an index of renal function¹⁹². Although urea is filtered by the glomerulus it is highly diffusible and may passively pass from the lumen to the tubular

²Phadebase, Pharmacia.

interstitium. Consequently, its clearance is always lower than creatinine. Furthermore, the clearance is dependent on urine flow and thus less than ideal as a measure of glomerular filtration¹⁹³. Other factors which influence BUN and urea clearance include hepatic function and the patients metabolic state, however the ratio of BUN to serum creatinine or urea clearance to creatinine clearance has been shown to correlate more closely to inulin clearance than either measurement independently¹⁷⁷.

2.1.3.4 γ -Glutamyltransferase (γ -GT).

γ -Glutamyltransferase (γ -GT) is a ubiquitous enzyme which is monitored in serum as an indicator of hepatocellular function¹⁹⁴. The highest concentration of γ -GT however, is in the proximal tubular epithelium of the kidney. It is localized predominantly in the brush border membrane, whose integrity is directly related to tubular function¹⁹⁵. Although its exact physiological function is unknown, it is thought to play an important role in the reabsorption of amino acids and peptides from the luminal filtrate by the tubule. γ -GT is able to be detected in the urine of normal patients, however elevated levels have been reported in a variety of renal diseases including glomerular nephritis, SLE, and mercury, cadmium and drug (aminoglycoside) nephrotoxicity¹⁹⁶. In general, it appears that when active inflammatory changes occur, particularly those of an immunological nature, urinary γ -GT concentration may rise. It is therefore a useful parameter in suspected tubular dysfunction, although non-specific as to the cause of inflammation.

2.1.3.5 Miscellaneous Biochemical Markers of Renal Function.

A multitude of biochemical and immunological markers have been shown to be present in the urine at elevated concentrations in a variety of kidney diseases. Although urine analysis is extremely valuable in many disorders, there is no universal marker present which would eliminate the necessity for the quantitative renal function estimations previously described.

Urinary protein analysis can be achieved by a variety of techniques including electrophoretic separation (SDS-Page, isoelectric focusing, cellulose acetate, isotachopheresis, and Iso Dalt 2-dimensional electrophoresis), molecular weight determinations (gel column chromatography, HPLC, GLC), and specific functional markers (immunoassays, immunodiffusion). The origin of proteins in urine is complex, however they can be categorized as i) Normal plasma proteins or fragments of them, ii) Proteins released into urine by various kidney cells, iii) Proteins arising from the urogenital tract, iv) Proteins from other tissues (either normally or as a result of disease), v) Hormones, vi) Pregnancy associated proteins, vii) Tumour associated proteins or antigens, and viii) Products of viral or bacterial infection. The measurement of these proteins is useful in the diagnosis of both renal and systemic diseases and has been the subject of various reviews¹⁹⁶⁻¹⁹⁸.

There are several other enzymes which are associated with normal kidney cells, which can be detected in the urine as a consequence of drug-induced changes in renal function, renal toxins, ischemia, renal diseases, hypertension, and surgery¹⁹⁹. Elevated enzymuria has been noted after high dose salicylates, aminoglycoside, and cytotoxic drug therapy although its sensitivity for demonstrating nephrotoxicity has not been shown superior to other indices¹⁹⁹⁻²⁰⁰. N-acetyl β -glucosaminidase (NAG) and leucine aminopeptidase (LAP) are two enzymes which originate from renal tubules and have been used to monitor renal tubular function²⁰⁰⁻²⁰¹. NAG is present in the basal cytoplasm of animal and human proximal tubules, while LAP is found in the straight portion of the proximal tubule, associated with the brush border microvilli. Elevated urine levels of NAG and LAP have been reported in cis-platinum induced nephrotoxicity in humans²⁰¹.

Lysosyme (muraminidase) is a basic protein enzyme of 14,000-15,000 daltons which originates from the lysosomes of phagocytic cells. Its presence in urine has been shown to correlate with the extent of tubular damage determined by kidney histology, as well as to the presence of urinary tract infections in animals, although not to date in

humans²⁰². The mechanism of elevated lysosyme levels in urine appears synonymous with that of β_2 -MG due to the incomplete reabsorption with proximal tubular damage.

Alkaline phosphatase and its isoenzymes have been studied in a variety of disease conditions and their presence in urine appears to parallel renal injury, particularly with tubular toxicity¹⁹⁹.

Immunological techniques have been reported for the determination of immune complexes, serum complement, tumour associated antigens (CEA, galactosyl transferase (GT)), and glomerular basement membrane (GBM) fragments in urine. These estimations rely on polyclonal or monoclonal antibody assays, such as RIA and ELISA, for determining the presence of the specific entities and their presence may indicate underlying disease conditions, including renal pathology¹⁹⁹.

2.1.3.6 Tamm-Horsfall Glycoprotein

Tamm and Horsfall^{203,204} first isolated the high molecular weight ($> 7.0 \times 10^6$ daltons) glycoprotein which now bears their collective names (T-H glycoprotein). The amino acid and carbohydrate constituents have been determined and show that about 25% of the T-H glycoprotein consists of carbohydrate structures²⁰⁵. Although individual sugar constituents vary, the main saccharides are hexose, fucose, N-Acetylhexosamine and Sialic (N-acetylneuraminic) acid. Glycolipid is present in low concentration²⁰⁵.

T-H glycoprotein is associated with epithelial cells of the kidney tubule²⁰⁶, limited to the ascending limb of the Loop of Henle and to a segment of the distal convoluted tubule below the macula densa²⁰⁷. It is the primary constituent of hyaline casts^{208,209} and is excreted into the urine of normal humans. It is excreted in excess quantities in patients with nephrotic syndrome and proteinuria, however its excretion is markedly reduced in patients with chronic renal failure²¹⁰. A significant correlation has been shown between T-H glycoprotein excretion/24 h and creatinine clearance, in patient studies and has been advocated as a measure of renal function estimation²¹⁰. It is able to bind to mercuric acid and ethacrynic acid and may play a role in active sodium and chloride transport by the

tubular cells²¹¹. A recent study by Ollier-Hartmann *et al.*²¹² has shown that T-H glycoprotein clearance increases from infancy to adulthood when related to body surface area. They conclude its usefulness as a measure of tubular mass and of distal tubular function in particular.

2.2 CIS-PLATINUM NEPHROTOXICITY

The antineoplastic agent cis-dichlorodiamine platinum (II) (cis-platinum) has been reported to be useful in the chemotherapy of numerous malignant conditions, both as a single agent and in combination with other cytotoxic agents. It is currently included in almost all treatment regimens for ovarian cancer, squamous cell carcinoma of the head and neck, seminomatous and non-seminomatous testicular cancer, bladder carcinoma and is often helpful in carcinoma of the lung and cervix. The clinical use of cis-platinum has been the subject of many reviews²¹³⁻²¹⁶ and will not be discussed in further detail. Nephrotoxicity remains one of the major limitations of its therapeutic use and has been reported as a dose-dependent phenomenon²¹⁷⁻²¹⁹.

2.2.0.1 Pathology

Renal alterations have been noted in mice and rats after the administration of single intraperitoneal doses of cis-platinum²²⁰. Early changes in the mitochondria and brush border membrane of proximal tubules have been shown to reflect the advanced complications of toxicity²²¹. Two weeks post-injection, the majority of tubules are dilated, have thickened basal lamella, and are devoid of microvilli. These lesions become more advanced at four weeks, involving the S₁ and S₂ segments of the proximal convoluted tubule, while at 6 months atrophy of the tubules and cysts is often noted²²²⁻²²⁴. The chronic toxicity can lead to permanent damage, resulting from lymphocyte infiltration and interstitial fibrosis²²².

Although the exact mechanism of tubular toxicity is unclear, it appears to be due to the metal ion of cis-platinum, and is analogous to the toxicity seen with other heavy

metals (Hg, Cd)^{223,225}. *In vitro* studies with isolated tubular cells have revealed generalized reduction of tubular metabolic function (ATPase) and diminished transport (PAH) after high dose cis-platinum treatment²²⁶. The glomerulus does not appear to be affected directly, although diminished hemodynamics may occur as a consequence of toxicity due to the activation of the renin/angiotensin II system, causing constriction of glomerular arterioles²¹⁷.

The nephrotoxic effects of cis-platinum is reported to be similar in dogs²²⁷, however in man, alterations in the distal convoluted tubule and the collecting duct are often noted to be the most affected regions of the nephron²²⁸. A reduction in the degree of nephrotoxicity can be achieved by induction of diuresis (mannitol or furosemide) and/or hydration^{229,230}.

2.2.0.2 Diagnosis of Cis-Platinum Nephrotoxicity.

Cis-platinum nephrotoxicity is generally investigated by standard methods including serum creatinine, creatinine clearance (CrCl), blood urea nitrogen (BUN)²³⁰, and urinary markers such as enzymes or proteins²⁰¹. Because cis-platinum renal toxicity may not necessarily result in changes of glomerular function, the measurement of GFR may not be appropriate as a measure of nephrotoxicity²⁰⁰. β_2 -MG clearance, and tubular enzymes NAG and LAP have been reported as more sensitive techniques for monitoring tubular function in cis-platinum therapy^{200,201}. Changes in the urinary parameters are observed earlier than subsequent changes in renal hemodynamics, resulting in increased sensitivity of these techniques. Radionuclide methods using ^{99m}Tc-DTPA or ¹²⁵I-OIH have been reported for the investigation of cis-platinum nephrotoxicity²³¹, but because of the limitations previously discussed, they may be insensitive for the early detection of changes in tubular function.

2.3 THE THOMSEN-FRIEDENREICH ANTIGEN.

There has been a resurgence of interest in the Thomsen-Friedenreich (T-F) recently, 50 years after its first discovery²³²⁻²³⁷. The history of this now important "marker" has been well reviewed recently²³⁴⁻²³⁷ and will not be the topic of further discussion here, although explanation of its current significance in modern immunology and histochemistry will.

The T-F antigen is a disaccharide entity consisting of β -D-Gal-(1 \rightarrow 3)- α -GalNAc which is glycosically linked to O serine or threonine of blood group protein, as well as some glycolipids²³⁹. Unlike the ABO antigens, the T-F antigen is not normally expressed on most normal tissues, although there are a few exceptions. In the vast majority of cases, including erythrocytes, it is in a cryptic or masked form with N-acetylneuraminic (sialic) acid linked to the terminal galactose or N-acetyl galactosamine residues²³⁷. Unmasked or free T-F antigen has been reported in a variety of animal and human carcinomas, and is thought to arise from malignant transformations occurring during differentiation, resulting in the synthesis of incomplete glycoprotein/glycolipid structures²³⁹. T-F antigen expression has been reported in most adenocarcinomas (tumours arising from epithelial cells) including breast, lung, gastrointestinal tract, bladder as well as melanoma²³⁹⁻²⁴². Many animal tumours including TA₁-Ha and RI in mice^{235,243-245}, ASPG-1 rat mammary carcinoma^{244,247} and a guinea pig hepatocarcinoma²⁴⁸ are reported to express free T-F antigen.

2.3.1 Anti T-F antibodies.

Anti T-F antibodies (mainly IgM class) are known to be present in the sera of all human adults as well as in animals²⁴⁹⁻²⁵¹ due to stimulation of the immune system by intestinal microflora²⁵²⁻²⁵⁴. These antibodies normally interact with tissue bound and circulating glycoproteins with exposed T-F antigen²⁴⁵, and it has been reported that patients with carcinomas of the breast²⁵⁰, G.I.T.²⁵⁶, and melanoma (including metastases)²⁵⁷ have reduced serum anti-T titres in comparison to controls. Decreased circulating levels are presumably due to adsorption to tumour-bound antigen or to circulating cells or fragments thereof.

(glycoproteins)²⁵⁰. Cell-mediated immunity is known to be induced in patients with adenocarcinomas expressing free T-F antigen structures, while normals only possess humoral immunity against T-F antigen^{240,250,258-259}.

The recent advances in hybridoma technology have been used to produce monoclonal anti-T antibodies against the T-F antigenic structures^{260,261}. Immunological and immunohistological characterization and distribution studies of T-F antigen structures is now possible using these specific antibodies²⁶¹.

2.3.2 M-, N-, T-F- and Tn- Glycoproteins.

The T-F antigen is the immediate precursor of the major antigens of the second human blood group system, MN^{262,263}. The immunodeterminant group of the T-F antigen has been shown to be the disaccharide β -D-galactosido(1 \rightarrow 3)-N-acetyl- α -D-galactosamine (β -D-Gal-(1 \rightarrow 3)- α -GalNAc)²³⁷.

T-F antigens prepared from N, M, or NM antigens have the same composition and react equally in hemagglutination inhibition assays with anti-T from animals or humans²⁶² or with peanut lectin (PNA)²⁶⁴. Enzymatic degradation of the disaccharide by α -D-galactosidase reveals the precursor antigen, Tn, which has the sugar N-acetyl-D-galactosamine (GalNAc) as its immunodeterminant structure²³⁶. As with T-F antigen, this is α -glycosidically linked to serine or threonine residues of the glycoprotein or glycolipid.

2.3.3 Composition and structure of the T-F and related antigens.

Klenk and Uhlenbruck²⁶⁶ first isolated the membrane glycoproteins from bovine erythrocytes in 1958, and Springer *et al.*²⁶⁷ subsequently isolated the T-F antigen from human red blood cell O and NN antigens. They reported the T-F antigen to be an aggregate of repeating, identical subunits of molecular weight 550,000 daltons. 40% of the structure was composed of carbohydrate, in which Gal and GalNAc were predominant. The protein portion was rich in threonine, serine and glutamic acid, while few aromatic or S-containing amino acids

were present²⁶⁷.

The T-F antigen has several closely related chemical entities including the desialated ganglioside asialo GM₁, a tetrasaccharide containing the terminal disaccharide structure β -D-Gal-(1 \rightarrow 3)- β -GalNAc glycosically linked β - rather than α ^{268,269}, and the Tn antigen, which lacks the terminal galactose residue²⁷⁰. The chemical structures of these are depicted in Figure 2.1 and 2.2.

Gangliosides, including GM₁, are the principal glycolipids of the CNS, are present in extraneural sites, and are thought to be the cholera toxin receptor of adipose and epithelial cells of the intestine²⁶⁹. GM₁ has been reported as a tumour-associated antigen in many animal and human tumours²⁶⁹⁻²⁷², while the asialo form (a-GM₁) has been demonstrated as a marker of mouse natural killer cells²⁷³ and murine fetal thymocytes²⁷⁴. Asialo-GM₁ has also been found as a tumour-associated marker of mouse lymphoma²⁷⁴ and human leukemic cells²⁷⁵.

The immunodeterminant structure of the Tn antigen is the monosaccharide N-acetyl galactosamine (GalNAc) and its expression is thought to be caused by a somatic mutation in adulthood at the pluripotent stem-cell level^{236,275}. It was originally discovered in a patient with haemolytic anaemia and polyagglutinability due to anti-Tn²⁷⁶. The Tn antigen on erythrocytes is caused by a genetic block of the enzymatic (β -galactosyltransferase) addition of D-galactose to GalNAc linked α to the hydroxyl group of serine or threonine in the amino-terminal region of the glycoprotein²⁷⁷. Humans are known to possess anti-Tn antibodies, analogous to those of anti T-F^{236,278}.

The T-F and Tn antigens have been shown to be present in large quantities on the membranes of many carcinomatous tissues by absorption assays with anti-T and anti-Tn^{239,279}, or by direct histological staining^{280,281}. Normal cell glycoproteins, in contrast, are usually covered by covalently linked carbohydrates, tertiary structures, or by high negative charge due to N-acetyl neuraminic (sialic) acid residues, but may be found in free form in "immunologically privileged" sites separated from the immune system²⁸². The structures of the T-F and Tn antigens have been verified by a variety of methods including lectin-binding studies

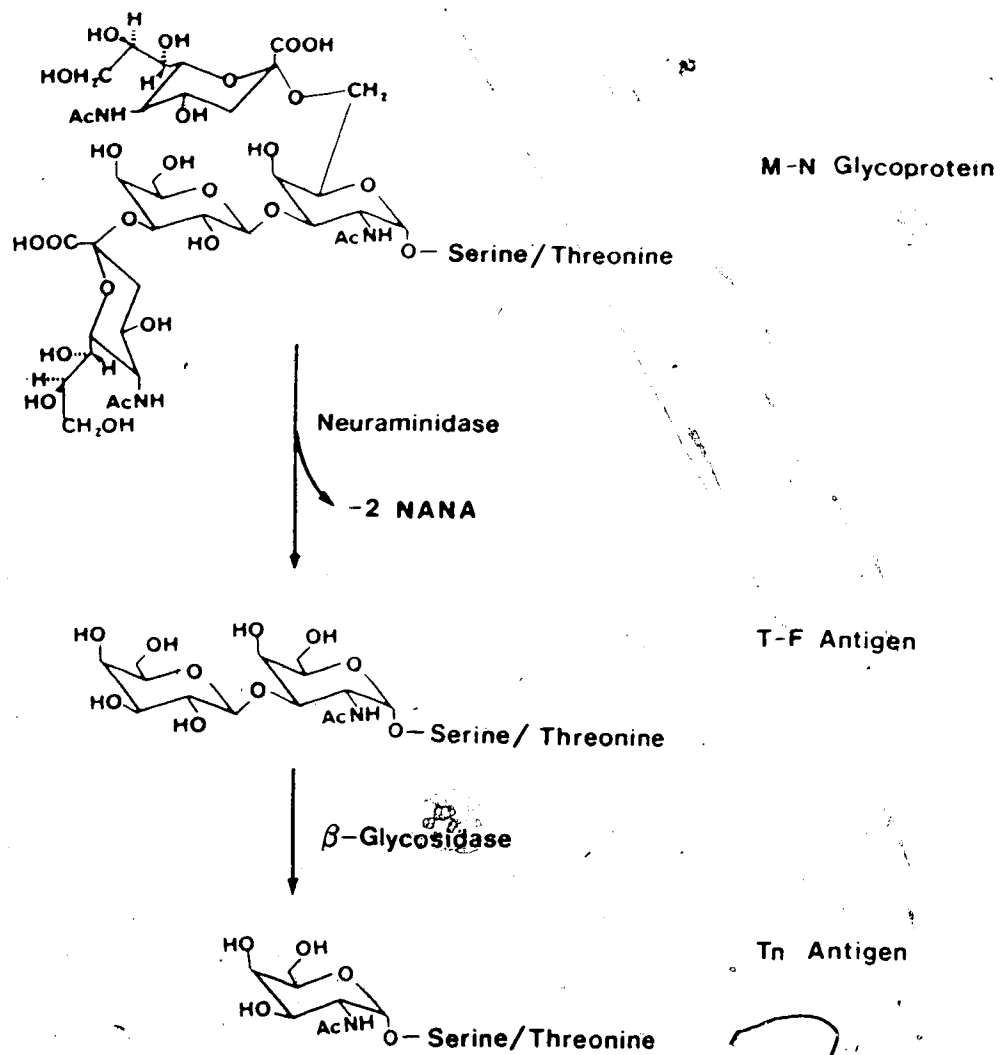


Figure 2.1 The chemical structure of the MN, T-F, and Tn antigens.

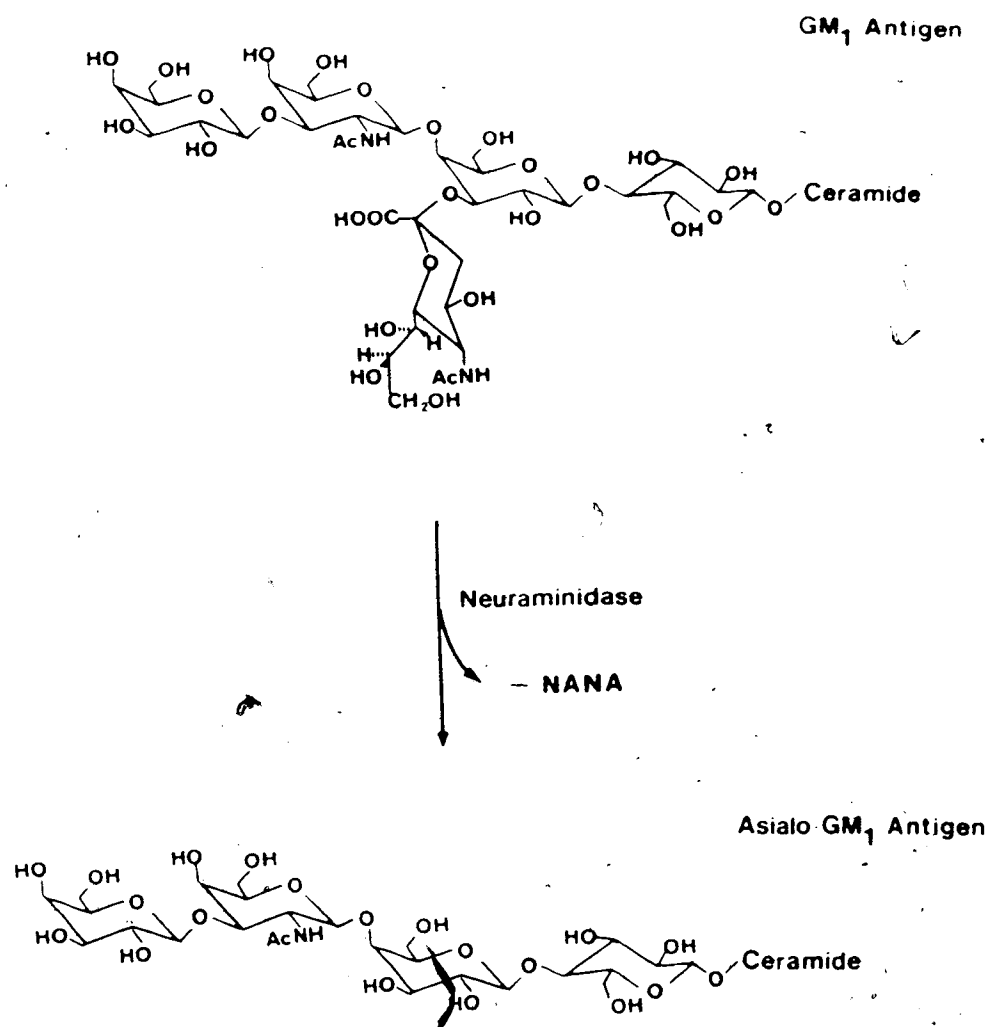


Figure 2.2 The chemical structure of the GM₁ and asialo-GM₁ antigens.

(the topic of later discussion), antibody-hapten inhibition studies²⁷⁹ and solid phase immunoassay²³⁶.

Synthesis of the antigen determinants in a form useful for monoclonal antibody production, binding studies and lectin purification has confirmed the chemical elucidation of these carbohydrate structures²⁸²⁻²⁸³.

Although both anti-T and peanut lectin are capable of binding to the T-F antigen, care must be taken in interpreting histochemical or serological results. Distinctions are made within the classification of T-F antigen receptors these being i) "True" T-F antigen which will bind both anti-T and PNA. Such receptors are found on the glycoprotein of desialated erythrocytes. ii) "Pseudo" T-F or "T-F like" receptors, which will bind only PNA due to reactivity of similar disaccharides such as that found on α -GM₁. iii) Cross-reacting receptors which will bind PNA, but are not due to β DGal(1 \rightarrow 3)GalNAc structures²³⁸.

2.3.4 T-F and Tn antigens in Tumour Aggressiveness and Adhesion.

Recent reports²⁶⁶⁻²⁷⁸ have indicated a correlation between the relative proportions of T-F and Tn and the aggressiveness of some tumours. The expression of T-F and Tn in large quantities appears to indicate a poorer prognosis, and higher metastatic potential in carcinomas (particularly, but not exclusively adenocarcinomas) of the lung, pancreas, breast, urinary bladder, G.I.T., and prostate²³⁶⁻²⁷⁸⁻²⁸⁴⁻²⁸⁶.

Adhesion of tumour cells expressing T-F or Tn antigens has been demonstrated to liver hepatocytes in animal cell inhibition studies²⁸⁷. Presumably this mechanism is analogous to the binding of circulating asialo-glycoproteins to the hepatic protein-binding (HBP) receptor originally described by Ashwell²⁸⁸, and may in part explain the organ-specific metastatic potential of some aggressive tumour lines. Further discussion of this important concept is beyond the scope of this survey but has been recently reviewed by Kieran and Longenecker²⁸⁹.

2.4 LECTINS.

2.4.1 Definition and Classification.

Considerable debate has arisen in the literature regarding the most appropriate definition for a class of proteins or glycoproteins which are collectively known as lectins. "Lectin" is derived from the latin *legere* 'to choose or to select', and was originally coined by Boyd and Shapleigh²⁹⁰ in 1954 to classify many carbohydrate-binding plant seed proteins/glycoproteins which were able to agglutinate human red blood cells according to their blood group. Expansion of this nomenclature was found necessary to include an ever increasing number of lectin-like substances isolated from a wide diversity of sources such as bacteria, fungi, fish, sera, snails and mammals²⁹¹. The nomenclature committee of the International Union of Biochemists (IUB) and the Joint Commission on Biochemical Nomenclature (JCBN) have adopted the definition proposed by Goldstein *et al.*²⁹² ie; that lectins are "sugar binding proteins or glycoproteins of non-immune origin which agglutinate cells and/or precipitate glycoconjugates". This definition also states that "lectins bear at least two sugar-binding sites, agglutinate animal and plant cells (most commonly erythrocytes, unmodified or enzyme treated) and/or precipitate polysaccharides, glycoproteins and glycolipids".

Although first discovered in plants, lectins have also been found in many other organisms, including mammals²⁹¹. A lectin may be soluble in biological fluids or membrane bound. Other types of sugar-binding proteins exist including enzymes (glycosidase, glycosyltransferases etc.), transport proteins, hormones (TSH, FSH etc.) and toxins (ricin, abrin, modeccin etc.) however they may or may not be included with this definition²⁹³. Under some circumstances enzymes with multiple binding sites may agglutinate cells, and hence be classified as lectins. Distinction is made with toxins in that they bear only one sugar-binding site and hence do not fit these criteria. Definitions such as "Antibody-like substances"²⁹⁴, "receptor-specific proteins"²⁹⁵, "sugar-specific"²⁹⁶ and "affinitin"²⁹⁷ have all been advocated for classification purposes, none of them being adequately definitive. Others feel that the

current definition does not encompass enough of the physiological or biochemical information known about proteins of this kind, and excludes compounds such as the toxins whose interactions are with single binding sites but are similar to "true" lectins in all other respects²⁹¹. No classification system has yet been described which unifies them in terms of their biological role.

2.4.1.1 Macromolecular Properties.

Affinity purification techniques utilizing solid supports of specific lectin binding carbohydrates is the procedure of choice for production of high purity lectins, and is the subject of past review²⁹². Each lectin purified has shown its individual chemical uniqueness although some common amino acid sequences in related lectins have been demonstrated^{300,301}. Most are composed of subunits of identical molecular weight, and although the number of subunits may vary, most have a common tetrameric structure²⁹³. Molecular weights are reported between 36,000-335,000 daltons³⁰⁰. The quaternary structure often requires the presence of metal ions (eg Mn^{2+} and Ca^{2+}) to maintain functional integrity²⁹¹. Most lectins are glycoproteins, although there are some notable exceptions such as peanut lectin (PNA), concanavalin A (Con A), and wheat germ lectin (WGA) which do not contain covalently bound carbohydrates as part of their structure³⁰⁰.

2.4.1.2 Functional Roles of Lectins

The diversity of functional roles suggested for lectins do not allow a unifying system for their classification based on biological function. Seed lectins have been implied as important for germination, cell differentiation, and defense against pathogens^{293,301}. Plant lectins may play roles in longitudinal cell growth, nitrogen fixation in legumes, transport, immobilization and storage of sugars, defence against plant pathogens or as enzymes for specific substrates^{293,301}. Animal lectins have been implicated in the removal of foreign or unmasked glycoproteins from circulation; in organization of cells during embryogenesis, and in cellular communication and/or adhesion³⁰².

2.4.2 Lectin Carbohydrate Specificity

The most logical approach in classifying lectins is via their specificity for carbohydrate moieties. Lectins are characteristically inhibited in their agglutination or precipitation reactions by competing sugars³⁰³. The sugars which are the "best", or rather, exhibit the strongest inhibition on the reactions have been reported for a number of lectins and are summarized in Table 2.3.

Stringent structural requirements exist for the interaction of lectins with their inhibitory carbohydrate. The C₁ and C₂ hydroxy groups of the sugars have been implicated as particularly important in lectin-sugar interaction²⁹¹. This is demonstrated with the monosaccharide binding lectins, an example being that the D-Galactose (D-Gal) binding lectins will not interact with D-Glucose or D-mannose or vice-versa²⁹¹. Not all lectins bind as strongly to monosaccharide as they do to disaccharide or even trisaccharide carbohydrates and hence the binding sites are obviously extended beyond the terminal sugar residue³⁰⁴. PNA and Con A both have extended binding sites demonstrable by their enhanced inhibition with di- and/or trisaccharides³⁰⁴.

The chemistry of lectin binding to complex oligosaccharides, glycoproteins and cell receptors is generally much more complex than that demonstrated with simple sugars²⁹¹. Non-specific and multivalent interactions result in higher association constants between lectins and these complexes and non carbohydrate related bonding such as hydrophobic interaction has also been reported³⁰⁰. Thus many lectins which possess similar binding affinity to monosaccharides may show large differences in affinity towards more complex heterosaccharides³⁰⁵. These differences make lectins powerful tools in differentiating fine structural variations in glycoconjugates and cell membrane glycoproteins or glycolipids³⁰⁵.

Because of the specific and reversible interactions that lectins and carbohydrates exhibit, they have been compared with the antibody-antigen reaction and lectins have been reported as "antibody-like substances"²⁹⁴. Like antibodies, lectins possess a definite combining site and binding can be inhibited by low molecular weight sugar "haptens", however they do not possess most of the other characteristics of antibodies (ie. those responsible for immunological

Table 2.3 Common Lectin Carbohydrate-binding Specificities.

Genus and Species	Common Name	Origin	Binding Specificity
<u>D-Mannose binding lectins</u>			
<i>Canavalia ensiformis</i> (Con A)	Jack-bean	plant	D-Man α 1
<i>Lens culinaris</i>	lentil	plant	D-Man α 1
<i>Pisum sativum</i>	pea	plant	D-Man α 1
<i>Vicia faba</i>		plant	D-Man α 1
<i>E. coli</i> , <i>Ps. aeruginosa</i>		bacteria	D-Man1
<u>N-Acetyl-D-Glucosamine binding lectins</u>			
	Livers	vertebrates	D-GlcNAc β 1
<i>Bandeiraea simplicifolia</i>	BS-II	plant	D-GlcNAc α 1
<i>Triticum vulgare</i> (WGA)	wheat germ	plant	(D-GlcNAc β 1 \rightarrow 4),
<i>Solanum tuberosum</i>	potato	plant	(D-GlcNAc β 1 \rightarrow 4),
<i>Datura stramonium</i>	jimson weed	plant	(D-GlcNAc β 1 \rightarrow 4),
<i>Phytolacca americana</i> (PHA)	pokeweed	plant	(D-GlcNAc β 1 \rightarrow 4),
<u>L-Fucose binding lectins</u>			
<i>Anguilla anguilla</i>	eel	vertebrate	L-Fuc α 1
<i>Ulex europaeus</i> I	gorse seed	plant	L-Fuc α 1 \rightarrow 2DGal β 1 \rightarrow 4GlcNAc β 1
<i>Lotus tetragonolobus</i>	asparagus pea	plant	L-Fuc α 1 \rightarrow 2DGal β 1 \rightarrow 4 -[L-Fuc α 1 \rightarrow 3]-DGlcNAc β
<u>Sialic acid</u>			
<i>Limulus polyphemus</i>	horseshoe crab	invertebrate	sialic acid
<u>N-Acetyl-D-Galactosamine binding lectins</u>			
	lobster lectin II	invertebrate	D-GalNAc1
<i>Helix pomatia</i>	snail	invertebrate	D-GalNAc α 1
<i>Phaseolus lunatus</i>	lima bean	plant	D-GalNAc α 1
	rabbit liver	vertebrate	D-GalNAc α 1
<i>Sophora japonica</i>	poganda tree	plant	D-GalNAc β 1
<i>Glycine max</i> (SBA)	soybean	plant	D-GalNAc α 1 \rightarrow 3-DGal β 1 \rightarrow 3GlcNAc
<i>Dolichos biflorus</i> (DBA)	horse gram	plant	D-GalNAc α 1 \rightarrow 3 -[L-Fuc α 1 \rightarrow 2]-DGal β 1
<u>D-Galactose binding lectins</u>			
<i>Dictyostelium discoideum</i>	slime mould	fungi	D-Gal β 1
<i>Ricinus communis</i> (RCA)	castor bean	plant	D-Gal β 1
<i>Cerianthus membranaceus</i>	sea anemone	invertebrate	D-Gal β 1
	liver, muscle, milk, lung, heart	vertebrate	D-Gal β 1
<i>Electrophorus electricus</i>	electric eel	vertebrate	D-Gal β 1
<i>Ps. aeruginosa</i>		bacteria	D-Gal β 1
	chick embryo	plant	D-Gal β 1 \rightarrow 3 (complex)
<i>Agaricus bisporus</i>	mushroom	fungi	D-Gal β 1 \rightarrow 3 (complex)
<i>Bauhinia purpurea</i>		plant	D-Gal β 1 \rightarrow 3
<i>Geodia cydonium</i>	sponge	sponge	D-Gal β 1 \rightarrow 4
	chick embryos	vertebrate	D-Gal β 1
<i>Axinella</i>	sponge	sponge	D-Gal β 1 \rightarrow 6
<i>Tridacna maxima</i>	clams	invertebrate	D-Gal β 1 \rightarrow 6
<i>Arachis hypogaea</i> (PNA)	peanut	plant	D-Gal β 1 \rightarrow 3DGalNAc

KEY: Fuc=fucose, Gal=galactose, GalNAc=N-Acetyl-D-galactosamine, GlcNAc=N-Acetyl-D-glucosamine, Man=mannose

responses, complement fixation or antigen memory)²⁹⁹. Lectins are present as cellular constituents and are not elicited by an immune response. Lectins possess a wide variety of structural diversity while antibodies have similarities in structure, dependent on their class and subclass. Lectin interaction is confined towards simple or complex carbohydrate residues whereas antibodies may be produced against a wide variety of haptens including amino acids, proteins, and nucleic acids^{299,300}. Despite the obvious differences, lectins can be used in place of antibodies for blood group typing and in the mitogenic stimulation of lymphocyte transformation³⁰⁰.

2.4.3 Uses of Lectins.

The high affinity that lectins possess for carbohydrate residues and the ability to label lectins with a variety of markers (fluorescein (FITC), Rhodamine, ferritin, peroxidase (HRPO), biotin, gold colloid or radionuclides [¹²⁵I, ¹³¹I]) has resulted in their use in many disciplines³⁰⁶. A major contribution has been made in determining the distribution and chemical heterogeneity of cellular glycoproteins and glycolipids by histochemical studies at both the light and electron microscopic level. This has been the subject of recent reviews^{306,307}. Modifications in glycosylated membrane constituents with many diseases (ie malignant vs normal), or at different stages of embryogenesis have also been reported using lectins³⁰⁸.

The specificity of most blood groups is dependent on cell-surface carbohydrate residues and lectins are valuable in clinical typing and study of blood group determinants^{299,309-310}.

Lectins often interact with cells causing agglutination or precipitation. This is a result of complex interactions between the cell membrane and the lectin, resulting in cross-linking and clumping³⁰⁹. Lectin receptor sites have been shown to aggregate into clusters facilitating the agglutination³⁰⁹. Significant differences in cell agglutinability has been shown between malignant and normal cells, embryonal and mature cells, mitotic and quiescent cells and between normal and enzymatically transformed cells³¹¹⁻³¹³. Although the number of binding sites of normal and transformed cells is similar, the differences in agglutination appear to be

the result of rearrangement of these sites, or increased mobility of receptors³⁰⁹. When the receptors are randomly dispersed or fixed by glutaraldehyde treatment, the transformed cells fail to be preferentially agglutinated^{309-311,312}.

Con A and PHA are mitogenic inducers of the growth and division of T-lymphocytes regardless of their antigenic specificity^{314,315} and this phenomenon is useful in immunological studies of lymphocyte function. The use of Con A in renal allograft perfusion has been reported to increase the survival of grafts in dogs³¹⁶. The mechanism is thought to be due to the masking of donor cellular antigens by Con A, resulting in diminished host humoral response^{316,317}.

The demonstration of selective *in vitro* binding to malignant and not to corresponding normal cells has led to the use of several lectins as *in vivo* carriers for both diagnostic and therapeutic purposes³¹⁸. Con A binds to certain tumours *in vitro* and can cause agglutination and cell death³¹⁹ and the *in vivo* administration of Con A has been demonstrated to increase the life span of tumour bearing mice. When methotrexate or chlorambucil was covalently attached to Con A, a significant increase in the anti-tumour effect over the lectin or the chemotherapeutic agent alone has been noted³²⁰⁻³²².

Immobilized lectins have also been used for affinity-chromatographic purification of glycoproteins, cells and fractionated cell subpopulations^{304,311,323}.

2.5 PEANUT LECTIN (PNA).

The peanut (*Arachis hypogaea*) lectin (PNA) is a readily available protein, which binds preferentially to oligosaccharides containing the terminal sequence

β -D-galactosyl-(1 \rightarrow 3)-N-acetyl-D-galactosamine (β Gal(1 \rightarrow 3)GalNAc)^{324,325}. Both the α and β configuration of this disaccharide are known to bind PNA^{325,326} ie, the

immunodeterminant groups of the T-F and a-GM₁ antigens. As previously mentioned, these antigens are important tumour-associated markers exposed on a wide number of tumour membranes and soluble glycoproteins. Exposed T-F antigen has been found in a variety of

adenocarcinomas including lung, gastrointestinal tract and breast³³⁶⁻³³⁸⁻³²⁷⁻³²⁹, and PNA demonstrated to bind to these epithelial cells but not to the corresponding normal cells both *in vitro* and *in vivo*³²⁹⁻³³⁰.

The affinity of PNA for reactive T-F antigen results in the agglutination of neuraminidase treated erythrocytes and has been designated an "anti-T agglutinin" since it gives the same immunological reaction as the anti-T antibody of mammalian sera³³¹.

2.5.1 Macromolecular Properties of PNA.

Lotan *et al.*³³³ determined the molecular weight of affinity-purified PNA to be 110,000 \pm 10,000 daltons, as determined by gel filtration and sedimentation velocity. Using sedimentation equilibrium centrifugation Terao *et al.*³³² found close agreement with this value (106,500 daltons), however Fish *et al.*³³³ reported a lower value of 98,000 \pm 3,000 daltons using similar techniques. Discrepancies may be due to i) variations in extraction methods resulting in slight aggregation, ii) higher protein concentrations used by Lotan and Terao or iii) isolectin variations³³³⁻³³⁴.

PNA is a relatively acidic (pI=5.95)³³², hydrophilic and compactly folded protein³³³. It is a tetrameric structure composed of four identical monomers of 24,000-27,000 daltons which are noncovalently linked³²⁵⁻³³²⁻³³³. One binding site exists per monomer (four per PNA molecule) as determined by equilibrium dialysis, and atomic absorption studies indicate each subunit contains one Ca²⁺ and Mg²⁺/Zn²⁺ atom (0.78 mole Mg²⁺/subunit and 0.11 mole Zn²⁺/subunit)³³⁵. The stability of the tetrameric structure is pH dependent and PNA reversibly dissociates to a globular dimeric structure (48,000 daltons) which lacks sugar binding capacity at pH 3.0³³³. The intrinsic sedimentation coefficient correspondingly decreases from 5.7 \pm 0.1s. to 3.8 \pm 0.2s at pH 3.0. In the presence of detergents (SDS) or denaturing conditions PNA dissociates to four identical subunits of 27,000 daltons which possess the same sequence for the last five NH₂-terminal amino acids³²⁵⁻³³²⁻³³³.

Amino acid sequencing studies of PNA has been reported by several investigators^{323,332,334-337}. Lotan *et al.*³²³ demonstrated a high content of acidic and hydroxylic amino acids, relatively little methionine, tryptophan and histidine and absence of cysteine. Terao *et al.*³³² reported conflicting data with that of Lotans' study of composition. They found considerably less threonine, serine, tryptophan and arginine than Lotan, an absence of methionine, but 16.6 moles of cysteine/mole PNA. The first 40 amino acids of the N-terminal end of PNA have been sequenced. Considerable homology exists between the first 25 and the first 40 residues of PNA and several other legume lectins (soybean, lentil and pea), suggesting a common ancestry for the genes coding these lectins³³⁶. A recent studies by Lauwereys *et al.*³³⁷ has elucidated 161 amino acids of PNA, 69 of which were identical to SBA, and 71 identical to favin.

The PNA molecule is an asymmetric orthorhombic crystal structure, as determined by X-ray diffraction studies³³⁸. About 57% of each molecule is occupied by solvent and the hydrodynamic radius of the molecule has been estimated as 35.5 ± 1.5 . Ultraviolet (u.v.) spectroscopy demonstrates a small absorption peak at 290 nm with a double maxima at 277 and 283 nm³³³. The extinction coefficient has been calculated as 0.96, while the absorption coefficient (A_{210}) is 7.7 cm^{-1} ³³⁵. In the presence of inhibition sugars, the u.v. spectrum shows saccharide-induced transition. The thermodynamic parameters (entropy and enthalpy) have been reported for the binding of PNA to β DGal(1 \rightarrow 3)GalNAc^{333,339}. Enthalpy (ΔH°) was calculated as $-78 \pm 5 \text{ kJ.mole}^{-1}$ and entropy (S°) as $-177 \pm 16 \text{ J.mole}^{-1}.\text{K}^{-1}$.

Unlike most other lectins, PNA does not contain any covalently bound carbohydrates³²³. The protein has been found to be stable within the concentration range $0.5\text{-}2.0 \text{ mg.mL}^{-1}$, between pH 3.0 and 10.75, and between $0.8\text{-}52^\circ\text{C}$ ³⁴⁰. Cryoinsolubility has been noted with PNA solutions of high concentration ($> 2 \text{ mg.mL}^{-1}$) at temperatures below 4°C ³⁴¹. This is most likely due to protein insolubility as polymerization or conformational changes are not observed. The presence of β DGal(1 \rightarrow 3)GalNAc results in preservation of solubility.

PNA is very stable both in solution and as a lyophilized powder. Crude saline extracts have shown no significant loss of agglutination ability when stored at 20°C for up to 6 months while lyophilized preparations have been reported stable up to 2 years³¹⁰.

2.5.2 Isolation and purification of PNA.

The anti-T-F activity associated with PNA was first found in crude saline extracts of peanuts (10% w/v NaCl solution)³³¹. Because peanuts contain up to 40% of their weight as lipid components, and these are present in saline extracts, pre-extraction of the crude peanut meal with organic solvents (ether, acetone) is advocated to remove the lipids^{323,332,342,343}. The proteins from the defatted saline extracts are usually salted out with neutral salts (eg. saturated Ammonium Sulphate precipitation) prior to centrifugation, reconstitution and dialysis/ultracentrifugation. The clear supernatant will still contain other peanut proteins such as the large molecular weight peanut globulins arachin (380,000 daltons) and conarachin³⁴⁴⁻³⁴⁷. PNA is isolated from this mixture by conventional protein purification techniques, affinity chromatography or a mixture of these techniques^{291,299,348}.

2.5.2.1 Isolectins: Multiple Molecular Forms of PNA.

Affinity purified PNA, found homogeneous by most protein purification techniques, has been reported to contain multiple molecular forms, known as isolectins^{334,349}. These have been demonstrated using polyacrylamide gel electrophoresis and isoelectric focussing where differences in electrophoretic mobilities were noted^{334,349}. The presence and relative abundance of the isolectins varies depending on the individual genotype of the peanut meal used³³⁴. Newman³⁴⁹ resolved the properties of several isolectins, reporting that all were composed of subunits of the same molecular weight (28,000 daltons), contained the same terminal amino acid (alanine), and had similar agglutination reactions to neuraminidase-treated erythrocytes. Cross-reactivity to a murine anti-PNA antibody was similar for each isolectin studied.

PNA has been reported present in 4556 genotypes of *Arachis hypogaea* and in 65 genotypes of species related to *Arachis*³³⁴. All but four of the wild species of *Arachis* contained seeds with PNA present. PNA from the variety 'Shulamit' was reported to have mitogenic properties towards desialylated lymphocytes, while PNA from unspecified genotypes of *Arachis hypogaea* has not been found to be mitogenic³³⁰. Presumably differences in isolectins account for the minor differences in PNA interaction with cellular glycoproteins.

2.5.3 Carbohydrate-Binding Specificity of PNA

Initial studies by Bird³³¹, using crude saline extracts of *Arachis hypogaea*, demonstrated the agglutination of neuraminidase-treated human erythrocytes (N'RBCs) independent of their ABO blood group type. The inhibitory effect of various mono- and oligosaccharides on the hemagglutination of N'RBCs or on glycoprotein precipitation have been reported by various investigators³³²⁻³³⁷⁻³⁵¹ as well as more direct measurements of carbohydrate binding including equilibrium dialysis³³⁵, u.v. difference spectroscopy³³⁵⁻³³⁹⁻³⁵², and carbon-13 nuclear magnetic resonance (NMR)³³³⁻³⁵⁴.

The monosaccharides D-galactose and α - and β -D-galactosides, such as lactose, were able to inhibit the agglutination of N'RBCs and it was postulated that β -glycosidically-linked D-galactosyl residues may be an important constituent of the T-F antigen³²⁴. Uhlenbruck *et al.*³²⁴ demonstrated very strong inhibition with 2-acetamido-2-deoxy-3-O- β -D-galactopyranosyl-D-galactose (β -D-Gal-(1 \rightarrow 3)- α -GalNAc) and by glycoproteins and gangliosides carrying this disaccharide in a non-reducing (or terminal) position. The desialated glycoproteins α_1 -acid glycoprotein, fetuin, glycophorin and the human blood group NN or MN antigens have also been reported as specific inhibitors of PNA binding to N'RBCs³²⁴⁻³²⁵⁻³⁵⁵. These compounds all contain the core structure β -D-Gal-(1 \rightarrow 3)- α -GalNAc upon desialation. Asialo-GM₁ has also been shown to inhibit PNA binding to N'RBCs with similar affinity to β -D-Gal-(1 \rightarrow 3)- α -GalNAc. Other sugars which have shown inhibition of PNA

(hemagglutination or glycoprotein precipitation) are summarized in Table 2.4.

In contrast to most other D-Galactose specific lectins, PNA is not inhibited by terminal N-acetyl-D-galactosamine^{324,325} and it is also one of the few lectins which is able to accommodate more than a single glycosyl residue in its combining site³³⁶. Its interaction with the disaccharide β DGal(1 \rightarrow 3)GalNAc appears very specific and has an affinity 50 times higher than the galactosyl monosaccharide suggestive of an extended binding site for PNA^{331,334,335}.

The structural features of carbohydrates required for binding and inhibition of PNA have been summarized as follows:

1. On C-6, an extracyclic chain was found necessary for the carbohydrate-lectin interaction and the orientation of the C-6 hydroxyl group is critical. Substitution of the C-6 hydroxymethyl resulted in decreased binding and therefore is also important for sugar-lectin binding.
2. A free hydroxyl or amino acid group on C-2 is required for interaction. Although a C-2 hydroxyl in an equatorial position is not essential for binding, the axial position of this OH was reported to diminish binding affinity^{325,333-337}.
3. A free hydroxyl on C-4 is necessary for binding, and the configuration of the C-4 terminal residue should be similar to D-galactose^{325,335}.
4. A methoxy group on C-1 favours binding, slight preference is seen for the α anomer. The O(1) atom appears to be involved in the glycosidic bonding while the second residue is involved in association with PNA. The β (1 \rightarrow 4) linkage favours association above α (1 \rightarrow 6) linkage, suggesting that C-1 configuration is also important^{325,336}.
5. Terminal sugars in the pyranose form are reported as more effective inhibitors than those in the furanose or 'open chair' form. Similar pyranose configuration of the penultimate GalNAc residue also confers increased inhibition³³³.

PNA-glycoprotein, glycolipid or polysaccharide interaction is more complex than that seen with simple mono- or disaccharides. This is due to the secondary binding stabilization beyond the combining site itself including multivalent binding, steric interaction, and

Table 2.4 Inhibitory effect of Carbohydrates on PNA hemagglutination or glycoprotein precipitation

Inhibitor	Relative Potency of Inhibition* of	
	Hemagglutination†	Precipitation‡
<u>Monosaccharides</u>		
D-Gal	1.0	1.0
D-Xyl	<0.4	
L-Fuc	<0.25	
D-Fuc	<0.4	0.6
D-Glu, DGluNH ₂ or GluNAc	<0.25	
DGalNH ₂	1.43-4.25	2.2
DGalNAc	<0.25	
6-0-methyl α DGal		1.0
methyl β DGal	1.25	1.5
p-Nitrophenyl β DGal	1.25-2.0	1.5
<u>Di- and oligosaccharides and glycoproteins</u>		
DGal β (1 \rightarrow 4)DGlc (lactose)	1.66-2.0	2.2
DGal β (1 \rightarrow 6)DGlc		2.2
DGal β (1 \rightarrow 4)DGlcNAc	1.66	4.0
DGal β (1 \rightarrow 3)DGlcNAc		0.6
DGal β (1 \rightarrow 3)DGalNAc (T-F antigen)	50	54.5
DGal α (1 \rightarrow 3)D-Gal-ol-NAc		2.2
DGal α (1 \rightarrow 3)D-Gal		0.9
DGal α (1 \rightarrow 6)D-Glc	0.8	0.6
DGalNAc α (1 \rightarrow 3)Gal		<0.5
Ch-3 (MN glycoprotein fragment)	20.0	
asialo-Ch-3	2,500	
MN glycoprotein	2.5	
asialo MN glycoprotein	5,000	

* Galactose assigned inhibitory potency 1.0, others calculated relative to this³²⁵.

† Based on concentration required for 50% inhibition of B-type N'RBCs (Lotan *et al.*³²⁵) or concentration required to completely inhibit 4 times the hemagglutination dose of AB-type N'RBCs (Terao *et al.*³²²).

‡ Based on concentration required for 50% inhibition of precipitation of blood group glycoprotein (Pereira *et al.*³²¹).

non-specific binding^{391,358,359}.

Because the determination of lectin-binding specificities by agglutination or precipitation merely reflect the relative binding constants of the different ligands, attempts have been made to study lectin-carbohydrate interactions using more sophisticated techniques such as u.v difference spectroscopy and NMR³⁵²⁻³⁵⁶. Matsumoto *et al.*³⁵², using u.v. difference spectroscopy, calculated an equilibrium constant of $2 \times 10^3 \text{ M}^{-1}$ for the PNA-lactose interaction at 21°C. Neurohr *et al.*^{337,338}, using the same technique, determined binding constants for PNA-methyl- α -D-galactopyranoside ($1.8 \times 10^3 \text{ M}^{-1}$), PNA-methyl- β -D-lactoside ($1.3 \times 10^3 \text{ M}^{-1}$) and PNA-methyl- β -D-galactopyranoside ($1.0 \times 10^3 \text{ M}^{-1}$) at 25°C. Results from NMR showed good correlation to those determined by the u.v. technique.

Neurohr *et al.*^{337,338} have proposed a two-step binding mechanism for PNA-ligand interaction. This involves a initial interaction (at close to diffusional rate) followed by conformational rearrangement resulting in the final complex. The mechanism appears similar for both mono- and disaccharides^{337,338,354}. Circular dichroism studies of PNA interaction demonstrated less conformational change associated with glycoprotein (asialofetuin) binding than that of simple sugars³⁶⁰. These results imply that the extended binding site for glycoproteins may be predetermined. The more intensive conformational changes that are required for simple sugar interactions results in lower binding constants, confirming existing data on relative binding strength^{353,354}. The binding constant (determined by extrapolation) has been estimated as $1 \times 10^7 \text{ M}^{-1}$ for PNA:T-F antigen binding³²⁵ and is in agreement with those values determined for other lectin:glycoprotein interactions.

2.5.4 Biological Binding of PNA.

Because of the specific interaction of PNA with the T-F antigen and with desialated glycoproteins and glycolipids containing cryptic antigenic determinants, PNA has gained wide spread use as a cell surface probe³⁶¹. Histological and immunological studies have been reported in a variety of tissues and cell populations, including neoplasias and has been the topic of recent

review³⁶²

2.5.4.1 Erythrocytes

The distribution of PNA positive cells in human peripheral blood is very low (about 5%) most of them being monocytes³⁶³. PNA, however, will bind and agglutinate N^oRBCs independent of their ABO blood group as previously discussed³⁶⁴⁻³⁶⁵. The T-F cryptoantigen has also been demonstrated on the membrane of erythrocytes by both serological and chemical methods³⁶⁶. Reductive cleavage of the erythrocyte membrane glycoprotein resulted in a tetrasaccharide N-acetylneuraminy(2→3)β-D-galactosyl-(1→3)-[N-acetylneuraminy(2→6)] N-acetyl-D-galactosaminol being released³⁶⁶. This structure is the major alkaline-labile oligosaccharide of the erythrocyte membrane, and is the antigen determinant of the human MN blood group³⁶⁶. The glycoprotein contains about 20.8 μmol of N-acetyl galactosamine and 48.7 μmol of sialic acid per milligram of glycoprotein. Thomas and Winzler³⁶⁶ further alluded that the T-F antigen (βDGal(1→3)GalNAc) is exposed when this tetrasaccharide is in the asialo form i.e. when treated with neuraminidase. In porcine and bovine erythrocyte glycoprotein it has been shown that the C-6 position of N-acetyl galactosamine is substituted with sialic acid³⁶⁶⁻³⁶⁸⁻³⁶⁹.

Several investigators have suggested the presence of two distinct antigens on erythrocyte membranes treated with neuraminidase, those with terminal D-galactose and those with terminal N-acetyl-D-galactosamine, and only the former responsible for binding PNA³⁷⁰⁻³⁷²⁻³⁷³. Aged RBCs show some differences in their binding to PNA after neuraminidase treatment, when compared to young erythrocytes. Senescent RBCs, which may contain only 70% of the sialic acid content of young RBCs, and cells with extruded nuclei do not bind PNA to the same extent as normal cells³⁶⁵. The probable cause of these differences may be due to the *in vivo* cleavage of exposed D-galactose by glycosidases such as β-galactosidase after desialation as it has been shown that older erythrocytes contain less galactose than younger cells³⁶⁵. Aging of RBCs however, does not result in unmasking

of N-acetyl-D-galactosamine residues.

2.5.4.2 Lymphocytes

The lymphoid system is comprised of numerous cell populations such as T and B lymphocytes, mature and immature cells differing in their immunological functions³⁷⁰. Although functional heterogeneity is demonstrated, morphological similarities exist and the various cells are often present in the same lymphoid tissue. Advances in immunology have resulted in the identification of lymphocyte membrane antigens which are able to distinguish between cell populations. Lectins, including PNA, have been found valuable tools in the identification of lymphocyte cell antigens and for the separation of various lymphocyte subpopulations³⁷¹⁻³⁷⁶.

Peripheral blood lymphocytes of humans, rats, mice and guinea pig have been shown to contain cryptic PNA binding sites which result in PNA binding after neuraminidase treatment³⁵⁰⁻³⁷¹. PNA has also been shown to stimulate mitogenic activity in unmasked human and rat lymphocytes, but not in untreated cells³⁵⁰. In lymphoid cells, exposed PNA membrane receptors are present on immature thymocytes and some neoplastic lymphocytes³²⁵⁻³⁵⁰. In mice, PNA receptors have been demonstrated on the membrane of thymus T lymphocytes (thymocytes) of cortical origin³⁷¹. The radiation and hydrocortisone sensitive PNA-binding thymocytes comprise the majority (80-90%) of the thymus cell population³⁷⁰. PNA is also known to bind to suppressor T-cells, and this has been used for differentiation and separation of suppressor T-cells from lymphocyte populations³⁷¹⁻³⁷².

PNA binds to small numbers of cells in bone marrow, spleen, and lymph-nodes³⁷³⁻³⁷⁴. The PNA-binding bone marrow cells in mice have been shown to be immature T-lymphocytes (prothromobocytes and lymphoid stem cells)³⁷¹⁻³⁷³. Umbilical cord lymphocytes of humans have also been noted to be PNA positive³⁷³ and this has led to the use of PNA binding as a method to study the ontogenesis of T-cells and hematopoietic stem-cell maturity³⁷¹. Since germinal centres in mice (Payers patches) and man (tonsils)

are also known to bind PNA^{376,377}, this lectin may also be a marker of immature B-cells.

Activated T-cells may acquire PNA receptors i.e. glycoprotein transformations may occur in cytotoxic T-cell membranes, even though they are derived from PNA negative lymphocytes or nodal cells³⁷⁸. This is a reversible transformation as these cells lose their ability to bind PNA when they transform back from the enlarged cells to small sized lymphocytes. This phenomenon is useful for the differentiation of various immature T-cells, B-cells and activated T-cell populations, and provides valuable information on cell-surface antigen expression during development and activation of lymphocytes³⁷⁹.

Several lymphoblastoid lines of T or B cells also express PNA receptors. Burkitt's lymphoma and several T-cell lines of leukemias (blast cells of acute lymphoblastic leukemia, stem cell leukemia, and myeloid leukemia) have been reported PNA positive³⁷⁴. Lymphocytes of most chronic lymphatic leukemias do not bind PNA³⁷³, while peripheral lymphocytes of children with acute lymphoblastic leukemia were often positive³⁷⁹. PNA binding may indicate poorer prognosis in these cases³⁷⁹, although recent data disputes these results, suggesting better prognosis with T-F positive leukemic cells³⁸⁰.

The murine RI lymphoma cell line has been shown to bind both PNA and anti-T antibodies^{235,243,330}. This radiation-induced RI lymphatic leukemia was initially isolated from CBA(H-2) mice by Hewitt³³¹ and has been passaged in mice in the ascites form or in cell culture by several investigators^{312,333}. Zabel *et al.*^{243,330} have demonstrated strong binding of PNA to RI cells *in vitro* as well as in subcutaneous solid tumours. The RI tumour is known to express the T-F antigen in unmasked form and is valuable as an animal tumour model for *in vivo* tumour uptake studies.

2.5.4.3 Platelets

PNA has been shown to bind to platelets after treatment with neuraminidase³¹⁴. The T-F antigen is expressed in a cryptic form on these cells and interaction with PNA does not occur with untreated platelets. Reductive (alkaline borohydrate) treatment of desialated platelet membranes has been shown to release the disaccharide

β DGal(1 \rightarrow 3)GalNAc, consequently detected by means of gas chromatography¹¹⁴.

2.5.5 PNA binding to tumour cells

As previously mentioned, the T-F antigen has been reported as an important tumour-associated antigen, and has been demonstrated in unmasked form in a variety of animal and human tumour cell lines. Using both histological and cell culture techniques the binding of PNA has been studied in detail in a variety of neoplasias.

2.5.5.1 Embryonal Carcinoma

Embryonal carcinoma (EC) cells are the stem cells of teratocarcinoma and have been studied as models of mammalian embryogenesis¹¹⁵. Several cell surface antigens have been identified on the membrane of mouse EC cells and these exhibit similarities to the antigens on the cells of embryos. Significant changes may occur in the arrangement and expression of these antigens during *in vitro* differentiation, and studies using PNA have demonstrated changes in localization, distribution and relative mobility of T-F antigen sugar residues at various stages of development¹¹⁶.

PNA has been found to bind to murine EC cells and detect subpopulations amongst multipotent EC cells¹¹⁶. Following *in vitro* differentiation these cells fail to bind PNA or express the glycoproteins responsible for binding¹¹⁷. Isolation and biochemical analysis of undifferentiated EC cell membrane glycoproteins has confirmed the presence of galactose and N-acetyl-D-galactosamine residues (presumably present as β DGal(1 \rightarrow 3)GalNAc) on undifferentiated cells^{117,118}.

2.5.5.2 Mammary Carcinomas

The T-F antigen expression has been extensively studied on various breast carcinomas and has been found to be present in unmasked form in most malignant cell types studied, although not in corresponding normal or benign breast tissue^{119,120,121,122}. The T-F antigen has been demonstrated in the cytoplasm and on the cell membrane in relatively

large quantities in many breast neoplasms^{300,390}, however PNA binding has also been reported in some benign lesions³⁹¹. Luminal duct and lobular membranes appear to stain PNA positive, and intraluminal secretions in benign conditions have occasionally shown T-F antigen expression³⁹¹.

In normal breast parenchyma, PNA binding has been reported along the luminal surface of the breast epithelium in the lobula as well as the ducts^{391,392}. Secretions found within the ducts are known to be rich in free and cryptic T-F antigen receptors and the intensity of PNA staining appears dependent on the secretory state of the epithelium³⁹¹. Milk fat globule membrane glycoproteins have been found to contain the appropriate structures for PNA interaction by independent chemical methods of analysis³⁹³.

The difference in PNA binding patterns in malignant conditions is thought to be due to the cellular localization of immune responses to the T-F or T-F antigen-like receptors and may reflect the aggressiveness of the tumour³⁹⁴.

In benign lesions, cryptic and free T-F antigen has been demonstrated in the apical region of epithelial cell membranes, particularly of the intraductal papillomas, as well as the cytoplasm³⁹¹. Cystically enlarged ducts have shown a variety of staining patterns, although they have generally been reported to be more strongly stained by PNA than normal parenchyma³⁹¹.

Most undifferentiated breast carcinomas have been shown not to possess either free or cryptic T-F antigens, although slight PNA staining was reported in some studies^{300,395,391}. Unsuccessful attempts have been made to correlate the histological grade of malignant breast lesions such as adenocarcinoma, infiltrating lobular carcinoma, infiltrating ductal carcinoma and medullary carcinoma, to the PNA staining pattern observed³⁹⁴. Light microscopical studies with peroxidase labelled PNA (HRPO-PNA) have demonstrated binding not only in the tumour cells mentioned above, but also in parts of the stroma of these lesions³⁹⁴.

Attempts have also been made to determine the correlation between the expression of PNA receptors and steroid receptors (oestrogen, progesterone, dihydrotestosterone and cortisol) in animal tumour models³³². It has been reported that in the presence of these receptors in concentrations above 25 fmol/mg cell protein, 68% of primary tumours and 60% of metastases were PNA reactive³³³. Only 23% of primary lesions and 0% of secondaries stained PNA positive in tumours with less than this concentration, or absence of steroid receptors. 45% of primary lesion stained PNA positive in the presence of oestrogen receptors alone (25% in secondaries), while in ovariectomized animals PNA was not seen to bind to any cells. The administration of 17β -oestradiol resulted in the re-expression of both cryptic and free PNA receptors, thus indicating an important correlation between oestrogen receptor positive and PNA positive lesions³³³. These findings have been verified by studies which have demonstrated the abolition of PNA receptors in hormone receptor positive tissue with the administration of Tamoxifen (an oestrogen antagonist)³³⁴. Furthermore, an 85% response to hormone therapy has been reported in PNA positive lesions, while a 24% response was noted in PNA negative lesions. It has been suggested that the synthesis of large quantities of PNA receptors may indicate neoplastic transformations occurring from a functionally undifferentiated state, with high proliferative activity, to a highly differentiated state with inhibition of mitotic activity, resembling, more closely, the lactating mammary gland. It appears that PNA binding studies may be useful in distinguishing hormone-sensitive from non-sensitive lesions in fixed tissue sections of both primary and metastatic breast lesions^{335,336}.

The strong binding of PNA to the spontaneous murine mammary adenocarcinoma TA₃-Ha of strain A mice has been reported by several investigators^{337-344,347}. This tumour line appears useful for the study of T-F antigen expression both in *in vitro* and *in vivo*, and has been shown to release a high molecular weight (500,000 daltons) glycoprotein composed largely of N-acetyl-galactosamine, galactose, sialic acid, serine and threonine known as epiglycanin (glycoprotein I)³⁴⁵⁻⁴⁰⁶. Epiglycanin has been reported to contain the

immunodeterminant structures of the T-F and NM antigens, is carcinoma-associated, and binds PNA avidly⁴⁰⁷⁻⁴⁰⁸. The intact cells are passaged in ascites but are capable of growing sub-cutaneously (s.c.)⁴⁰⁷. In addition, they readily metastasize to other organs, and metastatic variants, which selectively metastasize to either lung or liver, have been isolated⁴⁰⁹. These variants retain their T-F antigen expression, and are valuable models for *in vivo* studies with PNA or monoclonal antibodies against T-F antigen⁴⁰⁶.

The TA₃-St subline is a spontaneous variant of TA₃-Ha which, unlike the original cell-line, does not secrete epiglycanin⁴⁰¹⁻⁴⁰⁹. TA₃-St is only lethal in the synergistic strain A mice (the strain of origin) whereas TA₃-Ha is capable of growing in allogenic and even some xenogenic hosts⁴¹⁰⁻⁴¹². PNA binding to these tumour lines *in vivo* has been demonstrated and will be discussed in further detail later.

2.5.5.3 Carcinomas of the G.I.T.

Variability in PNA binding patterns to normal mucosal surface of the gastrointestinal tract has been demonstrated using histological techniques⁴¹³⁻⁴¹⁵. The isthmus cells of the gastric mucosa and epithelial cells of intestinal mucosa are known to strongly bind PNA. Free T-F receptors appear in the region of the golgi body of intestinal epithelial cells and are presumed to be a result of glycoprotein synthesis in this region⁴¹³. The cells of the cardiac, antral (gastric mucosa) and Brunner glands (intestinal mucosa) also show cytoplasmic, as well as golgi region staining with PNA. The invaginated membranes of parietal cells have been reported to weakly bind PNA, while chief cells are known to exhibit strong interaction⁴¹³⁻⁴¹⁵. Goblet cells of the small intestine exhibited PNA binding, while the corresponding cells in the large bowel were not stained⁴¹⁴. Surface mucous cells of the colon were devoid of free or cryptic PNA receptors, although some PNA binding was demonstrated to the glandular epithelial of the antral mucosa of stomach. The body of the stomach bound PNA only after neuraminidase treatment, while the remainder of the normal colon, ileum and stomach was reported to be devoid of T-F antigen even in the cryptic form⁴¹⁴.

Hyperplastic alterations of the gastric mucosa, resulting from malignant transformations or inflammation, have been noted to result in an increase in PNA binding in the mucous and isthmus cell golgi body and perinuclear regions⁴¹³. The extracellular mucous and the cell border of mucous cells in sections of gastric adenocarcinoma were PNA positive without neuraminidase treatment, in contrast to normal tissue⁴¹³.

The glycocalyx and cytoplasm of apical portions of large bowel carcinoma have also been noted to express free T-F antigen, whereas only the supranuclear portion of normal cells bound PNA⁴¹⁶. An explanation for the increased T-F antigen expression in these carcinomas has been proposed on the grounds of diminished glycotransferase levels in malignant cells resulting in incomplete biosynthesis of MN blood group glycoproteins on mucosal cell surfaces^{416,417}. As with breast malignancies, the degree of differentiation of rectosigmoid adenocarcinomas reflected the PNA staining pattern. Less differentiated lesions contained more cryptic antigens whereas highly differentiated tumours contained more free antigen structures⁴¹⁸. The aggressiveness of the tumour may also be related to the altered sialation of these cellular membrane glycoproteins⁴¹⁹.

Confirmation of the value of histological T-F antigen specific immunoperoxidase staining in colorectal carcinoma and in abnormalities of mucosa has been recently reported by Ørntoft *et al.*³²⁷. Tumour cells, as well as enteric ganglia nerve cells, were shown to bind PNA, presumably due to the presence of gangliosides (including GM₁). Although not true T-F antigen receptors, the gangliosides are known to contain carbohydrate structures capable of acting as PNA binding substrates. These authors further postulate that the heterogeneity of staining patterns in colon cancer cells may be a result of ganglioside content, shown to vary between clonal isolates from one malignantly transformed cell line by Murray *et al.*⁴²⁰.

2.5.5.4 Carcinomas of the bladder

T-F antigen expression has been reported in transitional cell carcinoma of the bladder both in cryptic and free form. Coon *et al.*⁴²⁴ demonstrated that T-F antigen was

limited to the carcinoma, and not to normal tissue. Free T-F antigen, determined by PNA histological staining, was more prevalent in high-grade carcinomas, but was also present in cryptic form in all grades of tumour. When present in unmasked form in low-grade lesions, it was an indicator of poor prognosis²¹⁵. Further studies by the same investigators have confirmed T-F antigen and ABH blood group antigen expression as a prognostic indicators of bladder carcinomas²¹⁶.

2.5.5.5 PNA binding in the skin

PNA receptors have been identified in the granular, and prickle cell layer of human skin in a free form, while the basal or horny layer does not appear to contain either free or cryptic receptors^{421,422}. In squamous cell carcinoma, PNA has been found to bind to tumour cells according to the degree of keratinization⁴²¹. The squamous component of basal cell carcinomas has also been shown to bind PNA, whereas keratocarcinoma does not appear to express cryptic or free T-F antigen structures⁴²².

2.5.6 PNA binding in the Kidney

Numerous investigators have reported the PNA binding characteristics in kidney sections of many animals and humans using HPRO, FITC, rhodamine and gold colloid labelled PNA⁴²³⁻⁴²⁶. Light microscopical studies on both paraffin fixed and frozen sections have been reported⁴²³ and considerable species-species variation in the cellular binding has been noted^{424,425}. A summary of PNA binding patterns in kidney sections of various species is contained in Table 2.5.

Schulte and Spicer⁴²⁶ studied the binding patterns of a variety of lectins, including PNA, labelled with HRPO, in paraffin sections of mouse and rat kidneys. They reported brush border staining of proximal tubules, particularly in the S₁ region, as well as the luminal surface and apical cytoplasm of cortical collecting ducts in several strains of mice. The Bowman's capsule was seen to bind HRPO-PNA while the remainder of cells along the nephron showed variable staining. Activity was faint in the Loop of Henle, slightly more positive on the luminal

Table 2.5 : PNA binding patterns in kidney sections of various animal species.

Species	Glomerulus	S ₁	Proximal tubule S ₁	S ₂	Loop of Henle Des. loop	Asc. loop	Distal tubule	Collecting duct
Mouse	++BC	++BB	++BB	++BB	+L	+L	++L	+++L,Cy
Rat		+++BB	++BB	++BB		+++L	++L,Cy	+++L,Cy ++BM
Guinea pig		++BB			not reported			not reported
Rabbit							+	++L
Dog					not reported		++	not reported
Human	to +BC					+L	++	+++L,B

KEY: Staining intensity reported from negative (-) to intense (+++)

Cell types and location reported: BC = Bowman's capsule, BB = Brush border, L = luminal membrane, Cy = cytoplasmic, BM = Basement membrane

surface of distal tubules, and strong on both the luminal membrane and cytoplasm of collecting ducts.

The staining pattern for rats was similar, although more intense staining was seen in the S₁ segment of the proximal tubule and diminished along its length⁴²⁶⁻⁴²⁷. The apical rim of luminal cells in the thick ascending limb of the Loop of Henle were PNA positive, continuing from the medulla to the junction of the cortical distal tubules and collecting ducts⁴²⁸⁻⁴²⁹. Some cytoplasmic staining was also noted, while the principal cells and, more particularly, the intercalated cells of the collecting duct were shown to strongly bind PNA⁴²⁸⁻⁴²⁹. The glomerulus, in contrast to that seen in mice, was completely negative, however upon neuraminidase treatment, intense staining was demonstrated⁴²⁸⁻⁴³⁰. The presence of cryptic T-F antigen in the epithelial plasmalemma of the rat glomerulus is a highly debated point at present. Early reports⁴³³⁻⁴³⁶ had suggested that the disaccharide β Gal(1 \rightarrow 3)GalNAc was an important constituent of podocalyxin, the major sialoglycoprotein of epithelial membranes in the rat glomerulus. After neuraminidase treatment this glycoprotein was reported to bind PNA. Recent biochemical analysis revealed that, although podocalyxin was rich in the sugars mannose, N-acetylglucosamine, galactose and sialic acid, it was completely devoid of N-acetylgalactosamine, the penultimate sugar of T-F antigen⁴³⁷. These findings raise questions as to what cryptic glycoprotein is responsible for PNA binding in desialated glomeruli.

Le Hir *et al.* reported the binding of PNA to cryostat sections of rabbit kidneys⁴³¹, as well as in perfused isolated cortical collecting ducts⁴³². The cortical staining was confined to the collecting duct and connecting tubule in fixed sections⁴³¹, while only intercalated cell staining was demonstrated in the lumen of perfused collecting ducts⁴³². The intercalated cells of the outer stripe of the medulla were PNA positive, while cells in the thin descending Loop of Henle in the inner medulla demonstrated light staining⁴³¹.

In sections of normal human kidney, PNA binding has been reported in the Bowman's capsule of the glomerulus, the thin limbs, distal convoluted tubules and to collecting ducts⁴³³⁻⁴³⁴. The proximal tubules were not stained in any studies even after neuraminidase

treatment. The treatment of sections with neuraminidase revealed the presence of cryptic receptors in the Bowman's capsule of humans⁴³⁸, similar to those seen in rat glomeruli. Intense glomerular staining has also been noted to occur in hemolytic-uremic syndrome of children, where the neuraminidase from pneumococcal infections is thought to expose cryptic T-F antigen structures⁴³⁹⁻⁴⁴⁰.

Diverse PNA staining patterns have been reported in cases of hypernephroma where both cytoplasmic as well as membrane-bound PNA receptors have been identified⁴⁴¹⁻⁴⁴³. The intensity of staining has been reported to be a function of the differentiation state of the tumour⁴⁴², although this appears simplistic⁴⁴³. It is thought that renal cell carcinomas are derived from epithelial cells of the proximal convoluted tubule⁴⁴⁴, cells which are known not to express even cryptic T-F antigen⁴⁴²⁻⁴⁴³. PNA binding has been attributed to malignant transformations resulting in the synthesis of altered membrane glycoconjugates although PNA binding would also be explained if the renal cell carcinoma were derived from other than proximal tubular epithelium⁴⁴¹⁻⁴⁴³.

These studies further highlight the usefulness of lectin-binding histological techniques in the identification of glycoprotein and antigen expression on various cell lines, and demonstrate the strain-strain heterogeneity of membrane glycoproteins in the kidney. The delineation of malignant from normal reactivity in renal cell carcinoma may provide information as to the glycoprotein transformations occurring in neoplastic conditions of the kidney. A recent report also indicates that lectin-binding studies, including PNA, may be valuable in the identification of blood cell infiltration of human glomeruli in immunological diseases of the kidney⁴⁴⁵.

2.5.7 In-vivo Studies with PNA.

Zabel *et al.*^{443,446-448} were the first to report on the use of PNA for the *in vivo* study of T-F antigen expressing neoplasms in mice. Using ¹²⁵I labelled PNA (¹²⁵I-PNA), they demonstrated the avid tumour uptake of this lectin by RI lymphoma cells transplanted into

CBA/CAJ mice using gamma scintigraphy. *In vitro* studies of ^{125}I -PNA and fluorescein labelled PNA confirmed the specific binding of PNA to this tumour line, and this was reversibly inhibited with the concomittant incubation with 0.1 M galactose. The subcutaneous (s.c.) innoculation of mice with RI tumour cells and the subsequent i.v. injection of ^{125}I -PNA resulted in tumour uptake of ^{125}I -PNA (tumour/blood ratio 7.5:1 at 72 h P.I.). Rapid deiodination of ^{125}I -PNA was noted and resulted in significant uptake of free iodide in the thyroid, stomach, and also contributed to the lowering of the circulating blood levels.

Further studies by Shysh *et al.*²⁴⁴ showed a more striking tumour uptake with subcutaneous (s.c.) TA₁-Ha tumour cells in AJ strain mice. Biodistribution was also reported in mice with TA₁-Ha in the ascites form. Differences were reported between the whole-body retention of ^{125}I -PNA in animals with ascites or s.c. tumour. In solid form, the blood clearance of ^{125}I -PNA was rapid and resulted in tumour/blood ratios of 70-85:1 at 72 h P.I. Rapid *in vivo* deiodination of ^{125}I -PNA was again noted resulting in thyroid, salivary and stomach retention. High kidney uptake of the radiopharmaceutical was noted, particularly at early times P.I., which could not be explained as a result of free iodide alone.

These authors also reported the results of acute toxicity studies in mice. Following i.v. injection of between 50-3,600 μg of PNA, weight gain was noted to be identical to control animals. Histological examination of mouse organs did not reveal any abnormalities at the light microscopical level.

The *in vivo* retention of ^{125}I -PNA binding has subsequently been reported by the same authors in liver and lung metastatic variants of the TA₁-Ha tumour cell line⁴⁴³.

Autoradiography with ^{125}I -PNA and fluorescent microscopy with FITC-PNA confirmed the active uptake of PNA in both lung and liver metastatic nodules, indicating that T-F antigen expression is maintained during metastasis. Clear delineation of the metastatic tumours in both the lungs and liver were also documented with scintigraphy after i.v. injection of ^{125}I -PNA.

Yokoyama *et al.*⁴⁴⁷ have reported the uptake of ^{125}I -PNA in tumour models Lewis lung carcinoma (LLC), B-16 melanotic melanoma (MM), Yoshida sarcoma (YS), and the Ehrlich

ascites tumour (EAT) in comparison to ^{67}Ga -citrate. They found superior delineation of LLC and EAT by ^{125}I -PNA scintigraphy, similar ^{125}I -PNA and ^{67}Ga -citrate uptake in YS and MM, while HAH did not appear to accumulate ^{125}I -PNA. The specificity of tumour ^{125}I -PNA uptake was reported higher than ^{67}Ga -citrate due to the lack of accumulation in abscesses, in contrast to ^{67}Ga .

The *in vivo* use of ^{125}I -PNA in humans was first reported by Suresh *et al.*⁴⁴ and subsequently by Holt *et al.*⁴⁵. Eight patients with metastatic cancer of the colon, lung, or breast were injected with 37-93 MBq (17-88 μg) ^{125}I -PNA. Serum radioactivity up to 48 h P.I. was monitored and demonstrated rapid elimination of ^{125}I -PNA, predominantly by the kidneys. Urine analysis revealed $82.5 \pm 5.3\%$ of the activity was excreted in the urine within 24 h P.I. The urinary activity appeared to be associated with protein (was precipitated with 10% trichloroacetic acid) while a GM_1 synsorb binding and gel-column chromatography indicated significant levels of intact immunoreactive ^{125}I -PNA in the urine.

Scintigraphic localization of ^{125}I -PNA was documented in only two out of eight patients with known metastatic lesions (one pulmonary secondary deposit from a breast primary, one hepatic secondary from cancer of the colon) as well as malignant pleural effusions in a further two patients. The remaining patients studied showed false negative scintigrams of multiple known metastatic sites⁴⁵. In all cases, the most prevalent organ to show ^{125}I -PNA uptake was the kidney. The mechanism of the renal excretion of PNA is the topic of further work in this thesis.

3. EXPERIMENTAL.

3.1 MATERIALS AND METHODS.

3.1.1 Protein solutions.

3.1.1.1 Peanut lectin.

Peanut lectin (PNA) was obtained as a lyophilized powder, sugar and salt free from Chembiomed, Edmonton, Alberta. The powder was weighed and dissolved in 0.01 M phosphate buffered saline (PBS) (Gibco Laboratories, Grand Island, NY.) at concentrations between 1-5 mg/mL. Solutions, when not in use, were stored at 4°C and used within 30 days of reconstitution.

3.1.1.2 Bovine Serum Albumin and Human Serum Albumin.

High grade Bovine serum albumin (BSA) and Human serum albumin (HSA) were purchased from Sigma Chemical Co., St Louis, MO., as crystalline powders. They were dissolved in 0.01 M PBS at concentrations between 0.1-5 mg/mL.

3.1.1.3 Asialo-GM₁-HSA.

Asialo-GM₁-HSA (a-GM₁-HSA) was synthesized by Dr S. Selvaraj, Faculty of Pharmacy and Pharmaceutical Sciences, University of Alberta, as recently described⁴³⁰. The analogue with 4 disaccharide units/HSA molecule was used throughout the experimental investigations, at concentrations of 1-5 mg/mL in 0.01 M PBS.

3.1.2 Radiolodination.

PNA, HSA, and a-GM₁-HSA were iodinated with ¹³¹I or ¹²⁵I by a modified iodogen method originally described by Fracker and Speck⁴³¹. One milligram of

1,3,4,6-tetrachloro-3- α -6- β -diphenylglycouril (Iodogen[®], Pierce Chemical Co., Rockford, IL.) was dissolved in 10 mL analytical-grade chloroform. Twenty microlitres (2 μ g Iodogen[®])

was dispensed into clean 3 mL glass Falcon® tubes (Becton-Dickinson, Mississauga, Ont.) and the solvent evaporated with a stream of N₂ gas passed through a sterile 0.22 µm Millex-SA® filter (Millipore Corp., Bedford, MA.). When dry, the protein to be iodinated was added to the tube in a volume of 100-200 µL 0.01 M PBS. Radioiodination-grade Na¹²⁵I or Na¹³¹I solution of high specific-activity (5,000-6,000 MBq/mL, A.E.C.L., Ottawa, Ont.) in 0.1 M NaOH solution was buffered with 20 µL 0.5 M Phosphate buffer (pH 7.4) and the appropriate activity (40-300 MBq) was added to the reaction tube. The solution was allowed to incubate at room temperature for 30-45 min and the reaction stopped by removing the solution to a clean glass tube. Twenty microlitres of freshly prepared carrier 1.0 M NaI solution, in deionized-distilled water, was subsequently added to the reaction mixture and allowed to stand for 15 min. The activity of the tube was calibrated in a Picker dose calibrator using the appropriate isotope settings.

3.1.3 Chromatographic Separation of Iodinated Protein.

The radioiodinated protein was separated from 'free' radioiodide by gel-column chromatography. Biogel P6-DG desalting gel with an exclusion limit of 6,000 daltons (Bio-rad Laboratories, Richmond, CA.) was swollen for at least 24 h in 0.01 M PBS, and packed into 1.5 x 25cm glass columns by gravity. The columns were washed with 0.5 mL of 1% w/v HSA or BSA, to reduce non-specific binding to the media, and further washed with up to 50 mL 0.01 M PBS.

The reaction mixture was added to the column, and eluted into the gel with 0.01 M PBS. The columns were run using 0.01 M PBS as eluent and 0.5 mL fractions collected into clean glass Falcon® tubes. The tubes were counted in the isotope dose calibrator, and the binding efficiency calculated by comparing the activity of the pooled void-volume fractions with the starting activity.

3.1.4 Quality Control.

3.1.4.1 Estimation of Protein Concentration.

The protein content of the iodinated material was measured by two methods. For PNA, protein estimation was initially made using u.v. spectroscopy, and calculation of concentration was made using the optical density of PNA at 280 nm. An absorbance coefficient of $E_{1\%}^{1\text{cm}} = 9.6$ was used to convert absorbance to concentration³²⁵.

In later studies the protein concentration was estimated by the Bio-rad® protein assay⁴³². This assay is also a spectrophotometric technique based on the absorbance of Coomassie Brilliant Blue G-250 at 595 nm when bound to protein⁴³³. Standard curves of PNA concentration (20 µg-2 mg/mL) were plotted, using the standard assay procedure and the microassay procedure, giving OD₅₉₅/concentration plots for PNA. Both curves were compared to those determined for a standard protein (bovine gamma globulin)⁴³².

The % protein recovery from gel-column chromatography (Biogel P6-DG, 1.5 x 25 cm columns) was determined for a standard sample (100 µg) of PNA using the Bio-rad® protein assay. This figure was used as a correction factor for subsequent chromatographic protein recovery estimations.

3.1.4.2 Trichloroacetic Acid Precipitation.

The % protein-bound radioactivity was determined by trichloroacetic acid (TCA) precipitation. Aliquots of the iodinated protein solutions were diluted with 1 mL of 1% BSA in PBS at 4°C, followed by 1 mL of 25% TCA at 4°C. The denatured protein mixture was inverted several times and allowed to stand in a refrigerator at 4°C for 15 min. The mixture was then centrifuged at 1000 x G for 10 min, the supernatant removed by Pasteur pipette, and both the supernatant and precipitate counted in a γ-spectrometer peaked for the appropriate isotope. The % protein-bound activity was calculated as the counts in the pellet/total activity of the two fractions.

3.1.4.3 Instant Thin Layer Chromatography (ITLC).

Ten to twenty microlitre aliquots were spotted onto ITLC-SG media (Gelman, Ann Arbor, MI.), allowed to air dry, and developed in 85% methanol to a distance of 10-15 cm. The strips were cut into 1 cm segments and counted in a γ -spectrometer calibrated for the appropriate isotope. The counts remaining at the origin (representing protein-bound activity) divided by the total counts of all segments was used to calculate the % protein-bound activity.

3.1.4.4 Carbohydrate-Binding Specificity of Iodinated PNA.

The immunoabsorbants T-synsorb and asialo-GM₁-synsorb were kindly provided by Chembiomed, Edmonton, Alberta. These products consist of the disaccharides β -D-Gal-(1 \rightarrow 3)- α -GalNAc (T-sorb) or β -D-Gal-(1 \rightarrow 3)- β -GalNAc (α -GM₁-sorb) covalently linked to an immobilized support¹¹².

Twenty milligrams of either synsorb were placed in an Eppendorf® mini centrifuge tube and mixed with 1 mL 1% BSA in PBS by an inversion mixer. After 1 h, the solution was aspirated and the sorbs washed x 3 with PBS. An aliquot of iodinated PNA (approximately 1 μ g), made up to 1 mL with PBS, was added to the tube and a 20 μ L aliquot removed (t=0). The tube was continuously mixed on the inversion mixer, and further 20 μ L aliquots removed at various times up to 24 h. These were counted in a γ -spectrometer and compared to the activity at t=0. Following their use, the synsorbs were washed with 1 M D-galactose for 24 h, washed x 3 with PBS, and dialyzed against several fresh PBS washes. The synsorbs were then suitable for reuse in subsequent PNA binding determinations.

3.1.5 ¹²⁵I-PNA for Human Administration.

3.1.5.1 Sterile Production of ^{131}I -PNA.

PNA, which was purified from peanuts by affinity chromatography under sterile conditions, was purchased from Chembiomed, Edmonton, Alberta. A sample of this material was reconstituted with sterile PBS and was tested for sterility (USP XIX sterility test), and pyrogens (USP XIX rabbit pyrogen test, B.C. Pyrogen Testing Laboratory, Vancouver, B.C.). The starting material was found to conform to monograms for i.v. administration.

Sterile iodination of PNA was performed by the iodogen method, as previously described, but under aseptic conditions. All reagents used in the iodination, with the exception of the Na^{131}I for iodination were prepared from sterile reagents, or were autoclaved (Barnstead Laboratory Sterilizer) at 121°C for 45 min and subjected to sterility testing (USP XIX) and Limulus Amoebocyte Lysate (LAL) pyrogen testing (MA Bioproducts Ltd, Walkersfield, MD.) prior to their use in sterile labelling. All glassware (chromatography columns, reaction tubes, and collection tubes) was autoclaved prior to use.

The reaction was performed in a vertical laminar flow cabinet (Canadian Cabinets Ltd, Ottawa, Ont.) and the solutions were transferred using sterile pipette tips and aseptic techniques. The chromatographic separation of ^{131}I -PNA from $^{131}\text{I}^-$ was achieved as previously described, however using Biogel P6 DG which had been autoclaved at 121°C for 45 min, and packed in steam sterilized glass columns by aseptic technique in the laminar flow cabinet. The void volume was collected into plain sterile glass tubes (B-D, Mississauga, Ont.). The ^{131}I -PNA fraction was made up to the appropriate specific activity and was terminally filtered into sterile 10 mL vials through a $0.22\ \mu\text{m}$ Millex GV sterile filter (Millipore Corp, Bedford, MA.), which was bubble tested after use, to ensure its integrity.

3.1.5.2 Sterility Testing.

One milliliter of the filtered ^{125}I -PNA solution was added to 50 mL thioglycollate blood broth (Microbiology Dept, University of Alberta) using aseptic technique. The medium was incubated at 37°C , and a duplicate at 4°C , for 14 days. The medium was inspected for turbidity, and if present, the solution was subcultured on blood agar plates, and the pathogens identified by standard techniques.

3.1.5.3 Pyrogen Testing.

Initial retrospective pyrogen testing was determined by the USP rabbit pyrogen test (B.C. Pyrogen Testing Laboratory, Vancouver, B.C.).

On-line pyrogen testing was determined on all batches of ^{125}I -PNA prepared for human studies by the LAL pyrogen test. One hundred microlitres of the ^{125}I -PNA solution were added to each LAL tube, as well as to positive control tubes (containing LAL + reference endotoxin). A negative control was also run using 100 μL of sterile saline as the test material. The reconstituted LAL tubes were then incubated in a non-agitating water bath at 37°C for 60 min. The tubes were carefully removed from the water bath and inverted 180° . Each tube was observed for gelation, and were judged negative if no gel was observed after incubation. A positive reaction was noted if the tube contained a solid gel on inversion.

Further quality control was determined on each batch of ^{125}I -PNA (TCA precipitation, asialo-GM₁-synsorb binding), as previously described.

3.2 ANIMAL STUDIES.

3.2.1 ^{125}I -PNA Biodistribution Studies in Mice.

3.2.1.1 Dose-Response in CBA/CAJ Mice.

The biodistribution of various doses (0.1-100 μg) of ^{125}I -PNA was determined in normal CBA/CAJ strain mice. Six to eight week old mice (body weight 18-22 g) were purchased from the Small Animal Program, University of Alberta, and housed in groups of 5-6 per cage. They were maintained on standard laboratory food (Wayne® Lab-Blox, Chicago, IL.) and tap water *ad libitum*.

Groups of six, weight and sex matched mice were injected i.v. (tail vein) with 0.13, 1.3, 10, 13, 50, or 100 μg ^{125}I -PNA. At 30 min P.I., the animals were exsanguinated by dry CO_2 /cardiac puncture, the organs of interest were excised in their entirety, blotted, and weighed in tared plastic counting tubes (Amersham Spectra® vials). The remaining carcass, tail (injection site), and a portion of trachea containing the thyroid were also placed (unweighed) in vials. The vials were counted in an automated γ -spectrometer (Beckman γ -8000), along with diluted standards of the injected material and background vials using the coincidence method for absolute determination of ^{125}I ⁴⁵⁴.

The percentage of radioactivity per organ or per gram of tissue was calculated from absolute counts using a computer biodistribution program.

3.2.1.2 ^{125}I -PNA Biodistribution in AJ, c57b, CBA/CAJ and CAF1/J Strain Mice.

The effect of strain difference on ^{125}I -PNA renal uptake was assessed in four different strains (AJ, c57b, CBA/CAJ and CAF1/J) of mice. Four groups (N=6) of sex and weight matched mice per strain were injected i.v. with 1 μg /100 kBq ^{125}I -PNA and were sacrificed at 30 min, 6, 24, and 48 h P.I. The organs were dissected, weighed and counted, as above, and the % injected dose in both kidneys determined. Results were statistically compared among species (students t-test).

3.2.1.3 Effect of Multiple Doses of PNA on the Biodistribution of ^{125}I -PNA in CBA/CAJ Mice.

Five groups (N=6) of CBA/CAJ mice were used to ascertain the effect of previous exposure to PNA on the biodistribution of ^{125}I -PNA.

- Group 1 Each mouse was injected i.v. with 1 μg PNA one week prior to biodistribution studies with 1 μg ^{125}I -PNA. The animals were sacrificed 24 h P.I. and the organs counted as previously described.
- Group 2 Each mouse was injected with two i.v. doses of PNA (1 μg) at one week intervals followed by ^{125}I -PNA a week later. The animals were sacrificed at 24 h P.I. and organs counted as above.
- Group 3 Each mouse was injected with three i.v. doses of PNA (1 μg) at one week intervals, followed by ^{125}I -PNA a week later. Twenty four hour biodistribution was determined as above.
- Group 4 Each mouse was injected with three s.c. doses of PNA (1 μg) mixed 1:1 v/v with Freund's Complete Adjuvant (Calbiochem-Behring, La Jolla, CA.), followed by ^{125}I -PNA a week later. Twenty four hour biodistribution was determined as above.
- Group 5 Control mice received only ^{125}I -PNA

The biodistribution results of each group were statistically compared using Analysis of Variance (ANOVA).

3.2.2 Dynamic ^{125}I -PNA Renal Scintigraphy in NZW Rabbits.

3.2.2.1 Normals.

Dynamic gamma-camera scintigraphic studies were acquired in four male NZW rabbits (body weight 1.5-1.9 kg), purchased from the Surgical and Medical Research Institute (SMRI), University of Alberta. Each animal was anaesthetized with an i.m. injection of 50 mg/kg Ketamine (Rogar/STB, Montréal, Qué.) and 10 mg/kg Xylazine (Cutter Laboratories, Mississauga, Ont.), and placed supine to a gamma-camera (Searle Pho-Gamma IV), with parallel-hole high-energy collimator, interfaced to a

computer (ADAC CAM II). The camera was calibrated to the 365 keV gamma-peak (20% window) with a standard of ^{131}I . The injection syringe containing approximately 18 MBq ^{131}I -PNA was imaged (100,000 counts) and stored on floppy disc (128 x 128 matrix) prior to the animal studies.

Dynamic data (0.5 min frames for 60 min, 64 x 64 matrix) was acquired and stored on disc after i.v. injection of ^{131}I -PNA (18 MBq/100 μg) via the lateral ear vein. At 60 min P.I., static images (128 x 128 matrix, 100,000 counts) were acquired on disc, as well as a residual of the injection syringe.

The dynamic studies were reconstructed on the computer, and regions of interest (ROIs) were drawn with a light pen around the heart, kidneys, and bladder, together with a background region distal to the left kidney. Background-corrected (matrix normalized) activity/time curves of the kidneys, heart pool, and bladder were plotted on the computer, and corrected to injected dose using the 60 min static image region counts and the injection standard (minus the residual dose). % injected dose-at-peak, and time-to-Peak estimates of each kidney were determined from the dynamic activity/time curve.

3.2.2.2 Comparative Studies.

Dynamic studies were obtained, as outlined above, in groups of two rabbits treated with the following agents:

a-GM₁ disaccharide

The asialo-GM₁ disaccharide (β -D-Gal-(1 \rightarrow 3)- β -GalNAc) was incubated with ^{131}I -PNA (1:1 molar ratio) for 30 min at 20°C, then injected i.v. into two NZW rabbits. Dynamic renal curves and parameters were calculated as above and results statistically compared to control animals injected with ^{131}I -PNA (ANOVA).

Furosemide

One hour prior to the dynamic study, each rabbit was injected i.p. with 1 mg/kg Furosemide (Hoechst, Montréal, Qué.). The renal parameters determined above were statistically compared using ANOVA analysis.

Probenecid

One hour prior to the dynamic study, each rabbit was injected i.p. with 10 mg/kg Probenecid (M.S.D., West point, PA.), and results statistically compared (ANOVA) to the control animals.

Polyclonal rabbit anti-PNA IgG

One hour prior to the dynamic study each animal was injected i.v. with 120 μ g polyclonal rabbit anti-PNA IgG antibody (Sigma Chemical Co., St Louis, MO.). Additional ROIs were obtained over the liver and the % injected dose at peak, time-to-peak, and kidney/liver ratio compared to controls.

Epiglycanin

Epiglycanin was kindly provided by Dr Longenecker, Dept. of Immunology, University of Alberta. One hour prior to the dynamic study, each animal was injected i.v. with 160 μ g epiglycanin. Liver and kidney dynamic parameters were compared to controls, as previously described.

3.2.3 Studies with asialo-GM₁-HSA.

The glycosylated HSA analogue asialo-GM₁ (a-GM₁-HSA) was synthesized in our unit, as recently described⁴⁵⁰, and was used for competition experiments with ¹³¹I-PNA in NZW rabbits. The analogue with 4 disaccharide units/HSA molecule was incubated for 30 min at 20°C with ¹³¹I-PNA (100 μ g) at molar ratios of 4:1, 2:1, 1:1, and 1:4 a-GM₁-HSA:¹³¹I-PNA, then injected i.v. into groups of two NZW rabbits. Using the same dynamic imaging protocol, the % injected dose in liver, kidneys, and bladder (30 and 60 min P.I.) was calculated for each treatment group as previously described. Results were statistically compared (ANOVA) to both ¹³¹I-PNA and ¹³¹I labelled a-GM₁-HSA (¹³¹I-a-GM₁-HSA) controls. Kidney/liver ratios were also calculated from the ROIs at 30 and 60 min P.I. These were averaged and statistically compared between groups using ANOVA.

3.2.3.1 ^{131}I -PNA: ^{125}I -a-GM₁-HSA Biodistribution Studies in TA₃-Ha Tumour-Bearing CBA/CAJ and CAF1/J Mice.

TA₃-Ha tumour cells were kindly provided by Dr Longenecker, Dept of Immunology, University of Alberta. These cells were grown from frozen stocks in RPMI 1640 media containing fetal calf serum (Gibco) and incubated at 37°C in 4-5% CO₂. The cells were subcultured every 2-3 days until a sufficient number were present for inoculation. The cell numbers were determined by aseptically removing an aliquot of the suspension, placing it on a hemocytometer, and counting under 150x magnification with a microscope. Cell viability was determined by adding a drop of trypan blue to the hemocytometer slide and observing cell staining. The cell culture was diluted to 10⁷ cells/mL with fresh RPMI media, pre-heated to 37°C in a water bath.

One hundred microlitres (10⁶ cells) were aseptically removed into tuberculin syringes and injected by subpannicular injection in a latero-dorsal site just above the rear legs of CAF1/J or CBA/CAJ mice. The tumours were allowed to grow for 10-14 days post-inoculation, or until palpable lesions of approximately 0.5 cm diameter were present.

PNA was iodinated with ^{131}I and a-GM₁ with ^{125}I by the iodogen method. Control biodistribution studies were performed with ^{131}I -PNA as well as ^{125}I -a-GM₁-HSA in TA₃-Ha tumour bearing mice, and dual isotope biodistributions were performed with mixtures of ^{131}I -PNA: ^{125}I -a-GM₁-HSA at molar ratios of 4:1, 1:2 and 1:4. Using a dual-isotope spillover correction program on the gamma-counter, the % injected dose/gram of tissue was determined for both the ^{131}I -PNA and ^{125}I -a-GM₁-HSA at various times (30 min-48 h) P.I. and at the various molar concentrations. Results for each isotope were statistically compared (students t-test) to the corresponding controls.

Further control biodistribution studies were performed with ^{131}I -HSA in CAF1/J mice and ^{131}I -PNA in CBA/CAJ mice with TA₃-Ha tumours by the standard method.

3.2.4 Dynamic and Static ^{131}I -PNA Scintigraphy in Dogs.

Four normal mongrel male dogs (17-21 kg) were purchased from SMRI, and anaesthetized with sodium pentobarbitone 20 mg/kg i.v. (Somnotol®, M.T.C., Hamilton, Ont.). A 19 gauge teflon angiocath (Deseret Medical Inc. Sandy, UT.) was inserted into a leg vein (either fore or hind limb), and a 3-way stopcock (B-D, Rutherford, NJ.) attached. The catheter patency was maintained by occasionally flushing with heparinized saline (1000 u/mL), and this venous access used for the drawing of blood samples. The animals were kept hydrated by the infusion of normal saline (100 mL/h) through an i.v. giving set (Travenol, Mississauga, Ont.) during anaesthesia.

The bladder was catheterized with a sterile neonatal feeding tube (Medi-craft Ltd., Malton, Ont.), and used for the withdrawal of urine contents, while the dogs were anaesthetized. The dogs were placed supine on an imaging table and the gamma-camera, calibrated for ^{131}I , positioned anteriorly over the kidneys and bladder. Each dog was injected i.v. with 200 μg ^{131}I -PNA (25-35 MBq), which had previously been statically imaged and stored (100,000 counts, 128 x 128 matrix). Dynamic computer frames were acquired at 0.5 min intervals (64 x 64 matrix) for 60 min and stored on floppy disc. A static image (128 x 128 matrix, 100,000 counts) was obtained over the bladder, the bladder contents aspirated, and the imaging repeated post-void. Further static images were also acquired, with consistent geometry and positioning, at 2, 3, 4 and 24 h P.I.

The dynamic background-corrected ROI curves over each kidney and the bladder, were reconstituted, as for the rabbit studies, and the % injected dose-at-peak and time-to-peak parameters derived from the resultant curves. The post-void scintigram was subtracted from the pre-void image, and the counts in the bladder, and kidney ROIs extracted. These were then corrected to % injected dose using the following formula:

$$\begin{aligned} \text{\% Inj. dose} &= \frac{\text{Counts in Kidney ROI}^*}{\text{Counts in Bladder ROI}^{**}} \times \frac{\text{Counts in Urine}^\dagger}{\text{Total counts injected}^\ddagger} \times \frac{100}{1} \\ &\text{Background-corrected.} \end{aligned}$$

- Pre-void minus post-void.
- † Urine aliquot counts determined in gamma-spectrometer and multiplied by total collected urine volume.
- ‡ Dose Standards counted in gamma-spectrometer and corrected for total counts injected.

3.2.5 ¹³¹I-PNA Plasma Pharmacokinetics and Clearance Studies in Dogs.

Studies to determine the plasma pharmacokinetics and clearance rate of ¹³¹I-PNA were determined simultaneously in each dog undergoing gamma-scintigraphy, as described above. Blood samples (2 mL) were drawn through the indwelling angiocath into heparinized tubes at 3, 5, 7, 10, 12, 15, 20, 30, 45 min and 1, 1.5, 2, 3, 4, 6, 9, 12, 24 and 48 h P.I. Plasma was generated by centrifuging the whole blood at 1000 x g for 10 min and 0.5 mL aliquots were counted in the γ -spectrometer, along with injection standards (0.5 mL of 1/1000 dilution of injected ¹³¹I-PNA). Normalized (100% at t=0) plasma activity/time curves were generated, entered into computer files, and analyzed by AUTOAN and NONLIN³ exponential curve-fitting programs, to determine pharmacokinetic and clearance parameters. Plasma aliquots were then treated with TCA (as previously described), supernatants and precipitates recounted, and the protein-bound pharmacokinetic curves plotted and analyzed as above.

3.2.5.1 Pharmacokinetic Model Calculations.

Standard pharmacokinetic parameters were derived for ¹³¹I-PNA plasma curves assuming a two compartment model described by the biexponential equation⁴³³:

$$A = A_0 e^{-\alpha t} + B_0 e^{-\beta t}$$

The half-life ($t_{1/2}$) of both the fast (α) and slow (β) exponentials was calculated from the stripped curve where:

$$t_{1/2} \alpha = \frac{0.693}{\alpha}$$

and

$$t_{1/2} \beta = \frac{0.693}{\beta}$$

³AUTOAN and NONLIN are exponential curve-fitting and curve-stripping programs developed by the Biomathematical Unit, Upjohn Co., Kalamazoo, MI.

The volume of distribution (V_d) was calculated from the plasma activity/time curves from the intercept of the curve ($A_0 + B_0$) at $t=0$, and relating this to the total injected dose:

$$V_d = \frac{\text{Total dose injected (cts/time)}}{A_0 + B_0}$$

The area under the plasma curve (AUC) was calculated using the equation:

$$AUC = \frac{A_1}{\alpha} + \frac{B_0}{\beta}$$

and the clearance (Cl/T_b) calculated from the equation:

$$Cl/T_b = \frac{\text{Total dose injected (cts/time)}}{AUC}$$

3.2.5.2 Red cell Binding.

Red cell binding was determined on all blood samples by counting aliquots of the packed cell volume (0.5mL) which had been washed and centrifuged x 3 in heparinized saline. The counts in the cell pellet were compared to the plasma aliquot counts given above, and % red cell binding determined.

3.2.5.3 Urine Collection and Analysis

Urine was collected throughout the study, initially by bladder catheterization, and subsequently from collections obtained while the dogs were housed in metabolic cages. The total radioactivity was determined for each collection period (0-1, 1-3, 3-6, 6-9, 9-24 and 24-48 h P.I.) together with % protein-bound activity (TCA precipitation) and % asialo-GM₁-synsorb binding.

Representative 1 h P.I. urine samples (2 mL) were analyzed by gel column chromatography (Biogel P 100, 2.5 x 50 cm, Bio-rad Laboratories, Richmond, CA.) with PBS as eluent. The column outlet was connected to a dual channel monitor, which simultaneously measured u.v. absorbance at 280 nm and ¹²⁵I radioactivity. The elution profile was plotted with a dual-pen chart recorder and this was compared to the elution profile of the ¹²⁵I-PNA injection material and Na¹²⁵I standards.

3.2.5.4 ^{131}I -PNA Renal Scintigraphy during Galactose Perfusion in Dogs.

Two dogs were subjected to ^{131}I -PNA renal scintigraphy, while D-galactose (an inhibitor of the PNA carbohydrate-binding site) was infused (2.5 g loading dose, 50 mg.min⁻¹ infusion) i.v. via an intravenous giving set. Dynamic parameters were determined, as previously described, and were compared to untreated dogs (ANOVA).

3.2.6 Renal PNA Deposition by Histopathology Techniques

The renal accumulation and cellular localization of PNA was studied in CAF1/J and CBA/CAJ mice, NZW rabbits, and mongrel dogs using histopathological techniques in collaboration with Dr D. Willans, Dept of Laboratory Medicine, Edmonton General Hospital. Initial studies were undertaken in CBA/CAJ mice using FITC-PNA and rhodamine-PNA (EY Laboratories, San Mateo, CA.). Ten micrograms FITC-PNA or rhodamine-PNA were injected i.v. into CBA/CAJ mice via the tail vein, and the animal were sacrificed at 1 and 3 h P.I. The animals were dissected, the kidneys removed and these were halved longitudinally. The tissue was washed with saline then immediately placed into formaldehyde solution and fixed for 24 h. The fixed tissues were then embedded in paraffin, and axial sections cut with a microtome. The sections were placed on clean microscope slides, and viewed by fluorescence microscopy at the appropriate incident wavelength. Mice, which were injected with normal saline only, were used as controls.

Although several of the kidney sections revealed good quality fluorescent sections of cellular localization, problems were encountered with this technique, resulting in autofluorescence in many of the sections, particularly with the FITC specimens. An immunoperoxidase technique was subsequently developed to overcome these limitations.

Doses of 1-100 μg PNA were injected i.v. into CAF1/J and CBA/CAJ mice, 10-500 μg into NZW rabbits, and 100-1000 μg into mongrel dogs. The animals were sacrificed at various times (10 min-24 h) P.I., the kidneys removed, and these were washed in cold saline at 0°C. The mouse kidneys were cut longitudinally, as above, while the rabbit and dog kidneys were cut

into axial blocks of about 0.5 cm thickness, and were embedded in O.C.T. (Lab-Tek Products, Naperville, IL.). The embedded tissue was then frozen in isopentane at -70°C and stored at -70°C until sectioned. One micrometer axial cryostat sections were cut, placed on slides and fixed in acetone. These were washed with PBS and incubated in diluted rabbit serum for 20 min to minimize non specific staining. Natural avidin substances were blocked by the application of Avidin reagent (Vector Laboratories Inc, Burlingome, CA.) for 15 min, washed with PBS and treated with Biotin blocking reagent (Vector) for a further 15 min. The sections were then incubated for 30 min with a 1/50 dilution of goat antiPNA IgG (Vector), followed by a 30 min incubation with biotinylated antigoat IgG antibody (Vector). The biotinylated sections were incubated for 60 min with Avidin peroxidase reagent (Vector), and were finally treated for 5 min with freshly prepared DAB- H_2O_2 solution. Duplicate immunoperoxidase stained slides were either counterstained with Harris's hematoxylin or not counterstained, and these were observed with conventional light microscopy.

3.2.7 ^{125}I -PNA Renal Parameters in Cis-platinum Induced Renal Toxicity in Dogs.

Four healthy male mongrel dogs (body weight 18-22 kg) were purchased from SMRI, were housed in standard pens, fed standard dog chow (Purina), and allowed water *ad libitum*. After at least one week of acclimatization, the dogs' renal function, serum biochemistry, and ^{125}I -PNA plasma and scintigraphic renal parameters were determined as previously described. The animals were then started on a 5 day single-cycle cis-platinum chemotherapy regimen. Five days following the completion of the cis-platinum schedule, the animals' renal function, serum biochemistry, and ^{125}I -PNA parameters were re-determined. The animals were sacrificed the following day, their kidneys removed and these were histologically examined (Dr D. Willans, Dept of Laboratory Medicine, Edmonton General Hospital) for signs and severity of renal toxicity. An outline of the study protocol is shown in Fig. 3.1.

3.2.7.1 Cis-platinum Treatment Regimen.

Five days following the pre-treatment assessment of renal function, each dog was commenced on a 5 day cis-platinum regimen.

Ten milligram vials of cis-platinum (Platinol®, Bristol-Meyers Laboratories, Ont.) were reconstituted with 10 mL of sterile saline. The solutions were allowed to stand for at least 30 min to ensure complete dissolution, then the contents drawn into 20 mL syringes. Doses of 0.5 mg/kg body weight were injected by slow i.v. injection each consecutive day for five days via a leg vein and 19 gauge butterfly (Cutter Laboratories.), followed by a saline flush of 10-20 mL. The dogs were retained on food and water *ad libitum*, and the volumes consumed were noted along with daily body weight. Five days following the final cis-platinum treatment dose, the animals' renal function and ^{131}I -PNA clearance were determined.

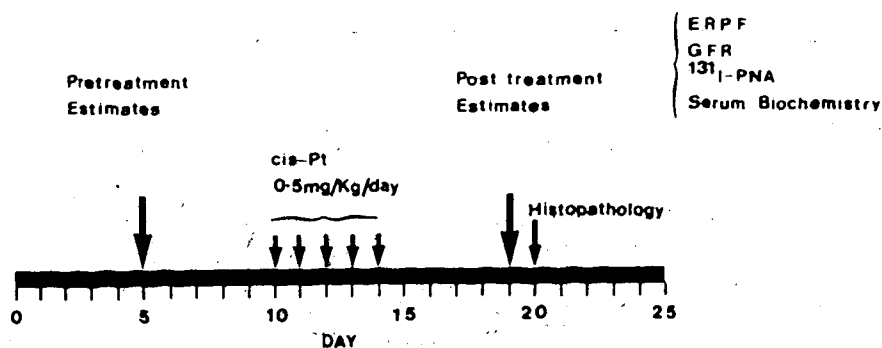


Figure 3.1 : Protocol of renal investigation for Cis-platinum treated dogs.

3.2.7.2 Serum Biochemistry.

Estimates of serum Na^+ , K^+ , Cl^- , Ca^{++} creatinine, blood urea nitrogen(BUN) and total protein were determined pre- and post- cis-platinum treatment. Blood samples were

drawn from a leg vein with a 20 mL syringe and 19 gauge needle. This was added to a plain red-top vacutainer tube (B-D, Mississauga, Ont.) and allowed to clot for several hours. The tubes were centrifuged at $1000 \times G$ for 10 min and the serum decanted with a sterile Pasteur pipette. The samples were sent to the SMRI biochemistry unit (Mrs M. McCubbin), and were assayed by a serum biochemistry Autoanalyser. The pre- and post-treatment results were compared (paired students t-test) and related to values of a normal dog pool ($N > 100$) analyzed by identical procedures.

3.2.7.3 Serum circulating T-F antigen titres

Serum T-F antigen titres were determined on each dog before and after cis-platinum treatment by an ELISA assay. The assay was conducted courtesy of Summa Biomedical Canada.

3.2.7.4 ERPF and GFR Estimations.

Effective renal plasma flow (ERPF) and glomerular filtration rate (GFR) were determined on each dog before and after cis-platinum treatment by a dual isotope technique.

Four megabecquerels of ^{131}I -labelled orthiodohippurate (^{131}I -OIH, Merck-Frosst, Montréal, Québec) and $10 \text{ MBq } ^{99\text{m}}\text{Tc-DTPA}$ ('in-house' preparation, see Appendix 1) were mixed together, made up to 1 mL with sterile saline, and injected i.v. into each dog via a leg vein. Blood samples (2 mL) were withdrawn from a contralateral leg vein into heparinized Falcon tubes at 5, 7, 10, 15, 20, 40, 60 min and 2, 4, 6 h P.I. Tubes were spun at $1000 \times G$ for 10 min and plasma aliquots (0.5 mL) were counted, along with injection standards and background tubes, in an automated gamma spectrometer (Beckman γ -8000) using a dual channel spillover correction program. Linear regression analysis of plasma activity/time plots was used to generate plasma t_1 values for both ^{131}I -OIH (0-60 min) and $^{99\text{m}}\text{Tc-DTPA}$ (2-6 h). These were computed with the appropriate volume of distribution (V_d) estimates (extrapolated) to calculate the ERPF and GFR. Pre- and

post-cis-platinum treatment values were expressed as % change ($\Delta S\%$) and statistically compared (paired students t-test) with other renal function tests determined in the same animals.

3.2.7.5 ^{131}I -PNA Plasma Clearance and Renal Studies in Cis-platinum Treated Dogs.

^{131}I -PNA plasma clearance and renal scintigraphic studies were determined in all dogs before and after cis-platinum treatment as previously described. Results were expressed as % change ($\Delta S\%$) and these were statistically compared to all other parameters by paired students t-test.

3.2.7.6 Renal Histopathology after Cis-platinum Treatment in Dogs.

One day after the post-treatment estimates were completed, the dogs were sacrificed, their kidneys removed and immediately fixed in formaldehyde. Paraffin embedded sections were cut with a microtome, stained with Harris's hematoxylin, and classified as to the degree of tubular damage demonstrated by light microscopy (Dr D. Willans).

3.3 HUMAN STUDIES.

Two studies were undertaken with ^{131}I -PNA in human patients. The first study involved the investigation of patients with known metastatic disease with ^{131}I -PNA as a tumour-seeking agent. Recent studies had indicated the potential usefulness of radioiodinated PNA as a tumour-seeking agent in mice^{243,244,330,440} and humans^{441,449}. A clinical trial was initiated to confirm these findings, and as a consequence of this study, further biodistribution parameters were determined which relate to the renal handling of ^{131}I -PNA in humans.

3.3.1 ^{131}I -PNA Scintigraphy in Patients with Metastatic Disease.

Seventeen patients with proven metastatic disease (breast carcinoma 7, colorectal carcinoma 4, small cell lung carcinoma 2, renal cell carcinoma 2, and one each of

adenocarcinoma of lung and carcinoma of stomach) were selected for scintigraphy of their known tumour sites. All patients were informed of the experimental nature of the study and their written consent obtained. Patients had their measurable tumour sites documented using standard clinical, radiological and nuclear medicine techniques, and routine biochemical profiles (including serum creatinine) were performed to assure normal renal function. Specific enquiry was made regarding allergies to iodine and peanuts.

Each patient was tested with a small dose (0.05 mL) of sterile PNA (1 mg/mL) intradermally, and the injection site was observed for at least 1 h for signs of skin sensitivity. Each patient received 10 drops of concentrated Lugol's iodine (5% w/v iodine and 10% potassium iodide, Drug Trading Co, Toronto, Ont.) daily for 5 days before and 3 days following ^{131}I -PNA scintigraphy, to minimize thyroidal uptake of ^{131}I .

Each patient was injected i.v. with 50 MBq ^{131}I -PNA (100-200 μg) via an antecubital vein. Whole body scintigrams (anteriorly and posteriorly) were acquired at 3, 6, 24, 48 and 72 h P.I. using a large field-of-view gamma camera (Searle LFOV) calibrated for ^{131}I and interfaced to a computer (Digital PDP 11/40).

In 5 patients, ^{131}I -PNA renal uptake was determined in conjunction with static scintigraphy. Following i.v. injection of ^{131}I -PNA, dynamic frames were acquired every 30 s for 45 min (64 x 64 matrix). Regions of interest (ROIs) were generated over each kidney, as well as adjacent background regions. Background-corrected activity/time curves were derived and area normalized. Exponential curve-fitting ($A = A_0[1 - e^{-\lambda t}]$) was used to describe the renal uptake curves and $t_{1/2}$ (uptake) and A_0 were determined for each kidney from the extrapolated 0-45 min dynamic curves. Expected vs. observed goodness of fit for each renal curve was determined by χ^2 testing. Curves were quantitated to % injected dose by comparison with injection standards and/or voided bladder counts, as previously described for animal studies.

3.3.2 ^{131}I -PNA Renal Studies in Patients undergoing Cis-platinum Chemotherapy.

Seven patients (4 with testicular carcinoma and 3 with ovarian carcinoma) were selected for detailed ^{131}I -PNA renal scintigraphy during their cis-platinum chemotherapy. Patients with known primary tumours who were to undergo cis-platinum chemotherapy, either as a single agent, or in combination with other antineoplastic therapy and/or radiotherapy, were informed of the experimental nature of the investigation, and were admitted to the study protocol.

3.3.2.1 Patient Eligibility.

All patients had histologically proven malignancy and were to commence cis-platinum chemotherapy, either alone or in combination with other drugs, and had no known renal dysfunction. Each patient selected was willing to be available for the entire study, had no known allergies to peanuts or iodine, and had a life expectancy greater than 12 weeks.

3.3.2.2 ^{131}I -PNA Renal Scanning and Pharmacokinetic Protocol.

Each patient was tested for tissue-type hypersensitivity one day prior to ^{131}I -PNA renal scintigraphy, by the intradermal injection of 5 μg PNA and observation for skin reaction. Each patient also received Lugol's iodine for the immediate study period, and this was repeated on each subsequent occasion prior to, during, and following ^{131}I -PNA scintigraphy.

Each patient was injected with 10 MBq of sterile ^{131}I -PNA (50-100 μg). Dynamic frames were acquired on the gamma camera/computer system every 60 s for 45 min. Static frames were also taken at 45 min P.I. in both the anterior and posterior projections, and individual kidney activity corrected for depth and tissue attenuation by standard computer techniques. Background-corrected Activity/time curves were generated for each kidney and were fitted to exponential curves ($A = A_0[1 - e^{-\lambda t}]$), as described for the previous study. Further analysis on the background-corrected and attenuation-corrected renal ROI curves was performed using computer quadratic equation fitting program ($A = ax + bx^2$)

to attain the slope of the initial renal curve for each kidney. The initial slope of the kidney curves were corrected to radioactivity/blood volume *in vivo* measurements by computing injected dose (MBq) over $V_d(L)$ determined from the plasma samples.

All patients were serially studied throughout their chemotherapy regime. A baseline study was performed the day prior to the commencement of cis-platinum chemotherapy, and was repeated following every second course of cis-platinum (0.5 mg/kg for 5 days, an interval of 14 days, then repeat of 5 day cycle). The average time required for the treatment protocol was 4-6 weeks. The results of the scintigraphy were compared between each occasion and against other estimates of renal function.

Early phase pharmacokinetic curves were determined during each study, and clearance determined as previously described. Blood samples (5 mL) were obtained from a contralateral antecubital vein directly into 10 mL plain vacutainer tubes at various times (2-60 min P.I.). Serum was generated by centrifuging at 1000 x G for 10 min and 0.5 mL aliquots were counted in a gamma-counter peaked for ^{131}I , along with injection standards. The Volume of distribution was calculated from the extrapolated log-linear curves and was computed with the decay constant, to calculate clearance (assuming single compartment model kinetics).

The % injected dose excreted in 24 h was determined by counting aliquots of 24 h urine collection and comparing these to the injected standards.

3.3.2.3 Serum Biochemistry and Creatinine Clearance.

Routine serum electrolytes, BUN, creatinine and liver function tests were determined on each patient, concomitantly with the ^{131}I -PNA renal studies, by standard techniques. Urinary creatinine was determined on the 24 h urine collections, and used to calculate creatinine clearance.

3.3.2.4 Anti-PNA Antibody Determinations.

Serum anti-PNA IgG, IgM, and IgE antibody titres were determined by ELISA assay on each patient a week prior to each ¹³¹I-PNA renal study.

A 96 well ELISA plate (Dynatech Immulon) was coated with PNA (1 µg in PBS/well) and incubated overnight at 4°C. The plate was emptied and washed x1 with PBS to remove any unbound PNA. The plate was blocked by incubating for 30 min at 37°C with 1% bovine serum albumin (BSA) in PBS and subsequently washed x1 with PBS.

The serum was diluted 1:10 with PBS and 200 µL and dispensed into the first wells for serial dilution up to 1:320. The remaining wells were filled with 100 µL PBS and the plate incubated at room temperature for at least 1 h, emptied and washed x2 with 200 µL washing solution (Mandel Scientific Co., Rockwood, Ont.). The wells were emptied and 50 µL of a 1:200 dilution of peroxidase-labelled goat-antihuman IgG, IgM, or IgE (Tago Systems, Burlingame, CA.) were added to groups of wells, the plate incubated for 1 h at room temperature and subsequently washed x4 with Washing solution. The plate was emptied and 50 µL of a 1:1 solution of ABTS (2,2'-azino-di[3-ethyl]-benzthiazoline sulphonate) and H₂O₂ (Mandel) substrate solution was added. They were then incubated for 15-20 min and the optical density at 412 nm was determined by an ELISA MR6000 plate reader (Dynatech Corp.).

Each patient's assay was compared to their pre-PNA determination, as well as to assays of pooled normal sera.

4. RESULTS AND DISCUSSION

4.1 RADIOIODINATION AND QUALITY CONTROL OF PEANUT LECTIN.

A major consideration in radiopharmacological studies for the investigation of *in vivo* behaviour of radiopharmaceuticals is the establishment of methodologies which will provide consistent products, whose biological properties will not vary from batch to batch. For this purpose PNA was used from one single manufacturer, and labelling techniques were kept consistent during all the experiments. Analysis of results from over 60 radioiodinations of PNA, with either ^{125}I or ^{131}I , has revealed a consistency in labelling efficiency, protein-bound radioactivity and sugar-binding characteristics of the radioiodinated PNA products. These data, spanning two and a half years of labelling experiments, are summarized in Table 4.1.

Table 4.1 Radioiodination efficiencies and quality control results of ^{125}I and ^{131}I -PNA batches.

		% Labelling efficiency	% TCA precipitation	% a-GM ₁ synsorb binding
^{125}I -PNA(N=9)	Mean \pm S.D.	57.2 \pm 5.7	98.4 \pm 1.2	90.6 \pm 2.8
	Range	43-71	83.2-98.6	84.6-93.8
^{131}I -PNA(N=53)	Mean \pm S.D.	60.3 \pm 4.6	97.6 \pm 1.8	89.8 \pm 2.4
	Range	41.4-68.9	80.1-98.2	79.4-93.2

The radioiodination technique employed in these labelling experiments gave consistent % labelling efficiencies, routinely in the range 45-65%, for both ^{125}I and ^{131}I . The resultant labelled PNA was shown to retain its biological sugar-binding specificity (immunoreactivity), as determined by asialo-GM₁ synsorb binding. Previous reports by Zabel³³⁰ and Eu⁴⁵⁶ have documented similar results and have also included results in which competitive inhibition of

PNA binding to α -GM₁ synsorb were described. Initial experiments on labelled batches of 125 I-PNA with 0.05 M galactose inhibition were also performed in this study, but because of consistency in finding, these have not been reported here.

ITLC-SG chromatography of radioiodinated PNA was also determined on initial batches of the product and again consistency was demonstrated with results of TCA precipitation, as reported by Eu⁴³. Because these results appeared superfluous to the determination of radiochemical purity, this technique was omitted from the quality control protocol in subsequent experiments.

4.1.0.1 Protein concentration determinations.

The protein content in PNA solutions was determined by two separate methods. Initially, u.v. spectroscopy at 280 nm was used to determine protein concentrations, however at concentrations of below 100 μ g/mL there was significant deviation from linearity, as demonstrated in Fig 4.1. In an attempt to improve the accuracy of the estimation of PNA concentration in solutions, particularly at dilutions <100 μ g/mL, the Bio-rad[®] protein assay was investigated, using the standard procedure, and the microassay technique, as described in the assay manual⁴². Serial dilutions (1 μ g-2 mg/mL) of PNA and also of the reference protein solution (bovine gamma globulin) provided Optical density at 595 nm (OD₅₉₅) vs. protein concentration standard curves with both the standard and microassay. Results demonstrated acceptable linear correlation of OD₅₉₅ vs. concentration of PNA and bovine gamma globulin using both the standard (Fig 4.2) and microassay (Fig 4.3) techniques. The assays were easy to perform, required minimal time, and appeared reproducible over several different experiments.

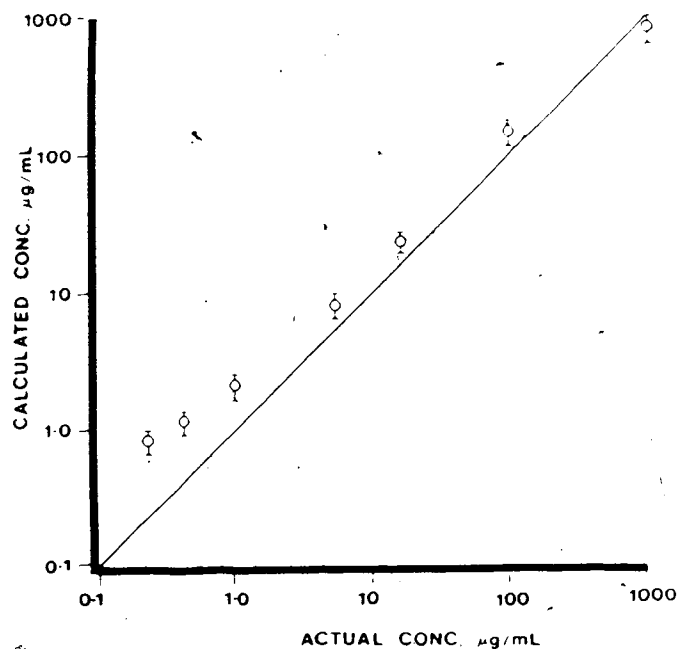


Fig 4.1: Calculated vs. Actual PNA concentration by u.v. spectroscopy at 280 nm.

Using the Bio-rad® protein assay, the protein recovery of a 1 mg/mL solution of PNA (100 μ L), applied to the standard gel-columns used for the separation of radioiodinated PNA from free iodide, was determined in four separate experiments. The % protein recovered from the columns was determined as $81.2 \pm 3.5\%$ and in subsequent chromatographic separations, this correction factor was used to estimate the recovered protein concentrations for all administered dose calculations.

4.1.0.2 Sterile preparation of ^{131}I -PNA.

Sterility and pyrogen testing of ^{131}I -PNA solutions for human studies (N=36), revealed no difficulties in the preparation of ^{131}I -PNA suitable for human administration. No solution tested contained micro-organisms (USP XIX), and all solutions lacked the ability to clot the LAL test vials, while positive controls showed a positive gelation reaction.

Asialo-GM₁-synsorb binding and TCA precipitation assays revealed retention of sugar-binding specificity and indicated >95% protein-bound activity (results are included

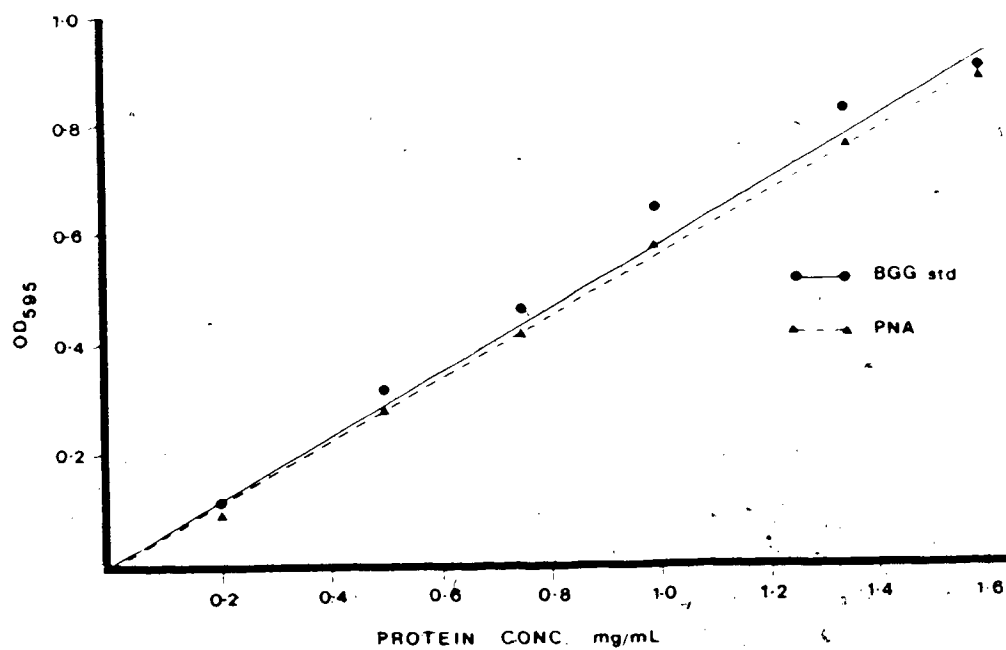


Figure 4.2 OD₅₉₅ vs. concentration of bovine gamma globulin and PNA (20 μ g-1.6 mg/mL) with the standard Bio-rad[®] protein assay.

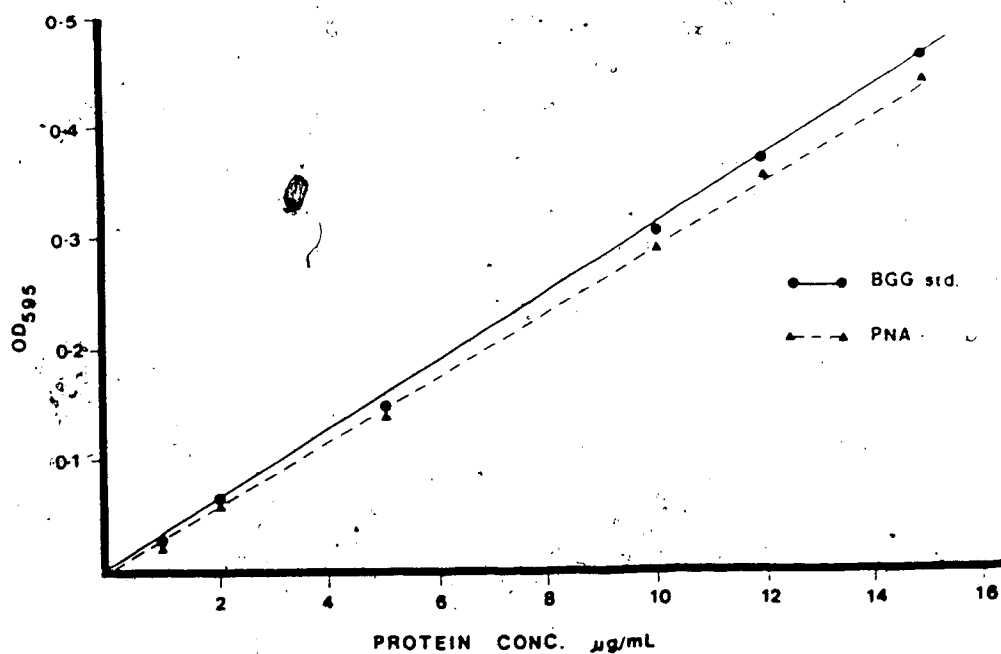


Figure 4.3 OD₅₉₅ vs. concentration of bovine gamma globulin and PNA (1-16 μ g/mL) with the Bio-rad[®] microassay.

in Table.4.1).

4.2 PNA BIODISTRIBUTION STUDIES IN ANIMALS AND HUMANS.

4.2.1 ^{125}I -PNA Biodistribution studies in mice.

4.2.1.1 Dose-response in mice.

The dose-response of ^{125}I -PNA was determined at 30 min P.I. in CBA/CAJ strain mice using doses ranging between 0.13-100 μg per animal. No significant difference was demonstrated in the % injected dose/g of blood or kidney tissue at doses below 1.3 μg per animal, however on increasing the doses above 10 μg per animal, there was a steady rise in the % injected dose/g in blood, and a corresponding decrease in the % injected dose/g in the kidneys, as summarized in Table 4.2. A plot of kidney/blood ratios vs. dose (Fig 4.4) shows a linear increase in this ratio, which peaks at around 10 μg per mouse. With doses in excess of 10 $\mu\text{g}/25\text{ g}$ mouse, a steady decline in this ratio is observed. These results suggest that the renal uptake of ^{125}I -PNA becomes saturated at around 10 μg per mouse (a dose corresponding to approximately 400 $\mu\text{g}/\text{kg}$ body weight).

Eu⁴⁵⁶ has recently reported a similar dose-response behaviour in the tumour uptake of ^{125}I -PNA in CBA/CAJ mice containing TA₃-Ha tumours. He found that a similar dose, (10 μg) per mouse, resulted in the optimal tumour uptake of ^{125}I -PNA, and at higher administered doses, the tumour/blood ratio declined, and concluded that this was due to saturation of PNA binding to the T-F antigen receptors in the tumour.

4.2.1.2 Renal uptake of ^{125}I -PNA in different strains of mice.

Previous biodistribution studies by Zabel⁴³⁰ and Eu⁴⁵⁶ have demonstrated an apparent difference in the degree of renal uptake and retention time of ^{125}I -PNA in several different strains of mice, although these experiments had used different sources of PNA and variations in the radioiodination technique (Chloramine-T or Iodogen method). In

Table 4.2 : DOSE RESPONSE OF ^{131}I -PNA IN CBA/CAJ MICE.
BLOOD AND RENAL ACTIVITY (30 MIN. P.I.)*

		AMOUNT ^{131}I -PNA INJECTED (μg)				
		0.13 (N=6)	1.3 (N=6)	10 (N=6)	50 (N=6)	100 (N=6)
<u>BLOOD</u>						
% DOSE/G		5.72	5.75	7.75	11.32	13.50
\pm S.D.		1.13	0.765	1.69	1.71	1.67
<u>KIDNEY†</u>						
% DOSE/G		21.55	27.35	41.45	37.25	33.19
\pm S.D.		4.64	6.15	10.37	5.21	3.50
% DOSE/ORGAN		11.85	11.37	17.22	13.89	13.41
\pm S.D.		2.68	1.82	3.35	2.20	2.50
<u>KIDNEY/BLOOD RATIO</u>		3.76	4.75	5.35	3.29	2.46
\pm S.D.		0.31	0.40	0.25	0.22	0.13

* BODY WEIGHT OF MICE = 21.7 ± 2.78

† KIDNEY WEIGHT = 391 ± 858

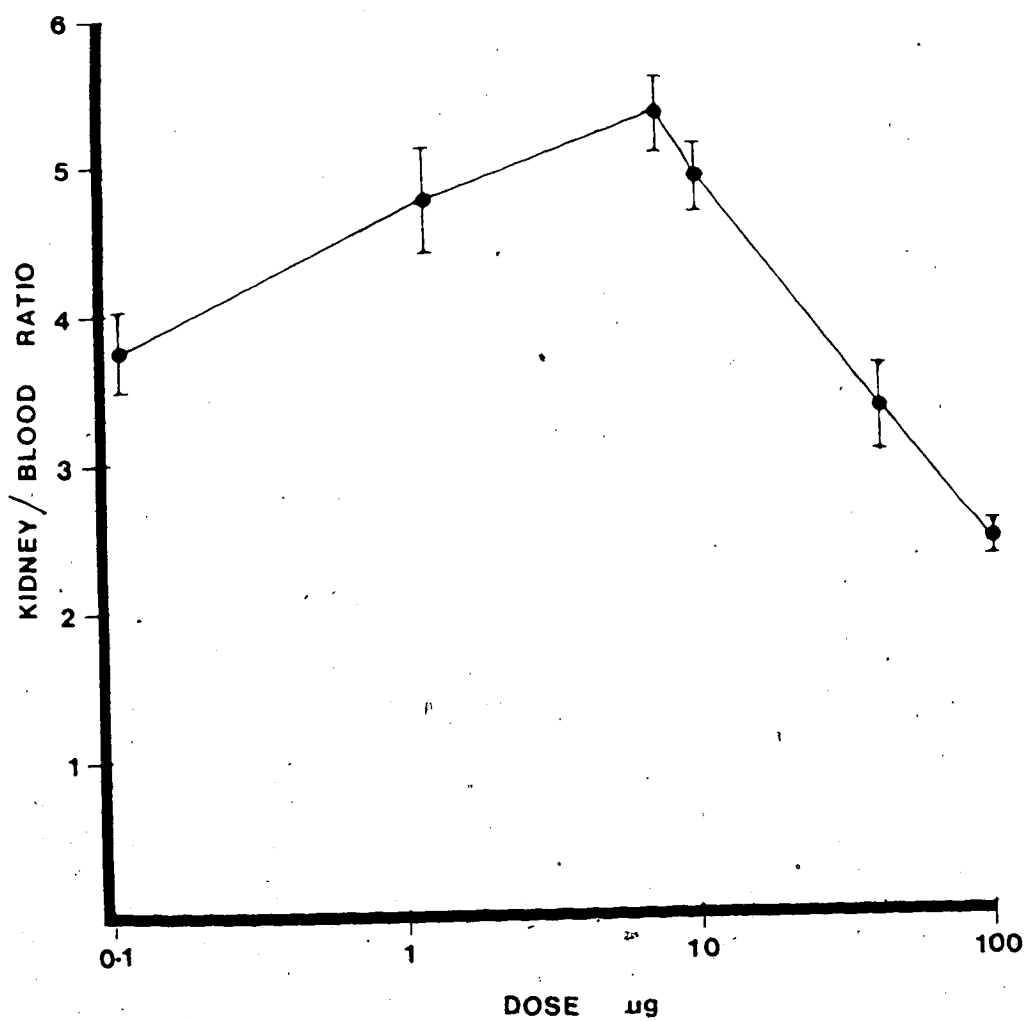


Figure 4.4 Kidney/blood ratio vs. injected dose of ^{125}I -PNA in CBA/CAJ mice.

order to establish whether these observations were true or whether the differences were dependent on the PNA stock material and labelling technique, an experiment was undertaken to compare the renal uptake of ^{125}I -PNA in four different strains of mice (AJ, c57b, CBA/CAJ and CAF1/J), using the same batch of ^{125}I -PNA labelled by the iodogen method. Although complete biodistribution studies were performed, only the % injected dose in kidneys is reported, as there appeared only minor differences in the ^{125}I -PNA levels in the remaining organ systems. Results confirm a strain-specific difference in the renal uptake and retention of ^{125}I -PNA in the kidneys of mice, as summarized in Table 4.3.

AJ and c57b mice showed similar % injected dose/organ estimates in the kidneys, with no significant difference demonstrated at 30 min, 6, 24 or 48 h P.I. CAF1/J mice demonstrated similar % injected dose/organ values in the kidneys at 30 min P.I. to AJ and c57b mice, however at later time points, the % injected dose/organ in kidneys was significantly lower than with AJ or c57b mice. These results appear to indicate a more rapid clearance of the radioactivity from the renal tissue into the urine, presumably because of a more efficient mechanism of tubular secretion of ^{125}I -PNA in CAF1/J mice.

A significant difference in the rate of renal accumulation and excretion of ^{125}I -PNA was seen in CBA/CAJ mice. The renal activity at 30 min P.I. was diminished in comparison to all other strains ($22.38 \pm 3.01\%$ Inj. dose/organ), and its clearance from the kidneys appeared to be of similar rate to the CAF1/J mice. These values obtained for CBA/CAJ mice appear to correspond more closely to those demonstrated in other animal species such as NZW rabbits, dogs and humans (see later results), and as such may indicate that this strain of mice is a more appropriate model for assessing the renal kinetics of PNA. It is also interesting to note that differences in the renal excretion rate of PNA in various strains of mice may, in part, explain the differences in tumour retention of PNA with murine tumour models such as the TA₁-Ha grown in AJ, CBA/CAJ or CAF1/J mice. The slower the renal excretion, the more likely the radiopharmaceutical is to localize within tumour tissue, resulting in higher tumour levels. This may support the differences in

Table 4.3: Renal Uptake of ^{125}I -PNA ($1\mu\text{g}$) in AJ, c57b, CBA/CAJ and CAF1/J strain mice*.

Time	Strain			
	AJ	c57b	CBA/CAJ	CAF1/J
30min.	37.42 ± 2.56	34.28 ± 2.65	$22.38 \pm 3.01^\dagger$	37.68 ± 2.04
6hrs.	9.11 ± 0.73	9.03 ± 1.96	$4.10 \pm 0.99^\dagger$	$6.36 \pm 0.55^\dagger$
24hrs.	1.50 ± 0.19	1.92 ± 0.22	$0.73 \pm 0.07^\dagger$	$1.18 \pm 0.06^\dagger$
48hrs.	0.73 ± 0.14	0.69 ± 0.22	$0.33 \pm 0.15^\dagger$	0.65 ± 0.10

* % injected dose in both kidneys (\pm S.D.).

† $p < 0.05$ (Students' t-test).

TA₃-Ha tumour activity demonstrated by Eu³³⁶ and Shysh *et al.*³⁴⁴ in previous reports.

Strain variations in the renal uptake of PNA may reflect fine differences in the distribution of membrane glycoproteins within the nephron, and thus indicate the sensitivity that PNA may offer in the respect to determining renal cellular glycoconjugates, receptor affinity, internalization rates, and tubular secretion rates. Eguchi *et al.*⁴³⁷ have also noted differences in the binding of the lectin Con A by the proximal tubule in two different strains of mice, indicating that there are often differences in the glycosyl content, as well as the density of membrane glycoproteins in the kidneys of various strains of mice.

4.2.2 Dynamic ¹³¹I-PNA renal scintigraphy in NZW Rabbits.

In order to study the renal uptake and excretion of ¹³¹I-PNA in more quantitative detail, NZW rabbits were employed as the test model. Dynamic gamma-camera renal scintigraphy was performed on control rabbits (N=4) and dynamic renal parameters were determined during the first hour P.I. These data were used as controls in subsequent experiments to determine the effect of various pharmacological agents on the rate of renal accumulation and excretion of ¹³¹I-PNA and are reported in Table 4.4.

Quantitative dynamic renal scintigraphy revealed consistent renal activity/time curves, resulting in consistent estimates of renal % Injected dose-at-peak and time-to-peak in four control NZW rabbits injected i.v. with ¹³¹I-PNA (Table 4.4, Figs. 4.5,4.6). Static scintigrams revealed that the kidney and bladder appeared to be the only major organ systems visualized up to 1 h P.I., confirming previous results with mice. The kidneys of control rabbits accumulated $19.6 \pm 4.3\%$ of the injected dose at peak (37.2 ± 6.9 min.), and $12.6 \pm 1.8\%$ of the dose was present in the bladder after 60 min. The kidney/liver ratio (calculated from normalized ROIs at 1 h P.I.) was 18.9 ± 1.8 in untreated animals.

Table 4.4 : 125 I-PNA Renal and Bladder Kinetics in NZW Rabbits*

PARAMETER	Controls (N=4)	A-GM ₁ disaccharide† (N=2)	Probenecid‡ (N=2)	Furosemide** (N=2)	Anti-PNA†† (N=2)	Epiglycanin††† (N=2)
Time-to-peak (min)	37.2 ±6.9	36.8 ±2.1	35.2 ±2.8	34.8 ±4.7	>60***	>60***
% Inj. Dose-at-peak (Both kidneys)	19.6 ±4.3	18.5 ±3.2	18.3 ±4.1	20.1 ±2.6	1.2*** ±0.6	5.9*** ±3.8
T 1/2 uptake (min)	13.7 ±3.6	13.9 ±1.8	14.6 ±2.2	13.9 ±2.8		
% Inj. Dose in bladder (1 h P.I.)	12.6 ±3.9	11.3 ±4.8	13.8 ±3.2	17.2 ±2.8	<1.0***	1.8***
Kidney/Liver ratio (1 h P.I.)	18.9 ±1.8	17.8 ±2.2	17.3 ±2.4	16.2 ±3.1	<0.01***	0.03***

* Derived from static and dynamic renal scintigraphy.

† 125 I-PNA:a-GM₁ disaccharide (1:1 molar ratio) incubated for 30 min prior to injection.

‡ 20 mg i.p. 30 min prior to 125 I-PNA.

** 2 mg i.p. 30 min prior to 125 I-PNA.

†† 120 μ g i.v. 30 min prior to 125 I-PNA.

††† 160 μ g i.v. 30 min prior to 125 I-PNA.

*** p < 0.01

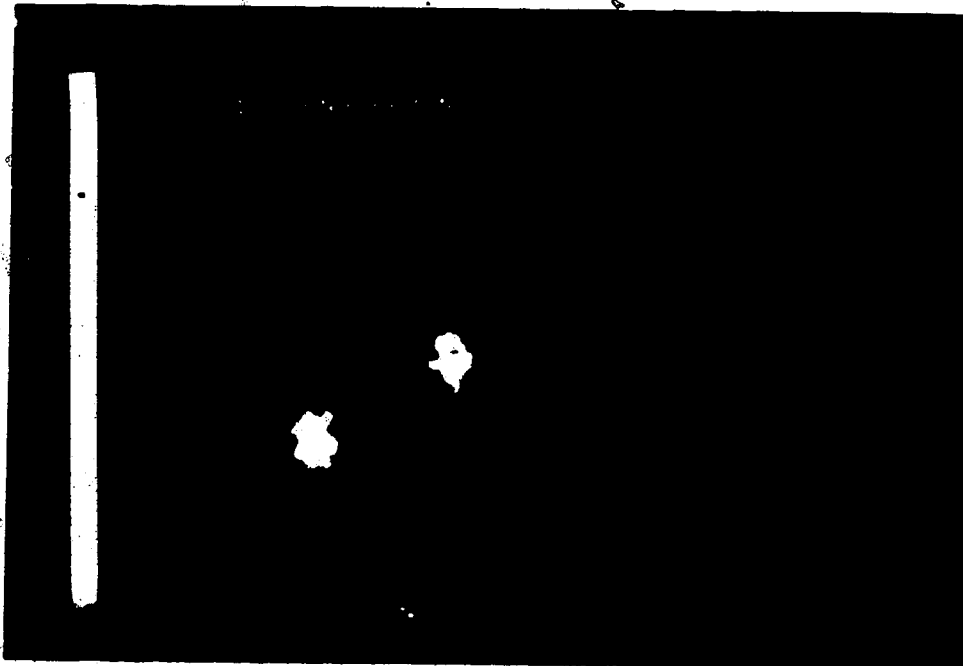


Figure 4.5 Static ^{131}I -PNA renal scintigram 60 min P.I. in NZW Rabbit.

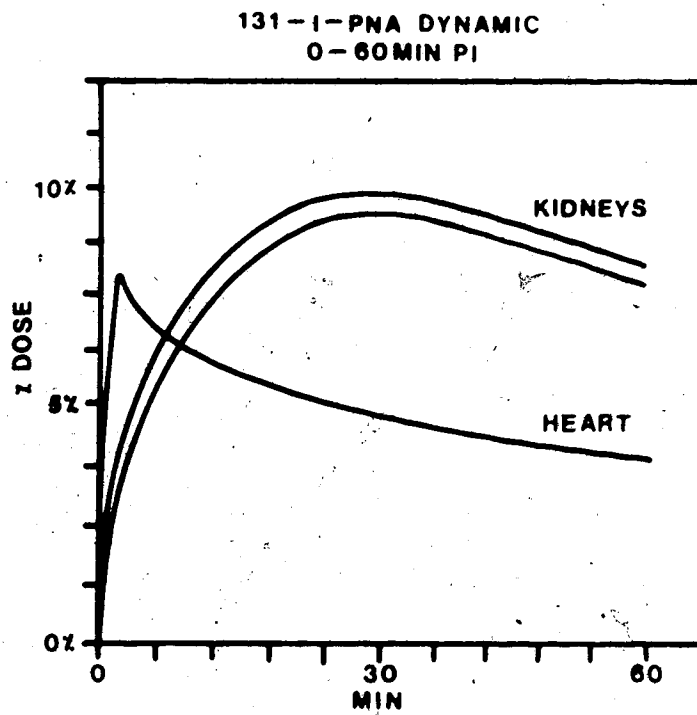


Figure 4.6 Dynamic Activity/time curve of ^{131}I -PNA in kidneys of NZW rabbit.

4.2.3 ^{131}I -PNA Dynamic and Static Renal Scintigraphy in Dogs.

Dynamic renal scintigraphy was determined in the four dogs for the first hour P.I., as described for the rabbit studies. Results indicated similar renal ROI kinetic profiles to those demonstrated for the rabbit studies, with the % injected dose-at-peak determined as $21.8 \pm 3.3\%$, and time-to-peak of 44.6 ± 4.8 min (Table 4.5). The % injected dose in bladder at 1 h P.I. was $12.8 \pm 5.3\%$, with little radioactivity demonstrated in the liver.

Table 4.5. Dynamic ^{131}I -PNA renal parameters in control and D-galactose infused dogs.

Parameter	Controls (N=4)	D-galactose† (N=2)
Time-to-peak (min)	44.6 ± 4.8	43.7 ± 3.8
% Inj. dose-at-peak (Both kidneys)	21.8 ± 3.3	10.9* ± 2.1
t $\frac{1}{2}$ uptake (min)	14.2 ± 2.8	15.2 ± 1.9
% Inj dose in bladder (1 h P.I.)	12.8 ± 5.3	4.7* ± 2.1
Kidney/liver ratio (1 h P.I.)	17.5 ± 2.8	14.2 ± 2.6

† 2.5 mg loading dose, 50 mg.min⁻¹ infusion.

* p < 0.05

Static scintigrams were determined at 1, 2, 3 and 24 h. P.I. and from the images obtained the % injected dose remaining in the kidneys was documented during the renal excretion phase of the ^{131}I -PNA 'renogram' (Fig 4.7). These data indicate that the activity in the kidneys declines at a similar rate to the plasma disappearance curve, resulting in only about 1% of the injected dose remaining in the kidneys at 24 h P.I.

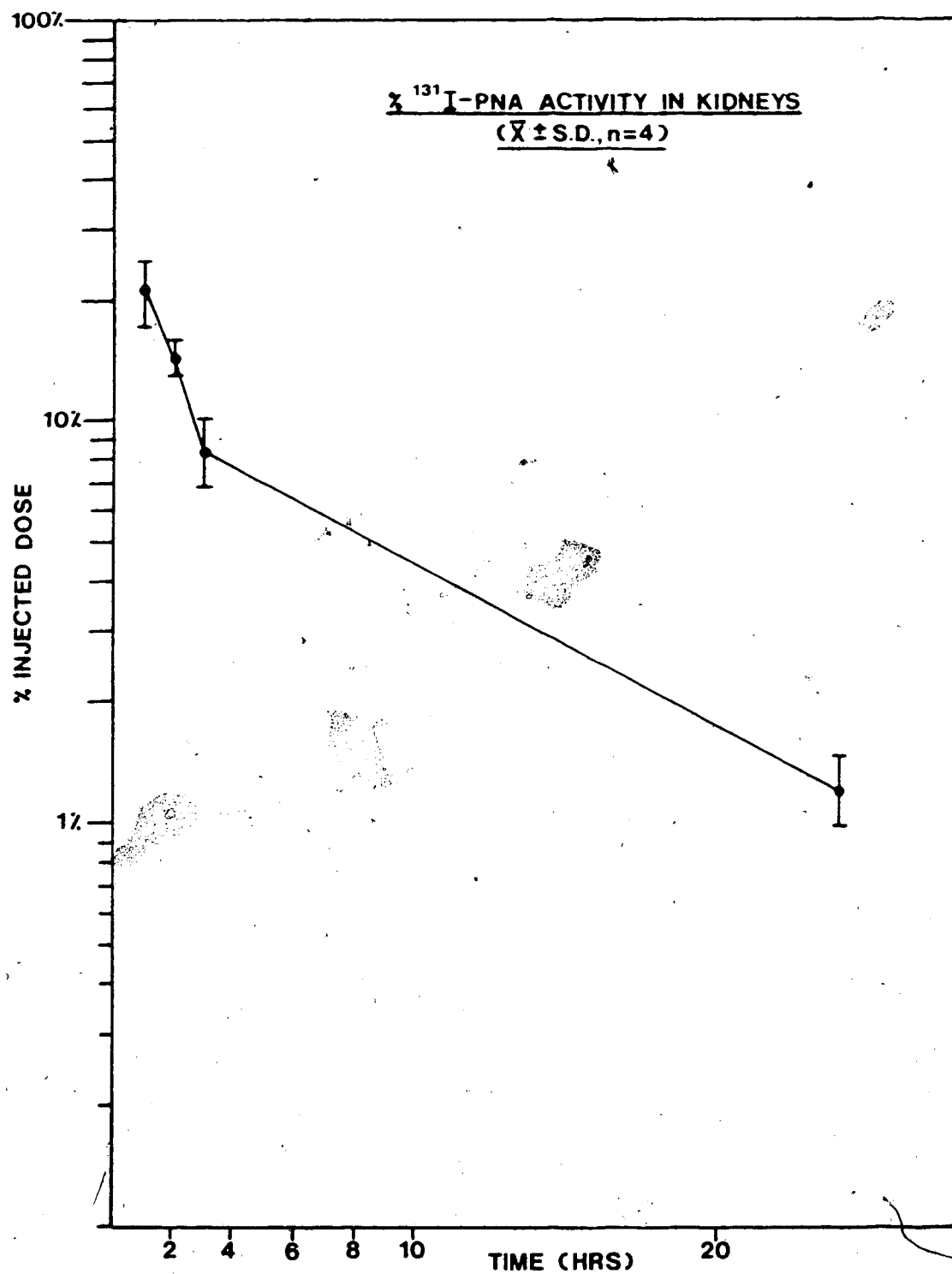


Figure 4.7 The % injected dose of ^{131}I -PNA remaining in kidney ROIs vs time in dogs.

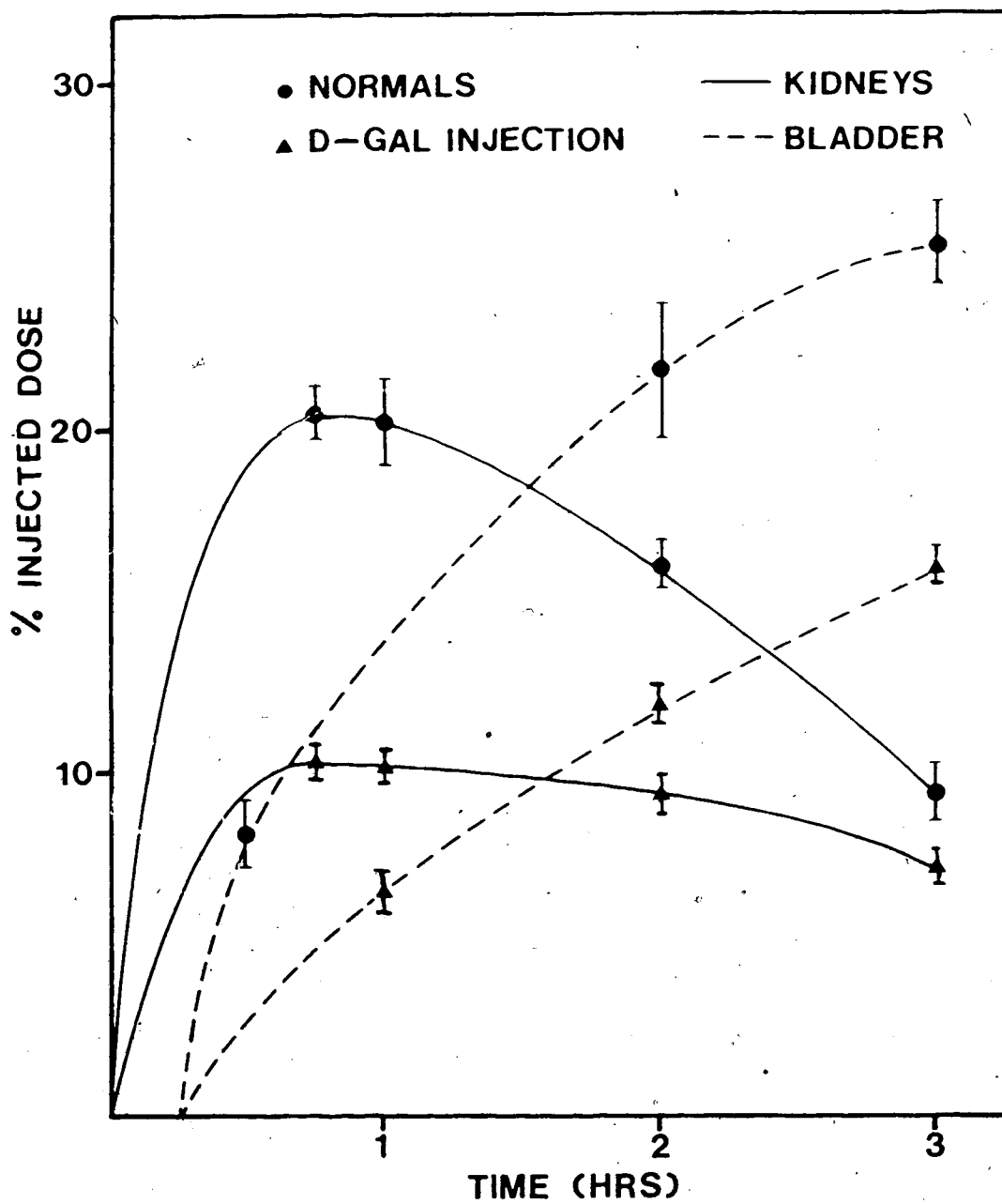


Figure 4.8 ^{125}I -PNA renal and bladder Activity/time curves in control dogs and dogs infused with D-galactose.

In order to study the effect of D-galactose (an inhibitor of PNA:T-F antigen interaction) on the renal ^{131}I -PNA kinetics, dynamic scintigraphy was undertaken in dogs during D-galactose infusion. The dogs were given an i.v. loading dose of 2.5 g D-galactose and this was followed by a constant infusion of $50 \text{ mg} \cdot \text{min}^{-1}$ during the study period. Five minutes after the commencement of the galactose infusion, $25\text{--}35 \text{ MBq } ^{131}\text{I}$ -PNA was injected i.v. and dynamic frames were acquired as previously described. The renal and bladder kinetic parameters were acquired as for the controls, and results statistically compared (students t-test).

A significant reduction in the % injected dose-at-peak and % dose in bladder at 1 h P.I. was demonstrated with the infusion of D-galactose ($p < 0.05$) while the time-to-peak was similar to control animals ($43.7 \pm 3.8 \text{ min.}$, Table 4.5, Fig 4.8) These results suggest that the sugar-binding site of PNA is an important configurational entity in the recognition of PNA by the kidney. D-galactose, being a specific inhibitor of the PNA:T-F antigen interaction, is able to inhibit the binding of PNA in the kidneys of dogs, when infused in high concentration. The most probable explanation for this finding is that PNA is bound to T-F antigen or 'T-F antigen like' receptors in kidney tissue. The rate of this interaction determines the rate of removal of PNA from plasma, and this can be altered by the infusion of inhibitory sugars, which competitively bind to the disaccharide binding site of PNA *in vivo*.

4.2.4 ^{131}I -PNA Scintigraphy in Patients with Metastatic Disease.

Tumour and dynamic renal scintigraphy was performed in 17 patients with known metastatic disease as part of a clinical trial to determine the efficacy of ^{131}I -PNA as a tumour imaging agent. As part of this trial, data was also determined as to the biodistribution pattern of ^{131}I -PNA in humans, with particular emphasis on the renal uptake of ^{131}I -PNA. Further information was derived as to the clinical the safety and tolerance of patients to the i.v. injection of ^{131}I -PNA.

4.2.4.1 Toxicity of PNA

No tissue-type sensitivity was noted in any patient with the intradermal injection of PNA prior to ^{131}I -PNA scintigraphy.

No hypersensitivity or anaphylactic reactions were observed following the i.v. injection of ^{131}I -PNA, and immediate or short term side effects were not present in any of the patients studied.

4.2.4.2 Tumour Scintigraphy with ^{131}I -PNA in Humans.

No visible uptake of ^{131}I -PNA on the analogue scintigrams (30 min-48 h) was evident at any site of known metastases in 16 of the 17 patients studied. A pulmonary metastatic lesion (measuring 3 cm in diameter), from a renal cell carcinoma, was visualized in one patient at 24 and 48 h P.I. Of interest, is that the solitary lesion visualized with ^{131}I -PNA in this study was in a patient who had a previous nephrectomy, and whose plasma clearance of ^{131}I -PNA was diminished in comparison to all others in the study group.

In a parallel study, Holt *et al.*⁴⁴ have demonstrated ^{131}I -PNA localization in two of eight patients with known metastases. Their imaging protocol included computer enhancement of the scintigraphic images, while no such manipulation was attempted in our study. In both studies, no lesion was demonstrated by ^{131}I -PNA scintigraphy, which was not evident on conventional radiology or nuclear medicine imaging. It appears from these preliminary studies that ^{131}I -PNA tumour scintigraphy holds little potential for the scintigraphic visualization of human tumours over existing radionuclide or radiological imaging techniques.

In eight patients, there was obvious uptake of ^{131}I -PNA demonstrated in the stomach at 6-48 h P.I. This activity did not appear to be associated with gastric contents, as it did not empty into the intestines at later times, and as such does not appear to be due to free ^{131}I . The specific binding of ^{131}I -PNA to gastric mucosa in some patients may indicate the presence of T-F antigen sites on these cells, a finding consistent with recent

histological findings of PNA receptors in the stomach⁴¹³. This finding was also noted in dogs administered ¹³¹I-PNA, particularly at later time points (>3 h P.I.).

In four patients, low-grade thyroidal uptake of activity was noted, despite the administration of Lugol's iodine, and is consistent with the presence of free iodide at later times (>6 h P.I.).

4.2.4.3 Renal Uptake and Excretion of ¹³¹I-PNA in Humans

All patients showed marked renal uptake of radioactivity following the injection of ¹³¹I-PNA (Fig. 4.9). Urinary bladder also contained significant activity within 30 min of injection, and the renal and bladder activity persisted for the duration of the imaging period (48 h).

Dynamic scintigraphy was performed in 5 patients and the dynamic renal parameters determined from the analysis of renal ROIs and exponential curve fitting of the activity/time curves (Table 4.6).

Three patients exhibited similar ¹³¹I-PNA renal uptake parameters (Mean % inj. dose-at-peak (both kidneys) = $20.5 \pm 0.7\%$, $t_{1/2}$ (uptake) = 18.8 ± 2.5 min, Table 4.6). One patient showed a slightly reduced rate of renal uptake in his single kidney ($t_{1/2}$ = 22.0 ± 1.2 min), however the % inj. dose-at-peak (18.2%) was similar to bilateral uptake in normal patients. A further patient demonstrated markedly reduced renal uptake of ¹³¹I-PNA in her single kidney, despite a normal serum creatinine. Interestingly, this patient was the only one who demonstrated discernable ¹³¹I-PNA uptake in her known metastatic lesion.

Holt *et al.*⁴⁴⁹ and Wilkinson *et al.*⁴⁵⁰ have reported that the ¹³¹I-PNA plasma disappearance curve in humans is best described by a two-compartment biexponential model, with $t_{1/2\alpha}$ = 44.5 ± 3.0 min, and $t_{1/2\beta}$ = 15.6 ± 2.0 . Urine collection recovered $26 \pm 11\%$, $34.8 \pm 8\%$, $60 \pm 5\%$, $79 \pm 9\%$, and $94 \pm 7\%$ of the injected dose at 2, 3, 9, 24, and 48 h P.I. respectively. The radioactivity present in the urine, particularly at early times P.I., was precipitable with TCA and appeared to maintain significant sugar-binding

Table 4.6 : Dynamic ^{125}I -PNA Renal Parameters in Humans.

PATIENT	SERUM CREATININE* ($\mu\text{mol.L}^{-1}$)	LEFT KIDNEY $t_{1/2}$ (min)	RIGHT KIDNEY $t_{1/2}$ (min)	LEFT KIDNEY AMPLITUDE (% Injected dose)	RIGHT KIDNEY AMPLITUDE (% Injected dose)	COMMENTS
T.H.	70†	14.9 ± 1.2	13.8 ± 1.3	9.8	10.2	Normal R.F.
N.O.	70	12.7 ± 1.1	16.8 ± 1.3	10.2	10.8	Normal R.F.
C.D.	80	18.3 ± 1.8	18.7 ± 1.8	9.4	9.9	Normal R.F.
R.O.	100	22.0 ± 1.2		18.2		Right Nephrectomy, Normal Left Kidney Function.
B.S.	90	N.D.		3.4		Right Nephrectomy, ?Impaired, Left Kidney Tubular Function

* Normal range 70 - 120 $\mu\text{mol.L}^{-1}$

† Not determined at time of study.

N.D. Not detected.

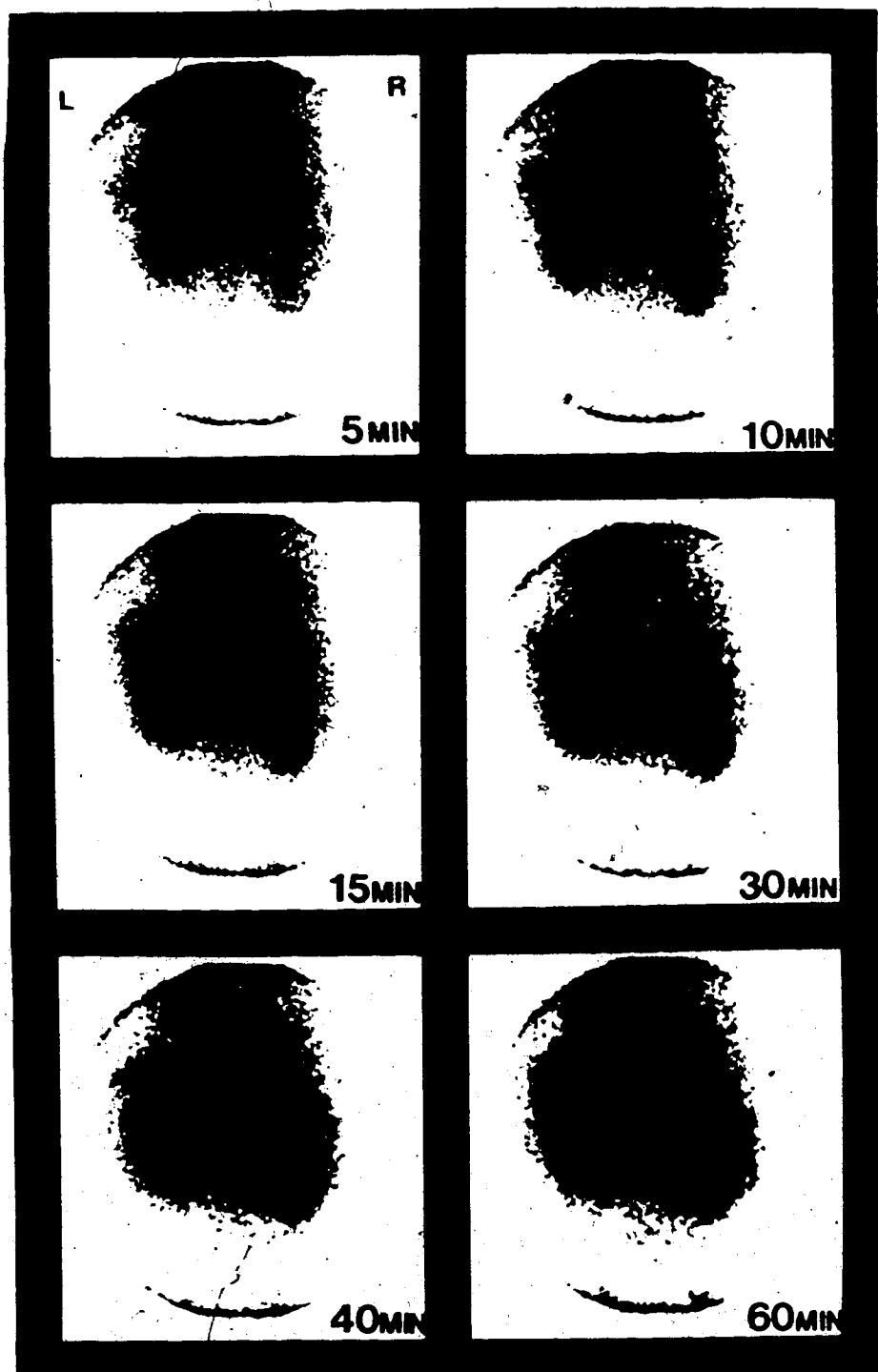


Figure 4.9 Typical Static ^{131}I -PNA renal scintigrams 0-60 min P.I. in humans.

specificity. Gel column chromatography on human urine has confirmed the presence of intact ^{131}I -PNA in the bladder contents of patients, a similar finding to ours in animal studies.

In detailed studies of the ^{131}I -PNA renal kinetics in humans, Wilkinson *et al.*⁴³ have indicated a % inj. dose-at-peak of slightly above 20%, and a time-to-peak of approximately 90 min in normal patients. Renal transit time for ^{131}I -PNA was calculated as 0.63 h, assuming a constant fractional rate, and was confirmed from the analysis of the plasma clearance data. Although detailed pharmacokinetic analysis was not performed in our patient study, qualitatively these results are in good agreement with our findings; and confirms the reproducibility of the ^{131}I -PNA renogram in normal patients.

4.3 THE MECHANISM OF RENAL UPTAKE AND EXCRETION OF ^{131}I -PNA.

The biodistribution studies performed above indicated that radiolabelled PNA is cleared from the plasma by the kidneys in mice, rabbits, dogs and humans. Further experiments were performed to quantify the plasma clearance and the rate of renal accumulation of iodinated PNA in animals, to study the cellular mechanism of PNA deposition, and to investigate the nature of the urinary excreted material observed in the animal experiments. These data have resulted in the postulation of a renal excretion pathway for PNA and the establishment of a dynamic renal model for the quantitation of the renal excretion of ^{131}I -PNA in animals and humans.

4.3.1 ^{131}I -PNA Plasma Pharmacokinetics and Clearance Studies in Dogs.

4.3.1.1 Plasma Pharmacokinetics and Clearance Determinations.

The plasma pharmacokinetic parameters of i.v. administered ^{131}I -PNA were determined in four normal mongrel dogs. Both the total plasma radioactivity/time curves and the protein-bound radioactivity/time curves (TCA precipitable counts) were analyzed by AUTOAN and NONLIN computer exponential curve fitting programs, and data was

normalized to 100% at $t=0$.

Both the total and protein-bound activity time curves (0-48 h. P.I.) were best described by a two compartment model ($r^2 = 0.998$ and 0.996 respectively) and showed reproducible results throughout the study (Fig 4.10, Table 4.7). There was a significant difference in the total and protein-bound plasma activity/time curves and the resulting parameters determined from pharmacokinetic curve fitting. The discrepancy in these values is due to the *in vivo* deiodination of the ^{131}I -PNA, resulting in the release of free ^{131}I .

For the protein-bound radioactivity, a rapid clearance is seen from plasma ($\text{Cl/TB} = 17.52 \text{ mL} \cdot \text{min}^{-1}$) from a volume of distribution of $1.27 \pm 0.48 \text{ L}$. The low V_d calculated from all dogs indicate that ^{131}I -PNA is distributed within the plasma compartment after administration, with little or no tissue or plasma protein binding. Red cell binding determinations indicated insignificant binding ($<1\%$) of ^{131}I -PNA to erythrocytes following i.v. injection.

^{131}I -PNA exhibits a rapid removal from plasma (as indicated by $t_{1/2\alpha}$ of $0.31 \pm 0.03 \text{ h}$ and $t_{1/2\beta}$ of $1.19 \pm 0.16 \text{ h}$). Although plasma decay is demonstrated beyond 6 h P.I., statistically the model could not distinguish the slope of this line from that of a straight line with slope of 1.

4.3.1.2 Urine analysis.

The urine from the dogs was collected for 48 h. following the i.v. injection of ^{131}I -PNA, initially by bladder catheterization, and then from gross collection while the dogs were housed in metabolic cages. The % of injected dose in urine was calculated for all collection periods and also for the complete collection period.

During the first hour P.I., $14.3 \pm 2.1\%$ of the injected dose was present in urine (Table 4.8), while the cumulative 24 and 48 h urine collection resulted in 65.4 ± 6.4 and $73.5 \pm 9.8\%$ of the dose being recovered respectively. TCA precipitation and asialo-GM₁ synsorb binding assays revealed that in the early period (0-6 h.) P.I., the majority of the excreted radioactivity was protein-bound, and retained specific binding to the immobilized

Table 4.7 : Normalized Biexponential curve-fitting estimates of ^{125}I -PNA Plasma Radioactivity in Dog†

	A_0 (%)	$T_{1/2\alpha}$ (H)	B_0 (%)	$T_{1/2\beta}$ (H)	V_d (L)	Cl/TB (mL.min ⁻¹)
TOTAL PLASMA COUNTS $R^2 = 0.998$ *	86.32 ± 8.27	0.45 ± 0.09	20.10 ± 8.21	14.78 ± 2.81	1.27 ± 0.48	8.25 ± 3.72
PROTEIN COUNTS $R^2 = 0.996$ *	68.23 ± 7.41	0.31 ± 0.03	39.75 ± 7.81	1.19 ± 0.16	1.27 ± 0.48	17.52 ± 8.74

† = From the biexponential equation $A = A_0 e^{-\alpha t} + B_0 e^{-\beta t}$

* = Correlation coefficient

Table 4.8 : Urine Analysis following i.v. Administration of ^{125}I -PNA in Dogs.
(Mean \pm S.D., N=4)

COLLECTION PERIOD (H)	% OF INJECTED DOSE IN BLADDER	% PROTEIN-BOUND RADIOACTIVITY (TCA precipitation)	% ASIALO-GMI SYNORB BINDING
0 - 1	14.3 \pm 2.1	92.4 \pm 2.1	67.1 \pm 4.2
1 - 3	15.8 \pm 4.9	90.7 \pm 4.0	60.2 \pm 5.4
3 - 6	13.7 \pm 3.2	75.4 \pm 5.2	51.8 \pm 6.2
6 - 9	11.8 \pm 1.9	59.3 \pm 4.1	35.4 \pm 4.1
9 - 24	9.9 \pm 2.0	23.1 \pm 2.7	18.6 \pm 2.9
24 - 48	8.1 \pm 3.2	15.2 \pm 3.1	11.2 \pm 3.2
CUMULATIVE 48 H URINE EXCRETION	73.5 \pm 9.8		

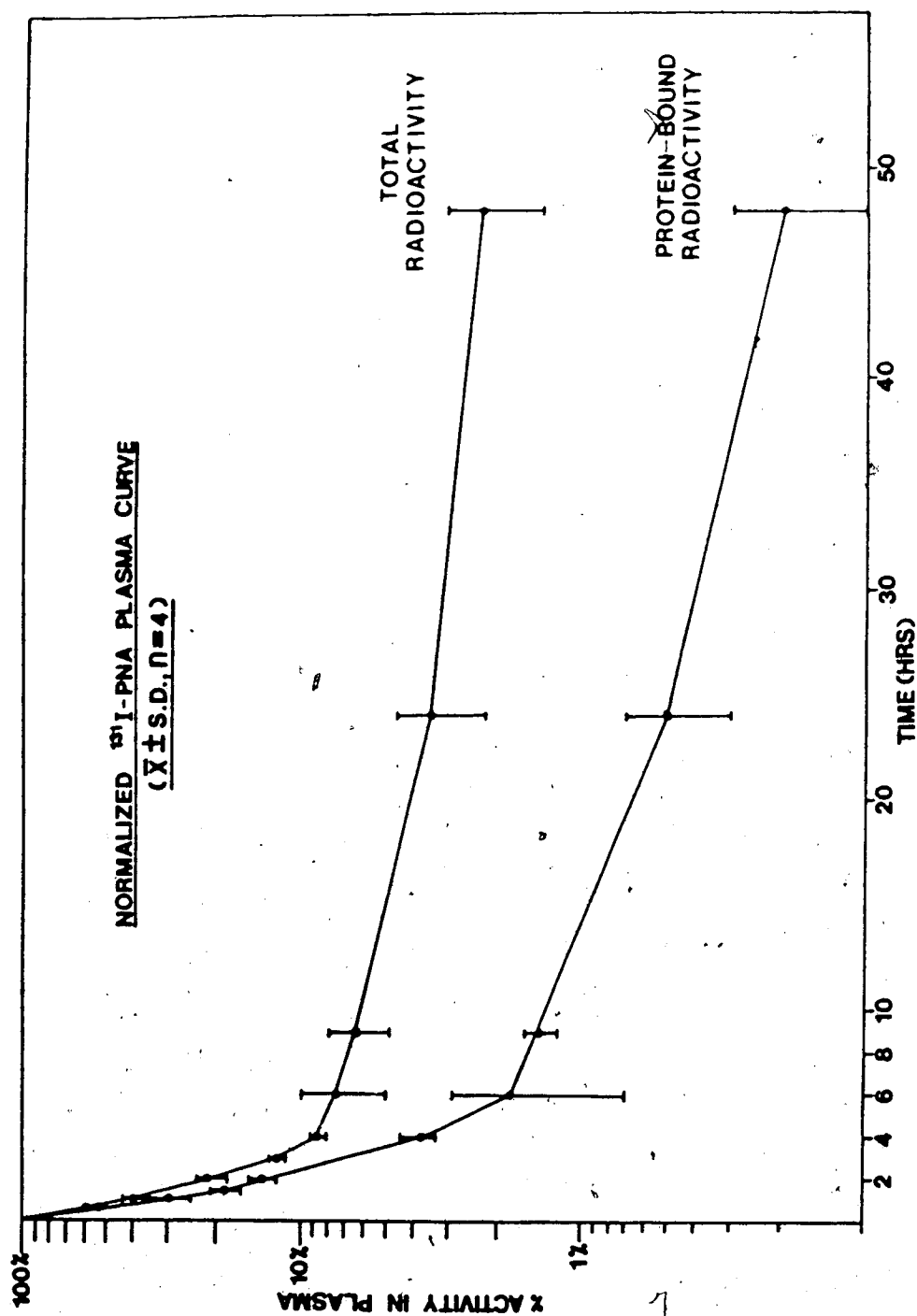


Figure 4.10 Normalized plasma activity/time curves of total radioactivity and protein-bound radioactivity following i.v. administration of 125 I-PNA in dogs

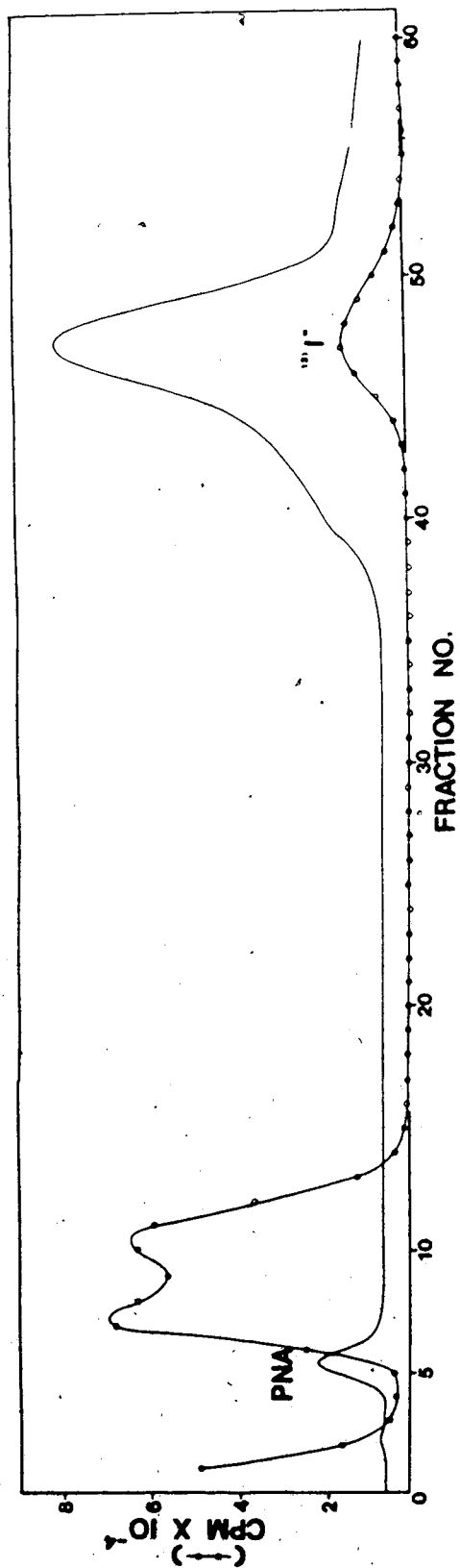


Figure 4.11 Biogel P100 gel column elution profile of urine contents 1 h following iv administration of ¹¹¹I-PNA in dogs

a-GM₁ disaccharide.

These results strongly indicate that ¹²⁵I-PNA is excreted by the kidneys in an intact form, a remarkable finding bearing in mind that PNA is a protein of 110,000 molecular weight, and is unlikely to be filtered by the glomerulus. To confirm these results and to further characterize the size of the urinary excreted material, aliquots of the recovered urine were subjected to gel column chromatography with Biogel P100 (exclusion limit 100,000 M.W), and both the radioactivity and protein elution profiles were determined. The elution profile determined for the 0-1 h urine aliquot confirmed that a significant proportion of the radioactivity co-eluted with PNA at the void volume. The elution profile also revealed the presence of lower molecular weight protein fragments, and a small proportion of free ¹²⁵I- (Fig 4.11). These are presumably proteolytic fragments from the degradation of PNA during renal transit. At later time points, the proportion of free ¹²⁵I increased relative to intact ¹²⁵I-PNA, a finding consistent with the TCA precipitation results reported in Table 4.8.

4.3.2 Histological determination of PNA binding in the kidneys of CBA/CAJ mice, NZW rabbits, and dogs.

In order to determine the cellular structures to which PNA binds after i.v. injection, histological examination of kidney slices was undertaken following the i.v. injection of fluorescein-labelled PNA (FITC-PNA) and rhodamine-labelled PNA (Rho-PNA), using fluorescent microscopy. Ten micrograms of either FITC-PNA or Rho-PNA were injected i.v. into CBA/CAJ mice, and the kidneys removed 3 h. P.I., fixed and examined by fluorescent microscopy (Fig 4.12).

Results revealed that fluorescence was confined predominantly to the proximal tubules of the cortex, with no staining seen in the glomerulus, and some faint staining evident in a small percent of medullary cells, which appeared to be either the distal tubular cells adjacent to the collecting ducts or early collecting duct parenchymal cells themselves. The most intense

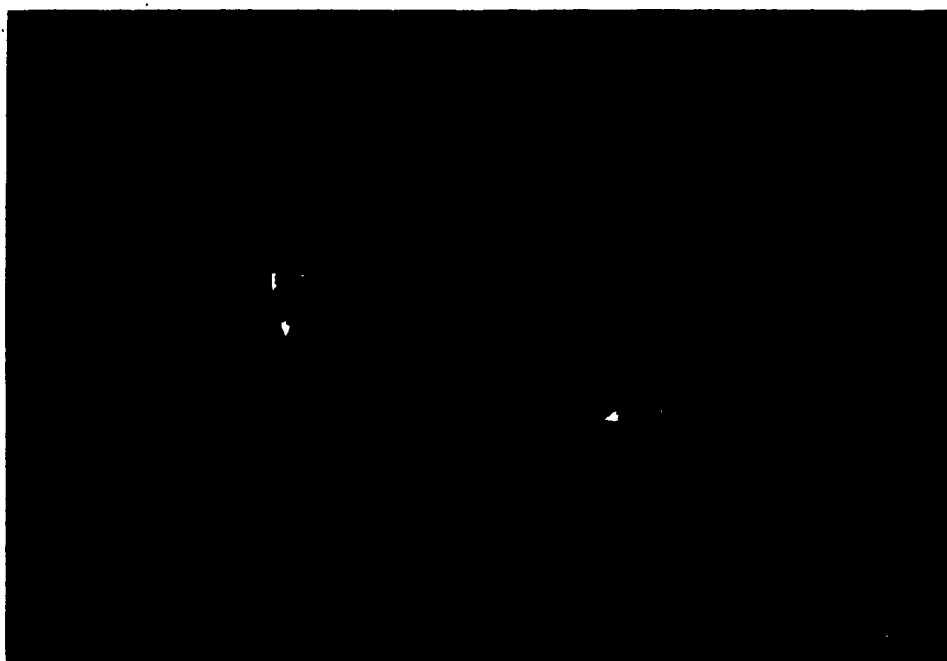


Figure 4.12 Fluorescent microscopical cortical section of CBA/CAJ mouse kidney 3 h following i.v. administered FITC-PNA. G = Glomerulus, PT = Proximal tubule.

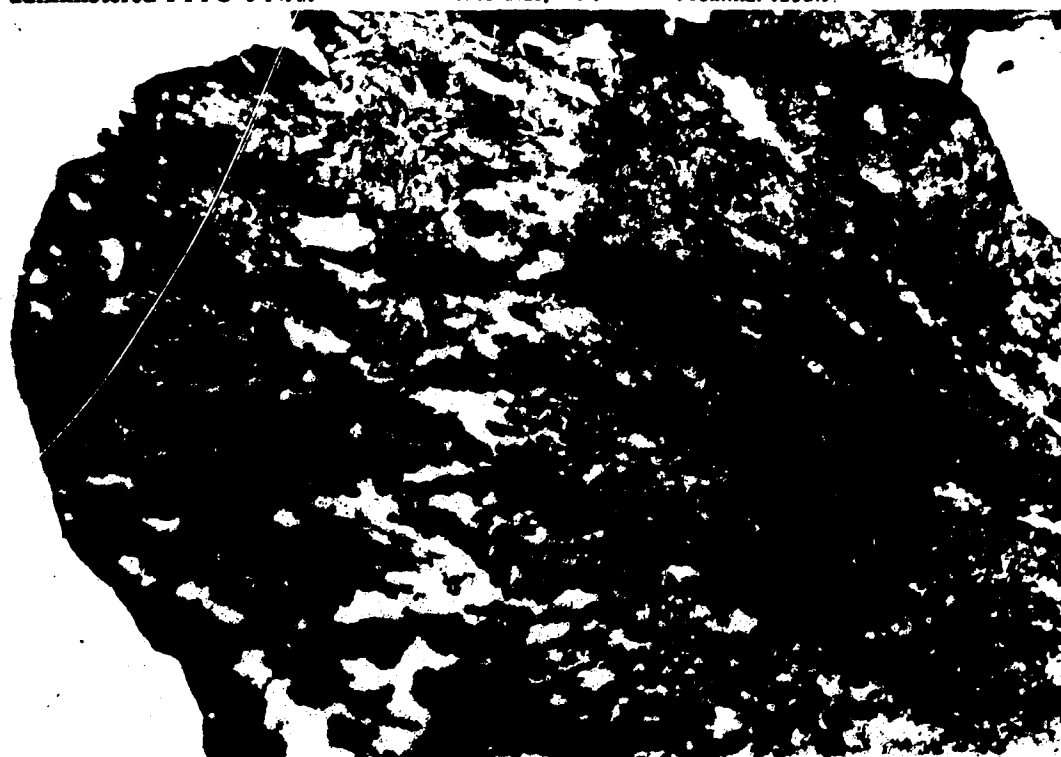


Figure 4.13 Immunoperoxidase stained section of whole CBA/CAJ mouse kidney (1 h P.I. PNA).



Figure 4.14 Immunoperoxidase stained cortical kidney section of CBA/CAJ mouse injected with PNA (1 h P.I.). bm = Basement membrane

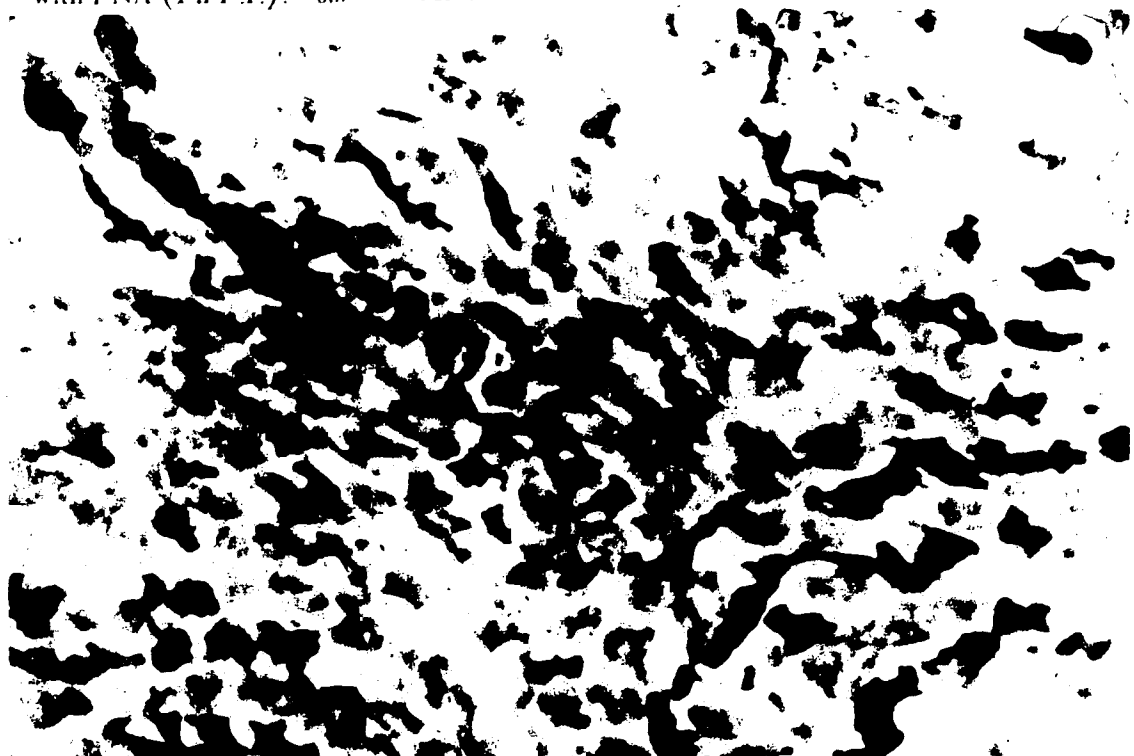


Figure 4.15 Immunoperoxidase stained medullary kidney section of CBA/CAJ mouse injected with PNA (1 h P.I.).

staining was demonstrated on the basement membrane of the proximal tubules, with staining also evident on the luminal membrane of these cells. Some fluorescence was seen intracellularly, however the exact localization of fluorescence was difficult to resolve. The collecting duct cells stained also showed prominent basement membrane and luminal membrane staining, as with the proximal tubules.

Using control animals, in which saline alone had been injected, some autofluorescence was seen in the cortical proximal tubules, which made interpretation of FITC-PNA micrographs difficult. Limitations were also expressed as to the specific nature of the fluorescent pattern seen in the kidneys, due to the inability of this technique to distinguish between free or PNA bound fluorescein. Because there existed the possibility that the FITC label may dissociate *in vivo*, thus indicating the presence of free fluorescein in the kidney, a new technique was developed using immunoperoxidase staining of kidney sections following i.v. PNA administration.

Following preliminary studies to determine the appropriate dose required for adequate staining, and the fixing and staining method most suitable for the visualization of PNA in the kidney, a study was undertaken in mice, rabbits and dogs using this technique. Animals were sacrificed between 10 min-24 h after the i.v. administration of 10 μ g PNA in CBA/CAJ mice, 300 μ g PNA in NZW rabbits and 500 μ g PNA in mongrel dogs.

The staining pattern determined showed marked similarities to the fluorescein results previously determined, except that control kidneys did not demonstrate significant background staining (Figs. 4.13,14,15). PNA was almost exclusively confined on the basement membrane of cortical proximal tubules and cells of the early collecting duct, at early times P.I. Internalized staining was demonstrated within the proximal tubules, as well as some luminal membrane staining, which became more evident at later times P.I. Staining intensity was noted to diminish in all sections with time, however the relative staining intensity between cortical and medullary cells remained constant throughout the 24 h study.

The staining pattern demonstrated was very similar in mice, rabbits, and dogs, with the proximal tubular basement membrane the most highly stained structure. The collecting duct cells stained in mice were also marked in rabbits and dogs, however the relative intensity of staining was diminished in the dogs, while in rabbits these cells appeared slightly more predominant. Again, internalized staining was seen within the proximal tubules, and luminal membrane staining was evident in all species studied.

Major differences exist in the PNA staining pattern seen in mouse, rabbit and dog kidney sections when PNA is used as a histological agent, as opposed to that seen following i.v. injection of PNA. In mice, the luminal membranes of proximal tubules, distal tubules, and collecting duct are the most predominantly stained structures, when PNA is applied to fixed sections^{426,427}. Staining has also been noted in the glomerulus, as well as to segments of the loop of Henle. In rabbits, LeHir *et al.*^{431,432} have documented staining to the luminal membrane of distal tubules, as well as intense interaction with collecting duct cells thought to be the intercalated cells. In the dog the luminal membrane of distal tubules interacts with PNA, while little staining is seen in other portions of the nephron⁴²⁴.

The delivery of PNA to the kidney via the renal blood supply results in a different staining pattern to that seen when PNA is incubated with fixed sections or perfused into isolated nephrons. Because the luminal structures are protected from interacting directly with PNA in plasma, these structures are not stained as predominantly as that seen in section. PNA delivery is limited initially to the basement membranes of the glomerulus, tubules and collecting ducts, with only those in the proximal tubules and collecting duct displaying selective staining. Intracellular PNA is demonstrated, indicating that PNA is actively transported into the tubular cell, and faint luminal staining is only evident after PNA has been transported to the lumen.

4.3.3 Proposed proximal tubular transport mechanism for PNA.

In view of the results determined in the above animal studies, it is clear that a unique transport mechanism is involved in the renal excretion of PNA. The immunoperoxidase studies

have revealed that the basement membrane of proximal tubules is largely responsible for the removal of PNA from the blood compartment, and further, that intracellular PNA can be identified in these cells. The identification of functionally intact PNA in the urine of dogs indicates that a significant proportion of the injected dose is excreted intact, while there is also evidence for some degradation of the protein during excretion. The rate of renal accumulation can be inhibited by D-galactose, a specific inhibitor of the PNA:T-F antigen interaction. It appears that there exists T-F antigen or 'T-F antigen-like' receptors on the basement membrane of mouse, rabbit and dog proximal tubular basement membranes, and that following the *in vivo* interaction with PNA, the receptor is internalized, and ultimately excreted into the lumen of the nephron. The rate of this transport is kinetically consistent within a single strain of mice, but may vary between strain, or between species.

Because PNA is an acidic protein ($pI = 5.95$) of high molecular weight (110,000 daltons)¹³² it is unlikely that it would be filtered by the glomerulus¹³⁰. This is confirmed by the absence of staining in the glomerulus, seen in the immunoperoxidase-stained kidney sections following i.v. administration of PNA. It is also unlikely to be passively transported from the peritubular capillaries to the lumen through the tight spaces of the tubular parenchymal cell, due to similar molecular weight limitations¹³⁰⁻¹³³. The transit of PNA from the peritubular capillaries to the lumen is most adequately explained by an active process of transport by proximal tubules, and to a lesser extent, by the intercalated cells of the collecting ducts. The mechanism is most likely one of endocytosis/exocytosis, which may result in some degree of protein degradation, although significant levels of intact PNA are still present in the urine. This is diagrammatically represented in Fig 4.16.

Receptor-mediated endocytosis is a pathway by which proteins, hormones, viruses and toxins enter cells, and has been the topic of recent review⁴⁴⁰⁻⁴⁴². Straus⁴⁴³ initially observed that several proteins were internalized by endocytosis in various segments of the nephron, a process which results in the production of coated vesicles⁴⁴⁴. Following protein interaction with the membrane receptor, clatherin-coated pits are formed⁴⁴⁵, which act as sites for internalization by

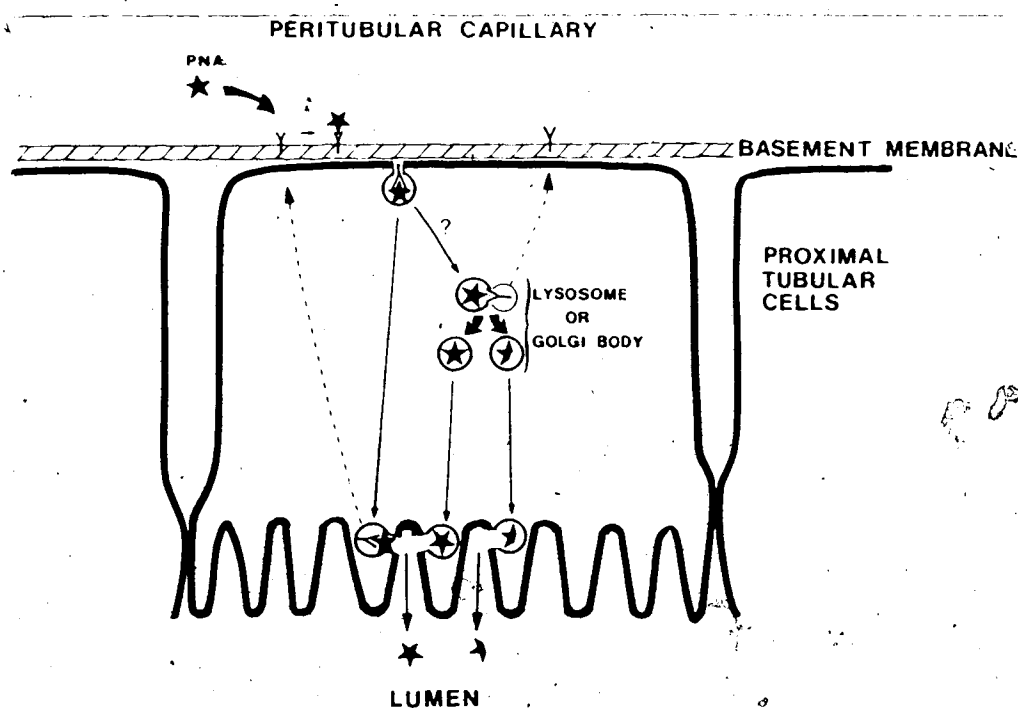


Figure 4.16-Proposed mechanism of PNA transport by proximal tubular cells of mouse, rabbit and dog.

pinocytosis⁴⁶². The receptor-ligand complexes either directly form receptosomes⁴⁶⁰, or are transported to pre-existing endosomes⁴⁶¹. The receptor-ligand complex undergoes dissociation within the acidic endosomal compartment, and results in the release of free ligand, which may undergo further catabolic degradation at the lysosome or golgi apparatus, while the receptor may be recycled back to the plasma membrane^{461,466}. This process has been identified in several cell lines including fibroblasts, macrophages, hepatocytes, as well as renal tubular cells^{460,462}. Other lectins, such as Con A, have been shown to be internalized via this mechanism⁴⁶⁷. The delivery time observed for the internalization and lysosomal deposition of protein is between 5-50 min.⁴⁶¹, which corresponds to the time of renal transit of PNA into the bladder of all animals studied.

The endocytotic pathway of proteins reabsorbed from the luminal membrane of proximal tubules has been extensively studied, as recently reviewed by Maunsbach⁴⁵⁹, and is known to be the major pathway for the reabsorption of proteins from the glomerular ultrafiltrate of the nephron. The two main cellular components involved in the protein uptake by the proximal tubule cells are the endocytic vacuoles and the lysosomes. The initial binding of protein molecules to the luminal plasma membrane induces the endocytotic process, but this is dependent on the affinity of the protein to the specific receptor. Receptors for ferritin, albumin, hemoglobin, as well as β_2 -MG, have been identified on the luminal membrane of proximal tubules⁴⁵⁹.

While the cellular uptake of proteins from the tubular lumen is well documented, peritubular uptake is more controversial. On the basis of studies with intact kidneys it has been suggested that some proteins, including insulin⁴⁶⁸ and β_2 -MG⁴⁶⁹, can be taken up by proximal tubular cells from the peritubular capillary blood. Peritubular endocytotic vesicles have been noted in the tubules of several submammalian species^{470,471}, however these have not been shown to be present in large quantities in higher species. Thus, this mechanism appears to be of little significance in the active transport of proteins by mammalian tubules. Our results suggest that PNA appears to be excreted by the proximal tubule in this manner, although it must be noted

that the isolation of the receptor or the *in vitro* study of this process has not been undertaken to date. Further work is warranted to characterize this process in more detail.

Although reabsorption of ^{131}I -PNA from the lumen of the nephron has not been studied, it appears that the similarities in rates of both plasma radioactivity and renal radioactivity following peak would suggest that this is not involved. In histological studies, the staining intensity of all cells was noted to diminish in a consistent manner, giving further evidence for the lack of tubular reabsorption. Further renal physiological studies are, however, required to exclude reabsorption conclusively as a contributing factor in the renal handling of ^{131}I -PNA.

4.4 FACTORS AFFECTING THE RENAL UPTAKE AND EXCRETION OF ^{131}I -PNA.

4.4.1 Agents present in the Circulation.

Previous studies in dogs had revealed that the inhibitory sugar D-galactose, reduces the renal binding of ^{131}I -PNA in dogs. A further series of experiments were subsequently performed to determine the effect of circulating agents such as glycoproteins, antibodies, and pharmacological agents (probenecid and furosemide) on the rate of renal uptake and excretion in various animal models.

4.4.1.1 ^{131}I -PNA:asialo GM_1 disaccharide renal scintigraphy in NZW rabbits.

The terminal disaccharide of the α - GM_1 antigen (β -D-Gal-(1 \rightarrow 3)- β -GalNAc) is a known inhibitor of PNA disaccharide binding²⁶. To determine if this disaccharide, incubated with ^{131}I -PNA, affected the renal binding kinetics of the lectin, an experiment was performed where the α - GM_1 disaccharide was mixed with ^{131}I -PNA (at 1:1 molar ratio) for 30 min prior to the i.v. injection of the mixture into NZW rabbits.

No significant difference was demonstrated in any of the renal or bladder parameters between controls or rabbits injected with ^{131}I -PNA incubated with the asialo- GM_1 disaccharide (Table 4.4).

4.4.1.2 ^{131}I -PNA renal scintigraphy in Probenecid and Furosemide treated NZW rabbits.

The pharmacologically active agents probenecid and furosemide are known to directly effect the transport of agents in the kidney. Probenecid inhibits the secretion of organic acids by the proximal tubules, while furosemide inhibits the reabsorption of both Na^+ and Cl^- in the ascending Loop of Henle⁴². The effect of therapeutic doses of probenecid and furosemide on the renal dynamics of ^{131}I -PNA in NZW rabbits was determined by comparing the renal dynamics of animals pretreated with these agents 30 min prior to the i.v. injection of ^{131}I -PNA.

No significant difference was demonstrated in the dynamic renal parameters determined for NZW rabbits injected i.p. with probenecid (10 mg/kg) 30 min prior to the ^{131}I -PNA study (Table 4.4).

Furosemide (1 mg/kg i.p.) treated rabbits showed a minor increase in the % injected dose in bladder at 60 min P.I., however this was within experimental error (Table 4.4). All other parameters were similar to controls. The minor increase in the bladder transit time is probably due to an increase in urine flow from the kidney, due to diuresis, or inhibition of the reabsorption of free I^- in the ascending Loop of Henle.

4.4.1.3 ^{131}I -PNA Renal Scintigraphy in NZW Rabbits injected with anti-PNA IgG Antibodies.

In order to determine the effect of circulating anti-PNA IgG antibodies on the biodistribution of ^{131}I -PNA, a set of experiments were undertaken in NZW rabbits which were primed with anti-PNA IgG antibodies. Renal scintigraphy was performed 1 h following the i.v. injection of 120 μg rabbit anti-PNA IgG antibodies, and the static and dynamic scintigrams were compared to control animals.

The administration of rabbit anti-PNA IgG antibody (120 μg) i.v. 1 h prior to the injection of ^{131}I -PNA had a dramatic effect on the whole body scintigraphic pattern seen with ^{131}I -PNA (Figs. 4.17, 4.18). Significant accumulation was demonstrated in the liver ($72.2 \pm 5.9\%$ of injected dose at 30 min P.I., time-to-peak 12.5 ± 2.5 min) while the spleen

was not visualized in the static scintiphotos. The activity visualized in the kidneys was virtually that of background, and thus difficult to quantify with any degree of accuracy. Because of the rapid accumulation of ^{131}I -PNA in the liver, in the presence of anti-PNA antibodies, it appears that the complexation to PNA is specific. These experiments do not elucidate the mechanism or site of the complexation, this may occur in plasma, or may occur at the liver hepatocyte membrane. It would appear from the scan findings that the resultant PNA-antibody complex is not cleared by the Kupffer cell phagocytosis but more likely by a specific mechanism by either Kupffer cells or hepatocytes. Reticuloendothelial clearance is usually associated with both spleen and liver uptake, analogous to that seen with radiocolloids, and the absence of splenic activity may indicate specific hepatic clearance in this case.

Recent studies with radiolabelled murine monoclonal IgG antibodies have indicated a mechanism of liver accumulation of injected Mab's in mice²³. The liver accumulation is thought to be due to binding of the Fc arm of the Mab's to a specific receptor situated on the hepatocyte cell surface. The liver accumulation is not demonstrated with Fab or F(ab'), fragments of the same antibody, and can be saturated by the administration of carrier Mab. It is therefore plausible that the anti-PNA antibody may localize on similar receptors in the rabbit liver, and may bind ^{131}I -PNA at this site following injection. Because the receptor appears specific for the Fc portion of the antibody, the antigen-recognizing arm may remain biologically intact and able to bind circulating ^{131}I -PNA at the membrane surface. It must be noted, however, that this finding is controversial and detailed studies have not been performed to elucidate this mechanism more fully.

4.4.1.4 ^{131}I -PNA Renal Scintigraphy in NZW Rabbits injected with Epiglycanin.

Peanut lectin is known to elicit strong binding to glycoproteins containing the terminal disaccharides of the T-F and α -GM₁ antigens³³⁹⁻³⁴⁶. In order to determine the effect of high circulating glycoprotein concentrations on the biodistribution of ^{131}I -PNA,

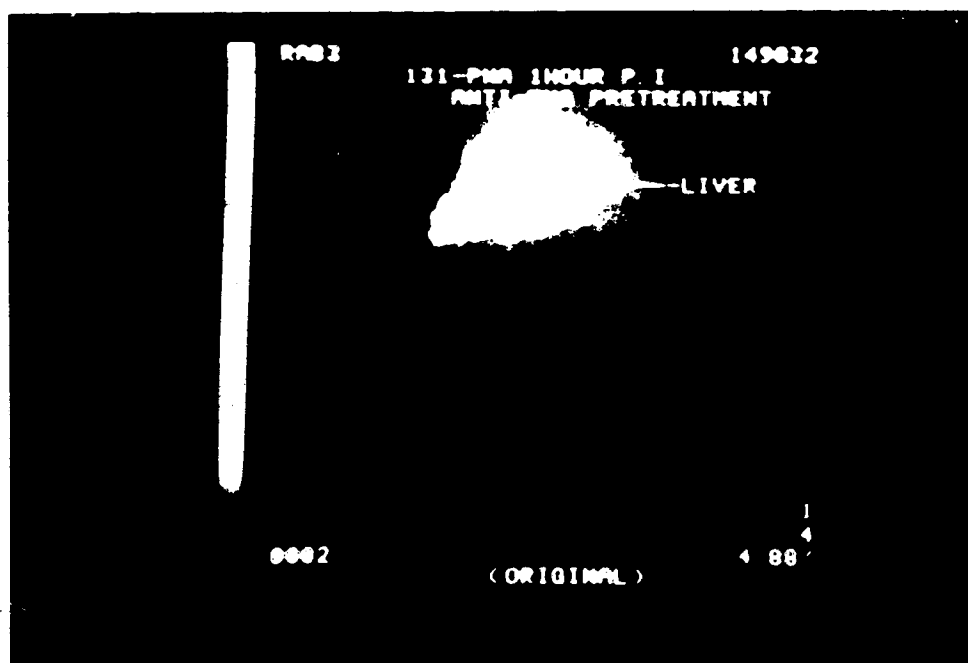


Figure 4.17 Static ^{131}I -PNA renal scintigram 60 min P.I. following administration of anti-PNA antibody in a NZW rabbit.

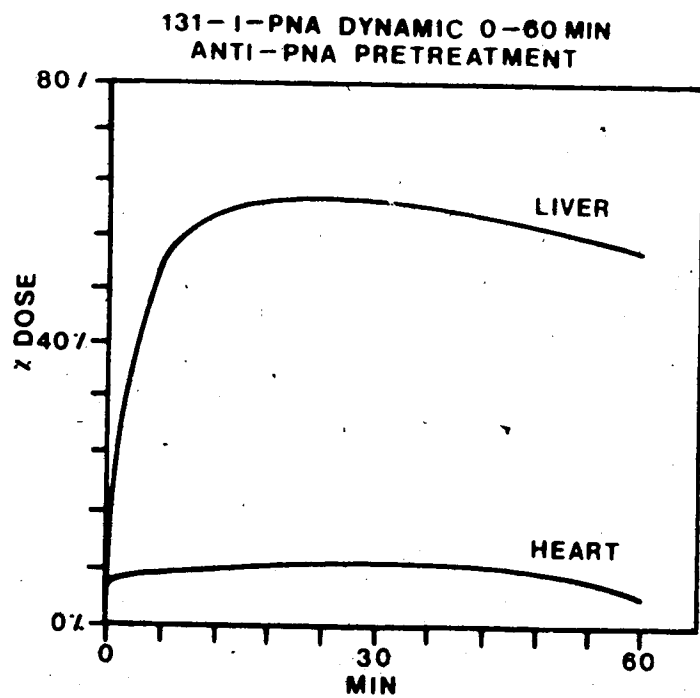


Figure 4.18 Dynamic liver Activity/time curve of ^{131}I -PNA following administration of anti-PNA antibody in a NZW rabbit.

biodistribution and renal dynamic scintigraphy was performed in NZW rabbits, which had previously been injected with a large i.v. dose of the glycoprotein epiglycanin.

Epiglycanin is a large (500,000 MW.) glycoprotein complex containing approximately 520 O-glycosyl-linked carbohydrate chains^{397,400}. It is derived from the TA₃-Ha ascites murine tumour line and is known to contain the immunodeterminant disaccharides of the T-F antigen (β -D-Gal-(1 \rightarrow 3)- α -GalNAc)^{402,406}. In the test-tube, epiglycanin binds strongly to PNA, resulting in the formation of a gelatinous material with high viscosity. This precluded our studying the biodistribution of *in vitro* formed ¹²⁵I-PNA:epiglycanin complex, however the *in vivo* studies reported appear to confirm the strong interaction that PNA and epiglycanin produce. The prior injection of epiglycanin (160 μ g) resulted in a significant change in the biodistribution of ¹²⁵I-PNA in rabbits (Figs. 4.19,4.20). The radiopharmaceutical was seen to rapidly accumulate in the liver (approximately 60% of the injected dose was contained in the liver at 15 min P.I.) while the lungs and spleen were also noted to contain significant amounts of the ¹²⁵I-PNA. The kidney activity was diminished in comparison to controls and this resulted in a significant difference in the kidney/liver ratio ($p < 0.05$).

It is uncertain from the scintigraphic results whether this interaction occurs in circulation, or whether, as postulated for anti-PNA/PNA, it occurs on the surface of hepatocytes. The main difference seen between the behaviour of ¹²⁵I-PNA in the presence of epiglycanin or anti-PNA antibodies, is the presence of lung and splenic localization. This scan pattern would be consistent with the plasma formation of large molecular weight complexes, which may be mechanically trapped by the capillaries of the lung field (analogous to that of particles above 10 μ m when injected i.v.) and phagocytosed by the Kupffer cells within the liver and spleen. However the hepatocytes of the liver⁴¹⁴ and alveolar macrophages of the lung⁴¹⁴ are known to contain specific receptors for glycoproteins containing terminal disaccharides such as β DGal-GalNAc, and this may result in membrane associated removal of ¹²⁵I-PNA-epiglycanin complex from the

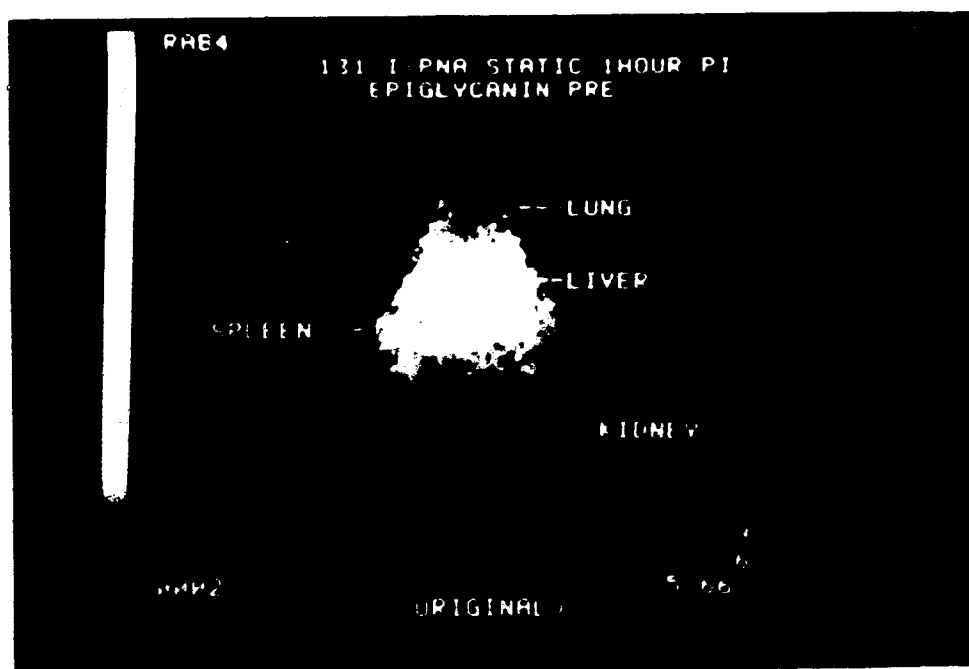


Figure 4.19 Static ^{131}I -PNA renal scintigram 60 min P.I. following administration of epiglycanin in a NZW rabbit

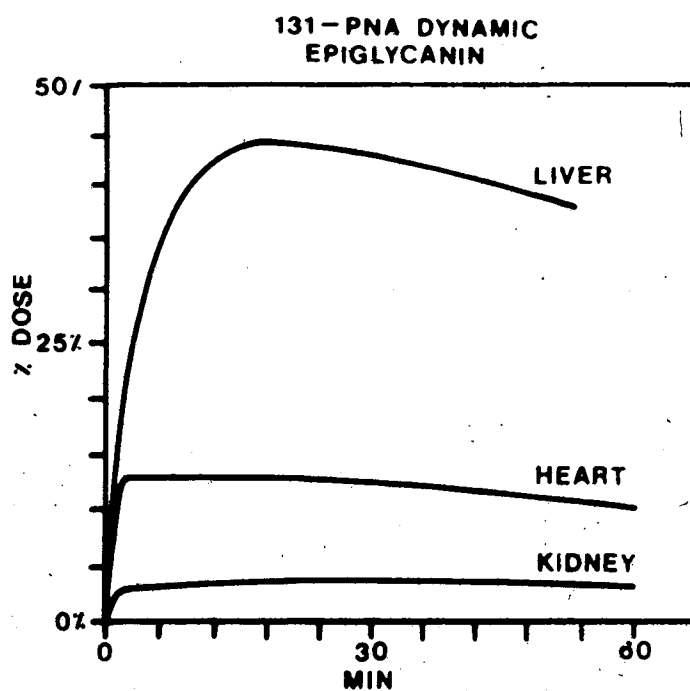


Figure 4.20 Dynamic liver Activity/time curve of ^{131}I -PNA following administration of epiglycanin in a NZW rabbit.

circulation.

4.4.2 Studies with asialo-GM₁-HSA and PNA in NZW rabbits and TA₁-Hla tumour-bearing CBA/CAJ and CAF1/J mice.

Based on previous liver-binding experiments⁴⁷³⁻⁴⁷⁸, Ashwell and Harford⁴⁷³ first identified the hepatocyte elimination of asialo-glycoproteins containing galactose in the terminal position. It was found that the circulation times for desialated glycoproteins were diminished in comparison to the corresponding sialated structures. Further research has also identified other sugars, including mannose, fucose and phosphomannose, as having specific receptors or liver lectins for their recognition and elimination from plasma⁴⁷⁴. The presence of these specific hepatocyte receptors has been implicated in the cellular recognition of 'foreign' asialo-glycoproteins and membrane fragments from plasma, as normal circulating structures and cellular glycoproteins are usually masked with N-acetyl neuraminic (sialic) acid and consequently protected from rapid elimination. Unmasked or desialated glycoproteins have been identified on many tumour cell lines, and have been implicated as markers of tumour aggressiveness⁴⁷⁵⁻⁴⁷⁹, and as important chemical markers in the specific mechanism of tumour metastasis to the liver⁴⁷⁹.

Vera *et al.*⁴⁸⁰⁻⁴⁸⁴ have advocated using this pathway for the study of liver function, via the use of radiolabelled asialo-glycoproteins and gamma-camera dynamic scintigraphy. Using ^{99m}Tc labelled neogalactoalbumin (^{99m}Tc-NAG), these authors have studied the kinetics of liver accumulation as a result of the saccharide density, and proposed a mathematical model for the calculation of receptor affinity and hepatic blood-flow⁴⁸⁵.

Recent clinical studies have indicated the usefulness of this radiopharmaceutical for quantifying liver perfusion and hepatic binding protein concentration in patients with parenchymal liver disease and liver transplant recipients⁴⁸⁶⁻⁴⁸⁷. We have also recently reported the possibility of using radiolabelled a-GM₁-HSA or T-HSA for the dynamic quantification of hepatocyte receptor function using the models proposed by the above investigators⁴⁸⁸.

In order to further investigate the specific renal clearance of ^{131}I -PNA in animals, and to attempt to inhibit the renal excretion of PNA, thus hopefully enhancing tumour uptake of PNA in tumour-bearing mice, studies were undertaken using asialo- GM_1 -HSA (a- GM_1 -HSA as an inhibitor of the PNA disaccharide binding site.

Asialo- GM_1 -HSA was synthesized in our laboratory by Dr S. Selvaraj using the methods previously reported by Ratcliffe *et al.*²⁸ and recently reported by us⁴⁹. The analogue of a- GM_1 -HSA containing four disaccharide units per HSA molecule was used in inhibition studies, and was successfully iodinated with ^{131}I or ^{125}I by the iodogen method, as previously described.

4.4.2.1 Renal scintigraphy with a- GM_1 -HSA/ ^{131}I -PNA in NZW rabbits.

Dynamic renal scintigraphy was undertaken in NZW rabbits, as previously described, with various molar ratios of a- GM_1 -HSA and ^{131}I -PNA, as well as ^{131}I -a- GM_1 -HSA controls and ^{131}I -PNA controls.

Control rabbits ($n=4$), injected i.v. with $100\text{ }\mu\text{g}$ (15 MBq) of ^{131}I -a- GM_1 -HSA, showed rapid liver accumulation of radiopharmaceutical in the liver (% inj. dose-at-peak = $85.2 \pm 1.6\%$, time-to-peak = 13.5 ± 1.5 min) with insignificant renal accumulation during the first hour P.I. (Table 4.9, Figs. 4.21, 4.22).

Dynamic renal and liver scintigraphy was performed in NZW rabbits with ^{131}I -PNA mixed with various molar concentrations of a- GM_1 -HSA (Table 4.9) and the % injected dose in kidneys, liver and bladder at 30 and 60 min P.I. were determined, along with kidney/liver ratios. When ^{131}I -PNA was in molar excess (4:1 molar ratio), no difference was seen in the biodistribution pattern when compared to controls. At a 1:1 ^{131}I -PNA to a- GM_1 -HSA molar ratio, slightly diminished renal accumulation was observed with a concomitant rise in the liver uptake of ^{131}I -PNA. The kidney/liver ratio was reduced to 3.1 compared to 18.6 for controls. When a- GM_1 -HSA was present in molar excess (1:2 and 1:4 ^{131}I -PNA:a- GM_1 -HSA), there was a significant change in biodistribution pattern resembling the scintigraphic distribution of ^{131}I -a- GM_1 -HSA. The

Table 4.9 : The Effect of Asialo-GM₁ on Gamma-camera derived ¹¹¹I-PNA Kidney and Liver Uptake Parameters.

		% Inj. Dose in Liver			% Inj. Dose in Kidneys			% Inj. Dose in Bladder			Kidney/Liver Ratio
		30 MIN P.I.	60 MIN P.I.		30 MIN P.I.	60 MIN P.I.		30 MIN P.I.	60 MIN P.I.		
¹¹¹ I-PNA controls											
		<2	<2		19.6	15.8		5.2	12.6		18.6 ₀
¹¹¹ I-a-GM ₁ IISA controls											
		79.2	75.8		<2	<2		<1	<1		<0.05
Molar ratio											
¹¹¹ I-PNA a-GM ₁ IISA											
4	1	<2	<2		20.2	16.9		4.1	10.2		17.6
1	1	4.8	5.2		17.4	14.8		3.5	8.7		3.1
1	2	35.6	33.8		14.3	12.5		<2	2.5		0.4
1	4	76.5	74.8		<2	<2		<1	<1		<0.05



Figure 4.21 Static scintigram of ^{131}I -a-GM₁-HSA in a NZW rabbit (60min. P.I.).

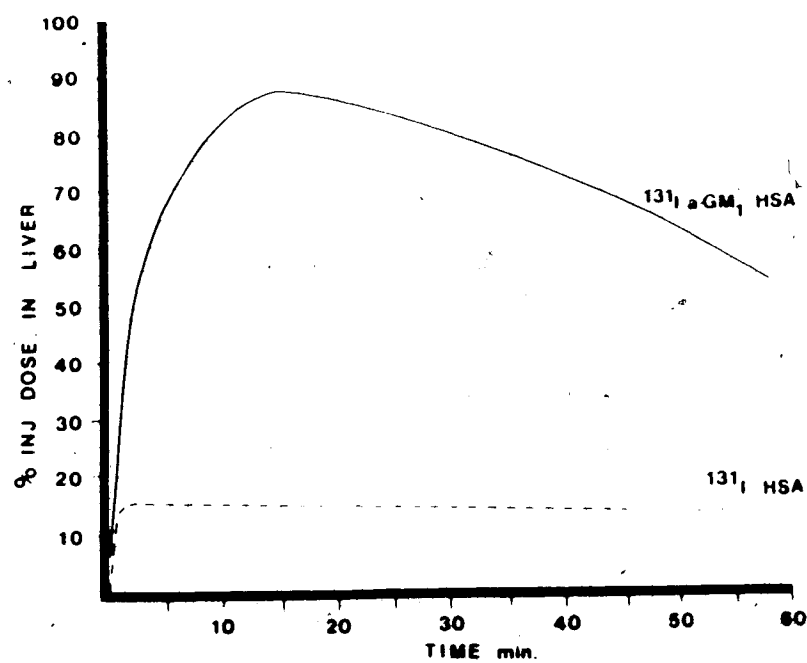


Figure 4.22 Dynamic Liver Activity/time curve following the administration of ^{131}I -a-GM₁-HSA in a NZW rabbit (0-60 min P.I.).

1:2 mixture showed a mixed pattern, indicating significant but incomplete complexation of ^{125}I -PNA to α -GM₁-HSA, while the 1:4 mixture appeared to result in complexation of the total amount of ^{125}I -PNA. This change in biological behaviour of ^{125}I -PNA in the presence of α -GM₁-HSA is further demonstrated in the static scintigraphic images obtained at 1 h P.I. (Fig 4.23).

As PNA contains four binding sites per molecule for the β -D-Gal-(1 \rightarrow 3)- β -GalNAc disaccharide residue²²², and the α -GM₁-HSA used in these experiments has an average of four disaccharide residues per molecule, it would be expected that a 1:1 molar ratio would result in the complete binding of ^{125}I -PNA to the α -GM₁-HSA. However, it is evident from our results that an excess of α -GM₁-HSA (1:4) is required to complex all the PNA. This may be due to weak binding of PNA to the glycosylated HSA derivative, or significant loss of binding *in vivo*. The weak sugar-binding capacity to the disaccharide residue is supported by the previous finding that the presence of the β -D-Gal-(1 \rightarrow 3)- β -GalNAc disaccharide did not significantly alter the scintigraphic localization of ^{125}I -PNA in rabbits at a molar ratio of 1:1 disaccharide to ^{125}I -PNA. It appears that there is some increased stability of the PNA binding to the protein-conjugated disaccharide in comparison to the free sugar, and this may be due to the extended binding site proposed for PNA, which infers higher stability²²³.

4.4.2.2 ^{125}I -PNA and ^{125}I -asialo-GM₁-HSA dual isotope biodistribution studies in CAF1/J mice bearing s.c. TA₃-Ha tumours.

In order to determine if altering the renal excretion rate of ^{125}I -PNA would result in a significant increase in the tumour localization of ^{125}I -PNA in CAF1/J mice bearing s.c. TA₃-Ha tumours, a series of experiments were completed using ^{125}I labelled α -GM₁-HSA as an inhibitor of ^{125}I -PNA renal excretion. During previous experiments in rabbits we had determined that ^{125}I -PNA mixed with α -GM₁-HSA at a molar ratio of 1:2 had caused an intermediate shift in the biodistribution when compared to controls. Renal excretion was diminished, but not totally at the expense of liver accumulation (as seen with

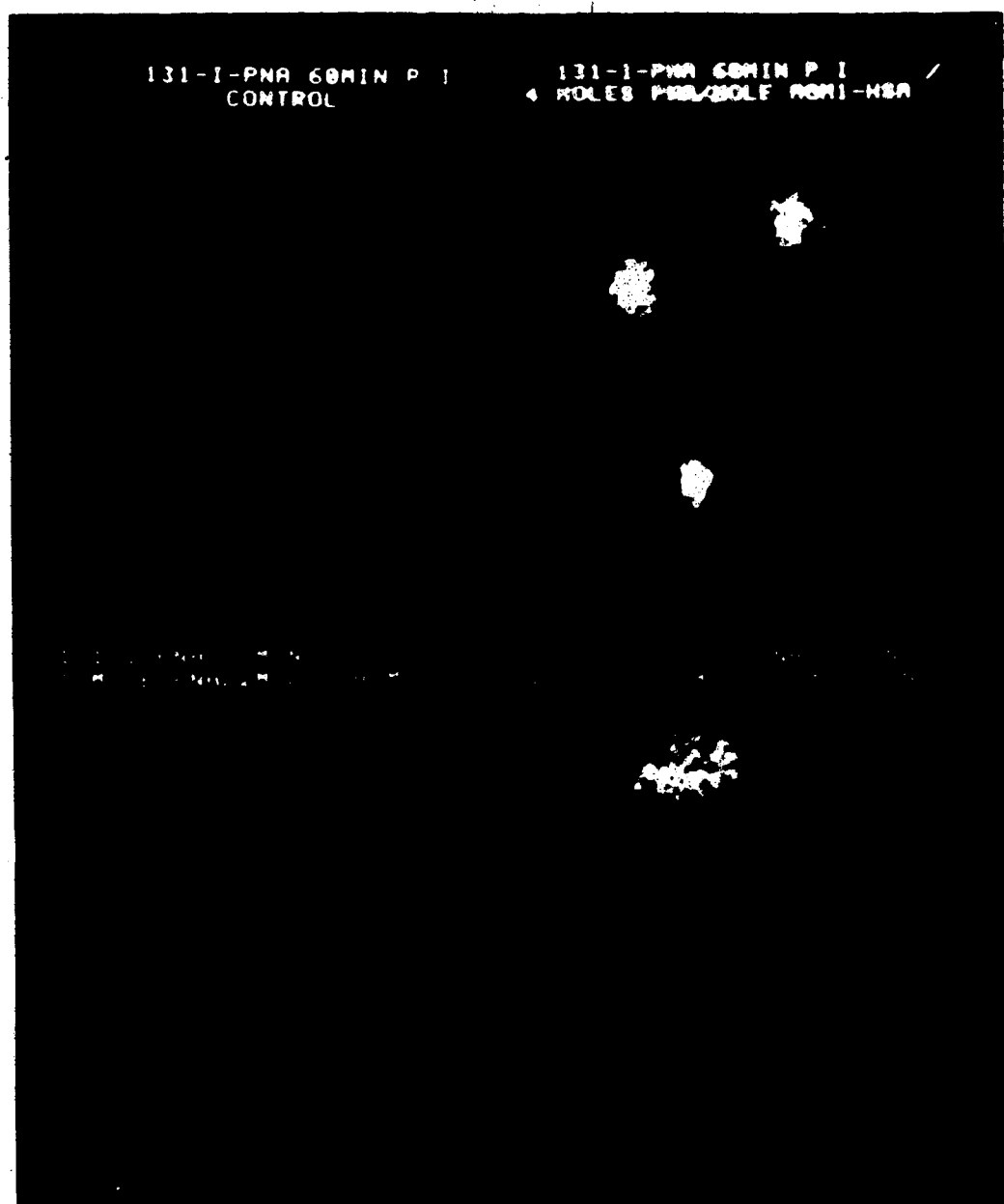


Figure 4.23 Static scintigrams of various molar ratios of ^{131}I -PNA: α -GM₁-HSA at 1 h post injection.

the 1:4 molar ratio mixture).

As a result of these observations, a dual isotope biodistribution study was performed in TA₃-Ha tumour bearing CAF1/J mice with ¹²⁵I-PNA and ¹²⁵I-a-GM₁-HSA at molar ratios of 4:1 and 1:2, along with controls of both ¹²⁵I-PNA and ¹²⁵I-a-GM₁-HSA. The animals were sacrificed at various times P.I (30 min-24 h) and the % injected dose/g tissue was compared for all major organs (Fig 4.24) (see Appendices 2-10 for full biodistribution data).

At 30 min P.I. there was a significant increase in liver and splenic uptake of the 4:1 mixture, while diminished accumulation was noted in stomach, salivary and tumour tissue when compared to controls receiving only ¹²⁵I-PNA (Table 4.10, $p < 0.05$). At 24 h. P.I. the liver and splenic increase in activity was again noted, along with a significant increase in the amount of dose remaining in the lungs (Table 4.11).

For the 1:2 molar ratio, a significant elevation in blood, liver spleen and whole body (as seen in the remaining carcass) activity was demonstrated over controls at 30 min P.I. (Table 4.10, $p < 0.05$). The elevated blood, liver, spleen and carcass activity remained at 24 h P.I., along with significant increases in GIT, renal and tumour activity (Table 4.11). The increase in liver, splenic and lung activity at all times P.I. with both the 4:1 and 1:2 molar ratio mixtures most likely reflects the formation of large molecular weight complexes, which are trapped by the cells of the RES in liver and spleen, and by capillaries in the lungs. This increase is more evident with the 1:2 mixture, which also shows elevated blood levels of ¹²⁵I-PNA at all times P.I. Although the tumour levels of ¹²⁵I-PNA in the 1:2 mixture are about twice that of controls, when the tumour/blood ratios are compared there is no significant difference from controls. Although the complexation of ¹²⁵I-PNA with a-GM₁-HSA results in diminished excretion from plasma, it does little to enhance the tumour uptake of ¹²⁵I-PNA. Perhaps this is not surprising, since by reacting the PNA with the glycosylated HSA analogue, we have in effect reduced the number of T-F antigen binding sites on the PNA, and consequently, unless the tumour antigen possessed a higher

Table 4.10 ^{125}I -PNA biodistribution in CAF1/J mice with s.c. TA₃-Ha tumours; effect of a-GM₁-HSA on tissue uptake at 30 min P.I.

ORGAN	% DOSE / GRAM OF TISSUE		
	CONTROL	^{125}I -PNA/a-GM ₁ -HSA	^{125}I -PNA/a-GM ₁ -HSA
	Mean ± S.D. (N = 5)	4 - 1 (N = 6)	1 - 2 (N = 6)
BLOOD	7.47 1.36	7.39 1.31	10.18* 0.83
LIVER	3.73 0.51	5.21* 0.47	7.63* 0.49
SPLEEN	3.78 0.59	22.39* 3.70	5.85* 0.16
STOMACH	17.77 4.76	5.70* 0.37	13.74 4.76
G.I.T.	2.35 0.48	2.31 0.26	2.94 0.44
KIDNEY	44.62 12.78	77.84 20.39	65.03 8.03
LUNG	4.66 0.54	6.86 1.64	5.83 0.38
MUSCLE	0.88 0.18	0.85 0.11	1.12 0.23
SALIVARIES	10.29 2.49	3.62* 3.62	12.16 3.59
TUMOUR	4.32 0.99	12.37* 0.70	5.62 0.62
CARCASS	2.06 0.47	2.84 0.34	3.50* 0.65

* p < 0.05

Table 4.11 ^{125}I -PNA biodistribution in CAF1/J mice with s.c. TA_1 -Ha tumours; effect of α - GM_1 -HSA on tissue uptake at 24 h. P.I.

% DOSE / GRAM OF TISSUE.			
ORGAN Mean \pm S.D.	CONTROL (N=6)	^{125}I -PNA/ α - GM_1 -HSA 4 1 (N=6)	^{125}I -PNA/ α - GM_1 -HSA 1 2 (N=6)
BLOOD	0.11 0.03	0.19 0.05	0.22* 0.01
LIVER	0.48 0.05	1.96* 0.23	3.52* 0.27
SPLEEN	0.33 0.07	2.13* 0.23	1.89* 0.26
STOMACH	0.58 0.40	1.00 0.41	0.85 0.11
G.I.T.	0.10 0.02	0.18 0.05	0.26* 0.03
KIDNEY	1.41 0.15	1.36 0.17	2.41* 0.27
LUNG	0.20 0.05	0.61* 0.06	0.32 0.03
MUSCLE	0.03 0.01	0.07 0.02	0.07 0.01
SALIVARIES	1.55 0.95	1.82 0.39	2.15 0.28
TUMOUR	0.57 0.24	0.40 0.08	1.14* 0.37
CARCASS	0.54 0.15	0.51 0.09	1.30* 0.13

* $p < 0.05$

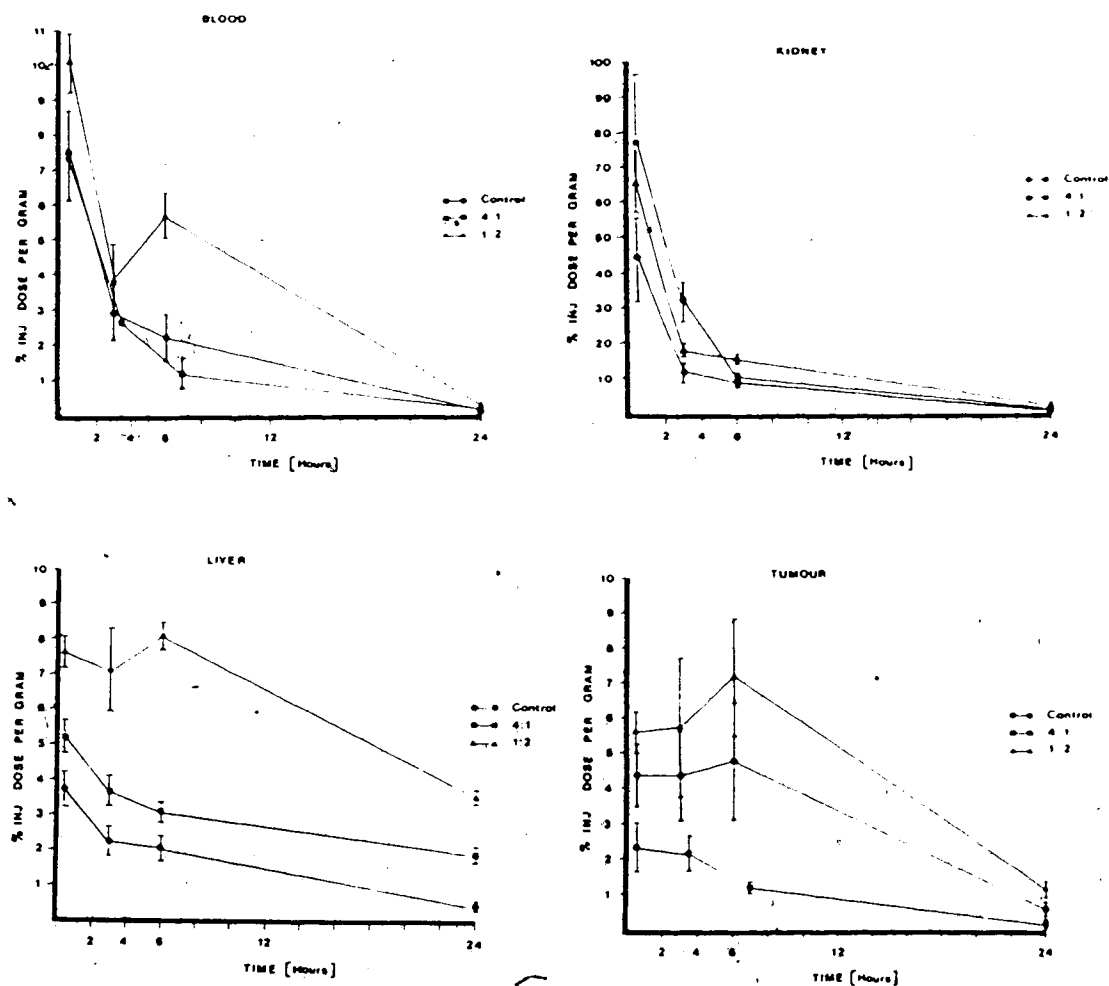


Figure 4.24 The blood, renal, liver and tumour % injected dose/g vs. time curves of ^{125}I -PNA, and ^{125}I -PNA: α -GM₁-HSA(4:1 and 1:2 molar ratios) in TA₃-Ha tumour-bearing CAF1/J mice.

binding affinity for PNA than α -GM₁-HSA, an increase in tumour retention should not be evident.

Interestingly, the % injected dose/g of kidney tissue with both the 1:2 and 4:1 ¹²⁵I-PNA: α -GM₁-HSA molar ratio mixtures is elevated at between 2 to 6 h. P.I. in comparison to controls. In previous experiments in rabbits, a marked diminution was noted in the pre-peak renal activity of ¹²⁵I-PNA when present with α -GM₁-HSA in similar molar ratios. In mice, it appears that α -GM₁-HSA does not elicit as strong an effect on the inhibition of renal binding of PNA, nor does it have as strong an affinity for the liver at a given molar ratio. This may be due to the rapid dissociation of the ¹²⁵I-PNA: α -GM₁-HSA complex, or the stronger affinity of the renal binding sites for PNA in the mouse.

4.4.3 The Effect of Multiple Doses of PNA on the Biodistribution of ¹²⁵I-PNA in CBA/CAJ mice.

Studies in rabbits have indicated that the presence of circulating anti-PNA antibodies (IgG's) elicits a pronounced effect on the biodistribution pattern of ¹²⁵I-PNA *in vivo*. Marked liver accumulation was noted, indicating *in vivo* complexation of antibody-PNA, which was subsequently rapidly removed by the liver. In order to determine if prior exposure to i.v. PNA, or s.c. PNA (complexed with Freund's Complete Adjuvant) had an effect on the *in vivo* biodistribution pattern, ¹²⁵I-PNA biodistribution studies were performed in CBA/CAJ mice which had previously been injected i.v. with multiple doses of PNA, or with s.c. PNA-Freund's adjuvant.

No significant difference in 24 h tissue levels of ¹²⁵I-PNA could be demonstrated in groups of mice which were previously exposed to 1, 2, or 3 i.v. doses of PNA (1 μ g) at one week intervals prior to the ¹²⁵I-PNA study. The liver, kidney, blood, spleen and lung levels of ¹²⁵I-PNA were not significantly different in all treatment groups when compared to controls (Table 4.12), and there were no obvious acute immunological reactions noted in any mice to the multiple PNA dosing regimen.

In contrast, a significant change in liver, spleen and lung levels of ^{125}I -PNA was observed when the animals were previously injected s.c. with 3 doses of PNA/Freund's mixture ($p < 0.05$). The resultant liver to kidney ratios were elevated (Fig 4.25), and these results appeared consistent with the production of antibodies against PNA in these animals.

Because PNA is a plant protein of non-immunological origin, it would be expected that antibodies may be produced against PNA, with multiple exposure to the protein. We have not been able to demonstrate changes in biodistribution of ^{125}I -PNA after up to three i.v. administrations of PNA in CBA/CAJ mice. However, when the PNA is injected s.c., complexed with Freund's complete adjuvant, a rise in RES-associated ^{125}I -PNA was noted. It appears that the i.v. route of administration may kinetically protect the animals from producing an immune response to PNA. As previously noted, the elimination kinetics of i.v. PNA are rapid and this may reduce the probability of antibody production. However, when PNA is administered s.c. with Freund's adjuvant, the exposure time to the antigenic material is prolonged, hence increasing the probability of an immune response to PNA. This is supported by the results reported here, however anti-PNA antibody titres were not determined in the mice studied. Antibody titres were, however, determined in humans exposed to multiple i.v. doses of PNA in subsequent studies (see later results).

4.5 THE EFFECT OF RENAL CELL FUNCTION ON THE RATE OF PNA RENAL BINDING AND EXCRETION.

4.5.1 ^{125}I -PNA Renal Kinetics of Cis-Platinum induced Nephrotoxicity in Dogs.

Cis-platinum is known to elicit metabolic and morphological changes in the function of renal tubular cells²²⁰⁻²²⁴, as previously discussed. In order to study the effect of cis-platinum induced tubular dysfunction on the rate of ^{125}I -PNA renal uptake and clearance, a study was performed in dogs administered a single-cycle cis-platinum chemotherapy regimen.

Table 4.12: Effect of Multiple Doses of PNA on the Biodistribution of ^{125}I -PNA in CBA/CAJ mice.

	% DOSE / GRAM OF TISSUE AT 24 H P.I					
	CONTROLS N=6	1 WEEK N=4	2 WEEKS N=5	3 WEEKS N=6	FREUND'S SC N=5	
BLOOD	Mean ±S.D.	0.19 0.02	0.12 0.03	0.15 0.07	0.12 0.04	0.14 0.03
LIVER	Mean ±S.D.	0.94 0.12	0.75 0.04	1.00 0.17	1.19 0.25	1.33* 0.25
SPLEEN	Mean ±S.D.	0.65 0.12	0.64 0.06	0.74 0.30	0.49 0.06	1.23* 0.36
STOMACH	Mean ±S.D.	0.43 0.15	0.52 0.25	0.58 0.25	0.52 0.17	0.47 0.14
G.I.T	Mean ±S.D.	0.10 0.03	0.09 0.02	0.12 0.03	0.11 0.03	0.11 0.02
KIDNEY	Mean ±S.D.	2.21 0.34	1.76 0.29	1.87 0.16	1.84 0.45	1.69 0.27
LUNG	Mean ±S.D.	0.30 0.07	0.36 0.03	0.28 0.05	0.20* 0.02	0.19* 0.04
MUSCLE	Mean ±S.D.	0.05 0.01	0.05 0.01	0.05 0.01	0.05 0.01	0.05 0.02
SALIVARY GLANDS	Mean ±S.D.	1.16 0.18	1.06 0.13	0.69 0.30	0.39 0.15	0.35* 0.15
CARCASS	Mean ±S.D.	0.52 0.18	0.42 0.14	0.88 0.23	0.97 0.24	0.28* 0.42
KIDNEY/LIVER RATIO	Mean ±S.D.	2.35 0.56	2.35 0.34	1.87 0.32	1.55 0.31	1.27* 0.54

* p < 0.05

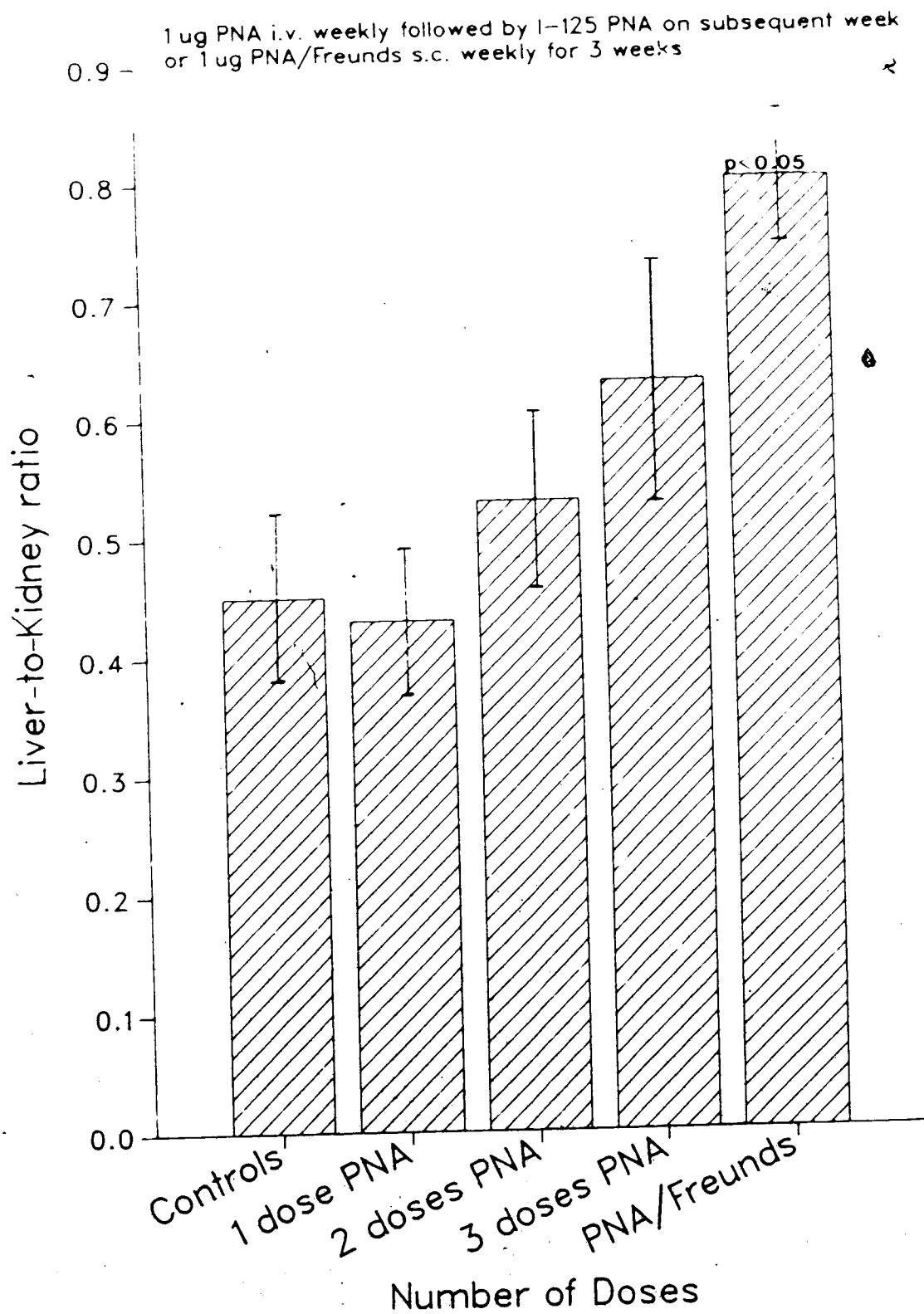


Figure 4.25 Liver/kidney ratios in CBA/CAJ mice previously exposed to multiple doses of PNA.

^{125}I -PNA plasma and renal pharmacokinetic studies were performed on dogs both before and following cis-platinum therapy, along with standard estimates of serum biochemistry, and renal function.

Serum biochemistry revealed no significant difference in electrolyte levels pre- and post-treatment (Table 4.13). There was an elevation in serum creatinine (Mean $\Delta\text{S\%} = 42.7\%$, $p < 0.05$) and BUN (Mean $\Delta\text{S\%} = 41.4\%$, $p < 0.05$), while total protein was noted to drop below normal range in three of the four dogs post cis-platinum treatment.

A marginal decline in ERPF ($\text{mL} \cdot \text{min}^{-1}$) was observed in all dogs, (Mean $\Delta\text{S\%} = 20.9 \pm 11.8\%$, Table 4.14) however did not gain statistical significance (students t-test). GFR showed a significant reduction in all dogs from a mean of $33.74 \pm 4.53 \text{ mL} \cdot \text{min}^{-1}$ to $18.27 \pm 5.31 \text{ mL} \cdot \text{min}^{-1}$ (Mean $\Delta\text{S\%} = 46.6 \pm 8.9\%$, $p < 0.05$). ^{125}I -PNA plasma levels were elevated in all dogs after cis-platinum treatment, resulting in a significant reduction in plasma clearance rate when compared to pretreatment values (Mean $\Delta\text{S\%} = 71.3 \pm 6.6\%$, $p < 0.05$). The pretreatment estimates showed a narrow standard deviation (Mean = $16.76 \pm 1.52 \text{ mL} \cdot \text{min}^{-1}$).

Gamma camera-derived renal curves demonstrated no significant differences in time-to-peak estimates pre- or post- cis-platinum treatment (Table 4.15), however there was a significant difference in the % injected dose-at-peak (Mean $\Delta\text{S\%} = 65.8 \pm 12.7\%$, $p < 0.05$). One hour bladder activity was also diminished by a similar magnitude (Mean $\Delta\text{S\%} = 67.6\%$).

The static scintiphotos at 1 h P.I. showed obvious differences in the renal accumulation of ^{125}I -PNA post-treatment (Fig. 4.26). One dog in particular, demonstrated a significant change in biodistribution, resulting in localization of ^{125}I -PNA predominantly in the liver. Renal accumulation was not evident and thus renal uptake parameters were difficult to assess. This animal showed the most severe signs of renal tubular toxicity as determined by histopathology. One plausible explanation for this is that under severe toxicity the tubular receptor antigen may be shed from the basement membrane and be released into the dog's circulation system. ^{125}I -PNA interaction may occur with this circulating antigen, resulting in the formation of a large molecular weight complex, which is subsequently removed by the liver.

Table 4.13 : Serum Biochemistry of Dogs Pre and Post Cis-platinum Chemotherapy.

		Na ⁺ mmol L ⁻¹	K ⁺ mmol L ⁻¹	Cl ⁻ mmol L ⁻¹	Ca ⁺⁺ mmol L ⁻¹	Creat umol L ⁻¹	BUN mmol L ⁻¹	Protein g L ⁻¹
NORMALS	Mean	146	4.1	114	5.0	79.5	6.1	58
	Range	136-151	3.4-4.7	105-124	4.25-6.00	53-97	4.2-8.2	49-63
PRE CIS Pt.	Mean±S.D.	138.5±5.7	3.67±0.29	111±3.5	5.75±0.70	77.3±8.5	6.29±0.59	44.9±11.5
	Range	135-147	3.50-4.90	107-118	4.00-6.25	66-90	5.4-7.2	38-59
POST CIS Pt.	Mean±S.D.	139.0±7.7	3.40±0.36	109.2±7.0	5.04±0.23	135.0±36.0	10.74±1.85	37.9±4.0
	Range	136-148	3.2-3.9	103-117	4.50-5.50	92-173	8.0-12.2	36-49
MEAN % CHANGE±S.D.						42.7* 7.8	41.4* 8.9	

* p < 0.05

Table 4.14 : Renal Function Estimates in Dogs Pre and Post Cis-platinum Chemotherapy.

DOG	E.R.P.F.(mL.min ⁻¹)		G.F.R.(mL.min ⁻¹)		¹²⁵ I-PNA CLEARANCE(mL.min ⁻¹)	
	PRE	CIS-Pt	POST	CIS-Pt	PRE	CIS-Pt
1	332.0		208.2	39.60	14.71	3.13
2	157.2		123.0	31.74	16.59	5.41
3	221.6		188.9	34.62	18.24	6.53
4	201.7		181.1	28.99	17.49	4.40
MEAN	228.1		175.3	33.74	16.76	4.87
±S.D.	74.3		36.7	4.53	1.52	1.45
MEAN % CHANGE±S.D.			20.9 11.8		46.6 8.9	71.3 6.6

• = p < 0.05

Table 4.15 : ¹¹¹I-PNA Gamma-camera Renal Dynamic Parameters in Dogs Pre and Post Cis-platinum Chemotherapy.

DOG	PRE CIS-Pt	POST CIS-Pt	TIME-TO-PEAK (MIN)	% INJ DOSE-AT-PEAK (RENAL)	PRE CIS-Pt	POST CIS-Pt	% INJ DOSE IN BLADDER (60 MIN Pt)	PRE CIS-Pt	POST CIS-Pt
1	21.51	9.6.	37.5		30.0	14.5	7.3		
2	20.61	8.6	41.5		39.5	9.9	4.5		
3	18.42	<3	32.5		N.D.	14.0	<3		
4	22.85	7.8	42.5		39.5	18.0	3.5		
MEAN ±S.D.	20.85 1.86	7.2 2.9	38.5 4.5		36.3 5.5	14.1 3.3	4.3 2.2		
MEAN % CHANGE±S.D.		65.8* 17.7			N.D.		61.6* 18.1		

* = p < 0.05

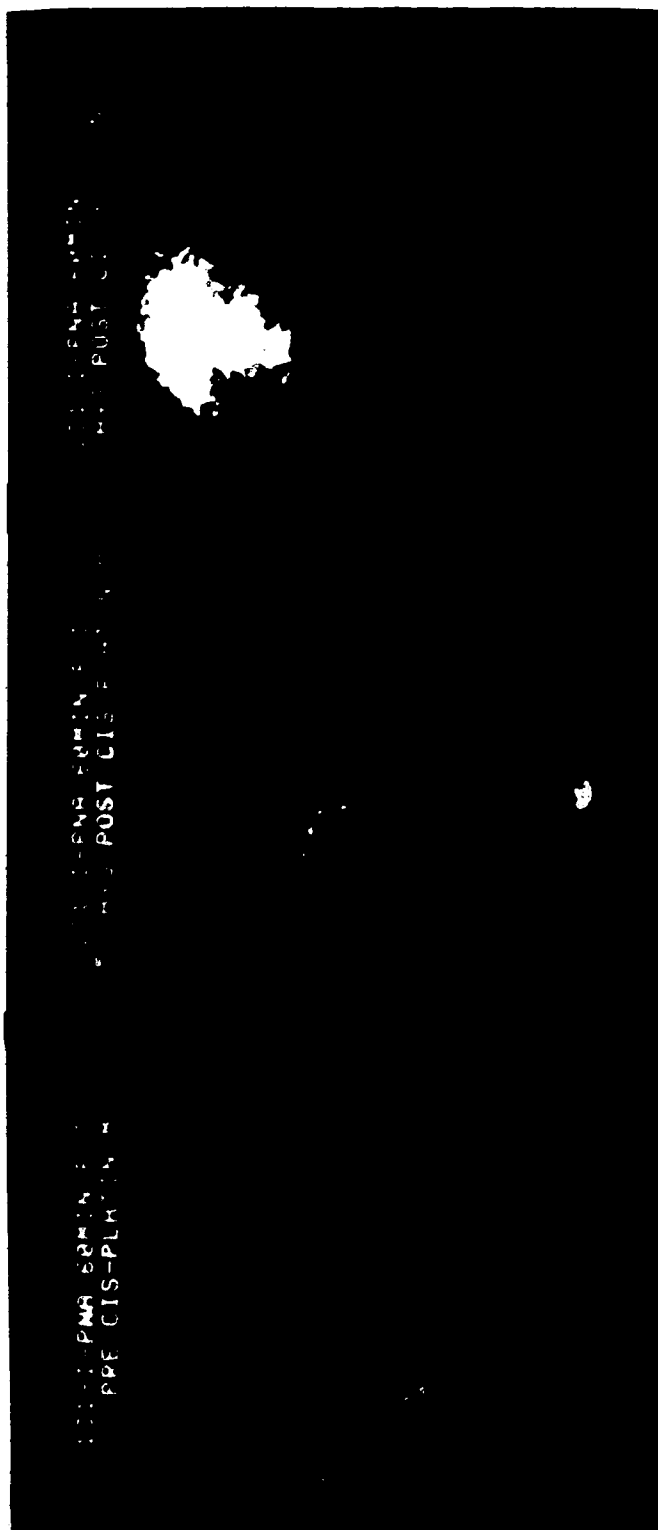
N.D. = Not Detected.

Evidence for this explanation is supported by the fact that high titres of serum T-F antigen were noted in this dog by ELISA assay. Only minor to moderate degrees of tubular toxicity were noted in the remaining dogs by histological examination. ^{125}I -PNA renal uptake was noted in the remaining dogs, however this was diminished in all cases, in comparison to their pretreatment scintigrams.

In all cases, the degree of reduction of the tubular function following cis-platinum treatment, (as determined by ^{125}I -PNA plasma clearance and renal uptake), was significantly greater than that predicted by methods which estimate glomerular function (serum creatinine, GFR). The mean change of serum creatinine post-treatment ($\Delta\text{S\%} = 42.7\%$) and $^{99\text{m}}\text{Tc}$ -DTPA GFR ($\Delta\text{S\%} = 46.6\%$) were of similar magnitude, however the mean ^{125}I -PNA clearance ($\Delta\text{S\%} = 71.3\%$) was statistically different ($p < 0.05$). A similar statistical difference was demonstrated with ^{125}I -PNA renogram-derived % injected dose-at-peak ($\Delta\text{S\%} = 65.8\%$) and % injected dose in bladder at 1 h P.I. ($\Delta\text{S\%} = 67.6\%$, $p < 0.05$).

Cis-platinum is known to cause dose-dependent toxicity to the kidneys in animals and humans²²⁷⁻²²⁹, and this nephrotoxicity has been reported as being the major dose-limiting factor in the treatment of patients with cis-platinum in a wide variety of neoplastic diseases²¹⁷⁻²¹⁹. The mechanism of toxicity to the kidney has been shown to be predominantly tubular although glomerular alterations may be demonstrated as a consequence of this²²⁶. Glomerular function may, however, remain essentially normal in spite of demonstrable tubular toxicity²⁰⁰, and therefore renal function estimations utilizing glomerular mechanisms of quantitation, such as GFR, serum creatinine and creatinine clearance, may be insensitive for detecting early tubular toxicity. Because of the predominant tubular toxicity, cis-platinum is also useful for studying specific tubular toxicity in animal models.

By altering the metabolic function of renal tubules by cis-platinum therapy, a dramatic reduction in the renal uptake and clearance of ^{125}I -PNA was observed in the above experiment. Reduced affinity for the basement membrane of the tubules was observed indicating either a reduction in the number of receptor sites present on the cell membrane or chemical alteration



A = NORMAL B = MILD TUBULAR DYSFUNCTION C = SEVERE TUBULAR DYSFUNCTION

Figure 4 26 Static Renal ^{111}I PNA scintigrams 1 h p.i. in dogs following cis platinum chemotherapy

of the glycoprotein receptor by cis-platinum. The degree of inhibition could neither be predicted by the concomitant monitoring of renal hemodynamics (ERPF), or glomerular function (GFR, serum creatinine).

The plasma clearance and renal uptake (slope-to-peak) can be readily quantified by standard plasma pharmacokinetic modelling and dynamic scintigraphy, allowing comparative estimates of ^{131}I -PNA clearance to be performed. Renal scintigraphy, however, seems preferable, due to the finding of ^{131}I accumulation with severe toxicity. Because of this change in biodistribution, monitoring of plasma pharmacokinetics alone may not accurately demonstrate the severity of tubular dysfunction.

4.5.2 ^{131}I -PNA Renal kinetics in Patients undergoing Cis-Platinum chemotherapy.

Encouraged by the apparent sensitivity of ^{131}I -PNA to detect changes in tubular function in dogs treated with cis-platinum, a prospective clinical trial was initiated in consenting patients who were to be treated with Cis-platinum as part of their chemotherapy régime. All patients were informed of the investigatory nature of the study, and had known neoplastic disease, documented by conventional radiology or nuclear medicine techniques.

Prior to the commencement of chemotherapy, each patient was challenged with a s.c. dose of PNA to determine the presence of tissue-type sensitivity to PNA, and serum anti-PNA IgG, IgM, and IgE titres were determined by ELISA assay. Each patient also received full biochemical and renal function (creatinine clearance) workup, and a baseline ^{131}I -PNA dynamic renogram study was performed, as previously described. Following each second course of chemotherapy, the patient was reinvestigated for PNA sensitivity, anti-PNA titres, serum biochemistry, renal function, and ^{131}I -PNA renal uptake.

Of the seven patients studied to date (16 administrations of ^{131}I -PNA) no patient has demonstrated any adverse reactions to the i.v. administration of ^{131}I -PNA. In all patients, evidence of tissue-type hypersensitivity has been absent (5 patients following 2 doses of ^{131}I -PNA, 2 patients following 3 doses of ^{131}I -PNA), nor have elevated titres of circulating

anti-PNA IgG, IgM, or IgE been demonstrated in any patient during the study period (Table 4.16).

Difficulties arose with the quantitative analysis of the renal uptake of ^{131}I -PNA in all patients. Initially, renal curves derived from ROI analysis, were fitted to an exponential equation ($A = A_0[1 - e^{-\lambda t}]$) and both the activity-at peak and $t_{1/2}$ uptake determined from the curves from each kidney. It was found, however, that the values derived from these curves were critically dependent on the selection of the background ROI, resulting in wide discrepancies of each parameter depending on where the region of interest was drawn. This stems from the fact that the peak activity estimates were calculated by the model from the renal curves which, at best, only described about half of the uptake curve for each kidney. In order to derive a parameter, which would describe the acquired curve alone, and be less reliant on the subjective selection of ROIs, the renal curves were reanalyzed using a quadratic equation ($A = ax + bx^2$). This model allows the calculation of the initial slope of the curve (a), which was further corrected to an *in vivo* radioactivity/volume measurement calculated from the relationship of injected dose (in MBq) to volume of distribution (V_d), determined from plasma sampling. The lump constant (kBq/mL) was used to normalize each renal slope (in counts/min/pixel) to an *in vitro* determined concentration of ^{131}I -PNA within the plasma.

In all patients studied to date, serum creatinine and creatinine clearance have remained within normal range, following up to four courses of cis-platinum (Table 4.16). Evidence of renal toxicity has not been demonstrated in any patients using the chemotherapy régimes used for the treatment of these tumours.

Analysis of the plasma clearance, and renal uptake of ^{131}I -PNA in patients has revealed variations following cis-platinum therapy, although the significance of these findings is difficult to interpret due to the limited number of patients studied to date. In two patients (R.S. and A.P.) who have received four courses of chemotherapy, a reduction in the renal uptake slope has been demonstrated (Table 4.17, Fig 4.27). A steady decline from a mean renal uptake rate of 0.339 counts/min/pixel pre-treatment to 0.223 and 0.155 counts/min/pixel following 2

Table 4.16 : Serum Creatinine, Creatinine Clearance, and Specific anti-PNA Antibody Titres in Patients undergoing Cis-Platinum Chemotherapy

PATIENT	STUDY PERIOD	SERUM CREATININE* ($\mu\text{mol.L}^{-1}$)	CREATININE CLEARANCE† (mL.min^{-1})	ANTI-PNA IgG	ANTI-PNA IgM	ANTI-PNA IgE
R.S.	Pre Cis-Pt	105	112	-ve	-ve	-ve
	Post Cis-Pt 2	100	111	-ve	-ve	-ve
	Post Cis-Pt 4	90	110	-ve	-ve	-ve
A.P.	Pre Cis-Pt	90	101	-ve	-ve	-ve
	Post Cis-Pt 2	80	122	-ve	-ve	-ve
	Post Cis-Pt 4	80	105	-ve	-ve	-ve
I.S.	Pre Cis-Pt	90	N.D.	-ve	-ve	-ve
	Post Cis-Pt 2	80	81	-ve	-ve	-ve
E.J.	Pre Cis-pt	100	90	-ve	-ve	-ve
	Post Cis-pt 2	90	95	-ve	-ve	-ve
A.G.	Pre Cis-Pt	100	N.D.	-ve	-ve	-ve
	Post Cis-Pt 2	90	92	-ve	-ve	-ve
L.S.	Pre Cis-Pt	90	126	-ve	-ve	-ve
	Post Cis-Pt 2	77	102	-ve	-ve	-ve
J.B.	Pre Cis-Pt	90	121	-ve	-ve	-ve
	Post Cis-Pt 2	80	85	-ve	-ve	-ve

* Normal range 70-120 $\mu\text{mol.L}^{-1}$ † Normal range 80-120 mL.min^{-1}

N.D. Not Determined.

Table 4.17 : ^{111}In -PNA Plasma and Renal Parameters in Patients undergoing Cis-Platinum Chemotherapy

PATIENT	STUDY PERIOD	Vd (L)	PLASMA CLEARANCE* ($\text{mL}\cdot\text{min}^{-1}$)	KIDNEY SLOPE† ($\text{cts}\cdot\text{min}^{-1}/\text{pixel}$)		% INJ. DOSE EXCRETED (24 h)
				RIGHT KIDNEY	LEFT KIDNEY	
R.S.	Pre Cis-Pt	3.51	25.8	0.328±0.047	0.351±0.043	66.9
	Post Cis-Pt 2	3.72	27.4	0.218±0.023	0.228±0.018	71.8
	Post Cis-Pt 4	3.82	29.0	0.157±0.017	0.154±0.016	69.8
A.P.	Pre Cis-Pt	3.32	25.9	0.183±0.021	0.197±0.021	86.2
	Post Cis-Pt 2	2.63	27.3	0.182±0.019	0.199±0.020	81.1
	Post Cis-Pt 4	2.75	28.2	0.125±0.018	0.144±0.016	89.0
I.S.	Pre Cis-Pt	2.80	31.3	0.104±0.013	0.105±0.013	88.6
	Post Cis-Pt 2	3.12	28.7	0.151±0.017	0.150±0.015	82.7
E.J.	Pre Cis-Pt	3.79	29.3	0.190±0.020	0.193±0.018	85.7
	Post Cis-Pt 2	3.57	31.2	0.130±0.019	0.141±0.016	86.2
A.G.	Pre Cis-Pt	4.62	32.7	0.110±0.017	0.143±0.018	89.8
	Post Cis-Pt 2	3.72	28.7	0.199±0.020	0.223±0.019	84.6
I.S.	Pre Cis-Pt	2.91	38.4	0.191±0.020	0.195±0.020	83.5
	Post Cis-Pt 2	2.98	32.5	0.221±0.018	0.256±0.019	89.2
J.B.	Pre Cis-Pt	2.59	29.9	0.172±0.019	0.196±0.018	89.4
	Post Cis-Pt 2	2.59	35.5	0.166±0.015	0.179±0.015	79.8

* Clearance calculated from plasma samples during the first 60 min P.I. (Fast phase of the plasma disappearance curve)

† Kidney slope derived from renal ROIs fitted to quadratic equation ($A = ax + bx^2$) Slope is corrected to plasma activity, and normalized to $3\text{kBq}/\text{mL}$.

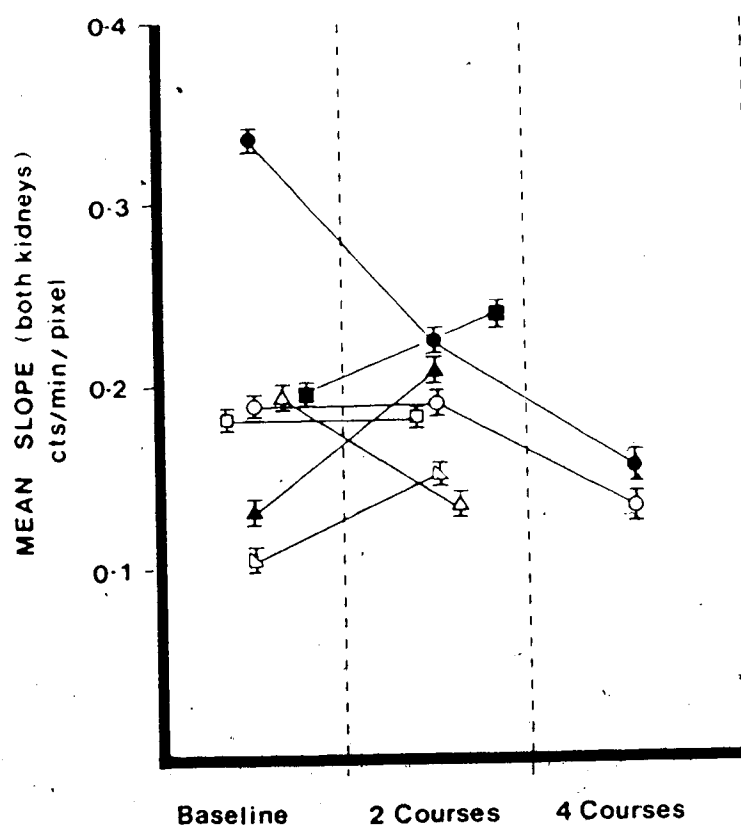


Figure 4.27 ^{131}I -PNA Mean Normalized Renal Slope Estimates in Patients before and after Cis-platinum chemotherapy.

and 4 courses of cis-platinum were seen in repeat studies in patient R.S., representing a change of 55.3% in the rate of renal uptake. This change in renal function was not confirmed by changes in creatinine clearance. Patient A.P also demonstrated a reduction in the mean renal uptake slope (30%) following four courses of cis-platinum, while her creatinine clearance remained within normal limits. A further patient in the study group (E.J.) showed a decrease (30%) in ^{131}I -PNA renal uptake slope following two courses of cis-platinum. Three patients (A.G., I.S. and L.S.), however, showed increased ^{131}I -PNA renal uptake slopes following two courses of cis-platinum. It appears therefore, that there is considerable variability in the renal uptake of ^{131}I -PNA in patients with neoplastic disease, although the significance of this is unclear. The variation may be due to the type and grade of the patient's neoplasia, the effect of the chemotherapy, the response of the tumour to the chemotherapy, or may be simply due to normal variations within the patient population. To date, we have not studied the renal uptake of ^{131}I -PNA in normal patients, nor have we any studies performed in patients with documented renal disease. It is, therefore, premature to comment on the sensitivity of ^{131}I -PNA renal scintigraphy in the diagnosis of tubular dysfunction.

As would appear from our data, there is a wide variability (approximately 200%) in patients whose creatinine clearance is within normal limits. Further studies are therefore warranted to document the variability of ^{131}I -PNA dynamic renal scintigraphy in a wider patient population, including controls, and to compare these results with those of patients with documented renal dysfunction, as well as further patients with neoplasia.

We have not, to date, been able to substantiate the findings of significant reductions in the rate of renal uptake of ^{131}I -PNA previously seen with dogs treated with cis-platinum. It must be noted, however, that in those experiments, renal toxicity was deliberately induced, while in our human study group, toxicity was avoided by the use of carefully controlled treatment régimes. Our study would appear to confirm the lack of renal toxicity induced by the cis-platinum treatment régimes used in these patients.

5. CONCLUSIONS.

1. Peanut lectin can be routinely iodinated with either ^{125}I or ^{131}I by the iodogen method. The radioiodinated material was adequately separated from free unreacted I by gel column chromatography (Biogel P6-DG, 0.01 M PBS) and the recovered protein retained its sugar-binding specificity, as determined by a-GM₁ synsorb binding assay.
2. The iodination procedure was satisfactorily adapted for sterile production, resulting in sterile and pyrogen-free ^{131}I -PNA suitable for human administration.
3. The i.v. administration of ^{125}I -PNA in mice resulted in rapid accumulation of ^{125}I -PNA in the kidneys with excretion into the bladder at times beyond 30 min P.I. A significant difference in the rate of renal uptake was observed in various strains of mice (AJ, c57b, CBA/CAJ, and CAF1/J), but was consistent within a single strain.
4. The renal uptake of ^{125}I -PNA at 30 min P.I. was saturable in CBA/CAJ mice, with doses in excess of 10 $\mu\text{g}/25\text{ g}$ mouse, resulting in elevated blood concentrations, and diminished kidney/blood ratios. This dose corresponded to a saturation dose of approximately 400 $\mu\text{g}/\text{kg}$ body weight.
5. The biodistribution of ^{125}I -PNA in CBA/CAF1/J mice was not affected by the prior injection of up to 3 i.v. doses of PNA over a one month period. The s.c. injection of PNA complexed with Freund's Complete Adjuvant, however, had a significant effect on the biodistribution of ^{125}I -PNA. This is consistent with the production of anti-PNA antibodies. The i.v. route of administration appears to reduce the risk of antibody production against PNA in CBA/CAJ mice.
6. ^{131}I -PNA dynamic renal scintigraphy in rabbits demonstrated consistent time-to-peak and % inj. dose-at-peak estimates in normal animals. Renal uptake was not affected by probenecid or furosemide but was inhibited by the prior administration of anti-PNA IgG antibodies and by the glycoprotein epiglycanin.
7. Asialo-GM₁-HSA, complexed to ^{131}I -PNA in excess molar concentration, effected the biodistribution pattern in both mice and rabbits resulting in liver accumulation of

- PNA- α -GM₁-HSA complex. No significant enhancement of tumour uptake of radioiodinated PNA, complexed with α -GM₁-HSA at 1:2 or 1:4 molar ratios, was noted in mice with s.c. TA₃-Ha tumours.
8. Dynamic ¹³¹I-PNA renal scintigraphy in normal dogs revealed consistent time-to-peak and % inj. dose-at-peak estimates, as determined from ROI analysis. Plasma pharmacokinetic analysis revealed a rapid clearance of protein-bound radioactivity from the blood following i.v. injection. The initial clearance (<2 h P.I.) appears due to the renal accumulation of ¹³¹I-PNA, however at later times P.I., the deiodination of ¹³¹I-PNA, and subsequent free iodide levels in plasma, complicates the quantitative determination of clearance. Both the renal uptake and plasma clearance estimates appear reproducible in normal dogs.
 9. Histological examination of kidney sections following the i.v. administration of PNA and FITC-PNA revealed accumulation of the protein, predominantly by cortical proximal tubules, although some staining was noted in medullary tubules, adjacent to the collecting ducts, in mice, rabbits and dogs. No glomerular accumulation of PNA was noted in any of the species studied. The protein was initially demonstrated on the basement membrane of the tubular cells (<3 h P.I.), while at later time points, intracellular protein was evident, together with luminal staining. It appears that intact PNA is secreted from the peritubular capillaries to the lumen by the proximal tubules. This process appears to be an active process, initiated by the binding of PNA to T-F antigen-like receptors on the basement membrane of the proximal tubules. The binding of PNA to the receptors can be inhibited by the infusion of D-galactose.
 10. The induction of tubular dysfunction in dogs by cis-platinum administration had a significant effect on the plasma clearance and renal uptake of ¹³¹I-PNA. At comparable human doses of cis-platinum, ¹³¹I-PNA renal uptake was diminished by $65.8 \pm 12.7\%$, while ERPF, GFR, and serum creatinine diminished by a lesser degree ($20.9 \pm 11.8\%$, $46.6 \pm 8.9\%$, and $42.7 \pm 5.7\%$ respectively).
 11. ¹³¹I-PNA renal studies in humans revealed similar % inj. dose-at-peak estimates to dogs

and rabbits ($20.2 \pm 1.8\%$) although the time-to-peak was extended to approximately 90 min P.I. in patients with normal renal function.

12. Sequential ^{125}I -PNA renal scintigraphy in patients undergoing cis-platinum chemotherapy has not revealed any acute or chronic toxicity following up to three repeated doses of ^{125}I -PNA. Circulating anti-PNA IgG, IgM or IgE antibodies have not been detected in any patient following multiple i.v. administrations of ^{125}I -PNA. Variations have been noted in the rate of renal accumulation of ^{125}I -PNA in patients with neoplastic disease, but with otherwise normal renal function (Creatinine clearance). The significance of these findings is uncertain at present and warrants further investigation.

6. REFERENCES

1. Oeser, H., Billion, H., *Functionelle Strahlendiagnostik durch etikettierte Röntgen Kontrastmittel*, *Forsch. Geb. Röntgenstrahl.*, 76: 431, 1952.
2. Kimbel, K. H., *Discussion of paper by W. Schlunbaum and H. Billion*, In "Radioaktiv Isotope in Klinik und Forschung Vorträge am Geister Internationalen Symposium," Vol II, Urban and Schartzburg, Berlin, 1956. pp 150.
3. Taplin, G. V., Meredith, O. M., Kade, H., et al., *The radioisotope renogram*, *J. Lab. Clin. Med.*, 48: 886, 1956.
4. Winter, C. C., Taplin, G. V., *A clinical comparison and analysis of radioactive Diotrast, Hypaque, Miokon and Urokon renograms as tests of renal function*, *J. Urol.*, 79: 573, 1958.
5. Tubis, M., Posnick, E., Nordyke, R. A., *Preparation and use of ^{131}I labeled sodium iodohippurate in kidney function tests*, *Proc. Soc. Exp. Biol. Med.*, 103: 497, 1960.
6. Swick, M., *Excretion Urography by means of the I.V. and oral administration of sodium ortho-iodohippurate with some physiological considerations*, *Surg. Gynec. Obstet.*, 56: 62, 1933.
7. Smith, H., Finkelstein, N., Alminosa, M., et al., *The renal clearance of substituted hippuric acid derivatives and other aromatic acids in dogs and man*, *J. Clin. Invest.*, 24: 388, 1945.
8. Mitta, A. E. A., Fraga, A., Veall, N., *A simplified method for preparing ^{131}I -labeled hippuran*, *Int. J. Appl. Radiat. Isot.*, 12: 146, 1961.
9. Elias, H., Arnold, C. H., Koss, G., *Preparation of ^{131}I -labeled m-iodohippuric acid and its behavior in kidney function studies compared to o-iodohippuric acid*, *Int. J. Appl. Radiat. Isotopes*, 24: 463, 1973.
10. Gillet, R., Cogneau, M., Mathy, G., *The preparation of I-123 labeled sodium-iodo hippurate for medical research*, *Int. J. Appl. Radiat. Isot.*, 27: 61, 1976.
11. Thakur, M. L., Chauser, B. M., Hudson, R. F., *The preparation of iodine-123 labeled sodium orthoiodohippurate and its clearance by the rat kidneys*, *Int. J. Appl. Radiat. Isot.*, 26: 319, 1975.
12. Sinn, H., Maier-Borst, W., Elias, H., *An efficient method for routine production of orthoiodohippuric acid labeled with ^{131}I , ^{125}I , or ^{123}I* , *Int. J. Appl. Radiat. Isot.*, 28: 809, 1977.
13. Zielinski, F. W., Holly, F. E., Robinson, G. D., et al., *Total and individual kidney function assessment with iodine-123 orthoiodohippurate*, *Radiology*, 125: 753, 1977.
14. Chervu, L. R., Blaufox, M. D., *Renal Radiopharmaceuticals, an update*, *Sem. Nucl. Med.*, 12: 224, 1982.
15. Haynie, T. P., Nafal, M., Carr, E. A., et al., *Scintillation scanning of the kidneys and*

- radiolabeled contrast media.*, Clin. Res., 8: 288, 1960.
16. McAfee, J. G., Wagner, H. N., Alminosa, M., et al., *Visualization of renal parenchyma: scintiscanning with ^{203}Hg neohydrin.*, Radiology., 75: 820, 1960.
 17. Sodee, D. B., *A new scanning isotope ^{197}Hg Neohydrin.*, J. Nucl. Med., 5: 74, 1964.
 18. Laa Kso, L., Lindgren, I., Rekonen, A., *Radiomercury and rat kidney. An autoradiographic study with neohydrin- ^{203}Hg .*, Acta. Radiol., 3: 304, 1965.
 19. McAfee, J. G., *Problems in evaluating the radiation dose for radionuclides excreted by the kidneys.*, In "Medical Radionuclides: Radiation Dose and Effects", Cloutier R. J., Edwards C. L., Snyder W. S., (eds), U.S.A.E.C., 1970.
 20. Reba, R. C., Wagner, H. N., McAfee, J. G., *Measurement of ^{203}Hg chloromerodrin accumulation by the kidneys for detection of unilateral renal disease.*, Radiology., 79: 134, 1962.
 21. Schlegel, J. V., Varela, R., Stanton, J. J., *Individual renal plasma flow determination without ureteral catheterization.*, J. Urol., 96: 20, 1966.
 22. Tabern, D. L., Kearney, J., Sohn, H., *The quantitative measurement of tubular chlormerodrin binding as an index of renal function: A study of 400 cases.*, Can. Med. Assoc. J., 103: 601, 1970.
 23. Gadbois, W. F., Corriere, J. N., *The use of segmental ^{197}Hg chlormerodrin delayed scans to evaluate and to follow individual renal function.*, J. Urol., 112: 420, 1974.
 24. Dayton, D. A., Maher, F. T., Elveback, L. R., *Renal clearance of technetium ($^{99\text{m}}\text{Tc}$) as pertechnetate.*, Mayo Clin. Proc., 44: 539, 1969.
 25. Blafox M. D., Gruskin, A., Sander, P., et al., *Radionuclide scintigraphy for detection of vesicoureteral reflux in children.*, J. Pediatr., 79: 239, 1971.
 26. Conway, J. J., King, L. R., Belman, B., et al., *Detection of vesicoureteral reflux with radionuclide cystography. A comparison study with roentgenographic cystography.*, Am. J. Roentgenol. Radium Ther. Nucl. Med., 115: 720, 1972.
 27. Harper, P. V., Lathrop, K. A., Hinn, G. M., et al., *Technetium- $^{99\text{m}}$ iron complex*, In Radioactive Pharmaceuticals. Andrews G. A., Kniseley R. M., Wagner H. N. (eds) U.S.A.E.C. 1966.
 28. Kountz, S. L., Yeh, S. H., Wood, J., *$^{99\text{m}}\text{Tc}$ (V) citrate complex for estimation of glomerular filtration rate.*, Nature, 215: 1397, 1967.
 29. Fleay, R. F., *$^{99\text{m}}\text{Tc}$ labeled E.D.T.A. for renal scanning.*, Aust. Radiol., 12: 265, 1968.
 30. Charamaza, O., Budikova, M., *Method of preparation of $^{99\text{m}}\text{Tc}$ -Sn-complex for renal scintigraphy.*, Nucl. Med., 8: 301, 1969.
 31. Eckelman, W. C., Richards, P., *Instant $^{99\text{m}}\text{Tc}$ -DTPA*, J. Nucl. Med., 11: 761, 1970.
 32. Brookeman, V. A., Williams, C. M., *Evaluation of $^{99\text{m}}\text{Tc}$ -DTPA acid as a brain scanning agent.*, J. Nucl. Med., 11: 733, 1970.

33. Subramanian, G., McAfee, J. G., Bell, E. G., et al., *New ^{99m}Tc -labeled radiopharmaceuticals for renal imaging*, J. Nucl. Med., 12: 399, 1971.
34. Lebowitz, E., Atkins, H. I., Hauser, W., et al., *^{99m}Tc -gelatin: a "compound" with high renal specificity*, Int. J. Appl. Radiat. Isotopes, 22: 786, 1971.
35. Winchell, H. S., Lin, M. S., Shipley, B., et al., *Localization of polypeptide caseidin in the renal cortex: A new radioisotope carrier for renal studies*, J. Nucl. Med., 12: 678, 1971.
36. Halpern, S., Tubis, M., Endow, J., et al., *^{99m}Tc -Pencillamine-Acetazolamide complex. A new renal scanning agent*, J. Nucl. Med., 13: 45, 1972.
37. Fliegel, C. P., Dewanjee, M. K., Holman, L. B., et al., *^{99m}Tc -tetracycline as a kidney and gall bladder imaging agent*, Radiology, 110: 407, 1974.
38. Lin, T. H., Khentigan, A., Winchell, H. S., *A ^{99m}Tc -Gluconate substitute for organoradiomercurial renal agents*, J. Nucl. Med., 15: 34, 1974.
39. Arnold, R. W., Subramanian, G., McAfee, J. G., et al., *Comparison of ^{99m}Tc -Complexes for renal imaging*, J. Nucl. Med., 16: 357, 1975.
40. Hagan, P. L., Ayres, P. R., Halpern, S. E., et al., *^{99m}Tc -thiomalic acid (TMA): A new non-stannous renal scanning agent. Preparation and evaluation*, J. Nucl. Med., 16: 531, 1975.
41. Subramanian, G., Singh, M. V., Chander, J., et al., *^{99m}Tc -Sn-acetylcysteine: A new renal scanning agent*, Eur. J. Nucl. Med., 1: 243, 1976.
42. Machida, T., Miki, M., Ueda, M., et al., *Basic studies of various ^{99m}Tc -labeled renal agents and clinical application of ^{99m}Tc -malate*, Nuklearmedizin, 16: 36, 1977.
43. Robinson, R. G., Bradshaw, D., Rhodes, B. A., et al., *A rapid one-step kit for the routine preparation of basic ^{99m}Tc -pencillamine*, Int. J. Appl. Radiat. Isotopes, 28: 919, 1977.
44. Fritzberg, A. R., Lyster, D. M., Dolphin, D. H., *^{99m}Tc -Ethyl-thiomethyl phosphonate: A new renal scanning agent*, Int. J. Nucl. Med. Biol., 4: 113, 1977.
45. Fritzberg, A. R., Lyster, D. M., Dolphin, D. H., *^{99m}Tc -Glutathione: Role of reducing agent on renal retention*, Int. J. Nucl. Med. Biol., 5: 87, 1978.
46. Vanlic-Razumenic, N., Johannsen, B., Spies, H., et al., *Complex of Tc (V) with 2,3-dimercaptopropanesulfonate (Unithiol): Preparation and Distribution in the rat*, Int. J. Appl. Radiat. Isotopes, 30: 661, 1979.
47. Fritzberg, A. R., Klingensmith, W. C., Whitney, W. P., et al., *Chemical and biological studies of ^{99m}Tc -N,N'-Bis(mercaptoacetamido)-ethylenediamine: A potential replacement for I-131 iodohippurate*, J. Nucl. Med., 22: 258, 1981.
48. Fritzberg, A. R., Kuni, C. C., Klingensmith, W. C., et al., *Synthesis and evaluation of Tc- 99m N,N'-bis(mercaptoacetyl)-2,3-diaminopropionate: A potential replacement for [^{131}I]o-iodohippurate*, J. Nucl. Med., 23: 592, 1982.
49. Chervu, L. R., Sundoro, B. M., Blafox, M. D., *Technetium- 99m -labeled P-aminohippuric acid analogue: A new renal agent: Concise communication*, J. Nucl. Med., 25: 1111, 1984.

50. Stewart, R. D. H., Forster, L., Ross, I. H., *Radionuclide imaging of the kidneys and bladder using technetium-99m gluconate*, Aust. N.Z. J. Med., 2: 336, 1972.
51. Boyd, R. E., Robson, J., Hunt, F. C., et al., *^{99m}Tc-gluconate complexes for renal scintigraphy*, Br. J. Radiol., 46: 604, 1973.
52. Kahn, P. C., Dewanjee, M. K., Brown, S. S., *Routine renal imaging after ^{99m}Tc-glucoheptonate brain scans*, J. Nucl. Med., 17: 786, 1976.
53. Halpern, S. E., Tubis, M., Golden, M., et al., *^{99m}Tc-PAC, A new renal scanning agent. II Evaluation in humans*, J. Nucl. Med., 13: 723, 1972.
54. Taylor, A., Davis, G., Halpern, S., et al., *^{99m}Tc-pencillamine: A renal cortical scanning agent*, J. Urol., 117: 418, 1977.
55. Carthy, H., *Dimercaptosuccinic acid imaging of the kidneys*. In "Non-invasive diagnosis of kidney disease.", Lubec, G. (ed), Karger, Basel, 1983. pp 280.
56. Handmaker, H., Young, B. W., Lowenstein, J. M., *Clinical experience with ^{99m}Tc-DMSA, a new renal imaging agent*, J. Nucl. Med., 16: 28, 1975.
57. Bingham, J. B., Maisey, M. N., *An evaluation of the use of ^{99m}Tc-DMSA as a static renal imaging agent*, Br. J. Radiol., 51: 599, 1978.
58. Wang, S. C., Ting, K. S., Woo, C. C., *Chelating therapy with Na-DMS in occupational and mercury intoxications*, Chinese Med. J., 84: 437, 1965.
59. Yee, C. A., Lee, H. B., Blafox, M. D., *^{99m}Tc-DMSA renal uptake: Influence of biochemical and physiologic factors*, J. Nucl. Med., 22: 1054, 1981.
60. Hosokawa, S., Kawamura, J., Yoshida, O., *Basic studies on the intrarenal localization of renal scanning agent ^{99m}Tc-DMSA*, INIS. Atomic Index, 9:417789, 1978.
61. Vanlic-Razumenic, N., Petrovic, J., *Biochemical studies of the renal radiopharmaceutical compound. Dimercaptosuccinate. I. Subcellular localization of ^{99m}Tc-DMS complex in the rat kidney in vivo*, Eur. J. Nucl. Med., 6: 169, 1981.
62. Van Luyk, W. H. J., Ensing, G. J., Piers, D. A., *Low renal uptake of ^{99m}Tc-DMSA in patients with proximal tubular dysfunction*, Eur. J. Nucl. Med., 8: 404, 1983.
63. Willis, K. W., Martinez, D. A., Hedley-White, E. T., et al., *Renal localization of ^{99m}Tc (Sn) Glucoheptonate and ^{99m}Tc (Sn) dimercaptosuccinate in the rat by frozen section autoradiography*, Rad. Res., 69: 475, 1977.
64. Kági, J. H. R., Himmelhoch, S. R., Whagner, P. D., et al., *Equine hepatic and renal metallothioneins*, J. Biol. Chem., 249: 3537, 1974.
65. Ikeda, I., Inoue, O., Kurata, K., *Chemical and biological studies on ^{99m}Tc-DMS. I: Formation of complexes by four different methods*, Int. J. Nucl. Med. Biol., 4: 56, 1977.
66. Ikeda, I., Inoue, O., Kurata, K., *Preparation of various ^{99m}Tc-DMSA complexes and their evaluation as radiotracers*, J. Nucl. Med., 18: 1222, 1977.
67. Razumenic, N. M. V., Gorkic, D., *Studies of chemical and biological properties of*

$^{99m}\text{Tc-DMSA}$, Eur. J. Nucl. Med., 1: 235, 1976

68. Ikeda, I., Inoue, O., Kurata, K., *Chemical and biological studies on $^{99m}\text{Tc-DMS}$ II. Effect of Sn(II) on the formation of various Tc-DMS complexes.*, Int. J. Appl. Radiat. Isotopes, 27: 681, 1976.
69. Krejcarek, G. E., Wicks, J. H., Heerwald, P. E., et al., *The structure of stannous dimercaptosuccinic acid chelates.*, J. Nucl. Med., 17: 565, 1976.
70. Blantz, R. C., Konnen, K. S., Tucker, B. J., *Glomerular filtration response to elevated ureteral pressure in both the hydropenic and plasma expanded rat.*, Circ. Res., 37: 819-829, 1975.
71. Deen, W. M., Robertson, C. R., Brenner, B. M., *Model of glomerular ultrafiltration in the rat.*, Am. J. Physiol., 223: 1178, 1972.
72. Brenner, B. M., Troy, J. L., Daugharty, T. M., *The dynamics of glomerular ultrafiltration in the rat.*, J. Clin. Invest., 50: 1776-1780, 1971.
73. Smith, H. W., *"Principles of Renal Physiology"*, Oxford University Press, New York, 1956.
74. Richards, A. N., Westfall, B. B., Bott, P. A., *Renal excretion of inulin, creatinine and xylose in normal dogs.*, Proc. Soc. Exp. Biol. Med., 32: 73, 1934.
75. Shannon, J. A., Smith, H. W., *The excretion of inulin, xylose and urea by normal and phlorizintized man.*, J. Clin. Invest., 14: 93, 1935.
76. Marlow, C. G., Sheppard, G., *$^{51}\text{Cr-EDTA}$, (hydroxymethyl- ^{14}C) inulin and inulin-T for the determination of glomerular filtration rate.*, Clin. Chim. Acta., 28: 479, 1970.
77. Cotlove, E., *^{14}C carboxyl-labeled inulin as a tracer for inulin.*, Fed. Proc., 14: 32, 1955.
78. Marlow, C. G., Sheppard, G., *Labeled tracers of inulin for physiological measurements.*, Clin. Chim. Acta., 28: 469, 1970.
79. Brooks, S. A., Davies, J. W. L., Graber, I. G., et al., *Labeling of inulin with radioactive iodine.*, Nature, 188: 675, 1960.
80. Concannon, J. P., Summers, R. E., Brewer, R., et al., *^{131}I allyl inulin for the determination of glomerular filtration rate.*, Am. J. Roentgenol. Radium Ther. Nucl. Med., 92: 302, 1964.
81. Haas, J. P., Prellwitz, W., *Die Bestimmung der renalen und totalen clearance mit ^{131}I -markiertem chlojodpropyl-Inulin.*, In "Radioaktive Isotope in Klinik und Forschung", Vol 7, Urban and Schwarzenberg, München, 1967, pp. 462.
82. Hör, G., Steinhoff, H., Heinze, H. G., et al., *^{131}I -inulin for quantitative determination of glomerular filtration rate.*, Acta. Radiol., 6: 579, 1967.
83. Adam, W. E., Hardt, H., Bonatz, K. G., et al., *Untersuchungen zur bestimmung des glomerulus filtrats mit radioaktive inulin.*, Klin. Wochenschr., 5: 818, 1967.
84. Johnson, H. E., Hartley, B., Gollan, F., *Preparation and properties of $\text{Cr-}^{51}\text{I}$ labeled*

- inulin., *J. Nucl. Med.*, 8: 97, 1967.
85. Nelp, W. B., Wagner, H. N., Reba, R. C., *Renal excretion of vitamin B₁₂ and its use in measurement of glomerular filtration rate.*, *J. Lab. Clin. Med.*, 63: 480, 1964.
 86. Breckenbridge, A., Metcalfe-Gibson, A., *Methods of measuring glomerular filtration. A comparison of inulin, vitamin B₁₂ and creatinine clearances.*, *Lancet*, 2: 265, 1965.
 87. Elwood, C. M., Sigman, E. M., *The measurement of glomerular filtration and effective renal plasma flow in man by iothalamate ¹³¹I and iodopyracet ¹³¹I.*, *Circulation*, 36: 441, 1967.
 88. Griep, R. J., Help, W. B., *Mechanism of excretion of radioiodinated sodium iothalamate.*, *Radiology*, 93: 807, 1969.
 89. Silkalns, G. I., Jeck, D., Earon, J., et al., *Simultaneous measurement glomerular filtration rate and renal plasma flow using plasma disappearance curves.*, *J. Pediatr.*, 83: 749, 1973.
 90. Barbour, G. L., Crumb, K., Boyd, M., et al., *Comparison of inulin, iothalamate, and ^{99m}Tc-DTPA for measurement of glomerular filtration rate.*, *J. Nucl. Med.*, 17: 317, 1976.
 91. Tessitore, N., LoSchiavo, Corgnati, A., et al., *¹²⁵I-iothalamate and creatinine clearances in patients with chronic renal disease.*, *Nephron*, 24: 41, 1979.
 92. Kimbel, K. H., Borner, W., *Über den Verbleib von ¹³¹I markiertem in Körper.*, *Naunyn-Schmiedeberg's Arch. Exper. Path. Pharmacol.*, 226: 262, 1955.
 93. Blafox, M. D., Sanderson, D. R., Tauxe, W. N., et al., *Plasmatic diatrizoate-¹³¹I disappearance and glomerular filtration in the dog.*, *Am. J. Physiol.*, 204: 536, 1963.
 94. Tauxe, W. N., Burbank, M. K., Maher, F. T., et al., *Renal clearances of radioactive orthiodohippurate and diatrizoate.*, *Mayo Clin. Proc.*, 39: 761, 1964.
 95. Bianchi, C., Hegesippe, E., Meozzi, A., et al., *Effect of autoradiolysis on the renal clearance of ¹³¹I labeled Hypaque and Hippuran.*, *Minerva Nucleare*, 9: 152, 1965.
 96. Maher, F. T., Nolan, N. G., Elveback, L. R., *Comparison of simultaneous clearances of ¹³¹I-labelled iothalamate (Glofil) and of inulin.*, *Mayo Clin. Proc.*, 46: 690, 1971.
 97. Foreman, H., Vier, M., Magee, M., *The metabolism of ¹⁴C labeled ethylenediaminetetraacetic acid in the rat.*, *J. Biol. Chem.*, 203: 1045, 1953.
 98. Foreman, H., Trujillo, T. T., *The metabolism of ¹⁴C labeled ethylene diamine-tetraacetic acid in the human being.*, *J. Lab. Clin. Med.*, 43: 566, 1954.
 99. Heller, J., Vostal, J., *Renal excretion of calcium-disodium ethylenediaminetetraacetic acid.*, *Experimentia*, 20: 99, 1964.
 100. Stevens, E., Rosoff, B., Weiner, M., et al., *Metabolism of the chelating agent diethylene triaminepentaacetic-¹⁴C-DTPA in man.*, *Proc. Soc. Exp. Biol. Med.*, 111: 235, 1962.
 101. Klopfer, J. F., Hauser, W., Atkins, H. L., et al., *Evaluation of ^{99m}Tc-DTPA for the measurement of glomerular filtration rate.*, *J. Nucl. Med.*, 13: 107, 1972.

102. Bianchi, C., Coli, A., Palla, R., et al., *The reliability of ^{140}La -DTPA for the determination of glomerular filtration rate.*, J. Nucl. Biol. Med., 15: 122, 1971.
103. Sziklas, J. I., Hosain, F., Reba, R. C., et al., *Comparison of ^{169}Yb -DTPA, ^{113}mIn -DTPA, ^{14}C -inulin and endogenous creatinine to estimate glomerular filtration.*, J. Nucl. Biol. Med., 15: 122, 1971.
104. Reba, R. C., Poulouse, K. P., Kirchner, P. R., *Radiolabeled chelates for visualization of kidney function and structure with emphasis on their use in renal insufficiency.*, Sem. Nucl. Med., 4: 151, 1974.
105. Hosain, F., Reba, R. C., Wagner, H. N., *Visualization of renal structure and function with chelated radionuclides.*, Radiology, 93: 1135, 1969.
106. Molnar, G., Pal, I., Stutzel, M., et al., *Determination of glomerular filtration rate with ^{51}Cr , ^{59}Co , ^{114}In , ^{115}In and ^{169}Yb labeled EDTA and DTPA complexes.*, In "Proceedings of Symposium on Dynamic Studies with Radioisotopes in Medicine", I.A.E.A., Vienna, 1971.
107. Stacy, B. D., Thorburn, G. D., *Chromium-51 ethylenediaminetetraacetate for estimation of glomerular filtration rate*, Science, 152: 1076, 1966.
108. Winter, C. C., Myers, W. G., *Three new testing agents for the radioisotope renogram: DISA- ^{131}I , EDTA- ^{51}Cr and Hippuran ^{125}I .*, J. Nucl. Med., 3: 273, 1962.
109. Garnett, E. S., Parsons, V., Veall, N., *Measurement of glomerular filtration rate in man using a ^{51}Cr edetic acid complex.*, Lancet, 1: 818, 1967.
110. Favre, H. R., Wang, A. J., *Simultaneous ^{51}Cr edetic acid, inulin and endogenous creatinine in 20 patients with renal disease*, B. Med. J., 1: 84, 1968.
111. Ditzel, J., Vestergaard, P., Brinklov, M., *Glomerular filtration rate determined by ^{51}Cr -EDTA complex. A practical method based upon the plasma disappearance curve determined from four plasma samples.*, Scand. J. Urol. Nephrol., 6: 166, 1972.
112. Brochner-Mortensen, J., Rodbro, P., *Selection of routine method for determination of glomerular filtration rate in adult patients.*, Scand. J. Clin. Lab. Invest., 36: 35, 1976.
113. Heidenreich, P., Kriegel, H., Hör, G., et al., *$^{99\text{m}}\text{Tc}$ -DTPA (Sn), Biologische und klinische Untersuchungen zur verteilung, kinetic und in-vivo-stabilität einer renin clearance-substanz.*, Strahlen-Therapie, 74: 174, 1975.
114. Hosain, F., *Quality Control of $^{99\text{m}}\text{Tc}$ -DTPA by double tracer clearance technique.*, J. Nucl. Med., 15: 442, 1974.
115. Kempi, V., Persson, R. B., *$^{99\text{m}}\text{Tc}$ -DTPA (Sn) dry-kit preparation: Quality control and clearance studies.*, Nucl. Med.(Stuttg), 13: 389, 1975.
116. Hilson, A. J. W., Mistry, R. D., Maisey, M. N., *$^{99\text{m}}\text{Tc}$ -DTPA for the measurement of glomerular filtration rate.*, Br. J. Radiol., 49: 794, 1976.
117. Rossing, N., Bølsen, J., Frederiksen, P. L., *The glomerular filtration rate determined with $^{99\text{m}}\text{Tc}$ -DTPA and a portable cadmium telluride detector.*, Scand. J. Clin. Lab. Invest., 38: 23, 1978.

118. Schlegel, J. U., Halikiopoulos, H. L., Prima, R., *Determination of filtration fraction using the gamma scintillation camera.*, J. Urol., 122: 447, 1979.
119. Bianchi, C., Bonadio, M., Donadio, C., et al., *Measurement of glomerular filtration rate in man using DTPA-99mTc.*, Nephron, 24: 174, 1979.
120. Carlsen, J. E., Moller, M. L., Lund, J. O., et al., *Comparison of four commercial Tc-99m (Sn) DTPA preparations used for the measurement of glomerular filtration rate.*, J. Nucl. Med., 21: 126, 1980.
121. McAfee, J. G., Gagne, G., Atkins, H. L., et al., *Biological distribution and excretion of DTPA labeled with Tc-99m and In-111.*, J. Nucl. Med., 20: 1273, 1979.
122. Chervu, L. R., Lee, H. B., Goyal, Q., et al., *Use of 99mTc-Cu-DTPA complexes as a renal function agent.*, J. Nucl. Med., 18: 62, 1977.
123. Anghileri, L. J., *A chromatographic study of the stability of iodine-131 labeled sodium o-iodohippurate.*, J. Nucl. Med., 4: 136, 1963.
124. Hotte, C. E., Ice, R. D., *The in vitro stability of ¹³¹I-O-iodohippurate.*, J. Nucl. Med., 20: 441, 1979.
125. Burbank, M. K., Tauxe, W. N., Maher, F., et al., *Evaluation of radioiodinated hippuran for the estimation of renal plasma flow.*, Mayo Clin. Proc., 36: 372, 1961.
126. Schwartz, F. D., Madeloff, M. S., *Simultaneous renal clearances of radiohippuran and PAH in man.*, Clin. Res., 9: 208, 1961.
127. Mailloux, L., Gagnon, J. A., *Measurement of effective renal plasma flow.*, In "Progress in Nuclear Medicine., Vol. 2. Evaluation of Renal Function and Disease with Radionuclides". Karger, Basel, 1972, pp 54.
128. Blafox, M. D., Orvis, A., Owen, C. A., et al., *Compartmental analysis of the radiorenogram and distribution of ¹³¹I-hippuran in dogs.*, Am. J. Physiol., 204: 1059, 1963.
129. Blafox, M. D., Merrill, J. P., *Simplified hippuran clearance measurement of renal function in man with simplified hippuran clearances.*, Nephron, 3: 274, 1966.
130. Blafox, M. D., Potchen, E. J., Merrill, J. P., *Measurement of effective renal plasma flow in man by external counting methods.*, J. Nucl. Med., 8: 77, 1967.
131. Wellman, H. N., Berke, R. A., Robbins, P. J., *Dynamic quantitative renal imaging with ¹³¹I-hippuran. A possible salvation of the renogram.*, J. Nucl. Med., 12: 405, 1971.
132. Chisholm, G. D., Short, M. D., Glass, H. I., *The measurement of individual renal plasma flow using ¹³¹I-hippuran and the gamma camera.*, Br. J. Urol., 46: 591, 1974.
133. Stadalnik, R. C., Vogel, J. M., Jansholt, A. L., et al., *Renal clearance and extraction parameters of ortho-iodohippurate (I-123) compared with OIH (I-131) and PAH.*, J. Nucl. Med., 21: 168, 1980.
134. *Product information ¹²³I-hippuran.*, Medipysics Corp., Richmond, California, 1985.
135. Klingensmith, W. C., Gerhold, J. P., Fritzberg, A. R., et al., *Clinical comparison of*

- Tc-99m N,N'-bis(mercaptoacetamido)ethylenediamine and [¹³¹I]ortho-iodohippurate for evaluation of renal tubular function: Concise communication.*, J. Nucl. Med., 23: 377, 1982.
136. Schneider, R. F., Subramanian, G., Feld, T. A., et al., *N,N'-bis (S-benzoylmercaptoacetamido) ethylenediamine and propylenediamine ligands as renal function imaging agents. Alternative synthetic methods*, J. Nucl. Med., 25: 223-229, 1984.
 137. McAfee, J. G., Subramanian, G., Schneider, R. F., et al., *Technetium-99m DADS complexes as renal function and imaging agents. II Biological comparison with Iodine-131 hippuran.*, J. Nucl. Med., 26: 375-384, 1985.
 138. Oster, Z. H., Som, P., Gil, M. C., et al., *⁹⁷Ru-DMSA for delayed renal imaging*, Radiology, 141: 185, 1981.
 139. Anghileri, L. J., Ottaviani, M., Ricard, S., et al., *Radioruthenium-2,3-Dimercapto propansulfonic acid complex- A potentially useful radiocompound for kidney studies*, Eur. J. Nucl. Med., 6: 403, 1981.
 140. Wenzel, M., Meinhold, H., Schachschneider, G., *⁹⁷Ru-labeled ruthenocenoyl-glycine: comparison of clearance with hippuran*, Eur. J. Nucl. Med., 10: 138, 1985.
 141. Dubrovsky, E. V., Russel, C. D., *Quantitation of renal function with glomerular and tubular agents.*, Sem. Nucl. Med., 12: 308, 1982.
 142. Taylor, A., *Quantitation of renal function with static imaging agents.*, Sem. Nucl. Med., 12: 330, 1982.
 143. Blafox, M. P., *Compartmental analysis of the radiorenogram and kinetics of ¹³¹I-hippuran.*, Prog. Nucl. Med., 2: 107, 1972.
 144. Sapirstein, L. A., Vidt, D., Mandel, M., et al., *Volumes of distribution and clearances of intravenously injected creatinine in the dog*, Am. J. Physiol., 181: 330, 1955.
 145. Tauxe, W. N., Maher, F. T., Taylor, W. F., *Effective renal plasma flow: Estimation from theoretical volumes of distribution of intravenously injected ¹³¹I-orthoiodohippurate*, Mayo Clin. Proc., 46: 524, 1971.
 146. Tauxe, W. N., Dubrovsky, E. V., Kid, T., *New formula for the calculation of effective renal plasma flow.*, Eur. J. Nucl. Med., 7: 51, 1982.
 147. Botsch, H., Lange, S., Golde, G., et al., *Estimation of effective renal plasma flow by a simplified method using a single plasma sample. Comparison with the two compartment analysis and other simplified methods*, In "Radionuclides in Nephrology." Hollenberg, N., Lange, S., (eds.), Thieme Stratton, Stuttgart, 1980. pp-59.
 148. Constable, A. R., Hussein, M. M., Albrecht, M. P., et al., *Renal clearance determination from single plasma sample*, In "Radionuclides in Nephrology." Hollenberg, N., Lange, S., (eds.), Thieme Stratton, Stuttgart, 1980. pp 62.
 149. Mathews, C. M. E., *The theory of tracer experiments with ¹³¹I-labeled plasma proteins*, Phys. Med. Biol., 2: 36-53, 1957.
 150. Tauxe, W. N., Dubrovsky, E. V., Kid, T., et al., *Prediction of urinary excretion of ¹³¹I-orthoiodohippurate*, Eur. J. Nucl. Med., 7: 102, 1982.

151. Cohen, M. L., Patel, J. K., Baxter, D. L., *External monitoring and plasma disappearance for the determination of renal function: Comparison of effective renal plasma flow and glomerular filtration.*, *Pediatrics*, 48: 377-392, 1971.
152. Blaurox, M. D., Potchen, E. J., Merrill, J. P., *Measurement of effective renal plasma flow in man by external counting methods.*, *J. Nucl. Med.*, 8: 77, 1967.
153. Taplin, G. V., Gore, E. K., Johnson, D. E., *The quantitative radiorenogram for total and differential renal blood flow measurements*, *J. Nucl. Med.*, 4: 404-409, 1963.
154. Britton, K. E., Brown, N. J. G., "Clinical Renography." Chicago Year Book, Medical Publishers, 1972.
155. Kenny, R. W., Ackery, D. M., Fleming, J. S., et al., *Deconvolution analysis of the scintillation camera renogram.*, *Br. J. Radiol.*, 48: 481-486, 1975.
156. Seckter-Walker, R. H., Coleman, R. E., *Estimating relative renal function*, *J. Urol.*, 115: 621-625, 1976.
157. Hayes, M., Brosman, S., Taplin, G. V., *Determination of differential renal function by sequential renal scintigraphy*, *J. Urol.*, 111: 556-559, 1974.
158. Taylor, A., *Delayed scanning with DMSA: A simple index of relative renal plasma flow.*, *Radiology*, 136: 449, 1980.
159. Daly, J., Jones, W., Rudd, T. G., et al., *Differential renal function using technetium-99m dimercaptosuccinic acid (DMSA): In vitro correlation.*, *J. Nucl. Med.*, 20: 63, 1979.
160. Kawamura, J., Hosokawa, S., Yoshida, O., et al., *Validity of 99mTc-DMSA renal uptake for an assessment of individual kidney function.*, *J. Urol.*, 119: 305, 1978.
161. Bailey, R. R., Réddy, J. R., Boniface, G. R., et al., *Estimating unilateral renal function with non-invasive methods*, *N.Z. Med. J.*, 96: 12, 1983.
162. Piepsz, A., Denis, R., Ham, H. R., et al., *A simple method for measuring separate glomerular filtration rate using a single injection of 99mTc-DTPA and the scintillation camera.*, *J. Pediatr.*, 93: 769, 1978.
163. Duffy, G. J., Casey, M., Basker, F., *A comparison of individual kidney GFR measured by Tc-99m-DTPA gamma camera renography and by direct collection of creatinine from each kidney*, In "Radionuclides in Nephrology." Academic Press Inc., London, 1982.
164. Enlander, D., Weber, P. M., dos Remedios, L. V., *Renal cortical imaging in 35 patients. Superior quality with 99mTc-DMSA.*, *J. Nucl. Med.*, 15: 743, 1975.
165. O'Reilly, P. H., Shields, R. A., Testa, H. J., "Nuclear Medicine in Urology and Nephrology." Butterworths, London, 1979.
166. Maxwell, M. H., Prozan, G. B., *Renovascular hypertension*, *Prog. Cardiovasc. Dis.*, 5: 1962.
167. Smith, G. W., Mullen, W. H., Beck, J. R., *Surgical results and the diagnostic evaluation of renovascular hypertension.*, *Ann. Surg.*, 167: 669, 1968.

168. Britton, K. E., Nimmon, C. C., Gruenewald, S. M., *Intrarenal plasma flow measurement noninvasively in man with 123-I orthodihydroxyphenylisodiphenylhydantoin*, J. Nucl. Med., 26: 81, 1985.
169. Clorius, J. H., Schmidlin, P., Raptou, E., et al., *Hypertension associated with massive bilateral, posture-dependent renal dysfunction*, Radiology, 140: 231, 1981.
170. Clorius, J. H., Schmidlin, P., *The exercise renogram. A new approach documents renal involvement in systematic hypertension*, J. Nucl. Med., 24: 104, 1983.
171. Kirchner, P. T., Rosenthal, L., *Renal transplant evaluation*, Sem. Nucl. Med., 12: 370, 1982.
172. Dubovsky, E. V., Logic, J. R., Reitheim, A. G., et al., *Comparative evaluation of renal function in the transplanted kidney*, J. Nucl. Med., 16: 1115, 1975.
173. Hilson, A. W. J., Maissey, M. N., Brown, C. B., et al., *Dynamic renal transplant imaging with Tc-99m DTPA (Sn) supplemented by a transplant perfusion index in the management of renal transplants*, J. Nucl. Med., 19: 994, 1978.
174. Leonard, J. C., Baumann, W. E., Pederson, J. A., et al., *^{99m}Tc-sulphur colloid scanning in diagnosis of renal transplant rejection*, J. Urol., 123: 815, 1980.
175. Fenech, H., Nicholls, A., Smith, S. W., *Indium (¹¹¹In)-labelled platelets in the diagnosis of renal transplant rejection: Preliminary findings*, Br. J. Radiol., 54: 325, 1981.
176. Forström, L. E., Loken, M. K., Cook, A., et al., *In-111-labeled leukocytes in the diagnosis of rejection and cytomegalovirus infection in renal transplant recipients*, Clin. Nucl. Med., 6: 146, 1981.
177. Duarte, C., "Renal Function Tests." Little, Brown & Co. Boston, 1980. pp 1.
178. Berlyne, G. M., Varley, H., Nilwarangkar, S., et al., *Endogenous creatinine clearance and glomerular filtration rate*, Lancet, 2: 874, 1964.
179. Husdan, H., Rapoport, A., *Estimation of creatinine by the Jaffe reaction: A comparison of three methods*, Clin. Chem., 14: 222, 1968.
180. Chasson, A. L., Grady, H. J., Stanley, M. A., *Determination of creatinine by means of automatic chemical analysis*, Am. J. Clin. Pathol., 55: 83, 1961.
181. Rapoport, A., Husdan, H., *Endogenous creatinine clearance and serum creatinine in the clinical assessment of kidney function*, Can. Med. Assoc. J., 99: 146, 1968.
182. Lubowitz, H., Slatopolsky, E., Shankel, S., *Glomerular filtration rate: Determination in patients with chronic renal disease*, J.A.M.A., 199: 252, 1967.
183. Kim, K. E., Onesti, G., Ramirez, Q., et al., *Creatinine clearance in renal disease: A reappraisal*, Br. Med. J., 4: 11, 1969.
184. Berggård, I., Bearn, A. G., *Isolation and properties of a low molecular weight β_2 -globulin occurring in human biological fluids*, J. Biol. Chem., 243: 4095, 1968.
185. Statius van Eps, L. W., Schardijn, G. H. C., *β_2 -microglobulin and the renal tubule*, In "Non-Invasive Diagnosis of Kidney Disease.", Lubec G. (ed) Karger Basel, 1983. pp 103.

186. Cunningham, B. A., Wang, J. L., Berggård, I., et al., *The complete amino acid sequence of β_2 -microglobulin*, Biochemistry, 12: 4811, 1973.
187. Peterson, D. A., Rask, L., Lindblom, J. B., *Highly purified papain-solubilized HLA antigens contain β_2 -microglobulin*, Proc. Nat. Acad. Sci. USA, 71: 35, 1974.
188. Thomson, D. M., Rauch, J. E., Weatherhead, J. C., et al., *Isolation of tumour specific antigens associated with β_2 -microglobulins*, Br. J. Cancer, 37: 753, 1978.
189. Creswell, P., Springer, T., Strominger, J. L., et al., *Immunological identity of the small subunit of HLA antigens and β_2 -microglobulin and its turnover on the cell membrane*, Proc. Nat. Acad. Sci. USA, 71: 2123, 1974.
190. Peterson, P. A., Evrin, P. E., Berggård, I., *Differentiation of glomerular, tubular and normal proteinuria: determinations of urinary excretion of β_2 -microglobulin, albumin and total protein*, J. Clin. Invest., 48: 1189, 1969.
191. Bernier, G. M., Post, R. S., *β_2 -microglobulin. A marker of renal homograft survival*, Transplantation, 15: 176, 1973.
192. Dunea, G., Freedman, P., *Renal clearance studies*, J.A.M.A., 205: 171, 1968.
193. De Wardener, H. E., "The Kidney: An outline of Normal and Abnormal Structure and Function." (4th Ed), Churchill/Livingston, Edinburgh, 1973. pp 33.
194. Albert, Z., Orlowska, J., Orlowski, M., et al., *Histochemical and biochemical investigations of gamma-glutamyl transpeptidase in the tissue of man and laboratory rodents*, Acta. Histochem., 18: 78, 1964.
195. Beck, P. R., *γ -Glutamyltransferase in kidney disease*, In "Non-invasive diagnosis of kidney disease." Lubec G. (ed) Karger, Basel, 1983. pp 2.
196. Clark, P. M. S., *Iso salt analysis of urinary proteins*, In "Non-invasive diagnosis of kidney disease." Lubec G. (ed) Karger, Basel, 1983. pp 144.
197. Pesce, A. J., "Proteinuria: an integrated review.", Marcel Dekker, New York, 1979.
198. Waldmann, T. A., Strober, W., Mogielpicki, R. P., et al., *The renal handling of low molecular weight proteins. II. Disorders of serum protein catabolism in patients with tubular proteinuria, the nephrotic syndrome or uremia*, J. Clin. Invest. 51: 2162, 1972.
199. Lubec, G., "Non Invasive diagnosis of kidney diseases". Karger, Basel, 1983.
200. Fleming, J. J., Child, J. A., Cooper, E. H., *Renal tubular damage without glomerular damage after cytotoxic drugs and aminoglycosides*, Biomedicine, 33: 251, 1980.
201. Jones, B. R., Bhalla, R.B., Mladek, J., et al., *Comparison of methods of evaluating nephrotoxicity of cis-platinum*, Clin. Pharmacol. Therap., 27: 557, 1980.
202. Gouswaard, J., Virella, G., *Role and value of Lysosyme determination for Non-invasive diagnosis of kidney disease*, In "Non invasive diagnosis of kidney diseases". Lubec G. (ed) Karger, Basel 1983. pp 19.
203. Tamm, I., Horsfall, F. L., *Characterization and separation of an inhibitor of viral*

- hemagglutination present in urine., *Proc. exp. Soc. Biol. Med.*, 74: 108, 1950.
204. Tamm, I., Horsfall, F. L., *A mucoprotein derived from human urine which reacts with influenza, mumps and Newcastle disease viruses*, *J. Exp. Med.*, 95: 71, 1952.
 205. Fletcher, A. P., Neuberger, A., Ratcliffe, W. A., *Tamm-Horsfall urinary glycoprotein. The chemical composition.*, *Biochem. J.*, 120: 417, 1970.
 206. McKenzie, J. K., McQueen, E. G., *Immunofluorescent localization of Tamm-Horsfall mucoprotein in human kidney.*, *J. Clin. Path.*, 22: 334, 1969.
 207. Hoyer, J. R., Sisson, S. P., Vernier, R. L., *Tamm-Horsfall glycoprotein. Ultrastructural immunoperoxidase localization in the rat kidney.*, *Lab. Invest.*, 41: 168, 1979.
 208. McQueen, E. G., *The nature of urinary casts.*, *J. Clin. Path.*, 15: 367, 1962.
 209. McQueen, E. G., *Composition of urinary casts.*, *Lancet*, i: 397, 1966.
 210. Grant, A. M. S., Baker, L. R. I., Neuberger, A., *Urinary Tamm-Horsfall glycoprotein in certain kidney diseases and its content in renal and bladder calculi.*, *Clin. Sci.*, 44: 377, 1973.
 211. Hartmann, L., Ambert, J. P., Ollier-Hartmann, M. P., et al., *Fixation du chlorure mercurique et de l'acide étacrinique sur l'uromucoïde ou protéine de Tamm-Horsfall.*, *Biomedicine*, 35: 30, 1981.
 212. Ollier-Hartmann, M. P., Pouget-Abadie, C., Bouillie, J., et al., *Variations of urinary Tamm-Horsfall Protein in humans during the first thirty years of life.*, *Nephron*, 38: 163, 1984.
 213. Sarna, G., Skinner, D. G., Smith, R. B., et al., *cis-Diamminedichloroplatinum(II) alone and in combination in the treatment of testicular and other malignancies.*, *Cancer Treat. Rep.*, 64: 1077, 1980.
 214. Hill, J. M., Speer, R. J., *Organo-Platinum complexes as antitumor agents.*, *Anticancer Res.*, 2: 173, 1982.
 215. Burchenal, J. H., *A clinical overview of dichlorodiamino platinum.*, *Biochimie*, 60: 915, 1978.
 216. Hall, D. J., Diasio, R., Goplerud, D. R., *Cis platinum in gynecological cancer. I. Epithelial ovarian cancer.*, *Am. J. Gynecol.*, 141: 299, 1981.
 217. Nitschke, R., *Renal complications of cis-diamminedichloroplatinum.*, *Ann. Clin. Lab. Sci.*, 11: 392, 1981.
 218. Goldstein, R. S., Norderwiler, B., Bond, J. T., et al., *Cis-dichloro-diammineplatinum nephrotoxicity: time course and dose response of renal functional impairment.*, *Toxicol. Appl. Pharmacol.*, 60: 163, 1981.
 219. Goldstein, R. H., Mayor, G. H., *The nephrotoxicity of cisplatin.*, *Life Sci*, 32: 685, 1983.
 220. Ward, J. M., Fauvie, K. A., *The nephrotoxicity of cis-diamminedichloroplatinum (II) (NSC-119875) in male F344 rats.*, *Toxicol. Appl. Pharmacol.*, 38: 535, 1976.

221. Kociba, R. J., Sleight, S. D., *Acute toxicological and pathological effects of cis-diamminedichloroplatinum (NSC-119875) in the male rat.*, Cancer Chemother. Rep., 55: 1, 1971.
222. Dobyan, D. C., Hill, D., Lewis, T., et al., *Cyst formation in rat kidney induced by cis-platinum administration.*, Lab. Invest., 45: 260, 1981.
223. Levi, J., Jacobs, C., Kalman, S., et al., *Mechanism of cis-platinum nephrotoxicity: I. Effects of sulphhydryl groups in rat kidneys.*, J. Pharmacol. Exp. Therap., 213: 545, 1980.
224. Dobyan, D. C., Levi, J., Jacobs, C., et al., *Mechanism of cis-platinum nephrotoxicity: II. Morphological observations.*, J. Pharmacol. Exp. Therap., 213: 551, 1980.
225. Choie, D. D., Longnecker, D. S., Del Campo, A. A., *Acute and chronic cisplatin nephrotoxicity in rats.*, Lab. Invest., 44: 397, 1981.
226. Guarino, A. M., Miller, D. S., Arnold, S. T., et al., *Platinate toxicity: past, present and prospects.*, Cancer Treat. Rep., 63: 1475, 1979.
227. Schaeppi, U., Heyman, I. A., Fleischman, R. W., et al., *Cis-dichlorodiammine-platinum II (NSC-119875): preclinical toxicological evaluation of intravenous injection in dogs, monkeys and mice.*, Toxicol. Appl. Pharmacol., 25: 230, 1973.
228. Gonzalez-Vitale, J. C., Hayes, D. M., Cvitkovic, E., et al., *The renal pathology in clinical trials of cis-platinum (II) diamminedichloride.*, Cancer, 39: 1362, 1977.
229. Lehane, D., Winston, A., Gray, R., et al., *The effects of diuretic pretreatment on clinical, morphological and ultrastructural cis-platinum induced nephrotoxicity.*, Int. J. Radiat. Oncol. Bio. Phys., 5: 1393, 1979.
230. Walker, E. M., Gale, G. R., *Methods of reduction of cisplatin nephrotoxicity.*, Ann. Clin. Lab. Sci., 11: 397, 1981.
231. Groth, S., Neilson, H., Pederson, A. G., *Nephrotoxicity of cis-platinum in man. A method for early detection.*, In "Proc. 3rd World Congress of Nuclear Medicine and Biology.", Raynaud, C. (ed), Pergamon Press, Paris, 1982. pp 580.
232. Thomsen, O., *Ein vermehrungsfähiges agens als veränderer des isoagglutinatorischen verhaltens der roten blutkörperchen, eine bisher unbekannte quelle der fehlbestimmungen.*, Z. Immunitätsforsch Immunobiol., 52: 85, 1927.
233. Friedenreich, V., *"The Thomsen hemagglutination phenomenon production of specific receptor quality in red cell corpuscles by bacterial activity."*, Levin and Munksgaard, Copenhagen, 1930.
234. Uhlenbruck, G., *The Thomsen-Friedenreich (TF) receptor: an old history with new mystery.*, Immunol. Commun., 10: 251, 1981.
235. Noujaim, A. A., Shysh, A., Zabel, P., et al., *The Thomsen-Friedenreich antigen: an important marker for the radioimmunodetection of cancer using macromolecular probes.*, In "Radioimmunoimaging and Radioimmunotherapy.", Burchiel, S. W., Rhodes, B. A. (Eds), Elsevier, 1983. pp 277.
236. Springer, G. F., *T and Tn, general carcinoma antigens.*, Science, 224: 1198, 1984.

237. Vaith, P., Uhlenbruck, G., *The Thomsen agglutinin phenomenon. A discovery revisited 50 years later.*, Z. Immun. Forsch., 154: 1, 1978.
238. Watkins, W. M., *Biochemistry and genetics of the ABO, Lewis and P blood group systems.*, Adv. Human Genet., 10: 1, 1980.
239. Springer, G. F., Desai, P. R., Murthy, M. S., et al., *Precursors of the blood group MN antigens as human carcinoma associated antigens.*, Transfusion, 19: 233, 1979.
240. Springer, G. F., Murphy, M. S., Desai, P. R., et al., *Patients' immune response to breast and lung carcinoma associated Thomsen-Friedenreich (T) specificity.*, Klin. Wochenschr., 60: 121, 1982.
241. Newman, R. A., Klein, P. J., *The presence and significance of the Thomsen-Friedenreich antigen in breast cancer.*, Cancer Res. Clin. Oncol., 93: 181, 1979.
242. Howard, D. R., Taylor, C. R., *An antitumour antibody in normal human serum reaction of anti-T with breast carcinoma cells.*, Oncology, 37: 142, 1980.
243. Zabel, P. L., Noujaim, A. A., Shysh, A., et al., *Radioiodinated peanut lectin: a potential radiopharmaceutical for immunodetection of carcinomas expressing the T-antigen.*, Eur. J. Nucl. Med., 8: 250-254, 1983.
244. Shysh, A., Eu, S.M., Noujaim, A. A., et al., *In vivo localization of Radioiodinated Peanut lectin in a murine TA3/Ha mammary carcinoma model.*, Eur. J. Nuc. Med., 10: 68, 1985.
245. Springer, G. F., Codington, J. F., *Surface glycoprotein from a mouse tumor cell as specific a specific inhibitor of anti-human blood group N agglutinin.*, J. Nat. Cancer Inst., 49: 1469, 1972.
246. Huggins, J. W., Trenbeath, T. P., Sherblom, A. P., *Glycoprotein differences in solid and ascites forms of the 13762 rat mammary adenocarcinoma.*, Cancer Res., 40: 1873, 1980.
247. Huggins, J. W., Trenbeath, T. P., *Redistribution and shedding of Conavalin A and peanut lectin receptor of ascites sublines of 13762 rat mammary adenocarcinoma.*, J. Supramol. Struc. (Suppl), 3: 212, 1979.
248. Springer, G. F., Cantrell, J. L., Desai, et al., *Human blood group M-, N-, T- and Tn-specific substances in lipidic extracts of line 10 hepatocarcinoma of strain Z Guinea Pigs.*, Clin. Immun. Immunopath., 22: 9, 1982.
249. Springer, G. F., Desai, P. R., Yang, H. J., et al., *Carcinoma-associated blood group MN precursor antigens against which all humans possess antibodies.*, Clin. Immunol., 7: 426, 1977.
250. Springer, G. F., Desai, P. R., *Increase in anti-T scores of breast carcinoma patients following mastectomy.*, Naturwissenschaften, 62: 587, 1975.
251. Springer, G. F., Desai, P. R., Scanlon, E. F., *Blood group MN precursors as human breast carcinoma-associated antigens and naturally occurring human cytotoxins against them.*, Cancer, 37: 169, 1976.
252. Springer, G. F., Tegtmeyer, H., *On the origin of anti-Thomsen-Friedenreich antibodies.*, Naturwissenschaften, 67: 317, 1980.

253. Boccardi, V., Attina, D., Girelli, G., *Influence of orally administered antibiotics on anti-T agglutinin of normal subjects and of cirrhotic patients.*, Vox Sang, 27: 268, 1974.
254. Springer, G. F., Tegtmeyer, H., *Origin of anti-Thomsen-Friedenreich (T) and Tn agglutinin in man and in white Leghorn chicks.*, Br. J. Haematol., 47: 453, 1981.
255. Springer, G. F., Desai, P. R., Murthy, M. S., et al., *Human carcinoma-associated precursor antigens of the blood group MN system and the host's immune responses to them.*, Prog. Allergy, 26: 42, 1979.
256. Bray, J., MacLean, G. D., Dusel, F. J., et al., *Decreased levels of circulating lytic anti-T in the serum of patients with metastatic gastrointestinal cancer: a correlation with disease burden.*, Clin. Exp. Immunol., 47: 176, 1982.
257. Thatcher, N., Hashmi, K., Chang, J., et al., *Anti-T antibody in malignant melanoma patients.*, Cancer, 46: 1278, 1980.
258. Springer, G. F., Murphy, M. S., Desai, P. R., et al., *Breast cancer patients' cell-mediated immune response to Thomsen-Friedenreich (T) antigen.*, Cancer, 45: 2949, 1980.
259. Springer, G. F., Desai, P. R., Murphy, M. S., et al., *Delayed-type skin hypersensitivity reaction (DTH) to Thomsen-Friedenreich (T) antigen as a diagnostic test for human breast adenocarcinoma.*, Klin. Wochenschr., 57: 961, 1979.
260. Rahman, R. A. S., Longenecker, B. M., *A monoclonal antibody for the Thomsen-Friedenreich cryptic T antigen.*, J. Immunol., 129: 2021, 1982.
261. Longenecker, B. M., Rahman, A. F. R., Barrington-Leigh, J., et al., *Monoclonal antibody against a cryptic-carbohydrate antigen of murine and human lymphocytes. I. Antigen expression in non-cryptic or unsubstituted form on certain murine lymphomas, on a spontaneous murine mammary carcinoma, and on several human adenocarcinomas.*, Int. J. Cancer, 33: 123, 1984.
262. Springer, G. F., Desai, P. R., *Common precursors of human blood group MN specificities.*, Biochem. Biophys. Res. Commun., 61: 470, 1974.
263. Springer, G. F., Desai, P. F., Murthy, M. S., et al., *Human carcinoma-associated precursor antigens of the NM blood group system.*, J. Surg. Oncol., 11: 95, 1979.
264. Skutelsky, E., Lotan, R., Sharon, N., et al., *Distribution of the T antigen on erythroid cell surfaces: studies with peanut agglutinin an anti-T specific lectin.*, Biochim. Biophys. Acta, 467: 165, 1977.
265. Desai, P. R., Springer, G. F., *Biosynthesis of human blood group T-N- and M- specific immunodeterminants on human erythrocyte antigens.*, J. Immunogenet., 6: 403, 1979.
266. Klenk, E., Uhlenbruck, G., *Über ein neuraminidasehaltiges mucoprotein aus rindererythrozytenstroma.*, Z. Physiol. Chem., 311: 227, 1958.
267. Springer, G. F., Tegtmeyer, H., Hyprkar, S. V., *Isolation and properties of human blood-group NM and Meconium-Vg antigens.*, Biochemistry, 5: 3254, 1966.
268. Hakomori, S., *Glycosphingolipids in cellular interaction, differentiation and oncogenesis.*, Ann. Rev. Biochem. 50: 733, 1981.

269. Nakahara, K., Ohashi, T., Oda, T., et al., *Asialo GM1, as well as a cell-surface marker detected in acute lymphoblastic leukemia.*, New Engl. J. Med., 302: 674, 1980.
270. Magnani, J. L., Brockhaus, M., Smith, D. F., et al., *A monosialoganglioside is a monoclonal antibody defined antigen of colon carcinoma.*, Science, 212: 55, 1981.
271. Keenan, T. W., Morre, D. J., *Mammary carcinoma enzymatic block in disialoganglioside biosynthesis.*, Science, 182: 935, 1973.
272. Yeh, M. Y., Hellstrom, I., Abe, K., et al., *A cell surface antigen which is present in the ganglioside fraction and shared by human melanomas.*, Int. J. Cancer, 29: 269, 1982.
273. Kasai, M., Iwamori, N., Nagai, Y., et al., *A glycolipid on the surface of mouse natural killer cells.*, Eur. J. Immunol., 10: 175, 1980.
274. Habu, S., Kasai, M., Nagai, Y., et al., Okumura, K., *The glycolipid asialo-GM1 as a new differentiation marker of fetal thymocytes.*, J. Immunol., 125: 2284, 1980.
275. Myllyla, G., Furuholm, U., Nordling, S., et al., *Persistent mixed field polyagglutinability: Electrokinetic and serological aspects.*, Vox. Sang., 20: 7, 1971.
276. Dausset, J., Moullec, J., Bernard, J., *Acquired haemolytic anaemia with polyagglutinability of red blood cells due to a new factor present in normal human serum (anti-Tn).*, Blood, 14: 1079, 1959.
277. Springer, G. F., Desai, P. R., Schachter, H., *Enzymatic synthesis of human blood group M-, N-, and T- specific structures.*, Naturwissenschaften, 63: 488, 1976.
278. Springer, G. F., Taylor, C. R., Howard, D. R., et al., *Tn, A carcinoma-associated antigen, reacts with anti-Tn of normal human sera.*, Cancer, 55: 561, 1985.
279. Kim, Z., Uhlenbruck, G., *Untersuchen uber T-antigen and T-agglutinin.*, Z. Immunitaetsforsch Immunobiol., 130: 88, 1966.
280. Anglin, J. H., Lerner, M. P., Nordquist, R. E., *Blood group-like activity released by human mammary carcinoma cells in culture.*, Nature, 269: 254, 1977.
281. Laurent, J. C., Noel, P., Faucon, M., *Expression of a cryptic cell surface antigen in primary cell cultures from human breast cancer.*, Biomed., 29: 260, 1978.
282. Ratcliffe, R. M., Baker, D. A., Lemieux, R. U., *Synthesis of the T (beta-D-gal (1-3) and D-gal NAc) antigenic determinant in a form useful for the preparation of an effective artificial antigen and the corresponding immunoadsorbent.*, Carbohydr. Res., 93: 35, 1981.
283. Kaifu, R., Osawa, T., *Synthesis of O-beta-D-galactopyranosyl-(1-3)-O-(2-acetamido-2-deoxy-alpha (and beta)-D-galactopyranosyl)-N-acetyls-L-serine and their interaction with D-galactose-binding lectins.*, Carbohydr. Res., 69: 79, 1979.
284. Coon, J. S., Weinstein, R. S., Summers, J. L., *Blood group precursor T-antigen expression in human urinary bladder carcinoma.*, Am. J. Clin. Path., 77: 692, 1982.
285. Coon, J. S., Weinstein, R. S., Summers, J. L., *Combination of ABH and T antigen detection in prognosis of urinary bladder carcinoma.*, Lab. Invest., 46: 15, 1982.

286. Summers, J. L., Coon, J. S., Ward, R. M., et al., *Prognosis in carcinoma of the urinary bladder based upon tissue blood group ABH and Thomsen-Friedenreich antigen status and karyotype of the initial tumour.*, Cancer Res., 43: 934, 1983.
287. Springer, G. F., Cheingsong-Popov, R., Schirmacher, V., et al., *Proposed molecular basis of murine tumor cell-hepatocyte interaction.* J. Biol. Chem., 258: 5702, 1983.
288. Ashwell, G., Harford, J., *Carbohydrate-specific receptors of the liver.*, Ann. Rev. Biochem., 51: 531, 1982.
289. Kieran, M. W., Longenecker, B. M., *Organ specific metastasis with special reference to avian systems.*, Cancer Met. Rev., 2: 165, 1983.
290. Boyd, W. C., Shapleigh, E., *Specific precipitating activity of plant agglutinins (lectins).*, Science, 119: 419, 1954.
291. Goldstein, I. J., Hayes, C. E., *The Lectins: carbohydrate binding proteins of plants and animals.*, Adv. Carbohydrate Chem. Biochem., 35: 127, 1978.
292. Goldstein, I. J., Hughes, R. C., Monsigny, M., et al., *What should be called a lectin?*, Nature, 285: 66, 1980.
293. Rüdiger, H., *Lectins: an introduction.*, In "Lectins: Biology, Biochemistry, Clinical Biochemistry." Vol 1., Boghansen, T. C. (ed.), Walter de Gruyter, 1981. pp 1.
294. Gold, E. R., Phelps, G. F., *Provisional classification of receptor-specific proteins (Antibody like substances).*, Z. Immun. Forsch., 143: 430, 1972.
295. Gold, E. R., Balding, P., *Receptor specific proteins: plant and animal lectins.*, Excerpta Medica, Amsterdam, 405, 1975.
296. Balding, P., *Lectins: Sugar-specific or receptor-specific proteins?*, In "Lectins: Biology, Biochemistry, Clinical Biochemistry." Vol 1., Boghansen, T. C. (ed.), Walter de Gruyter, 1981. pp 11.
297. Franz, H., Ziska, P., Boghansen, T. C. (Ed), *Affinitins: Combining sites-containing proteins.*, In "Lectins: Biology, Biochemistry, Clinical Biochemistry." Vol 1., Boghansen, T. C. (ed.), Walter de Gruyter, 1981. pp 17.
298. Kocourek, J., Horejsi, V., *A note on the recent discussion on definition of the term "lectin".*, In "Lectins: Biology, Biochemistry, Clinical Biochemistry." Vol 3., Boghansen, T. C., Spengler, G. A., (eds.), Walter de Gruyter, 1983. pp 3.
299. Lis, H., Sharon, N., *Affinity chromatography for the purification of lectins (A review).*, J. Chromatography, 215: 361, 1981.
300. Lis, H., Sharon, N., *Lectins: their chemistry and application to immunology.*, The Antigens, 4: 429, 1977.
301. Goldstein, I. J., Lamb, J. E., Roberts, D. D., et al., *Structural homologies of some leaf and seed lectins.*, Prog. Clin. Biol. Res., 138: 21, 1983.
302. Barondes, S. H., *Lectins: their multiple endogenous cellular functions.*, Ann. Rev. Biochem., 50: 207, 1981.

303. Ochoa, J. L., Cordoba, F., *On the Specificity and Hydrophobicity of lectins*. In "Lectins- Biology, Biochemistry, Clinical Biochemistry." Vol 1., Boghansen, T. C. (ed.), Walter de Gruyter, 1981. pp 73.
304. Lotan, R., Nicolson, G. L., *Purification of cell membrane glycoproteins by lectin affinity chromatography*, Biochim. Biophys. Acta, 559: 329, 1979.
305. Wu, M., *Differential binding characteristics and applications of DGal β (1 \rightarrow 3)DGalNAc specific lectins*. Mol. Cell. Biochem., 61: 131, 1984.
306. Coggi, G., Dell'Orto, P., Bonoldi, E., et al., *Lectins in diagnostic pathology*. In "Lectins- Biology, Biochemistry, Clinical Biochemistry." Vol 3., Boghansen, T. C., Spengler, G. A., (eds.), Walter de Gruyter, 1983. pp 87.
307. Horisberger, M., Tacchini-Volanthen, M., *Stability and steric hinderance of lectin-labelled gold markers in transmission and scanning electron microscopy*. In "Lectins- Biology, Biochemistry, Clinical Biochemistry." Vol 3., Boghansen, T. C., Spengler, G. A., (eds.), Walter de Gruyter, 1983. pp 189.
308. Howard, D. R., Ferguson, P., Batsakis, J. G., *Carcinoma associated cytoskeletal antigenic alterations. Detection by lectin binding*. Cancer, 47: 2872, 1981.
309. Judd, W. J., *The role of lectins in blood group serology*. CRC Crit. Rev. Clin. Lab. Sci., 12: 171, 1980.
310. Judd, W. J., *The use of purified lectins in immunohematology*. Transfusion, 19: 768, 1979.
311. Nicolson, G. L., *Lectin-interactions with normal and tumour cells and the affinity purification of tumour cell glycoconjugates*. Cancer markers. Diagnostic and development significance. Humana Press U.S.A., 403, 1980.
312. Nicolson, G. L., *The interactions of lectins with animal cell surfaces*. Int. Rev. Cytol., 39: 89, 1974.
313. Rapin, A. M. C., Burger, M. M., *Tumour cell surfaces: general alterations detected by agglutinins*. Adv. Cancer Res., 20: 1, 1974.
314. Stadler, B. M., Liechti, J., Bonnard, G. D., *T-cell stimulating lectins are mitogenic inducers but not mitogens*. In "Lectins- Biology, Biochemistry, Clinical Biochemistry." Vol 3., Boghansen, T. C., Spengler, G. A., (eds.), Walter de Gruyter, 1983. pp 37. 7: 1966.
315. Berke, G., *T-lymphocyte-mediated cytotoxicity. IV. How do mitogenic and non mitogenic lectins mediate lymphocyte-target interactions?*. In "Lectins- Biology, Biochemistry, Clinical Biochemistry." Vol 3., Boghansen, T. C., Spengler, G. A., (eds.), Walter de Gruyter, 1983. pp 55.
316. Toledo-Pereyra, L. H., Ray, P. K., Callender, C. O., et al., *Renal allograft prolongation using phytomitogens to mask graft antigens*. Surgery, 76: 121, 1974.
317. Ray, P. K., Simmons, R. L., *Masking of cellular histocompatibility antigens with phytomitogens*. J. Immunol., 110: 1693, 1973.
318. Ghose, T., Blair, A. H., *Antibody-linked cytotoxic agents in the treatment of cancer: current status and future prospects*. JNCI, 61: 657, 1978.

319. Lin, H., Bruce, W. R., Walcroft, M. J., *Concanavalin A: its action on experimental tumour cells and possible use in cancer chemotherapy.*, Cancer Chemother., 59: 319, 1975.
320. Lin, J. Y., Li, J. S., Tung, T. C., *Lectin derivatives of methotrexate and chlorambucil as chemotherapeutic agents.*, JNCI., 66: 523, 1981.
321. Kitao, T., Hattori, K., *Concanavalin A as a carrier of duanomycin.*, Nature, 265: 81, 1977.
322. Tsuruo, T., Yamori, T., Tsukagashi, S., et al., *Enhanced cytotoxic action of methotrexate by conjugation to concanavalin A.*, Int. J. Cancer, 26: 655, 1980.
323. Roth, J., *The lectins' molecular probes in cell biology and membrane research.*, Exp. Path. Suppl., 3: 7, 1978.
324. Uhlenbruck, G., Pascoe, G. I., Bird, G. W. G., *On the specificity of lectins with a broad agglutination spectrum. II Studies on the nature of the T-antigen and the specific receptors for the lectins of Arachis hypogaea (ground nut).*, Zeitschrift fur Immunitäts Forschung Allergic und Klinische Imm., 138: 423, 1969.
325. Lotan, R., Skutelsky, E., Danon, D., et al., *The purification, composition and specificity of the Anti-T lectin from peanut (Arachis hypogaea).*, J. Biol.Chem., 250: 8518, 1975.
326. Momoi, T., Tokunaga, T., Nagai, Y., *Specific interactions of peanut agglutinin with the glycolipid Asialo GM1.*, FEBS Letters, 141: 6-10, 1982.
327. Ørntoft, T. F., Mors, N. P. O., Eriksen, G., *Comparative immunoperoxidase demonstrations of T-antigens in human colorectal carcinomas and morphologically abnormal mucosa.*, Cancer Res., 45: 447, 1985.
328. Springer, G. F., Desai, P. R., Banatwala, I., *Blood group MN antigens and precursors in normal and malignant human breast glandular tissue.*, J. Nat. Cancer Inst., 54: 335, 1975.
329. Newman, R. A., Klein, P. J., Rutland, P. S., *Binding of peanut lectin to breast epithelium, human carcinomas and a cultured rat mammary stem cell: use of the lectin as a marker of mammary differentiation.* JNCI., 63: 1339, 1979.
330. Zabel, P. M., *¹²⁵I antibodies and PNA for tumour detection.*, MSc Thesis, University of Alberta, 1982.
331. Bird, G. W. G., *Anti-T in peanuts.*, Vox Sang., 9: 748, 1964.
332. Terao, T., Irimura, T., Osawa, T., *Purification and characterization of a hemagglutinin from Arachis hypogaea.*, Hoppe Seylers Z Physiol. Chem., 356: 1685, 1975.
333. Fish, W. W., Hamlin, L. M., Miller, R. L., *The macromolecular properties of peanut agglutinin.*, Arch. Biochem. Biophys., 190: 693, 1978.
334. Pueppke, S. G., *Multiple molecular forms of peanut lectin: classification of isolectins and isolectin distribution among genotypes of the genus Arachis.*, Arch. Biochem. Biophys., 212: 254, 1981.
335. Neurohr, K. J., Young, N. M., Mantsch, H. H., *Determination of the carbohydrate-binding properties of peanut agglutinin by ultraviolet difference spectroscopy.*, J. Biol. Chem., 255: 9205, 1980.

336. Foriers, A., deNeve, R., Strosberg, A. D., *Lectin sequences as a tool for chemotaxonomical classification*, *Physiol. Veg.*, 17: 597, 1979.
337. Lauwereys, A., Foriers, A., Sharon, N., et al., *Sequence studies of peanut agglutinin*, *FEBS Letters*, 181: 241-244, 1985.
338. Salunke, D. M., Khan, M. I., Surolia, A., *Crystallization and preliminary X-ray studies of the anti-T lectin from peanut (Arachis hypogaea)*, *J. Mol. Biol.*, 154: 177, 1982.
339. Neurohr, K. J., Bundle, D. R., Young, N. M., et al., *Binding of disaccharides by peanut agglutinin as studied by ultraviolet difference spectroscopy*, *Eur. J. Biochem.*, 123: 305, 1982.
340. Howard, D. R., *Expression of T-antigen on polyagglutinable erythrocytes and carcinoma cells: preparation of T-activated erythrocytes, anti-T lectin anti-T absorbed human serum and purified anti-T antibody*, *Vox Sang.*, 37: 107, 1979.
341. Decastel, M., Bourrillon, R., Frenoy, J. P., *Cryoinstability of peanut agglutinin effects of saccharides and neutral salts*, *J. Biol. Chem.*, 256: 9003, 1981.
342. Majumdar, T., Surolia, A., *A large scale preparation of peanut agglutinin on a new affinity matrix*, *Prep. Biochem.*, 8: 119, 1978.
343. Sutoh, K., Rosenfield, L., Lee, Y. C., *Isolation of peanut lectin by affinity chromatography on polyacrylamide (coallyl α -D-galactopyranoside)*, *Analyt. Biochem.*, 79: 329, 1977.
344. Dawson, R., *Comparison of fractionation of groundnut proteins by two different methods*, *Analyt. Biochem.*, 41: 305, 1971.
345. Neucere, N. J., Conkerton, E. J., *Some physicochemical properties of peanut protein isolates*, *J. Agric. Food Chem.*, 26: 683, 1978.
346. Neucere, N. J., *Isolation of alpha-arachin, the major peanut globulin*, *Analyt. Biochem.*, 27: 15, 1969.
347. Basha, S. M., Pancholy, S. K., *Isolation and characterization of two cryoproteins from florunner peanut (Arachis hypogaea L) seed*, *J. Agric. Food Chem.*, 30: 36, 1982.
348. Merry, A. H., Rawlmsom, V. I., Stratton, F., *A rapid purification method for peanut anti-T lectin*, *Immunol. Commun.*, 10: 265-273, 1981.
349. Newman, R. A., *Heterogeneity among the anti-T lectins derived from Arachis hypogaea*, *Hoppe Seyler's Z Physiol. Chem.*, 358: 1517, 1977.
350. Novogrodsky, A., Lotan, R., Ravid, A., et al., *Peanut agglutinin: a new mitogen that binds to galactosyl sites exposed after neuraminidase treatment*, *J. Immunol.*, 115: 1243, 1975.
351. Periera, M. E. A., Kabat, E. A., Lotan, R., et al., *Immunochemical studies on the specificity of the peanut (Arachis hypogaea) agglutinin*, *Carbohydr. Res.*, 51: 107, 1976.
352. Matsumoto, I., Jimbo, A., Kitagaki, H., et al., *Detection of lectin-sugar interaction by ultraviolet difference spectroscopy*, *J. Biochem.*, 88: 1093, 1980.

353. Neurohr, K. J., Mantsch, H. H., Young, N. M., et al., *Carbon-13 nuclear magnetic resonance studies on lectin-carbohydrate interactions: binding of specifically carbon-13-labeled methyl-beta-D-lactoside to peanut agglutinin.*, *Biochem.*, 21: 303, 1982.
354. Neurohr, K. J., Young, N. M., Smith, I. C. P., et al., *Kinetics of binding of methyl α and β -D-galacto pyrananoside to peanut agglutinin: a carbon-13 nuclear resonance study.*, *Biochem.*, 20: 3499, 1981.
355. Irimura, T., Kawuguchi, T., Terao, T., et al., *Carbohydrate-binding specificity of the so-called galactose-specific phytohemagglutinins.*, *Carbohydr. Res.*, 39: 317, 1975.
356. Ohanessian, J., Caron, M., *A spectrophotometric study of the carbohydrate binding site of peanut lectin.*, In "Lectins- Biology, Biochemistry, Clinical Biochemistry.", Vol 3., Boghansen, T. C., Spengler, G. A., (eds.), Walter de Gruyter, 1983. pp 623.
357. Caron, M., Ohanessian, J., Becquart, J., et al., *Ultraviolet difference spectroscopy study of peanut lectin binding to mono- and disaccharides.*, *Biochim. Biophys. Acta.*, 717: 432, 1982.
358. Sharon, N., *Lectins.*, *Sci. Am.*, 236: 108, 1977.
359. Jimbo, A., Matsumoto, I., *Involvement of the tyrosyl residue in the interaction of peanut lectin with lactose.*, *J. Biochem.*, 91:: 945, 1982..
360. Young, N. M., Neurohr, K. J., Williams, R. E., *Unique effects of glycopeptides on the circular dichroism of concanavalin A peanut agglutinin and the peanut lectin.*, *Biochim. Biophys. Acta*, 701: 142, 1982.
361. Springer, G. F., Desai, P. R., Murthy, M. S., *Histochemical methods for the demonstration of Thomsen- Friedenreich antigen in cell suspensions and tissue sections.*, *Klin. Wochenschr.*, 56: 1225, 1978.
362. Cooper, H. S., *Lectins as probes in histochemistry and immunohistochemistry.*, *Human Pathol.*, 15: 904, 1984.
363. London, J., Perrot, J. Y., Berrih, S., et al., *Peanut agglutinin IV. a tool for studying human mononuclear cell differentiation.*, *Scand. J. Immunol.*, 9:451, 1979.
364. Glöckner, W. M., Newman, R. A., Dahr, W., et al., *Alkali-labile oligosaccharides from glycoproteins of different erythrocyte milk fat globule membranes.*, *Biochim. Biophys. Acta*, 443: 402, 1976.
365. Dahr, W., Uhlenbruck, G., Knott, H., *Immunochemical aspects of the MNS blood group system.*, *J. Immunogenet.*, 2: 87, 1975.
366. Dahr, W., Uhlenbruck, G., Bird, G. W. G., *Cryptic A-like receptor sites in human erythrocyte glycoproteins: proposed nature of Tn-antigen.*, *Vox Sang*, 27: 29, 1974.
367. Dahr, W., Uhlenbruck, G., Bird, G. W. G., *Further characterization of some heterophile agglutinins reacting with alkali-labile carbohydrate chains of human erythrocyte glycoproteins.*, *Vox Sang*, 28: 133, 1975.
368. Thomas, D. B., Winzler, R. J., *Structural studies of human erythrocyte glycoproteins. Alkali labile oligosaccharides.*, *J. Biol. Chem.*, 244: 5943, 1969.

369. Newman, R. A., Uhlenbruck, G., *Investigation into the occurrence and structure of lectin receptors on human and bovine erythrocytes, milk fat globule and lymphocyte membrane glycoproteins.*, Eur. J. Biochem., 76: 149, 1977.
370. McConnell, I., Munroe, A., Waldmann, H., "The Immune System.", 2nd Ed. Blackwell, Oxford, 1981.
371. London, J., Berrih, S., Bach, J., *Peanut agglutinin I. A new tool for studying T lymphocyte subpopulations.*, J. Immunol., 121: 438, 1978.
372. Nakamura, T., Tanimoto, K., Nakano, K., et al., *Isolation of human suppressor T cells by Peanut agglutinin.*, Int. Archs. Allergy Appl. Immun., 68: 338, 1982.
373. Reisner, Y., Biniaminov, M., Rosenthal, E., et al., *Interaction of peanut agglutinin with normal human lymphocytes and with leukemic cells.*, Proc. Nat. Acad. Sci. USA., 76: 447, 1979.
374. Ballet, J. J., Fellous, M., Sharon, N., et al., *Reactivity of human lymphoid and lymphoblastoid cells with peanut agglutinin: detection of a blood cell subset which lacks detectable membrane HLA.*, Scand. J. Immunol., 11: 555, 1980.
375. Sharon, N., Lis, H., *Lectins: cell-agglutinating and sugar specific proteins.*, Science, 177: 949, 1972.
376. Rose, M. L., Malchiodi, F., *Binding of peanut lectin to thymic cortex and germinal centres of lymphoid tissue.*, Immunol., 42: 583, 1981.
377. Rose, M. L., Habeshaw, J. A., Kennedy, R., et al., *Binding of peanut lectin to germinal centre cells: a marker for β -cell subsets of follicular lymphoma?*, Br. J. Cancer, 44: 68, 1981.
378. Schrader, J. W., Chen, W. F., Scollay, R., *The acquisition of receptors for peanut agglutinin by peanut agglutinin-negative thymocytes and peripheral T-cells.*, J. Immunol., 129: 545, 1982.
379. Levin, S., Russell, E. C., Blanchard, D., et al., *Receptors for peanut agglutinin (Arachis hypogaea) in childhood acute lymphoblastic leukemia: possible clinical significance.*, Blood, 55: 37, 1980.
380. Veerman, A. J. P., Hogeman, P. H. G., Huismans, D. R., et al., *Peanut agglutinin, a marker of T-cell acute lymphoblastic leukemia with a good prognosis.*, Cancer Res., 45: 1890, 1985.
381. Hewitt, H. B., *Studies on the dissemination and quantitative transplantation of a lymphocytic leukemia in CBA mice.*, Br. J. Cancer, 12: 378, 1958.
382. Zola, H., *Modulation of the immune response to transplantation antigens. I The effects of immunization using adjuvants on the immune response in mice to a tumour allograft.*, Clin. Exp. Immunol., 11: 585, 1972.
383. Bessel, E. M., Courtenay, V. D., Foster, A. B., et al., *Some in vivo and in vitro antitumour effects of the deoxyfluoro-D-glucopyranosides.*, Eur. J. Cancer, 9: 463, 1973.
384. Glöckner, W. M., Kaulen, H. D., Uhlenbruck, G., *Immunochemical determination of the*

- Thomsen-Friedenreich antigen (T-antigen) on platelet plasma membranes.* Thrombos. Haemostas., 39: 186, 1978.
385. Jacob, F., *Mouse teratocarcinoma and embryonal antigens*, Immunol. Rev., 33: 3, 1977.
 386. Reisner, Y., Gachelin, G., Dubois, P., et al., *Interaction of peanut agglutinin, a lectin specific for non-reducing D-galactosyl residues with embryonal carcinoma cells.*, Dev. Biol., 61: 280, 1977.
 387. Muramatsu, T., Gachelin, G., Damonville, M., et al., *Cell surface carbohydrates of embryonal carcinoma cells: polysaccharide side chains of F9 antigens and of receptors to two lectins. FBP and PNA.*, Cell, 18: 183, 1979.
 388. Prujansky-Jacobovitis, A., Gachelin, G., Muramatsu, T., et al., *Surface galatosyl glycopeptides of embryonal carcinoma cells.*, Biochem. Biophys. Res. Comm., 89: 448, 1979.
 389. Springer, G. F., Desai, P. R., Banatwala, I., *Blood group MN specific substances and precursors in normal and malignant human breast tissues.*, Naturwissenschaften, 61: 457, 1974.
 390. Coon, J. S., Weinstein, R. S., *Blood groups antigens in tumor cell membranes.*, Biomembranes, 11: 173, 1983.
 391. Klein, P. J., Newman, R. A., Muller, P., et al., *The presence and the significance of the Thomsen-Friedenreich antigen in mammary gland. II. Its topochemistry in normal hyperplastic and carcinoma tissue of the breast.*, J. Cancer Res. Clin. Onco., 93: 205, 1979.
 392. Klein, P. J., Newman, R. A., *Histochemical methods for the demonstration of T-F antigen in cell suspensions and tissue sections.*, Klin. Wochenschr., 56: 761, 1978.
 393. Klein, P. J., Vierbuchen, M., Fischer, J., et al., *The characterization of milk proteins by lectins and antibodies in hormone dependent breast cancer.*, In "Lectins- Biology, Biochemistry, Clinical Biochemistry.", Vol 3., Boghansen, T. C., Spengler, G. A., (eds.), Walter de Gruyter, 1983. pp 157.
 394. Calafat, J., Hageman, P. C., Janssen, H., *Ultrastructural localization of peanut agglutinin receptors on the cells of human mammary tumors.*, In "Lectins- Biology, Biochemistry, Clinical Biochemistry.", Vol.3., Boghansen, T. C., Spengler, G. A., (eds.), Walter de Gruyter, 1983. pp 131.
 395. Vierbuchen, M., Klein, P. J., Rossel, S., et al., *Endocrine therapeutical studies on carcinogen-induced rat mammary carcinomas characterized by hormone dependent lectin-binding sites.*, In "Lectins- Biology, Biochemistry, Clinical Biochemistry.", Vol 3., Boghansen, T. C., Spengler, G. A., (eds.), Walter de Gruyter, 1983. pp 145.
 396. Klein, P. J., Vierbuchen, M., Wurz, H., et al., *Secretion-associated lectin-binding sites as a parameter of hormone dependance in mammary carcinoma.*, Br. J. Cancer, 44: 746, 1981.
 397. Springer, G. F., Codington, J. F., *Surface glycoprotein from a mouse tumour cell as a specific inhibitor of antihuman blood group N agglutinin*, JNCI., 49: 1469, 1973.
 398. Miller, D. K., Cooper, A. G., Brown, M. C., et al., *Reversible loss in suspension culture of a major cell surface glycoprotein of the TA3-Ha mouse tumor.*, JNCI., 55: 1249, 1975.

399. Miller, S. C., Codington, J. F., Klein, G., *Further studies on the relationship between allotransplantability and the presence of the cell surface glycoprotein epiglycanin in the TA3-MM mouse mammary carcinoma ascites cell.*, JNCI., 68:981, 1982.
400. Van den Eijnden, D. H., Evans, N. A., Codington, J. F., et al., *Chemical structure of epiglycanin, the major glycoprotein of the TA3-Ha ascites cell.*, J. Biol. Chem., 254: 12153, 1979.
401. Sanford, B. H., Codington, J. F., Jeanloz, R. W., *Transplantability and antigenicity of two sublines of the TA3 tumor.*, J. Immunol., 110: 1233, 1973.
402. Codington, J. F., Cooper, A. G., Miller, D. K., et al., *Isolation and partial characterization of an epiglycanin-like glycoprotein from a new non-strain-specific subline of TA3 murine mammary adenocarcinoma.*, JNCI, 63:153-161, 1979.
403. Codington, J. F., Van den Eijnden, D. H., Jeanloz, R. W., et al., *Structural studies on the major glycoprotein of the TA3/ Ha ascites tumor cell.*, In "Cell Surface Carbohydrate Chemistry." , Acad. Press, N.Y., 1978. pp 49.
404. Codington, J. F., Cooper, A. G., Brown, M. C., et al., *Evidence that the major cell surface glycoprotein of the TA3-Ha carcinoma contains the Vicia graminea receptor sites.*, Biochem., 14: 855, 1975.
405. Cooper, A. G., Codington, J. F., Brown, M. C., *In Vivo release of glycoprotein I from the Ha subline of TA3 murine tumour in ascites fluid and serum.*, Proc. Nat. Acad. Sci. USA., 71: 1224, 1974.
406. Codington, J. F., Linsley, K. B., Jeanloz, R. W., et al., *Immunochemical and chemical investigations of the structure of glycoprotein fragments obtained from epiglycanin, a glycoprotein at the surface of the TA3-Ha cancer cell.*, Carbohydr. Res., 40: 171, 1975.
407. Friberg, S., *Comparison of an immunoresistant and immunosusceptible ascites subline from murine tumor TA3. I. Transplantability, morphology, and some physiochemical properties.*, JNCI., 48:1463, 1972.
408. Shysh, A., Eu, S.M., Noujaim, A.A., et al., *Radioimmuno-detection of murine mammary adenocarcinoma (TA3/ Ha) lung and liver metastases with radioiodinated PNA.*, Int. J. Cancer, 35: 113, 1985.
409. Matsumoto, I., Codington, J. F., Jannke, R. E., et al., *Comparative lectin-binding and agglutination properties of the strain-specific TA3-st and the non-strain-specific TA3-Ha, murine mammary carcinoma ascites sublines, further studies of receptors in epiglycanin.*, Carbohydr. Res., 80: 179, 1980.
410. Friberg, S., *Comparison of an immunoresistant and an immunosusceptible ascites subline from murine tumor TA3. II. Immunosensitivity and antibody binding capacity In Vitro and immunogenicity in allogeneic mice.*, JNCI., 48:1477, 1972.
411. Miller, S. C., Hay, E. D., Codington, J. f., *Ultrastructural and histochemical differences in cell surface properties of strain-specific and nonstrain- specific TA3 adenocarcinoma cells.*, J. Biol. Chem., 72: 511, 1977.
412. Cooper, A. G., Codington, J. F., Miller, D. K., et al., *Loss of strain specificity of the TA3-St subline: Evidence for the role of epiglycanin in mouse allogenic tumor growth.*

JNCI., 63:163, 1979.

413. Fischer, J., Klein, P. J., Vierbuchen, M., et al., *Histochemical and biochemical characterization of glycoprotein components in normal gastric cancers with lectins*, In "Lectins- Biology, Biochemistry, Clinical Biochemistry.", Vol 3., Boghansen, T. C., Spengler, G. A., (eds.), Walter de Gruyter, 1983. pp 167.
414. Klein, P. J., Osmers, R., Vierbuchen, M., et al., *The importance of Lectin binding sites and carcinoembryonic antigen with regard to normal, hyperplastic, adenomatous, and carcinomatous colonic mucosa*, Rec. Res. Cancer Res., 79: 1, 1981.
415. Fischer, J., Klein, P. J., Vierbuchen, M., et al., *Lectin binding properties of glycoproteins in cells of normal gastric mucosa and gastric cancers: a comparative histochemical and biochemical study*, In "Proc. 1st Int. Conf. on Human Tumor Markers.", 1983. pp 137.
416. Cooper, H. S., *Peanut lectin-binding sites in large bowel carcinoma*, Lab. Invest., 47: 383, 1982.
417. Schachter, H., Roseman, S., *Mammalian glycosyltransferases: their role in synthesis and function of complex carbohydrates*, In "The Biochemistry of Glycoproteins and Proteoglycans.", Lennarz W. J. (ed), Plenum Press, New York, 1980, pp 85.
418. Boland, C. R., Montgomery, C. K., Kim, Y. S., *Alterations in human colonic mucin occurring with cellular differentiation and malignant transformation*, Proc. Nat. Acad. Sci. USA, 79: 2051, 1982.
419. Yogeeswaran, G., Salk, P. L., *Metastatic potential is positively correlated with cell surface sialation of cultured murine tumour cell lines*, Science, 212: 1514, 1981.
420. Murray, R. K., Yogeeswaran, G., Sheinin, R., et al., *Glycosphingolipids of clonal lines of transformed mouse fibroblasts adrenocortical cells*, In "Tumour Lipids, Biochemistry and Metabolism.", Wood, R. (ed) AQCSP Press, Champaign, 1973. pp 285.
421. Hyun, K. H., Nakai, M., Kawamura, K., et al., *Histochemical studies of lectin binding patterns in keratinized lesions, including malignancy*, Virchow Arch. A., 402: 337, 1984.
422. Hyun, K. H., Hosaka, M., Fukui, S., et al., *Lectin binding sites in basal cell epitheliomas*, Acta. Histochem. Cytochem., 17: 504, 1984.
423. Viale, G., Dell'Orto, P., Colombi, R., et al., *Lectin binding sites on semithin sections of epoxy-embedded tissues*, In "Lectins- Biology, Biochemistry, Clinical Biochemistry.", Vol 3., Boghansen, T. C., Spengler, G. A., (eds.), Walter de Gruyter, 1983. pp 199.
424. Holthöfer, H., *Lectin binding sites in kidney: a comparative study of 14 animal species*, J. Histochem. Cytochem., 31: 531-537, 1983.
425. Holthöfer, H., Miettinen, A., et al., *Comparison of lectin binding sites in the kidneys of different animal species*, In "Lectins- Biology, Biochemistry, Clinical Biochemistry.", Vol 3., Boghansen, T. C., Spengler, G. A., (eds.), Walter de Gruyter, 1983. pp 205.
426. Schulte, B. A., Spicer, S. S., *Histochemical evaluation of mouse and rat kidneys with lectin-horseradish peroxidase conjugates*, Am. J. Anatomy, 168: 345, 1983.
427. Brown, D., Kunz, A., Wohlwend, A., et al., *Ultrastructural detection of glycocalyx*

- heterogeneity in convoluted and straight proximal tubules of rat kidney, using lectin gold complexes.*, C. R. Acad. Sc., 10: 501, 1983.
428. LeHir, M., Dubach, U. C., *The cellular specificity of lectin binding in the kidney. I. A light microscopical study in the rat.*, Histochemistry, 74: 521, 1982.
 429. Roth, J., *Applications of immunocolloids in light microscopy. II. Demonstration of lectin-binding sites in paraffin sections by the use of lectin-gold or glycoprotein complexes.*, J. Histochem. Cytochem., 31: 547, 1983.
 430. Murata, F., Tsuyama, S., Suzuli, S., et al., *Distribution of glycoconjugates in the kidney studied by use of labeled lectins.*, J. Histochem. Cytochem. 31: 139, 1983.
 431. LeHir, M., Dubach, U. C., *The cellular specificity of lectin binding in the kidney. II. A light microscopical study in the rabbit.*, Histochemistry, 74: 531-540, 1982.
 432. Faraggiana, T., Malchiodi, F., Prado, A., et al., *Lectin-peroxidase conjugate reactivity in normal human kidney.*, J. Histochem. and Cytochem., 30: 451, 1982.
 433. Holthöfer, H., Virtanen, I., Pettersson, E., et al., *Lectins as-fluorescence microscopic markers for saccharides in the human kidney.*, Lab. Invest., 45: 391, 1981.
 434. Scherberich, J. E., Gauhl, C., Hess, H., et al., *Comparative studies on lectin receptors of plasma-membranes (PM) from human kidney and renal adenocarcinoma.*, Eur. J. Cell Biol., Suppl. 4: 17, 1983.
 435. Kerjaschki, D., Sharkey, D. J., Farquhar, M. G., *Identification and characterization of podocalyxin- the major sialoprotein of the renal glomerular epithelial cell.*, J. Cell. Biol., 98: 1591, 1984.
 436. Moho, S. C., Skoza, L., *Glomerular sialoprotein.*, Science, 164: 1519, 1969.
 437. Kerjaschki, D., Vernillo, A. T., Farquhar, M. G., *Reduced sialylation of podocalyxin- the major sialoprotein of the rat glomerulus- in aminonucleoside nephrosis.*, Am. J. Pathol., 118: 343, 1985.
 438. LeHir, M., Kaissling, B., Koeppen, B. M., et al., *Binding of peanut lectin to specific epithelial cell types in the kidney.*, Am. J. Physiol., 11: C117, 1982.
 439. Klein, P. J., Bulla, M., Newman, R. A., et al., *The significance of pneumococcal neuraminidase for the development of haemolytic-uraemic syndrome.*, In "Dialysis and Kidney Transplantation in Children.", Bulla, M. (ed), Bibliomed, Melsungen, 1981. pp 183,
 440. Klein, P. J., Bulla, M., Newman, R. A., et al., *Thomsen-Friedenreich antigen in haemolytic-uraemic syndrome.*, The Lancet, 1024, 1977.
 441. Vierbuchen, M., Klein, P. J., Uhlenbruck, G., et al., *The significance of lectin receptors in the kidney and in hypernephroma (renal adenocarcinoma).*, In "Recent Results in Cancer Research, Cancer Chemotherapy and Immunopharmacology. Mathe, G., Muggia, F. M. (Eds), Springer-Verlag, N.Y., 1983. pp 68.
 442. Raedler, A., Boehle, A., Otto, U., et al., *Differences of glycoconjugates exposed on hypernephroma and normal kidney cells.*, J. Urol., 128: 1109, 1982.

443. Ortmann, M., Klein, P. J., Vierbuchen, M., et al., *The importance of lectin receptors in the diagnosis of infectious immunologic and neoplastic diseases of the kidney.*, In "Renal Insufficiency in Children.", Bulla, M. (ed.), Springer-Verlag., Cologne, 1981. pp 31.
444. Wallace, A. C., Nairn, R. C., *Renal tubular antigens in kidney tumours.*, Cancer, 29: 977, 1972.
445. Holthöfer, H., Virtanen, I., Törnroth, T., et al., *Lectins as markers for cells infiltrating human renal glomeruli.*, Virchow Arch. B., 46: 119, 1984.
446. Zabel, P. L., Noujaim, A. A., Shysh, A., et al., *Radiiodinated peanut lectin: a potential radiopharmaceutical for the detection of tumours expressing the T-antigen.*, In "Proc. 3rd World Congress of Nuclear Medicine and Biology.", Raynaud, C. (ed.), 1982.
447. Yokoyama, K., Aburano, T., Watanabe, N., et al., *Tumor affinity of radiolabeled Peanut agglutinin compared with that of Ga-67 citrate in animal models.*, J. Nucl. Med., 26: P111, 1985.(abst).
448. Suresh, M. R., Wilkinson, A. A., Holt, S., et al., *The biodisposition of Peanut lectin in humans.*, In "Proceedings of the 3rd International Symposium of Radiopharmacology.", Freiburg, 1983.
449. Holt, S., Wilkinson, A., Suresh, M.R., et al., *Radiolabelled Peanut Lectin for the scintigraphic detection of cancer.*, Cancer Lett., 25: 55, 1984.
450. Boniface, G. R., Selvaraj, S., Suresh, M. R., et al., *Synthetic Glycosylated H.S.A. analogues for Hepatocyte Imaging.*, In "Proceedings of the 4th International Symposium of Radiopharmacology.", Banff, 1985.
451. Fraker, P. J., Speck, J. C., *Protein and cell membrane iodinations with sparingly soluble chloramide 1,3,4,6-tetrachloro-3- α -6- β -diphenylglycouril.* Biochem. Biophys. Res. Commun., 80: 849, 1978.
452. *Instruction Manual, Biorad Protein Assay.* Bio-Rad Laboratories, Richmond, California.
453. Bradford, M. *A rapid and sensitive method for the quantitation of microgram quantities of protein utilizing the principle of protein-dye binding.* Anal. Biochem., 72: 248, 1976.
454. Ediss, C., Abrams, D. N., *Implementation of the coincidence method for determining ¹²⁵I activity with an estimate of error.* J. Radioanal. Chem., 65: 341, 1981.
455. Gibaldi, M., Perrier, D., *Pharmacokinetics. 2nd Ed.*, Marcel Dekker Inc., New York, 1982.
456. Eu, S. M., *Radiiodinated Peanut lectin and Monoclonal Antibodies for the detection of T-Antigen expressing tumours and metastases.* M.Sc. Thesis., University of Alberta, 1985.
457. Eguchi, M., Poon, K. C., Spicer, S. S., *Alterations in the proximal nephron of beige mice with Chediak-Higashi syndrome.*, Am. J. Pathol., 106: 95, 1982.
458. Wilkinson, A. A., Holt, S., Matte, G., et al., *Renal excretion of radiiodinated Peanut lectin in Humans: Postulating receptor-mediated endocytosis and exocytosis by renal tubular cells.* Under preparation.

459. Maunsbach, A. B., *Cellular mechanisms of tubular protein transport*. In "International Review of Physiology: Kidney and urinary tract Physiology II, Vol II", Thurau, K. (ed), University Park Press, Baltimore, 1976. pp 145.
460. Pastan, I., Willingham, M. C., *Journey to the centre of the Cell: Role of the receptosome*. Science, 214: 504, 1981.
461. Helenius, A., Mellman, I., Wall, D., et al., *Endosomes*. Trends Biochem. Sci., 7: 245, 1983.
462. Steinman, R. M., Mellman, I., Muller, W. A., et al., *Endocytosis and recycling of Plasma Membrane*, J. Cell Biol., 96: 1, 1983.
463. Straus, W., *Occurrence of phagosomes and phago-lysosomes in different segments of the nephron in relation to the reabsorption, transport, digestion and extrusion of intravenously injected horseradish peroxidase*. J. Cell Biol., 21: 295, 1964.
464. Roth, T. F., Porter, K. R., *Yolk protein uptake in the oocyte of the mosquito Aedes aegypti L.*, J. Cell Biol., 20: 313, 1964.
465. Pearse, B. M. F., *Clathrin: a unique protein associated with intracellular transfer of membrane coated vesicles*. Proc. Natl. Acad. Sci. USA., 73: 1255, 1976.
466. Tycko, B., Maxfield, F. R., *Rapid acidification of endocytic vesicles containing α_2 -macroglobulin*, Cell, 28: 643, 1982.
467. Pastan, I., Willingham, M. C., *Receptor-mediated endocytosis: Coated pits, receptosomes and the golgi*, Trends Biochem. Sci., 7: 250, 1983.
468. Katz, A. I., Rubenstein, A. H., *Metabolism of proinsulin, insulin and C-peptide in the rat*, J. Clin. Invest., 52: 1113, 1973.
469. Ravnskov, U., Johansson, B. G., Göthlin, J., *Receptor-mediated endocytosis: Coated pits, receptosomes and the golgi*, Scand. J. Clin. Lab. Invest., 30: 71, 1972.
470. Feria-Velasco, A., *The ultrastructural bases of the initial stages of renal tubular excretion. A cytochemical study using horseradish peroxidase as a tracer*, Lab. Invest., 30: 190, 1974.
471. Kessel, R. G., *The permeability of dragonfly malpighian tubule cells to protein using horseradish peroxidase as a tracer*, J. Cell Biol., 47: 299, 1970.
472. Goodman, L. S., Gilman, A., *The Pharmacological Basis of Therapeutics*, 5th Ed., MacMillan Publishing Co. Inc., New York, 1975.
473. DeNardo, G. L., DeNardo, S. J., Peng, J. S., et al., *Evidence of a saturable receptor for mouse monoclonal antibodies*. J. Nucl. Med., 26: P67, 1985. (abst).
474. Stahl, P. D., Rodman, J. S., Millar, M. J., et al., *Evidence for receptor-mediated binding of glycoproteins, glycoconjugates and lysosomal glycosidases by alveolar macrophages*. Proc. Natl. Acad. Sci. USA., 75: 1399, 1978.
475. Gregoriadis, G., Morell, A. G., Sternlieb, I., et al., *Catabolism of desialylated ceruloplasmin in the liver*. J. Biol. Chem., 245: 5833, 1970.

476. VanDen Hamer, C., Morell, A. G., Scheinberg, I., et al., *Physical and chemical studies on ceruloplasmin IX: The role of galactosyl residues in the clearance of ceruloplasmin from the liver.* J. Biol. Chem., 245: 4397, 1970.
477. Morell, A. G., Gregoriadis, G., Scheinberg, I., et al., *The role of sialic acid in determining the survival of glycoproteins in the circulation.* J. Biol. Chem., 246: 1461, 1971.
478. Van Lenten, L., Ashwell, G., *The binding of desialylated glycoproteins by plasma membranes of rat liver.*, J. Biol. Chem., 247: 4633, 1972.
479. Hakomori, S., *Tumour-associated carbohydrate antigens.*, Ann. Rev. Immunol., 2: 103, 1984.
480. Vera, D. R., Krohn, K. A., Stadalnik, R. C., *Liver imaging via labeled hepatic binding protein ligands.*, J. Nucl. Med., 19: 685, 1978.
481. Vera, D. R., Krohn, K. A., Stadalnik, R. C., *Radioligands that bind to cell-specific receptors: Hepatic binding protein ligands for hepatic scintigraphy.*, In "Radiopharmaceuticals II.", Sodd, V. J., Allen, D. R., Hoogland, D. R. Ice, R. D. (Eds), Society of Nucl. Med., N.Y., 1979. pp 565.
482. Vera, D. R., Krohn, K. A., Stadalnik, R. C., et al. *Tc-99m Galactosyl-neogalactoalbumin: Preparation and preclinical studies.*, J. Nucl. Med., 26: 1157, 1985.
483. Vera, D. R., Krohn, K. A., Stadalnik, R. C., et al. *Tc-99m Galactosyl-neogalactoalbumin: In vivo characterization of receptor-mediated binding to hepatocytes.* Radiology., 151: 191, 1984.
484. Vera, D. R., Krohn, K. A., Stadalnik, R. C., et al. *Tc-99m Galactosyl-neogalactoalbumin: In vivo characterization of receptor-mediated binding.* J. Nucl. Med., 25: 779, 1984.
485. Krohn, K., Vera, D. R., Stadalnik, R. C., *A complementary radiopharmaceutical and mathematical model for quantitating hepatic-binding protein receptors.*, In "Receptor-binding Radiotracers, Vol II.", Eckelman, W. C. (Ed), CRC Press, Boca Raton, Florida, 1982. pp 41.
486. Woodle, E. S., Ward, R. E., Vera, D. R., et al., *Technetium-99m Galactosyl-Neogalactoalbumin (Tc-NGA) liver imaging: Application in liver transplantation.*, J. Nucl. Med., 26: P9, 1985. (abst).
487. Stadalnik, R. C., Vera, D. R., Woodle, E. S., et al., *Technetium-99m NGA Functional Hepatic Imaging: Preliminary Clinical Experience.*, J. Nucl. Med., 26: 1233, 1985.

7. APPENDICES

APPENDIX 1

Preparation of ^{99m}Tc -DTPA

1. Dissolve 100 mg Diethylene triamine penta acetic acid (Sigma Chemical Co., St Louis, Mo) and 2 mg Stannous chloride in 10 mL of 0.1 N HCl.
2. Heat at 90-100°C for 15 min, cool, and make up to 100 mL with Water for Injection.
3. Adjust pH to 7 with 1 N NaOH and purge with N_2 for 15 min.
4. Dispense 2 mL aliquots into sterile 10 mL vials through a 0.22 μm Sterile Millex-SA filter, using aseptic technique.
5. Freeze solutions at 4°C until used.
6. Reconstitute thawed solution with $^{99m}\text{TcO}_4^-$ solution to the appropriate specific activity and determine radiochemical purity using ITLC-SG chromatography with Acetone as solvent.
7. Use within 2 h after reconstitution.

APPENDIX 2: ¹²⁵I-PNA BIODISTRIBUTION IN CBA/CAJ MICE WITH TA3/IIa TUMOUR (S.C.).

		% DOSE / GRAM OF TISSUE				
		30 MIN N=5	3.5 HRS N=6	7 HRS N=5	24 HRS N=6	48 HRS N=6
BLOOD	Mean ±S.D.	6.13 1.37	3.21 0.68	1.20 0.44	0.13 0.01	0.07 0.01
LIVER	Mean ±S.D.	6.67 1.79	5.92 0.53	5.62 0.35	3.02 0.33	2.60 0.42
SPLEEN	Mean ±S.D.	8.30 2.31	8.02 1.64	4.69 0.70	3.19 1.31	2.91 0.56
STOMACH	Mean ±S.D.	14.08 2.11	26.67 3.35	2.12 2.30	0.50 0.13	0.27 0.04
G.I.T.	Mean ±S.D.	2.92 0.76	2.64 0.50	1.08 0.34	0.14 0.02	0.08 0.01
KIDNEY	Mean ±S.D.	62.33 24.54	11.53 3.13	4.34 0.52	1.12 0.06	0.63 0.09
LUNG	Mean ±S.D.	10.32 5.70	4.46 0.81	2.84 1.22	0.37 0.07	0.30 0.11
MUSCLE	Mean ±S.D.	1.23 0.10	1.08 0.51	0.30 0.08	0.08 0.02	0.06 0.02
SALIVARIES	Mean ±S.D.	6.10 2.06	6.05 0.70	6.72 3.93	1.42 0.20	0.77 0.19
TUMOUR	Mean ±S.D.	3.73 1.13	3.99 1.39	1.45 0.41	0.45 0.08	0.30 0.05
CARCASS	Mean ±S.D.	3.76 0.53	3.44 0.72	1.58 0.31	0.68 0.19	0.41 0.13

APPENDIX 3: ¹²⁵I-PNA BIODISTRIBUTION IN CAF1/J MICE WITH TA3/II₁ TUMOUR (S.C.).

	% DOSE / GRAM OF TISSUE				
	30 MIN N=5	3.0 HRS N=6	6 HRS N=6	24 HRS N=6	48 HRS N=6
BLOOD	Mean ±S.D. 7.47 1.36	2.91 0.84	2.27 0.73	0.11 0.03	0.09 0.03
LIVER	Mean ±S.D. 3.73 0.51	2.22 0.42	2.16 0.37	0.48 0.05	1.62 0.12
SPLEEN	Mean ±S.D. 3.78 0.59	2.31 0.49	1.91 0.33	0.33 0.07	0.90 0.19
STOMACH	Mean ±S.D. 17.77 4.76	21.77 6.54	20.21 7.73	0.58 0.40	0.29 0.16
G.I.T.	Mean ±S.D. 2.35 0.48	1.77 0.41	1.57 0.43	0.10 0.02	0.10 0.04
KIDNEY	Mean ±S.D. 44.62 12.78	11.74 3.11	8.48 0.92	1.41 0.15	1.39 0.22
LUNG	Mean ±S.D. 4.66 0.54	2.54 0.84	2.07 0.51	0.20 0.05	0.19 0.04
MUSCLE	Mean ±S.D. 0.88 0.18	0.55 0.17	0.39 0.10	0.03 0.01	0.04 0.01
SALIVARIES	Mean ±S.D. 10.29 2.46	25.05 10.31	37.55 11.98	1.55 0.95	0.74 0.32
TUMOUR	Mean ±S.D. 4.12 0.99	4.40 1.38	4.84 1.72	0.57 0.24	0.51 0.28
CARCASS	Mean ±S.D. 2.06 0.47	1.66 0.39	1.59 0.39	0.54 0.15	0.55 0.20

APPENDIX 4: ^{131}I -CM₁-H.S.A. BIODISTRIBUTION IN CBA/CAJ MICE.

		% DOSE / GRAM OF TISSUE				
		30 MIN N=5	60 MIN N=5	3 HRS N=4	6 HRS N=5	24 HRS N=6
BLOOD	Mean ±S.D.	24.47 1.78	18.32 1.35	16.99 3.30	23.58 1.75	2.78 0.19
LIVER	Mean ±S.D.	32.08 3.71	15.64 2.00	9.10 1.39	10.80 1.64	0.88 0.03
SPLEEN	Mean ±S.D.	4.64 0.34	3.70 0.47	4.12 0.83	6.53 0.77	0.59 0.07
STOMACH	Mean ±S.D.	21.04 3.16	27.91 8.18	50.45 10.93	101.40 31.66	1.27 0.13
G.I.T.	Mean ±S.D.	4.56 0.52	4.65 0.95	5.28 0.99	9.30 1.89	0.53 0.03
KIDNEY	Mean ±S.D.	9.97 0.85	9.59 0.33	9.85 1.17	11.88 1.29	1.08 0.11
LUNG	Mean ±S.D.	10.67 0.94	8.66 1.24	9.80 1.68	12.42 1.56	1.47 0.11
MUSCLE	Mean ±S.D.	1.71 0.12	1.73 0.23	2.08 0.43	3.28 0.40	0.37 0.02
SALIVARIES	Mean ±S.D.	10.28 0.85	12.74 2.65	17.50 4.75	38.31 5.47	1.40 0.09
CARCASS	Mean ±S.D.	3.36 0.38	3.45 0.38	4.87 0.78	7.90 0.96	1.75 0.29

APPENDIX 5: ^{125}I -a-GM1-H.S.A. BIODISTRIBUTION IN C3H/101 MICE WITH TA3/IIa TUMOUR (S.C.).

		% Ixuse μ GRAM OF TISSUE				
		30 MIN	3 HRS	6 HRS	24 HRS	48 HRS
		N=6	N=6	N=6	N=6	N=6
BLOOD	Mean	25.42	14.64	13.65	2.47	0.72
	\pm S.D.	3.44	0.99	1.36	0.38	0.11
LIVER	Mean	20.82	8.51	7.76	0.85	0.31
	\pm S.D.	3.27	1.26	1.34	0.22	0.03
SPLEEN	Mean	4.52	3.32	3.54	0.42	0.13
	\pm S.D.	0.64	0.26	0.43	0.15	0.02
STOMACH	Mean	39.94	63.17	69.34	5.15	1.08
	\pm S.D.	5.34	9.23	15.54	3.48	0.33
G.I.T.	Mean	6.12	5.48	6.76	0.71	0.18
	\pm S.D.	1.14	0.60	0.77	0.34	0.03
KIDNEY	Mean	9.96	6.66	6.90	0.84	0.27
	\pm S.D.	1.58	0.55	0.59	0.25	0.04
LUNG	Mean	9.96	7.00	6.73	1.25	0.45
	\pm S.D.	1.43	0.79	0.91	0.29	0.07
MUSCLE	Mean	2.09	1.92	1.95	0.25	0.08
	\pm S.D.	0.25	0.27	0.17	0.07	0.01
SALIVARIES	Mean	19.56	35.64	22.94	2.50	0.57
	\pm S.D.	4.87	3.19	6.60	2.35	0.16
TUMOUR	Mean	10.69	10.30	11.13	1.73	0.51
	\pm S.D.	1.66	1.18	0.98	0.52	0.08
CARCASS	Mean	4.59	4.74	5.03	1.62	1.23
	\pm S.D.	0.46	0.38	0.22	0.44	0.18

APPENDIX 6: ¹²⁵I-HSA BIODISTRIBUTION IN CAF1/J MICE WITH TA3/II_a TUMOUR (S.C.).

	% DOSE / GRAM OF TISSUE					
	30 MIN. N=6	3 HRS N=6	6 HRS N=6	24 HRS N=6	48 HRS N=5	
BLOOD						
Mean	41.88	22.48	17.17	3.48	0.93	
S.D.	5.55	1.14	2.14	0.31	0.18	
LIVER						
Mean	11.25	6.11	5.48	0.99	0.33	
S.D.	1.06	0.76	0.70	0.12	0.06	
SPLEEN						
Mean	5.61	3.17	2.79	0.54	0.21	
S.D.	0.74	0.27	0.41	0.08	0.07	
STOMACH						
Mean	26.40	34.11	36.06	3.97	0.89	
S.D.	2.90	3.59	9.05	2.00	0.26	
G.I.T.						
Mean	4.94	4.35	4.50	0.74	0.18	
S.D.	0.89	0.55	0.47	0.19	0.04	
KIDNEY						
Mean	15.31	7.95	6.94	1.20	0.39	
S.D.	2.67	0.78	0.98	0.18	0.09	
LUNG						
Mean	14.30	8.73	6.80	1.63	0.55	
S.D.	2.43	0.83	1.18	0.24	0.11	
MUSCLE						
Mean	1.88	1.65	1.49	0.31	0.12	
S.D.	0.34	0.28	0.20	0.07	0.21	
SALIVARIES						
Mean	14.26	19.65	13.19	2.55	0.57	
S.D.	3.46	5.71	3.91	1.38	0.18	
TUMOUR						
Mean	10.50	9.98	9.75	2.20	0.63	
S.D.	2.21	1.57	1.03	0.49	0.12	
CARCASS						
Mean	5.30	4.93	4.59	1.38	0.79	
S.D.	0.58	0.44	0.17	0.28	0.14	

APPENDIX 7: ¹²⁵I-PNA-¹²⁵I-α-GM-128 S.A. BIODISTRIBUTION IN CAF1/J MICE WITH TA3/HA₂ TUMOUR (S.C.), 4 : 1 CONJUGATION.

		% DOSE / GRAM OF TISSUE				
		30 MIN. N=6	3.5 HRS N=5	7 HRS N=6	24 HRS N=6	48 HRS N=6
BLOOD	Mean ±S.D.	7.39 1.31	2.67 0.32	1.24 0.30	0.19 0.05	0.06 0.01
LIVER	Mean ±S.D.	5.21 0.47	3.62 0.44	3.02 0.33	1.96 0.23	1.58 0.15
SPLREEN	Mean ±S.D.	22.39 3.70	8.66 3.02	3.95 1.00	2.13 0.23	2.03 0.55
STOMACH	Mean ±S.D.	5.70 0.37	16.05 1.96	9.82 3.02	1.00 0.41	0.26 0.06
G.I.T.	Mean ±S.D.	2.31 0.26	2.41 0.38	1.27 0.40	0.18 0.05	0.08 0.02
KIDNEY	Mean ±S.D.	77.84 20.39	32.68 8.11	10.32 2.36	1.36 0.17	0.71 0.05
LUNG	Mean ±S.D.	6.86 1.64	3.42 0.37	2.35 0.23	0.61 0.06	0.26 0.06
MUSCLE	Mean ±S.D.	0.85 0.11	0.79 0.14	0.45 0.11	0.07 0.02	0.03 0.03
SALIVARIES	Mean ±S.D.	3.63 0.47	2.83 3.41	2.52 2.50	1.82 0.39	0.83 0.32
TUMOUR	Mean ±S.D.	2.37 0.70	2.18 0.50	1.27 0.18	0.40 0.08	0.22 0.06
CARCASS	Mean ±S.D.	2.84 0.34	2.77 0.42	1.72 0.38	0.51 0.09	0.48 0.13

APPENDIX 8: ¹²⁵I-1-CM-H.S.A.:¹²⁵I-PNA BIODISTRIBUTION IN CAF1/J MICE WITH TA3/IIa TUMOUR (S.C.). 1 : 4 M/M CONJUGATION.

	% DOSE / GRAM OF TISSUE				
	30 MIN. N=6	3.5 HRS N=6	7 HRS N=6	74 HRS N=6	48 HRS N=6
BLOOD	Mean ±S.D.	13.78 1.87	8.07 1.82	5.09 0.78	1.14 0.10
LIVER	Mean ±S.D.	19.67 3.72	4.50 1.02	3.04 0.64	0.63 0.06
SPLREEN	Mean ±S.D.	2.92 0.49	2.42 0.62	1.26 0.23	0.28 0.05
STOMACH	Mean ±S.D.	16.70 1.80	30.35 7.59	17.33 5.67	1.37 0.54
G.I.T.	Mean ±S.D.	3.12 0.41	3.11 0.80	1.70 0.44	0.36 0.06
KIDNEY	Mean ±S.D.	6.69 1.24	4.31 1.03	3.76 1.46	0.66 0.09
LUNG	Mean ±S.D.	8.10 1.33	4.92 1.14	2.98 0.73	0.83 0.09
MUSCLE	Mean ±S.D.	0.95 0.17	1.25 0.28	0.69 0.17	0.17 0.02
SALIVARIES	Mean ±S.D.	6.63 1.36	12.25 6.40	11.12 4.08	1.64 0.45
TUMOUR	Mean ±S.D.	2.61 0.55	3.69 1.26	2.47 0.51	0.92 0.20
CARCASS	Mean ±S.D.	2.36 0.42	3.44 0.86	2.23 0.44	0.87 0.14

APPENDIX 2: ^{125}I -FNA: ^{125}I -GM, H.S.A. BIODISTRIBUTION IN CAF1/J MICE WITH TA3/HA TUMOURS (S.C.). 1 : 2 M/M CONJUGATION.

	% DOSE / GRAM OF TISSUE					
	30 MIN. N=5	3 HRS N=6	6 HRS N=6	24 HRS N=5	48 HRS N=5	
BLOOD	Mean S.D.	3.81 1.40	5.76 0.74	0.22 0.01	0.10 0.01	
LIVER	Mean S.D.	7.63 0.49	8.08 0.38	3.51 0.24	2.35 0.23	
SPLEEN	Mean S.D.	5.85 0.16	5.19 0.56	5.33 0.43	1.89 0.26	1.40 0.30
STOMACH	Mean S.D.	13.74 4.76	19.57 10.16	23.72 7.92	0.85 0.10	0.19 0.11
G.I.T.	Mean S.D.	2.94 0.44	2.62 0.86	3.76 0.52	0.26 0.03	0.11 0.02
KIDNEY	Mean S.D.	65.03 8.03	17.34 3.52	15.26 2.10	2.40 0.26	1.21 0.13
LUNG	Mean S.D.	5.83 0.38	3.42 0.88	4.31 0.50	0.32 0.03	0.18 0.03
MUSCLE	Mean S.D.	1.12 0.23	0.85 0.27	1.14 0.13	0.07 0.01	0.05 0.02
SALIVARIES	Mean S.D.	12.16 3.59	24.28 13.11	58.63 3.86	2.15 0.28	0.65 0.17
TUMOUR	Mean S.D.	5.62 0.62	5.71 2.10	7.19 1.73	1.14 0.38	0.30 0.01
CARCASS	Mean S.D.	3.50 0.65	2.70 0.96	4.19 0.35	1.30 0.13	0.72 0.32

APPENDIX 10: ¹²⁵I-IGM-H.S.A.¹²⁵I-PNA BIODISTRIBUTION IN CAFL/J MICE WITH TA3/II₁ TUMOUR (S.C.). 2 : 1 M/M CONJUGATION.

		% DOSE / GRAM OF TISSUE				
		30 MIN N=5	30 HRS N=6	6 HRS N=6	24 HRS N=5	48 HRS N=5
BLOOD	Mean ±S.D.	19.36 2.67	15.07 2.45	16.80 0.77	2.44 0.28	1.10 0.15
LIVER	Mean ±S.D.	17.18 4.51	5.80 1.72	7.14 0.68	0.19 0.04	0.00 0.00
SPLEEN	Mean ±S.D.	2.45 0.22	1.94 0.91	3.60 0.37	0.00 0.00	0.00 0.00
STOMACH	Mean ±S.D.	21.95 3.65	31.50 15.16	37.71 12.43	2.09 0.16	0.41 0.20
G.I.T.	Mean ±S.D.	4.10 0.45	3.97 1.19	5.62 0.47	0.49 0.05	0.17 0.03
KIDNEY	Mean ±S.D.	0.00 0.00	3.52 1.11	6.42 0.45	0.49 0.09	0.27 0.07
LUNG	Mean ±S.D.	7.88 1.96	7.56 1.12	8.39 0.80	1.12 0.16	0.58 0.12
MUSCLE	Mean ±S.D.	11.29 0.14	1.47 0.36	2.12 0.22	0.23 0.05	0.08 0.02
SALIVARIES	Mean ±S.D.	17.83 3.99	40.31 19.99	90.36 3.72	4.06 0.45	0.50 0.16
TUMOUR	Mean ±S.D.	5.81 0.97	7.59 2.35	9.97 1.27	1.38 0.17	0.41 0.04
CARCASS	Mean ±S.D.	2.50 -0.24	3.37 0.79	4.79 0.23	1.96 0.16	0.94 0.27